DEVELOPMENT OF HYBRID SILICA MEMBRANE MATERIAL FOR MOLECULAR SIEVE APPLICATIONS

Hany Hassan Hussein Abdel Aziz

Dipòsit Legal: T.1370-2013

Hany Hassan Hussein Abdel Aziz El-Feky

DEVELOPMENT OF HYBRID SILICA MEMBRANE MATERIAL FOR MOLECULAR SIEVE APPLICATIONS

DOCTORAL THESIS

Supervised by

Dr. Tània Gumí Caballero

Dr. Kelly Cristina Briceño Mejías

Department of Chemical Engineering

UNIVERSITAT ROVIRA I VIRGILI

Tarragona

2013

UNIVERSITAT ROVIRA I VIRGILI
ESCUELA TÈCNICA SUPERIOR D'ENGINYERIA QUÍMICA
DEPARTMENT D'ENGINYERIA QUÍMICA

Avinguda Països Catalans, 26
Campus Sescelades
43007 Tarragona (Spain)
Tels. 977 55 96 03/04
Fax 977 55 96 21
e.mail:secdeq@urv.cat
http://www.etseq.urv.cat/DEQ

I STATE that the present study, entitled "Development of Hybrid Silica Membrane Material for Molecular Sieve Applications", presented by Hany Hassan Hussein Abdel Aziz for the award of the degree of Doctor, has been carried out under my supervision at the Department of Chemical Engineering of this university, and that it fulfils all the requirements to be eligible for the international doctorate award.

Tarragona, 25 July 2013
Doctoral Thesis Supervisors

Dr. Tània Gumí Caballero

Dr. Kelly Cristina Briceño Mejías

The present thesis has been possible thanks to the award of a doctoral grant from "Departament d'Economia i Coneixement" de la "Generalitat de Catalunya" and its department of Support to Universities and Research (SUR del DEC), together with Fons Social Europeu (FSE) for the period 2010-2013.

Acknowledgments

First and foremost, all praises and thanks are due to **Allah**, for giving me the power, health and patience to finish my PhD thesis. For providing me every day the enthusiasm and wisdom to proceed successfully and for giving me the great opportunity to step in the wonderful world of science ''*Alhamdu lillah*''

I am very grateful to my supervisor Dr. Tània Gumí, who gave me the opportunity to carry out my master and PhD under her supervision. Thanks Tània for your patience, encouragement, help whenever I needed it, and guides during all these years. You have been supportive and have given me the freedom to pursue researches without objection. Indeed, you helped and showed me the first steps to be a researcher.

Also I would like to express my appreciation to Dr. Kelly Briceño, my advisor and friend, for giving me guidance and counsel, and for having faith and confidence in me, also for her supervision and encouragement during the experimental work and preparation of the thesis.

I owe my deepest gratitude to Inorganic Membranes research group at University of Twente (Enschede, Holland) for their guidance and hospitality during my research stay there. Thanks to all my friends with whom I shared my time in Enschede.

The members at Servei de Recursos Científics i Tècnics (Universitat Rovira i Virgili) are acknowledged for their kindly guidance and advices through my samples analysis and characterization.

I would like to thank and acknowledge the support and help of chairmen, managers and my friends at Abu Qir Fertilizers and Chemicals Industries Company (Alexandria, Egypt). It is with immense gratitude that I acknowledge Dr. Eng. Hasseib Ibrahim El-Feky for his support, encouragement and help.

I have been fortunate to have many friends, from different countries all over the world, who cherish me despite my eccentricities. It gives me great pleasure in acknowledging the support and help of the members, and former members, of my research group (METEOR). Thanks to Brisa Peña, Cinta Panisello, Diana Dubert, Krzysztof Bogdanowicz, Ania Trojanowska**,** Joandiet Castañeda Padrón and all friends at Universitat Rovira i Virgili. Kamila Szałata is acknowledged for her contribution and assistance to finish my work.

Pepa (Habeby), I cannot find words to express my gratitude to you. Thanks so much for your help, support and everything you have done for me when I joined the group.

I owe great thanks to all my Egyptian friends that I have met in Tarragona and Holland, special thanks to Hatem and his wife Reham. My deep thanks to Obai and Hamdi (Sudan), Radouane, Houda and Enqira (Morocco), Ibrahim and Abdel Rahman (Saudi Arabia) and Bribi and Rachid (Algiria). Rachid, thanks so much for everything you have done for me and your help. Indeed, my dear friends your friendships are invaluable for me.

I am indebted to my family for their support and encouragement during my study. Mohamed, my oldest brother, whatever I'm going to say, it is not enough to express my gratitude to you and to your lovely wife Reham. Really I have enjoyed my time being with your family and my playing with my nephew, my sweet heart, Eyad (Dodo). I'm so desirous to see your lovely and sweet newcomer daughter. Mohamed and Reham thanks from my deep heart for everything you have done for me.

Last but not least, how I wish the two most important persons in my life, my parents, were alive and beside me at this moment. This work and all what I achieved in my life would not have been possible unless I remembered their encouragement words.

*Ya **Allah** ''the most merciful and beneficent'' bless their spirits.*

For spirits of my parents, this thesis is dedicated.

Hany Hassan El-Feky

CONTENTS

Summary i
List of abbreviations xiii
List of Figures xvii
List of Tables xxi
Scope of the thesis 1
I. An overview 2
II. Structure of the thesis 5
1. General introduction 11
1.1. Membrane technology: State-of-the-art 12
1.2. An introduction to gas separation using membranes 13
1.3. Inorganic Membranes for gas separation 17
1.3.1. Dense inorganic membranes 21
1.3.2. Porous inorganic membranes 21
1.3.3. Gas transport and separation mechanisms in porous inorganic membranes 23
1.3.3.1. An overview 23
1.3.3.2. Single gas mechanisms 24
1.3.3.3. Gas mixtures mechanisms 27
1.4. The need for gas separation 29
1.5. References 33
2. Sol- gel technique 39
2.1. Introduction 40
2.1.1. Chemical reactions during the sol-gel process 44
2.1.2. Processing 48
2.2. Sol-gel derived microporous silica membranes 48
2.2.1. Preparation of microporous silica membranes 50
2.2.1.1. Colloidal suspension route 51
2.2.1.2. Polymeric sol-gel route 51
2.2.2. Tailoring the porosity of microporous silica materials 53
2.2.2.1. Solvent-templating 53
2.2.2.2. Surface derivatization 54
2.2.2.3. Template-based approaches 55
2.2.3. Modified microporous silica membranes 55
2.3. Characterization techniques for microporous silica membranes 61

2.3.1. Hydrophobicity of the microporous silica membranes 61
2.3.1.1. Contact angle measurements 61
2.3.1.2. Hydrophobicity index 63
2.3.1.3. Water adsorption isotherms 63
2.3.2. Thermogravimetric Analysis (TGA) 64
2.3.3. Fourier Transform Infrared-Attenuated Total Reflectance Spectroscopy (FTIR-ATR) 64
2.3.4. X-Ray Diffraction (XRD) 64
2.3.5. Solid-state silicon-29 nuclear magnetic resonance spectroscopy (^{29}Si NMR) 66
2.3.6. Gas adsorption/desorption measurements 67
2.4. References 71
3. General objectives of the thesis 79
4. Novel silica membrane material for molecular sieve application 83
4.1. Introduction 84
4.2. Experimental part 86
4.2.1. Materials and methods 86
4.2.2. Preparation of silica membrane materials 87
4.2.3. Characterization of the silica membrane materials 89
4.3. Results and discussion 90
4.3.1. Hydrophobicity of the modified silica membrane materials 90
4.3.2. Infrared spectroscopy 92
4.3.3. X-ray analysis for the metal-doped membrane materials 92
4.3.4. Solid-state ^{29}Si NMR spectroscopy 95
4.3.5. Thermal stability of the membrane materials 97
4.3.6. Micropore structure 98
4.4. Conclusions 104
4.5. References 105
5. Characterization of metal-doped methylated microporous silica for molecular separations 111
5.1. Introduction 112
5.2. Experimental part 114
5.2.1. Materials and methods 114
5.2.2. Xerogels preparation 115

5.2.3. Characterization of the xerogels 116
5.3. Results and discussion 117
5.3.1. Thermogravimetric analysis 117
5.3.2. Infrared spectroscopy 118
5.3.3. X-ray analysis 121
5.3.4. Solid-state ^{29}Si NMR spectroscopy 121
5.3.5. Micropore structure 125
5.4. Conclusions 132
5.5. References 133
6. Thermally enhanced methylated microporous silica for molecular sieve applications 139
6.1. Introduction 140
6.2. Experimental part 143
6.2.1. Materials and methods 143
6.2.2. Xerogels preparation 143
6.2.3. Characterization of the xerogels 144
6.3. Results and discussion 145
6.3.1. Thermogravimetric analysis 145
6.3.2. Infrared spectroscopy 146
6.3.3. X-ray analysis 148
6.3.4. Micropore structure 148
6.4. Conclusions 157
6.5. References 159
7. Novel hydrophobic silica membrane for gas separation 165
7.1. Introduction 166
7.2. Experimental part 168
7.2.1. Materials and methods 168
7.2.2. Unsupported hydrophobic silica membranes preparation 169
7.2.3. Supported hydrophobic silica membranes preparation 170
7.2.4. Membranes Characterization 172
7.2.5. Gas permeance measurements 173
7.3. Results and discussion 173
7.3.1. Membranes hydrophobicity 173
7.3.2. Characterization of the sols 175
7.3.3. Thermogravimetric analysis 177
7.3.4. Micropore structure 181

7.3.5. Permenace of the hydrophobic membranes. 184
7.3.5.1. Tubular hydrophobic silica membranes 184
7.3.5.2. Disk-shaped hydrophobic silica membranes 192
7.4. Conclusions 200
7.5. References 202
8. General conclusions and future work 209
9. List of publications and congresses contributions 215
10. Curriculum Vitae 219

Summary

In the present thesis, a new methodology for modification of silica membrane materials, in order to achieve and enhance these materials, towards molecular sieve applications such as gas separation is proposed. The way for doing that is by combining two different approaches that have been used for silica membrane materials modification.

Microporous silica membranes suffer from water sorption due to the interaction between water molecule and silanol (hydroxyl) surface groups of silica membranes. Therefore, microporous silica membranes are an effective separation way only for dry gases. This has encouraged an increasing research for developing new approaches for silica modification and enhancement. One approach is template-based approach that depends on incorporation of organic template within the silica matrix to form hybrid materials. The benefit from this approach is the surface and microstructural properties of these hybrid silica materials, as a membrane material precursor, can be modified and enhanced by the processing gas used for the heat treatment, during calcination process. Under inert atmosphere the silica membranes are rendered hydrophobic feature. On the other hand, under oxidizing atmosphere the pyrolysis of these organic templates take place, therefore, it results in micropores network formation. However, the thermal stability of these organic constituents was reported to be between 400 °C and 500 °C in both atmospheres. The other approach is the metal-doped approach that was designed to reduce the degradation of the hydrophilic silica membranes. Several metal and/or metal oxides-doped silica membranes were prepared and used for molecular sieve applications such as gas separation. For instance, metal oxides such as Co_3O_4, TiO_2 and NiO have been trialed and in most cases provide membranes with improved performance. However, metal-doped silica membranes still showed the hydrophilic effect, as they can adsorb water, but less than the conventional silica membranes.

In the present thesis, the novel material, cobalt-doped hybrid silica material, was prepared by the acid-catalyzed hydrolysis and condensation process of tetraethylorthosilicate (TEOS) and methyltriethoxysilane (MTES). The preparation involved cobalt-doping within the matrix of organic templated silica material (hybrid silica). The synthesis and surface properties of the novel unsupported silica membrane were revealed by surface and microstructural techniques, such as TGA, FTIR, X-ray, solid-state ^{29}Si MAS NMR and N_2 adsorption measurements. The initial

results on the synthesis and surface properties of the novel unsupported silica membrane showed enhanced properties as well as the same properties that the blank and modified unsupported silica membranes, hybrid and metal-doped, posses.

For instance, calcination of unsupported TEOS/MTES silica membrane under inert atmosphere resulted in hydrophobic membrane material. On the other hand, calcination of the novel unsupported membrane under oxidizing atmosphere resulted in silica membrane that rendered hydrophobic feature. Moreover, the novel material showed high thermal stability in inert and oxidizing atmosphere compared with the non-doped material. The thermal stability of the novel unsupported silica membrane was enhanced up to temperature range between 500 °C and 600 °C in oxidizing atmosphere. Such enhancement in the silica properties could be attributed to the presence of cobalt as covalently bound cobalt strongly interacting with the siloxane matrix forming Si–O–Co, as well as crystal of Co_3O_4 as confirmed by FTIR where tiny small bands at ~ 570 and 660 cm^{-1} were assigned to Co_3O_4. Furthermore, this enhanced thermal stability methylated microporous silica exhibited a trend towards micropores formation by possessing narrow pore size distribution. This was confirmed by solid-state ^{29}Si MAS NMR where the resonance Q^2 and Q^3 were observed. These two resonances correspond to silica matrix with smaller pore size.

It was reported that the non-doped hybrid materials showed pyrolysis, decomposition process of the organic templates due to heat treatment in oxidizing atmosphere, and hence formation of micropores network. Removal of these organic constituents is mainly depending on the temperature at which pyrolysis process occurs, i.e. between 400 °C and 500 °C. However, these materials showed virtually complete densification resulting from heat treatment around 550 °C. This had a significant effect on the membrane performance in separation of CO_2 from CH_4. Therefore, investigation of this behavior concerning the novel unsupported silica membrane was studied in the present thesis, especially at temperature below and above the pyrolysis of the organic templates. For that purpose, cobalt-doped organic templated silica xerogels, with different MTES amount and constant cobalt to be doped were prepared. Contrary cobalt-doped organic templated silica xerogels, with different cobalt to be doped and constant MTES amount were prepared. These materials showed high thermal stability regardless the MTES content and cobalt content as well. Higher template concentration and heat treatment (calcination process) induced the collapse of the xerogel matrix due to capillary stress promoting

dense xerogel as well as a broader pore size distribution. Whereas cobalt content (over 3 wt%) resulted in xerogels with approximately the same structure parameters even after heat treatment. This could be attributed to the fact that the dispersion of the cobalt particles was homogeneous. Therefore, this opposed the silica structure collapse. In any case, the heat treatment led to structural change of the silica xerogels such as a decreased micropore volume and surface area. However, despite of their structural change, these materials exhibited a trend towards micropores formation even after the removal of the organic templates, which occurred at temperature range higher than that of non-doped materials. Hence, a complete densification can occur at high temperature compared with the non-doped one.

On the other hand, this thesis also includes the preparation and performance of the novel supported membrane. Membranes were prepared by two different methodologies, preparation under normal conditions and under clean room conditions. The cobalt-doped hybrid membranes showed better results compared with the non-doped hybrid one. The doping process and dilution of the coating sol resulted in sol with low polydespersity as indicated by dynamic light scattering (DLS) measurements. The cobalt-doped hybrid membrane prepared under normal conditions showed selectivity over or on the boundary of Knudsen values, whereas the non-doped membrane do showed. For example, the selectivity of H_2/N_2 = 4.7, He/N_2 = 3.35 and H_2/He = 1.41 (Knudsen values are 3.74, 2.65 and 1.41, respectively). Therefore, in this case the support had a significant effect on the membrane performance in terms of transport mechanisms, and hence the gases transport was governed by the coexistence of more than one transport mechanism. The membrane prepared under clean room conditions exhibited an activated transport mechanism resulting from the formation of thin top selective silica layer. The novel membrane prepared with a sol of 20-fold dilution showed high selectivity, varying with temperature, compared with the other membranes prepared with a sol of 6-fold dilution. For example, the selectivity of H_2/N_2 = 14-40, H_2/CH_4 = 20-60 and CO_2/CH_4 = 5-24 (Knudsen values are 3.74, 2.83 and 1.66, respectively).

In general, the findings reported in this thesis concerning the hydrophobic and thermally enhanced methylated microporous silica material will open new frontiers in the field of microporous silica materials for molecular sieve applications. Moreover, this novel material can be considered as a promising membrane material for the particular application of gas separation.

Resum

En la present tesi, es proposa una nova metodologia per a la modificació de materials de membrana de sílice, per tal d'assolir i millorar aquests materials, per a la seva aplicació com a tamís molecular en la separació de gasos. La forma de fer-ho és mitjançant la combinació de dos enfocaments diferents que s'han utilitzat anteriorment per a la modificació de materials de membrana de sílice.

Les membranes microporoses de sílice són propicies a absorbir aigua a causa de la interacció entre les molècules d'aigua i dels grups silanol que es troben en la superfície d'aquestes membranes. Per tant, les membranes microporoses de sílice són aplicables només per a la separació de gasos secs. Això ha estimulat un augment de la investigació per al desenvolupament de nous sistemes de modificació i millora dels material de sílice. Una de les solucions investigada és la incorporació de material orgànics dins de la matriu de sílice per formar materials híbrids. El benefici d'aquest procés és la superfície i les propietats microestructurals finals que posseeixen aquests materials de sílice híbrids, com a precursors de materials de membrana, que seran modificades durant el procés de calcinació. Tractades sota atmosfera inerta les membranes de sílice híbrides es comporten com a matèria hidròfoba. D'altra banda, la piròlisi dels grups orgànics, que té lloc sota atmosfera oxidant, implica la formació de microporus. L'estabilitat tèrmica d'aquests constituents orgànics arriba als 400 °C i 500 °C en ambdós ambients. La segona solució estudiada consisteix en dopar el material de membrana amb un metall, fet que permet reduir la degradació de les membranes de sílice hidròfiles. S'han considerat diversos metalls i/o òxids metàl·lics i s'han utilitzat per a aplicacions de tamís molecular en la separació de gasos. Un exemple, és l'ús d'òxids metàl·lics com ara Co_3O_4, TiO_2 i NiO obtenint en la majoria dels casos membranes amb un rendiment millor. No obstant això, algunes membranes de sílice dopades amb metall encara mostren efectes hidròfils, poden adsorbir aigua, però sempre menys que les membranes convencionals de sílice.

En aquesta tesi doctoral, s'ha desenvolupat un nou material que és a la vegada de sílice híbrid i dopat amb cobalt. Aquest va ser preparat per hidròlisi mitjanant catàlisi àcida i seguidament per condensació amb ortosilicat de tetraetil (TEOS) i metiltrietoxisilà (MTES). La preparació va incloure també el dopatge de la matriu de sílice híbrida amb cobalt. Les propietats superficials dels materials obtinguts han estat analitzats mitjançant les tècniques següents: TGA, FTIR, Raigs X, ^{29}Si MAS NMR d'estat sòlid i adsorció de N_2. Els resultats inicials de la síntesi i de les propietats de la

superfície de la membrana de sílice no suportada van mostrar propietats millorades, mantenint al mateix temps les propietats ambdós tipus de materials combinats: sílice no modificada, sílice híbrida i sílice dopada amb metall. Així doncs, la calcinació de TEOS/sílice MTES sota atmosfera inert va donar lloc a un material hidròfob; la calcinació del material dopat sota atmosfera oxidant va resultar en una sílice hidròfoba; i el nou material va mostrar una alta estabilitat tèrmica en atmosfera inert i oxidant en comparació amb el material no dopat. Per tant; s'aconsegueix així una millora de l'estabilitat tèrmica de la membrana de sílice fins a valors de temperatura entre 500 °C i 600 °C en atmosfera oxidant. Aquesta millora de les propietats de sílice podria atribuir-se a la presència de cobalt fortament unit amb la matriu de siloxà Si-O-Co, així com a la presència de Co_3O_4 confirmat per FTIR (s'observen petites bandes a 570 i 660 ~ cm^{-1}). D'altra banda, aquesta elevada estabilitat tèrmica del metilat de sílice (sílice híbrida) va augmentar la tendència de formació de microporus amb una distribució de mida estreta. Això va ser confirmat per ^{29}Si MAS-RMN en estat sòlid on es van observar la ressonància Q^2 i Q^3. Aquestes dos ressonàncies corresponen a la matriu de sílice amb mida de porus més petit.

És conegut que els materials híbrids no dopats poden sotmetre's a processos de piròlisi donant lloc a la formació d'una xarxa de microporus. Aquest procés implica l'eliminació dels constituents orgànics que depèn principalment de la temperatura a la que es produeix el procés de piròlisi (entre 400 °C i 500 °C). No obstant això, aquests materials mostren una densificació pràcticament completa amb un tractament tèrmic al voltant de 550 °C. Aquest fet va implicar un efecte significatiu en el rendiment de la membrana per a la separació de CO_2 i CH_4. Per tant, es va aprofundir en l'estudi d'aquest comportament, a temperatures just per sota i per sobre de la temperatura de piròlisi. Per aquest propòsit, es van preparar varies mostres de sílice híbrides i dopades amb cobalt que contenien diferents quantitat de MTES i de cobalt Aquests materials van mostrar, tots ells, una alta estabilitat tèrmica, independentment del contingut MTES i del contingut de cobalt. Una major concentració de constituents orgànics van induir el col·lapse de la matriu de xerogel, durant el tractament tèrmic (procés de calcinació), degut a l'estrès per capil·laritat, així com una distribució de mida de porus més ampli. En canvi el contingut de cobalt (més de 3% en pes) va donar lloc a xerogeles amb aproximadament els mateixos paràmetres de l'estructura, fins i tot després del tractament tèrmic. Això podria atribuir-se al fet que la dispersió de les partícules de cobalt va ser homogènia. Per

tant, això s'oposa el col·lapse de l'estructura de sílice. Per tant, aquest fet s'oposa al col·lapse de l'estructura de sílice. En qualsevol cas, el tractament tèrmic ha aportat canvis estructurals dels xerogels de sílice com ara una disminució del volum de microporus i de l'àrea superficial. No obstant això, malgrat el canvi estructural, aquests materials exhibeixen una tendència cap a la formació de microporus fins i tot després de l'eliminació dels constituents orgànics, que es va produir en un rang de temperatura més alta que la dels materials no dopats. Per tant, una densificació completa pot produir-se a alta temperatura en comparació amb el material no dopat.

D'altra banda, aquesta tesi també inclou la preparació i l'estudi del rendiment d'una nova membrana suportada. Les membranes es van preparar per dos metodologies diferents, la preparació en condicions d'ambient normals i en sala blanca. Les membranes híbrides dopades amb cobalt van mostrar millors resultats en comparació amb les híbrides no dopades. El procés de dopatge i la dilució del revestiment de sol-gel va resultar en un sol-gel amb baixa polidispersitat de mida de partícules, com s'indica per la dispersió dels mesuraments de llum dinàmica (DLS). La membrana suportada dopada amb cobalt, preparada en condicions d'ambient normal, va mostrar selectivitat sobre o en el límit de Knudsen. Per exemple, la selectivitat de H_2/N_2 = 4,7, He/N_2 = 3,35 i H_2/He = 1,41(els valors Knudsen són 3,74, 2,65 y 1,41, respectivament). En aquest cas el suport va tenir un efecte significatiu en el comportament de la membrana en termes de mecanismes de transport, i per tant el transport dels gasos es regeix per la coexistència de més d'un mecanisme de transport. La membrana preparada sota condicions de sala blanca va exhibir un mecanisme de transport actiu resultant de la formació de la capa superior prima de sílice selectiva. La nova membrana preparada amb un sol-gel diluït 20 vegades va mostrar una alta selectivitat, variant amb la temperatura, en comparació amb les altres membranes preparades amb un sol-gel diluït tan sols 6 vegades. Per exemple, la selectivitat de H_2/N_2 = 14-40, H_2/CH_4 = 20-60 i CO_2/CH_4 = 5-24 (els valors Knudsen són 3,74, 2,83 i 1,66, respectivament).

En general, els resultats que es presenten en aquesta tesi relatius al comportament relativament hidròfob i a l'estabilitat tèrmica del material de sílice permetran obrir noves fronteres en el camp dels materials microporosos de sílice per a aplicacions de tamís molecular. D'altra banda, aquest nou material pot ser considerat com un material de membrana prometedor per a l'aplicació particular de la separació de gasos.

Resumen

En la presente tesis, se propone una nueva metodología para la modificación de materiales de membrana de sílice, con el fin de alcanzar y mejorar estos materiales, para su aplicación como tamiz molecular en la separación de gases. La forma de realizarlo es mediante la combinación de dos enfoques diferentes que han sido utilizados anteriormente.

Las membranas microporosas de sílice son propicias a absorber agua debido a la interacción entre las moléculaa de agua y los grupos silanol de la superficie de estas. Por lo tanto, las membranas microporosas de sílice aplicables solo a la separación de gases secos. Eso ha estimulado un aumento de la investigación para el desarrollo de nuevos sistemas para la modificación y mejora de estos materiales. Una de las soluciones investigada es la incorporación de constituyentes orgánicos dentro de la matriz de sílice para formar materiales híbridos. El beneficio de este proceso es la superficie y propiedades microestructurales finales de estos materiales de sílice híbridos, como precursores de material de membrana, que son modificados durante el proceso de calcinación. Tratados bajo atmósfera inerte las membranas de sílice híbridas se comportan de forma hidrófoba. Por otro lado, la pirólisis de los constituyentes orgánicos, que tiene lugar bajo atmósfera oxidante, da lugar a la formación de microporos. La estabilidad térmica de estos constituyentes orgánicos alcanza los 400 °C y 500 °C en ambos ambientes. La segunda solución consiste en dopar el material de membrana con un metal, consiguiendo así reducir la degradación de las membranas de sílice hidrófilas. Se han considerado varios metales y/o óxidos metalicos y se han utilizado para aplicaciones de tamiz molecular en la separación de gases. Un ejemplo, es el uso de óxidos metálicos tales como Co_3O_4, TiO_2 y NiO proporcionando en la mayoría de los casos un rendimiento mejor de la membrana. Sin embargo, las membranas de sílice dopadas todavía muestran efectos hidrófilos, pudiendo adsorber agua, aunque menos que las membranas convencionales de sílice.

En esta tesis, se ha desarrollado un nuevo material de sílice que es a la vez híbrido y dopado con cobalto. Dicho material fue preparado por hidrólisis mediante catalisis ácida y seguidamente por condensación de ortosilicato de tetraetilo (TEOS) y metiltrietoxisilano (MTES). La preparación involucró también el dopaje de la matriz de sílice híbrida con cobalto. Las propiedades superficiales de los materiales obtenidos han sido analizados mediantes las técnicas siguientes: TGA, FTIR, Rayos X,

^{29}Si MAS NMR de estado sólido y adsorción de N_2. Los resultados iniciales de la síntesis y de las propiedades de la superficie del nuevo material mostraron propiedades mejoradas, manteniendo al mismo tiemo las mismas propiedades de las membranas de sílice no modifcadas, sílice híbrida y sílice dopada con metal. Así pues, la calcinación de TEOS/ sílice MTES bajo atmósfera inerte dio lugar a un material hidrófobo; la calcinación de la membrana dopada bajo atmósfera oxidante resultó en membrana de sílice con comportamiento hidrófobo; y el nuevo material mostró una alta estabilidad térmica en atmósfera inerte y oxidante en comparación con el material no dopado. Por lo tanto, se consigue así una mejora de la estabilidad térmica de la membrana de sílice hasta valores de temperatura entre 500 °C y 600 °C en atmósfera oxidante. Tal mejora en las propiedades de sílice podría atribuirse a la presencia de cobalto fuertemente unido a la matriz de siloxano Si-O-Co, así como a la presencia de Co_3O_4 confirmado mediante FTIR (se observan pequeñas bandas a 570 y 660 ~ cm^{-1}). Por otra parte, la elevada estabilidad térmica del metilato de sílice incrementó la tendencia hacia de formación de microporos con una distribución estrecha de tamaño de poro. Eso fue confirmado por ^{29}Si MAS-RMN en estado sólido en donde se observaron las resonancias Q^2 y Q^3. Estas dos resonancias corresponden a la matriz de sílice con tamaño de poro más pequeño.

Es conocido que los materiales híbridos no dopados pueden someterse a processos de pirólisis dando lugar la formación de una red de microporos. Dicho proceso implica la eliminación de los constituyentes orgánicos que depende principalmente de la temperatura a la que se produce el proceso de pirólisis (entre 400 °C y 500 °C). Sin embargo, estos materiales muestran una densificación prácticamente completa con un tratamiento térmico en torno a 550 °C. Este fenómeno tuvo un efecto significativo en el rendimiento de la membrana para la separación de CO_2 de CH_4. Por lo tanto, se estudió en detalle este comportamiento a temperaturas justo por debajo y por encima de la temperatura de pirolisis. Con ese propósito, se prepararon varias muestras de de sílice hríbrida y dopada conteniendo diferentes cantidades de MTES y cobalto. Estos materiales mostraron, todos ellos, una notable estabilidad térmica, independientemente del contenido MTES y del contenido de cobalto. Una mayor concentración de constituyentes orgánicos indujo al colapso de la matriz de xerogel (por estrés de capilaridad) duranto el tratamiento térmico (proceso de calcinación), así como una distribución de tamaño de poro más amplio. El contenido de cobalto (más de 3% en peso) dio lugar a xerogeles con

aproximadamente los mismos parámetros de la estructura, incluso después del tratamiento térmico. Esto podría atribuirse al hecho de que la dispersión de las partículas de cobalto fue homogénea. Por lo tanto, esto se opuso el colapso de la estructura de sílice. Por lo tanto, este hecho se opuso al colapso de la estructura de sílice. En cualquier caso, el tratamiento térmico produjo cambios estructurales de los xerogeles de sílice tales como una disminución del volumen de microporos y del área superficial. Sin embargo, a pesar de los cambios estructural, estos materiales exhiben una tendencia hacia la formación de microporos incluso después de la eliminación de los constituyentes orgánicos, que se produjo en un rango de temperatura mayor que la de los materiales no dopados. Por lo tanto, una densificación completa puede producirse a alta temperatura en comparación con el material no dopado.

Por otro lado, esta tesis también incluye la preparación y el estudio del comportamiento de la nueva membrana soportada. Las membranas se prepararon mediante dos metodologías diferentes, la preparación en condiciones de ambiente normal y bajo condiciones de sala blanca. Las membranas híbridas dopadas con cobalto mostraron mejores resultados en comparación con las híbridas no dopadas. El proceso de dopaje y la dilución del revestimiento de sol-gel resultaron en una solución con baja polidispersidad de tamanyo de partícula como indica la dispersión de las mediciones de luz dinámica (DLS). La membrana preparada bajo condiciones de ambiente normal mostró selectividad sobre o en el límite de Knudsen, mientras que la membrana no dopada no. Por ejemplo, la selectividad de H_2/N_2 = 4.7, He/N_2 = 3.35 y H_2/He = 1.41 (los valores Knudsen son 3,74, 2,65 y 1,41, respectivamente). En este caso el soporte tuvo un efecto significativo en el comportamiento de la membrana en términos de mecanismos de transporte, y por lo tanto el transporte de los gases se rigió por la coexistencia de más de un mecanismo de transporte. La membrana preparada bajo condiciones de sala blanca exhibió un mecanismo de transporte activo resultante de la formación de la capa superior delgada de sílice selectiva. La membrana sintetizada mediante un sol-gel diluido 20 veces mostró una alta selectividad, variando con la temperatura, en comparación con las otras membranas preparadas con un diluido únicamente 6 veces. Por ejemplo, la selectividad de H_2/N_2 = 14-40, H_2/CH_4 = 20-60 y CO_2/CH_4 = 5-24 (los valores Knudsen son 3,74, 2,83 y 1,66, respectivamente)

En general, los resultados que se presentan en esta tesis que conciernen el comportamiento relativamente hidrófobo y la estabilidad térmica del material de

sílice van a permitir abrirán nuevas fronteras en el campo de los materiales microporosos de sílice para aplicaciones de tamiz molecular. Por otra parte, este nuevo material puede ser considerado como un material de membrana prometedor para la aplicación particular de la separación de gases.

List of abbreviations

VOC	Volatile organic compounds
IUPAC	International Union of Pure and Applied Chemisrty
CVD	Chemical Vapor Deposition
K_n	Knudsen number
λ	Average free path length of the gas molecule
d_p	Characteristic pore diameter
J	Membrane flux
Q	Total amount of gas permeated through the membrane
A	Membrane area (m^2)
F	Membrane permeance ($mol.m^{-2}.s^{-1}.Pa^{-1}$)
ε	Porosity
μ_p	A shape factor
τ	Tortuosity
$\bar{r}$	Modal pore radius (m)
P_m	Mean pressure (Pa)
R	Gas constant ($J.mol^{-1}.K^{-1}$)
T	Temperature (K)
η	Gas viscosity ($N.s.m^{-2}$)
L	Membrane thickness (m)
M	Molecular mass ($g.mol^{-1}$)
D	Diffusion coefficient
dC/dz	Concentration gradient
E_a	Apparent activation energy of permeance ($kJ.mol^{-1}$)
E_m	Mobility energy of the permeant ($kJ.mol^{-1}$)
Q_{st}	Isosteric heat of adsorption ($kJ.mol^{-1}$)
K_0 and D_0	Temperature independent proportionality constants
$S_{i/j}$	Membrane selectivity of component *i* over component *j* in a mixture
$S°_{i/j}$	Permselectivity of gas *i* over gas *j*
α_i	The separation factor of component *i* from a multicomponent mixture
WGS	Water gas shift reaction
MSS	Molecular sieve silica
TEOS	Tetraethylorthosilicate
MTES	Methyltriethoxysilane

MPTMA	3-(Trimethoxysilyl)propyl methacrylate
TFPTES	(trifluoropropyl)triethoxysilane
SN	Nucleophilic substitution reaction
SN^2	Bimolecular nucleophilic substitution
P_C	Capillary stress
V_m	Molar volume of the pore liquid
K_0	Initial network bulk modulus at the gel point
h_0	Film thickness at the gel point
h	Final film thickness.
θ	Contact angle
HI	Hydrophobic index
TGA	Thermogravimetric Analysis
FTIR-ATR	Fourier transform infrared-Attenuated total reflectance spectroscopy
XRD	X-ray diffraction
^{29}Si NMR	Solid-state silicon-29 nuclear magnetic resonance spectroscopy
B-Si	Blank silica membrane material
Hyd-Si	Hydrophobic silica membrane material
Co-Si	Cobalt-doped silica membrane material
Hyd-Co-Si	Hydrophobic cobalt-doped silica membrane material
PSD	Pore size distribution
NLDFT	Non Localized Density Functional Theory
Q^n	Distribution describe silicon center in the silica matrix
T^n	Distribution describe silicon center in the silica matrix (organosiloxane matrix)
P/P_0	Relative pressure
V	Volume adsorbed at a given P/P_0
V_0, V_{micro}	Micropore volume
E	Energy of adsorption
β	Affinity coefficient of the adsorbate
V_T	Total pore volume
V_{meso}	Mesopore volume
BET	Brunauer, Emmett and Teller
V_n	Narrow micropore volume
S_{BET}	Surface area
DTA	Differential thermal analysis
3x	3- fold dilution

6x	6- fold dilution
20x	20- fold dilution
PVA	Polyvinylalcohol
DLS	Dynamic light scattering
R_H	Hydrodynamic radius (nm)
SEM	Scanning electron microscopy
PC	Pressure controller
PI	Differential pressure indicator
TC	Temperature controller
FI	Flow indicator
R_H	Hydrodymanic radius
d_k	Kinetic diameter

List of Figures

Figure I. The membrane demand by market 4

Figure II. The membrane preparation set-up employed in METEOR research group, URV, Tarragona, Spain 6

Figure III. Set-up for testing the membrane permeance employed in METEOR research group, URV, Tarragona, Spain 7

Figure V. Dip-coating machine for membrane preparation in clean room employed in IM group, University of Twente, Holland 7

Figure IV. Set-up for testing the membrane permeance employed in IM group, University of Twente, Holland 8

Figure 1.1. An overview of membrane systems used in different energy processes 15

Figure 1.2. Classification of inorganic membranes 15

Figure 1.3. comparative searches for different membrane materials used in gas separation 16

Figure 1.4. Depiction showing the kinetic diameter of different gases 19

Figure 1.5. Depiction showing the structure of an inorganic membrane 19

Figure 1.6. Picture and SEM magnification of a ceramic microporous gas-sieving disk presented in the thesis 20

Figure 1.7. Commercial inorganic membranes (a) Tubular and (b) Disk-shaped (flat) membranes 20

Figure 1.8. Gas transport mechanisms in porous membranes 30

Figure 1.9. Schematic representation of two reactions (steam-reforming + WGS) in a membrane reactor with catalyst 32

Figure 2.1. Formation of sols and gels 42

Figure 2.2. Contracting surface forces in pores of different size during drying 43

Figure 2.3. Applications of sol-gel technique 43

Figure 2.4. Formation of gel via condensation reactions of silanols 46

Figure 2.5. Possible intermediates generated during sol-gel process of $Si(OR)_4$ via hydrolysis and condensation reactions. Each intermediate can, in principle, undergo either hydrolysis or condensation reactions 47

Figure 2.6. Acid-catalyzed reactions where the oxygen atom in Si-OH or Si-OR is protonated and H-OH or H-OR are leaving groups. The electron density are shifted from the Si atom, making it more accessible for reaction with water (hydrolysis) or silanol (condensation) 47

Figure 2.7. Base-catalyzed reactions where nucleophilic attack by OH- 48

or Si-O- on the central Si atom. These species are formed by dissociation of water or Si-OH. The reactions are of SN^2 type where OH- replaces OR- (hydrolysis) or silanolate replaces OH- or OR- (condensation)

Figure 2.8. Inductive and steric effects on hydrolysis rate 49

Figure 2.9. Schematic process of sol–gel method for preparing MSS membranes 51

Figure 2.10. Selected interactions typically applied in hybrid materials and their relative strength 56

Figure 2.11. Condensation of a hydrolyzed trialkoxysilane to the silica surface 57

Figure 2.12. Water drop behavior and contact angle values at solid of different hydrophobicity 62

Figure 2.13. Types of physisorption isotherms (left) and types of hysteresis loops (right) 68

Figure 4.1. Contact angles of silica membrane materials surface 93

Figure 4.2. FTIR spectra of a) dried and b) calcined silica membrane materials 94

Figure 4.3. XRD diffractogramms of Hyd-Co-Si, (a) 3 wt% Co, (b) 10 wt% Co calcined at 400 °C, (c) 10 wt% Co calcined at 500 °C and (d) mixture of SiO_2 and Co_3O_4. Solid circles represent Co_3O_4 reference pattern 94

Figure 4.4. Solid-state ^{29}Si MAS NMR spectra of the silica membrane materials 96

Figure 4.5. TGA curve, relative weight loss vs. temperature for silica/modified silica membrane materials 98

Figure 4.6. a) N_2 at -196 °C and b) CO_2 at 0 °C adsorption isotherms for the silica /modified membrane materials 100

Figure 4.7. Pore size distributions of the silica membrane materials, calculated according to NLDFT model (cylindrical pore-equilibrium model), from N_2 adsorption data at -196 °C 103

Figure 5.1. TGA (solid lines) and DTA (dashed lines) of 50% MTES (top left) and Co-X% MTES 119

Figure 5.2. FTIR spectrum of sample Co-50% MTES. Inset shows the FTIR spectra of samples Co-60% and Co-80% MTES calcined at 600 °C 120

Figure 5.3. Deconvoluted solid-state ^{29}Si NMR spectrum of sample Co-20% MTES at a) 400 °C and b) 600 °C 123

Figure 5.4. N_2 adsorption isotherms of Co-X% MTES calcined at a) 400 °C and b) 600 °C 127

Figure 5.5. PSD of Co-X% MTES calcined at a) 400 °C and b) 600 °C 128

Figure 6.1. TGA (a) and DTA (b) of different cobalt content organic templated silica xerogels 147

Figure 6.2. FTIR spectrum of 10%-Co 147

Figure 6.3. XRD diffractogramms of X%-Co calcined at 400 °C (a) 3%-Co, (b) 5%-Co, (d) 8%-Co and (f) 10%-Co. Samples calcined at 600 °C (c) 5%-Co, (e) 8%-Co and (g) 10%-Co. (i) SiO_2+Co_3O_4 mixture and solid circles represent Co_3O_4 reference pattern 149

Figure 6.4. N_2 adsorption isotherms of X%-Co calcined at a) 400 °C and b) 600 °C 151

Figure 6.5. PSD of X%-Co calcined at a) 400 °C and b) 600 °C 152

Figure 6.6. Structural changes in surface and micropore surface area 155

Figure 7.1. Experimental set-up for tubular hydrophobic membranes 174

Figure 7.2. Experimental set-up for disk-shaped hydrophobic membranes 174

Figure 7.3. Contact angles of the support and hydrophobic silica membranes 176

Figure 7.4. Drop of water on Hyd-Co-Si membrane (M6) 176

Figure 7.5. Particle size distribution of the non-diluted and diluted sols. Intenisty (left), volume (middle) and number (right) distribution curves 178

Figure 7.6. Weight losses vs. temperature (a) and differential weight loss curves (b) in inert atmosphere 179

Figure 7.7. Weight losses vs. temperature (a) and differential weight loss curves (b) in oxidizing atmosphere 180

Figure 7.8. N_2 adsorption isotherms of the unsupported hydrophobic membranes 182

Figure 7.9. PSD of the unsupported hydrophobic membranes 183

Figure 7.10. Gas permeance vs. pressure difference for M1 where a) at 25 °C, b) at 50 °C, c) at 100 °C and d) at 150 °C 185

Figure 7.11. Gas permeance vs. pressure difference for M2 where a) at 25 °C, b) at 50 °C, c) at 100 °C and d) at 150 °C 186

Figure 7.12. Gas permence vs. kinetic diameter for M1 and M2 at (Δ P = 2 bar) and 150 °C 187

Figure 7.13. Gas permence vs. temperature for a) M1 and b) M2 187

Figure 7.14. Selectivity of M1 (hollow symbols) and M2 (solid symbols). Dashed lines represent Knudsen selectivity (Δ P = 2 bar) 188

Figure 7.15. Gas permeance vs. molecular weight $^{-1/2}$ for different gases a) M1 and b) M2 (Δ P = 2 bar) 190

Figure 7.16. Temperature dependency for several gases a) M1 and b) M2 (Δ P = 2 bar) 191

Figure 7.17. SEM images of cross-sections of the membranes prepared in clean room 192

Figure 7.18. Gas permence vs. kinetic diameter for M3 to M6 194

Figure 7.19. Gas permence vs. temperature for a) M3, b) M4, c) M5 and d) M6 (Δ P = 2 bar) 196

Figure 7.20. Temperature dependency for several gases for a) M3, b) M4, c) M5 and d) M6 (Δ P = 2 bar) 197

List of Tables

Table 1.1. Different applications performed by membranes gas separation 16

Table 2.1. Characteristic bands (cm^{-1}) in FTIR spectra of silica/modified silica membrane materials 65

Table 4.1. Molar compositions of the used sols 88

Table 4.2. Solid-state ^{29}Si MAS NMR of silica membrane materials 97

Table 4.3. Compilation of structural parameters deduced from N_2 adsorption data at -196 °C and CO_2 adsorption data at 0 °C 101

Table 5.1. Weight losses between 500-800 °C of different Co-X% MTES 118

Table 5.2. Solid-state ^{29}Si MAS NMR of Co-X% MTES. 124

Table 5.3. Compilation of structural parameters deduced from N_2 adsorption data at -196 °C for Co-X% MTES calcined at 400 °C 130

Table 5.4. Compilation of structural parameters deduced from N_2 adsorption data at -196 °C for Co-X% MTES calcined at 600 °C 130

Table 6.1. Compilation of structural parameters deduced from N_2 adsorption data at -196 °C for X%-Co calcined samples at 400 °C 153

Table 6.2. Compilation of structural parameters deduced from N_2 adsorption data at -196 °C for X%-Co calcined at 600 °C 153

Table 7.1. Molar compositions of the used sols for hydrophobic silica membranes preparation 171

Table 7.2. Membranes notations in the present study 172

Table 7.3. Characteristics of the sols used for the preparation of hydrophobic membranes 179

Table 7.4. Compilation of structural parameters deduced from N_2 adsorption data at -196 °C for the unsupported hydrophobic membranes 183

Table 7.5. M1 and M2 permeance depending on the d_k of the probe molecule at (Δ P = 2 bar) and 150 °C 186

Table 7.6. Apparent activation energies for M1 and M2 at (ΔP= 2 bar) 191

Table 7.7. M3 to M6 permeance depending on the d_k of the probe molecule at (Δ P = 2 bar) and 200 °C 194

Table 7.8. Apparent activation energies for M3 to M6 at (ΔP= 2 bar) together with reported data in the literature 198

Table 7.9. Permselectivity of M3 to M6 membrane at (ΔP= 2 bar) 199

Scope of the Thesis

I. An Overview

The beginning of research work on Nanotechnology and Nanoscience can be traced back over 40 years, first described in a lecture entitled, ´´There's Plenty of Room at the Bottom´´ in 1959 by *Richard P. Feynman*. Over the last decade, Nanotechnology went through a variety of fields from materials science to electrical engineering and from chemistry to biology. Nowadays, scientists are creating the tools and developing the know-how to bring Nanotechnology out of the research labs and into the market place. Nanotechnology can be defined as the design and synthesis of functional materials within nanometer scale in at least one dimension (up to 100 nm) and control and exploitation of novel properties and phenomena in different fields such as physics, chemistry and biology depending on this length scale.

The need for new energy sources has attracted renewed and ever-increasing attention around the world in recent years. Hydrogen as a high-quality and clean energy carrier has attracted researchers' attention around the world in the last years, mainly due to developments in fuel cells and environmental pressures including climate change issues. Hydrogen is one of the most promising energy carriers for the future. It is a high efficiency, low polluting fuel that can be used for transportation, heating, and power generation in places where it is difficult to use electricity. Hydrogen as a gas (H_2), however, does not exist naturally on Earth it is found only in compound form. Combined with oxygen, forming (H_2O) and combined with carbon; it forms organic compounds such as methane (CH_4), coal, and petroleum. Today, hydrogen is mostly produced using steam reforming technology of fossil fuels such as methane; this technology is mature and well established in industrial field. About 80% of the energy used world-wide comes from fossil fuels, and this share is expected to increase until at least year 2020. To develop the way of hydrogen production and purification, the economic impact cost should be taken into account.

Facile, cheap and effective ways for synthesis of nanoporous materials thanks to Nanotechnology that can be exploited for that purpose. In recent years, membrane reactor technology has become an important way for hydrogen production and purification. Moreover, development of membrane materials for that purpose is increasingly gaining importance. In the last years, membrane processes for gas separation are gaining a larger acceptance in industry and in the market, and are competing with consolidated operations such as pressure swing absorption and cryogenic distillation. Figure I show the membrane demand by market. Membranes

have been long utilized in industry for separation of gas mixtures. Thanks to their chemical, physical, and thermodynamic stability, as well as for their high durability at elevated temperatures and high permeation flux, ceramic membranes have become especially popular in the field. Today, the volume of research and development on inorganic membranes has grown considerably and a large diversity of potential applications and development directions has emerged.

Sol-gel technique is the most common method in Nanotechnology that has been used to produce high quality microporous materials (pore diameter less than 2 nm). Hence, this technology has attracted researchers' attention to produce thin selective separation membrane layer. Moreover, it is possible to use sol-gel technique to modify the microporous membrane materials to achieve new materials with enhanced chemical and physical properties. Microporous silica materials can be easily synthesized by sol-gel technique; therefore they are the most common materials that are using to prepare thin selective separation membrane layer. The most common precursor to prepare microporous silica materials by sol-gel technique is tetraethylorthosilicate (TEOS). As these materials showed hydrophilicity behavior and could not work in presence of steam. This has encouraged an increasing research to overcome these limitations and to enable these materials to be used in large-scale industrial applications.

One strategy that was used for that purpose is template-based approach which depends on the preparation of new hybrid organic-inorganic silica-based microporous materials. The most common organic template that is using for that approach is methyltriethoxysilane (MTES). By doing so, the incorporation of organic groups in the silica network enhances the silica surface and their molecular sieving properties. Another strategy for modification of microporous silica materials is metal-doped approach. This approach was designed to reduce the degradation of the hydrophilic silica membranes. Several metal and/or metal oxides-doped silica membranes were prepared and used for molecular sieve applications such as gas separation. However, metal-doped silica membranes still showed the hydrophilic effect, as they can adsorb water, but less than the conventional silica membranes.

In the present thesis these two approaches are combined to develop and achieve novel silica material that can be used as silica membrane precursor for molecular sieve silica applications such as gas separation.

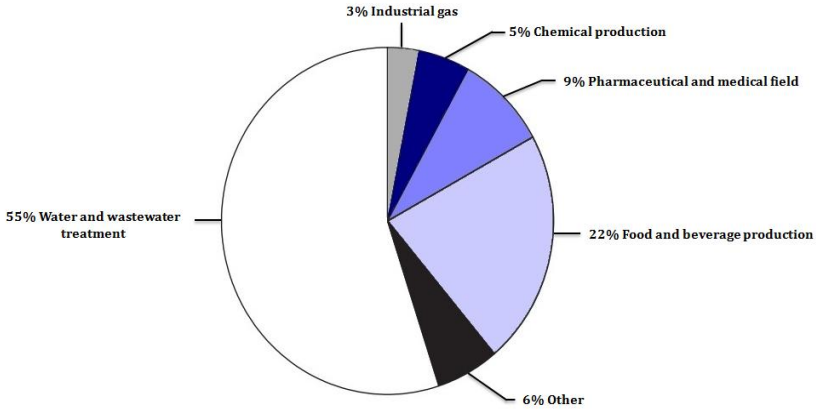

Figure I. The membrane demand by market.

The thesis thus consists of the following parts:

Part I. *Preparation and characterization of unsupported silica membranes*

This is the major work that was done and reported in the present thesis. This was done at METEOR research group, Universitat Rovira i Virgili (URV), Tarragona, Spain. In this part the initial synthesis of the novel material and comparison with other silica and modified silica materials was reported. Besides, investigation of the heat treatment (calcination process) with different contents of organic template as well as different cobalt content was performed especially under oxidizing atmosphere. Material characterization was carried out by fourier transform infrared (FTIR), solid-state ^{29}Si nuclear magnetic resonance (NMR), Thermogravimetric analysis (TGA) and N_2 adsorption measurements, in order to study the effect of the preparation parameters or conditions on the material final properties. The idea of focus on studies the effect of these aspects (MTES and cobalt contents) on the microporosity of silica materials, because it is the key factor for molecular sieve applications.

Part II. *Preparation and characterization of supported silica membranes*

It impels the first trial to prepare the novel silica membrane by simple way and out of clean room, i.e. preparation under normal conditions. This was done at METEOR research group, URV, Tarragona, Spain. Later the novel silica membrane was prepared under clean room conditions at the Inorganic Membrane (IM) group,

University of Twente, Holland. In both cases the novel membrane (cobalt-doped hybrid silica membrane) was compared with the non-doped one. Figure II and III shows the experimental set-up that was used to prepare, under normal conditions, and test the membranes performance, respectively. On the other hand, Figure IV and V shows dip-coating machine that was used to prepare the membrane under clean room condition and the experimental set-up for testing the membranes performance.

II. Structure of the thesis

Outline the thesis scope

Chapter 1: General introduction

In this chapter a brief description concerning the membrane technology and state-of-the-art is presented. Besides, Classification of membranes for gas separation and especially porous inorganic membranes and their architecture is briefly mentioned. The common mechanisms for gas transport and separation mechanisms in porous inorganic membranes are discussed as well.

Chapter 2: Sol-gel technique

This chapter is general overview on the sol-gel technique to produce high quality microporous silica membrane materials, and the most characterization techniques that are used for these materials.

Chapter 3: General objectives of the thesis

Chapter 4: Novel silica membrane material for molecular sieve applications

This is the first work on the synthesis of the novel silica membrane material. This chapter describes the initial results on the synthesis and surface properties of the novel silica membrane material together with a comparison of these aspects with blank and modified silica membrane materials.

Chapter 5: Characterization of metal-doped methylated microporous silica for molecular separations

This chapter describes the effect of different MTES content with constant cobalt content to be doped. The effect of heat treatment (calcination process) was studied under oxidizing atmosphere.

Chapter 6: Thermally enhanced methylated microporous silica for molecular sieve applications

This chapter describes the effect of different cobalt content to be doped within the silica matrix with constant MTES content. The effect of heat treatment (calcination process) was studied under oxidizing atmosphere.

Chapter 7: Novel hydrophobic silica membrane for gas separation

This chapter is related to the novel silica membrane (supported material). Membrane preparation under normal conditions as well as under clean room conditions is discussed. Gas permeance for the novel silica membrane and the governed mechanism for the membrane performance are reported as well. Besides, it discusses the characterization of the novel silica membrane material after dilution process. The novel doped-metal hybrid membrane is compared with the non-doped one.

Chapter 8: Overall conclusions and prospects for the future

Figure II. The membrane preparation set-up employed in METEOR research group, URV, Tarragona, Spain.

Figure III. Set-up for testing the membrane permeance employed in METEOR research group, URV, Tarragona, Spain.

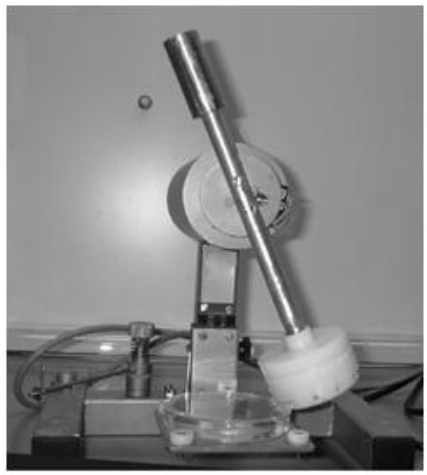

Figure IV. Dip-coating machine for membrane preparation in clean room employed in IM group, University of Twente, Holland.

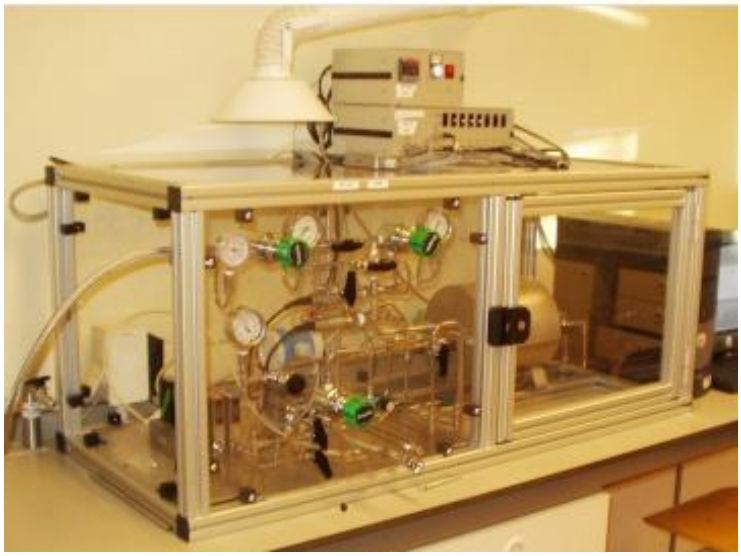

Figure V. Set-up for testing the membrane permeance employed in IM group, University of Twente, Holland.

Chapter 1

General Introduction

This chapter describes a brief introduction concerning the state of the art of membrane technology and its importance in molecular sieve applications such as gas separation. In recent years, because of the important characteristics and applications of membrane separation processes, therefore this technology was implemented and stand out as alternatives to conventional processes for the chemical, biochemical or pharmaceutical, biotechnological and food industries. The main attractions of these processes are the low energy consumption, reduction in number of processing steps, greater separation efficiency and improved final product quality. A great deal of researches have been investigating to improve the membrane materials for gas separation as well as to study the separation and transport of gases by membranes. Silica-based membranes have attracted the researchers' attention thanks to their facile synthesis via sol-gel technique, and their molecular sieving properties which is very useful in the gas separation field.

1.1. Membrane technology: State-of-the-art

Membrane technology is recognized today as powerful separation technique as it is becoming a competitive technology compared to the conventional separation unit technology in the last decades. They offer several advantages over conventional separation methods, e.g., cryogenic distillation, chemical and physical absorption. The advantages of membrane separation technology are: in some cases minimum space requirement for plant operation, lower time consumption, improve final product quality, energy efficient, they offer a relative cheap technology, more effective in processing dilute solutions, membrane process is gentle and mild, hence retaining chemical identity of the feed component and they are environmentally respectful [1, 2]. Membrane separation technology for gas separation is considered as a more energy efficient way to perform a pressure-driven separation processes [3, 4]. Using membranes can reduce the energy consumption by a factor of 6 to 10 as compared to thermally driven processes, such as raw material refining within the industrial sector of some processes, which intrinsically require high-temperatures to occur economically [3]. Therefore, the field of membrane technology is a growing market in the petro-chemical industry; waste water treatment and food and beverage industry being the largest markets [5].

The development and enhancement of microporous materials towards molecular sieve applications is an ever-growing area of research. Gas separation processes, as one of molecular sieve applications, is an example of a field in which membrane technology is increasingly gaining importance. Gas separation membranes are an example of those materials that emerged from laboratory to adapt rapidly on industrial applications, being an attractive alternative to conventional, expensive and contaminant methods for gas separation. Baker in 2002 estimated the market scale of membrane gas separation technology in year 2020 to be five times that of year 2000 [6]. As the need for reducing the environmental impact and costs of industrial processes are taking into account, it is expected that membrane gas separation will play an increasingly important role and can potentially compete with some traditional separation methods in terms of energy requirements and economic costs [1, 4]. During the last two decades, membrane gas separation has played an important role in various environmental and energy processes, such as natural gas sweetening [7, 8], CO_2 capture [9, 10], volatile organic compounds (VOC) recovery

[11] and hydrogen production [12, 13]. Figure 1.1 shows an overview of membrane systems for environmentally friendly energy processes from materials to applications.

1.2. An introduction to gas separation using membranes

The first experiment on gas permeation through polymer was done by Thomas Graham in 1829 [14]. A membrane is defined by International Union of Pure and Applied Chemistry (IUPAC) as a structure, having lateral dimension much greater than its thickness, through which mass transfer occurs under a variety of driving forces. This is the most general definition about membranes. However this description or definition does not include the main function of a membrane. Membranes are mainly prepared for separating things. The most characteristic feature of a membrane processes is that the feed flow is divided in two streams called the retentate and the permeate. The retentate is the stream that has been separated from the permeant by the membrane. The permeant is what passes through the membrane; the streams containing the permeant that leaves a membrane module is called permeate [15].

Membranes can be classified into organic, inorganic and hybrids of organic/inorganic systems. Organic membranes can be further divided into polymeric and biological constituents [16, 17]. Whereas inorganic ones were divided by Hsieh [18] into two major categories based on its structure: porous inorganic membranes and dense (non-porous) inorganic membranes as shown in Figure 1.2. Besides that, porous inorganic membranes have two different structures: asymmetric and symmetric. An authoritative summary of basic concepts and definitions for membranes is available in an IUPAC report [15]. Commercialized membrane applications have been strongly or exclusively dominated by polymer membranes. Although inorganic membranes are more expensive than organic polymeric membranes, the share of inorganic membranes is currently estimated to be about 12% [18]. However, inorganic membranes will have their share of the future growth of membrane technology, if their strong characteristic features, being advantages over the polymeric membranes, can be used. These characteristic features are [19]:

- Their relatively high chemical stability and good corrosion resistance, compatible with highly aggressive media, allowing filtration in, for example,

strong solvents such as aprotic solvents that dissolve all currently existing polymeric membranes; in addition, allowing very aggressive cleaning, opening even economical implementation of ceramic membranes in drinking water production from difficult surface waters.

- Their biocompatibility facilitating their use in highly certified industries such as the pharmaceutical and food industry.
- Their noncompactability under high pressure, allowing application at more moderate pressures and without lengthy pretreatments.
- Their relatively high thermal stability, compatibility with high-temperature operations, and suitable for real reaction–filtration integration, allowing therefore, for example, a shift of the reaction equilibrium as in membrane reactors.
- Their mechanical strength.
- Their long lifetime.
- The possibility of surface modification to improve hydrothermal stability.

These advantageous characteristics encouraged many researchers in the early 1980s, when the first membrane for hydrogen recovering was patented, to investigate the gas separation properties of these membranes, especially porous inorganic membranes. Besides, hydrogen separation and purification by membrane technology are in constant development [20, 21]. Depending on the application both dense and porous membranes include a large variety of materials where polymers are the most widely reported. Figure 1.3 shows a comparative view of different materials used on for gas separation [22]. As it can be observed, over the last two decades different membrane materials have encountered many applications in the field of gas separation and the using of membrane technology was gaining a considerable attraction. On the other hand the processes of applications of the membrane technology are usually denominated from the target they can achieve, such as separation, recovery, enrichment, removal of undesired components, desiccation, purification, recycling and reuse of specific substances. Most of the applications where membranes are employed to separate gases are listed in Table 1.1.

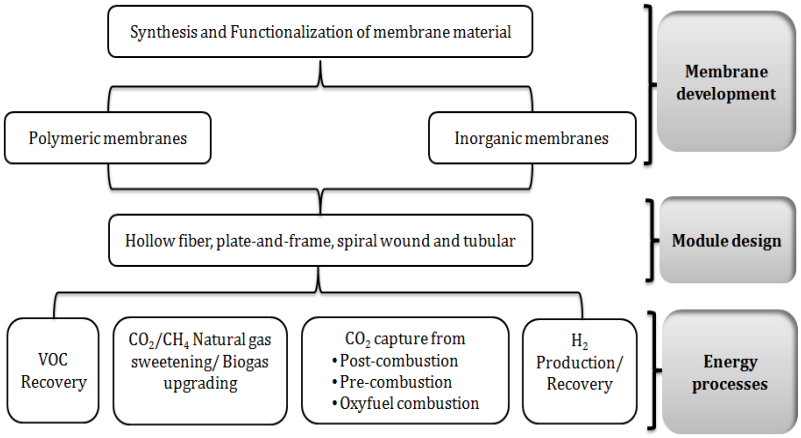

Figure 1.1. An overview of membrane systems used in different energy processes.[1]

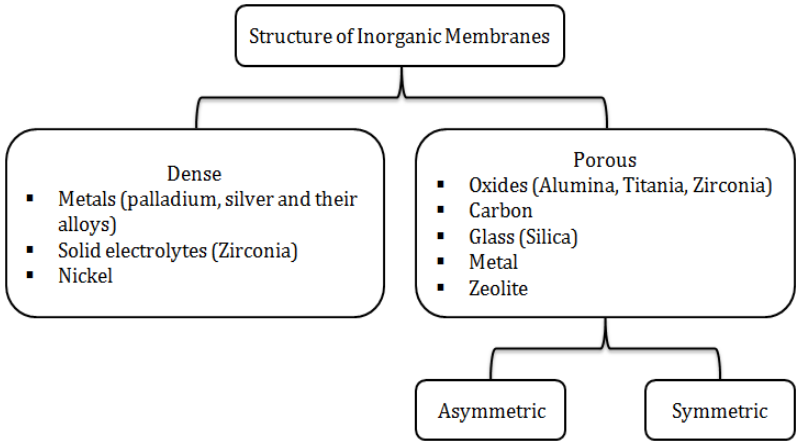

Figure 1.2. Classification of inorganic membranes.[18, 20]

Table 1.1. Different applications performed by membranes gas separation.

Process	Target	Source	Ref.
Separation	H_2	H_2/N_2	[23]
Separation	CO_2	Landfill gas (CH_4 50% and CO_2 40%)	[21]
Recovery	He	Natural gas	[24]
Removal	H_2S	Natural gas	[7, 25]
Removal	Water vapour	Natural gas	[7, 25, 26]
Enrichment	O_2	Air for metallurgical purposes	[27]

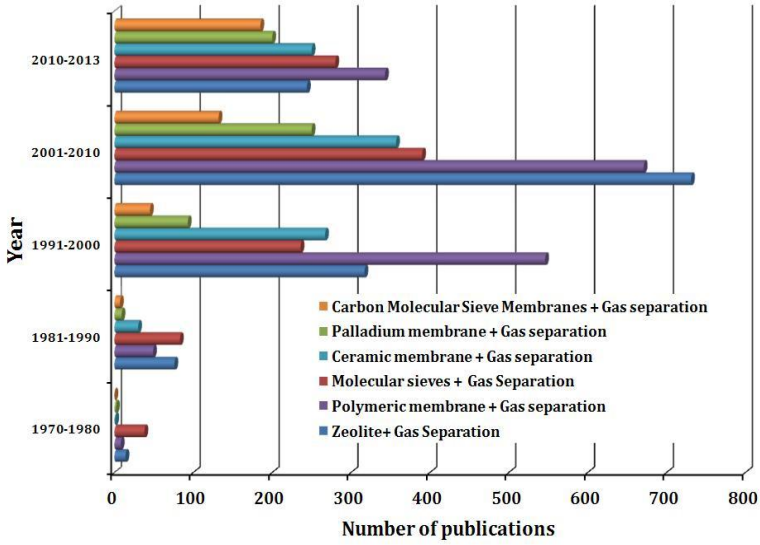

Figure 1.3. Comparative searches for different membrane materials used in gas separation.[22]

1.3. Inorganic Membranes for gas separation

Over the last decades, inorganic membranes have became an important area of increasing research interest in the field of membrane science and technology which, until recently, was dominated by the earlier developed polymer membranes. This is because of their characteristic features, as mentioned earlier in the previous section. As is common for recent developments, the field of inorganic membranes is still undergoing rapid change and innovation. Inorganic membranes are a relatively new product. However, in fact, their development started in the 1940s. Today, a wide variety of inorganic membranes exist in the market, covering not only the whole range of liquid filtrations, including pervaporation, but also a whole range of materials from different ceramics, over glass to metals [19]. Gas separation using inorganic membrane is a challenge for researchers; this is because of the smaller kinetic diameter of gases as shown in Figure 1.4. The architecture of an inorganic membrane for gas separation is consisting of mainly three layers:

- Porous support or substrate, which provides the necessary mechanical suitability for real applications.
- Primary layer or an intermediate layer, one or more intermediate layers between support and top layer take into account a gradual decrease of the pore size in the multilayer composition.
- Top separation layer(s), porous or dense layer.

This structure is represented by Figure 1.5 and an example the architecture of an inorganic ceramic membrane, one of membranes that are presented in the present thesis as will be mentioned in chapter 7, is presented in Figure 1.6. The main challenge for high quality top layers is to avoid defects in the layer. Indeed, these defects will decrease the final selectivity. It is obvious that this requirement is more stringent for microporous and dense membranes, than for more open-porous membranes. Hence, as the top separation layer consists of very narrow pores, especially in few nanometres or angstrom rang; this will enhance the inorganic membrane for gas separation. This multilayer composition provides a convenient way to combine a high flux and high selectivity in the final membrane. According to IUPAC classification for porous materials, pores with diameters exceeding 50 nm are called macropores; mesopores have diameters between 50 nm and 2 nm and, if a pore has a diameter less than 2 nm, it is called a micropore [28].

Despite the wide pore-size range of all existing inorganic membranes, their syntheses show some common aspects. All synthesis begins from an appropriate powder preparation from precursor or material. Subsequently, these powder particles are packed with a certain shape (flat or tubular). This can be done by wet or dry shaping techniques, facilitated by using one or more organic additives (in the role of binders, dispersants, and plasticizers). The pore size that can be obtained in this processing depends on the particle size of the starting powders [19]. Some commercial inorganic membranes, as the tubular one and disk-shaped (flat) one that were used in the present thesis, in use today, are shown in Figure 1.7. The intermediate layers and the fine porous or dense top layers coated on the porous supports are produced using other specific techniques such as sol–gel techniques or chemical vapor deposition (CVD). The dense or fine-porous membrane layers also require a temperature treatment similar to that of the porous supports, to consolidate their microstructure.

The most common inorganic membrane materials for membrane preparation are silica, alumina, ceramic, zeolites, Vycor glass and carbon-silica [29-35]. Important considerations should be taken into account during preparation of gas separation membranes, especially for small molecular kinetic diameter as Hydrogen:

- The porosity modification of the mesoporous support or substrate.
- The final membrane must be defect-free membrane.
- The thickness of the membrane itself, since the permeation rate is maximised when the thickness is minimised. Additionally, during its performance the membrane must withstand the pressure drop in combination with aggressive reagents and/or high temperatures.

It is well documented in the literature that, for example, the support modification can be performed by using any commercial material such as Locron alumina sols or Boehmite (γ-A1OOH) sols [36-39]. Other methods for support modification have been reported, such as intermediate layers of silica-zirconia composites, with smaller pores sizes are typically employed [40, 41]. For preparation a defect-free membrane, membrane is prepared under clean room conditions [42, 43]. However, in the present thesis we demonstrate the possibility of membrane preparation under normal conditions and the preparation under clean room conditions. In the latter case, the support modification was performed using a

boehmite colloidal suspension sol. For high-temperature gas separation applications, the two types of inorganic membranes (dense and porous) are suitable for that purpose. Therefore, a brief description will be mentioned related to these two types of inorganic membranes. On the other hand, concerning the membrane support there is a trend towards using other membrane support as porous stainless steel in order to prepare inorganic membrane such as supported silica membrane [44, 45].

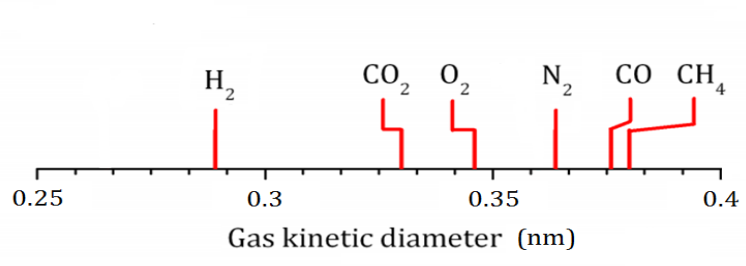

Figure 1.4. Depiction showing the kinetic diameter of different gases.

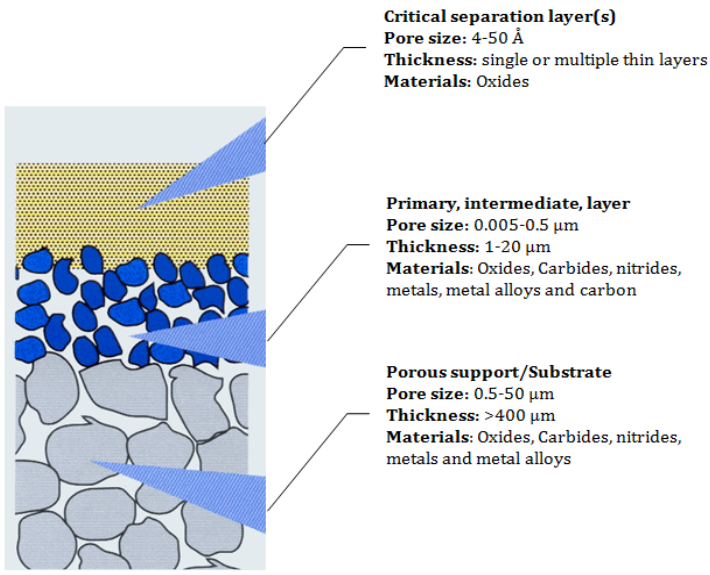

Figure 1.5. Depiction showing the structure of an inorganic membrane.

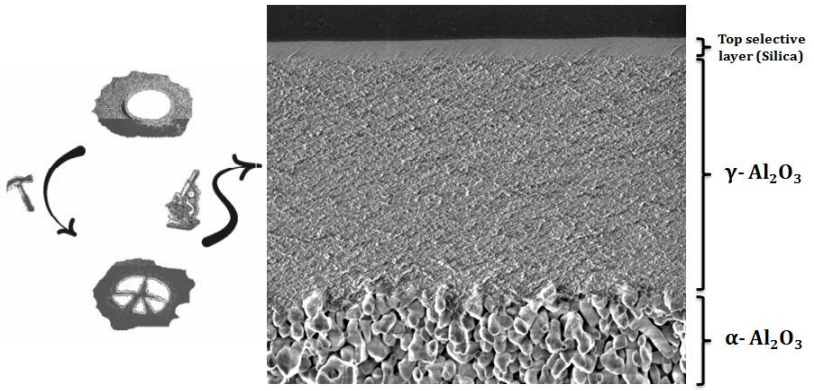

Figure 1.6. Picture and SEM magnification of a ceramic microporous gas-sieving disk presented in the thesis.

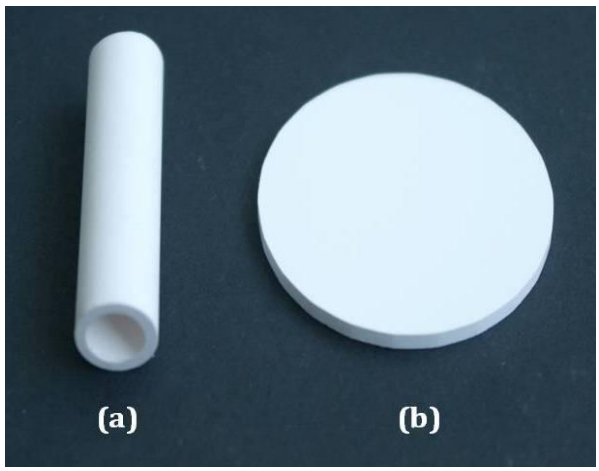

Figure 1.7. Commercial inorganic membranes (a) Tubular and (b) Disk-shaped (flat) membranes.

1.3.1. Dense inorganic membranes

These membranes are prepared as unsupported ones as well as thin films on porous supports. They are made of polycrystalline ceramic material, in particular perovskites, or metal (palladium), which allows specific gas species to permeate the dense material. Depending on the nature of the dense membrane material, specific gas as hydrogen selectively permeates in atomic (Pd alloys), molecular (dense SiO_2) or protonic (proton-conductive solid electrolytes) form. Dense membranes are impermeable to all gases except for a very limited number of gases that can permeate the material (i.e. H_2 through Pd) or can be incorporated into the structure of the membrane and transported through the material (i.e. O_2 through perovskites). Palladium and its alloys are usually the first choice for dense metal membranes to separate hydrogen. Palladium membrane allows transport of hydrogen, but is very expensive and has low durability as well as a complex process that contains several steps as mentioned elsewhere [46-48].

1.3.2. Porous inorganic membranes

Although dense inorganic membranes can achieve high separation factors, gas fluxes through porous membranes are much higher. Therefore, many works have been done and reported in the literature used a porous structure material as substrate, and covered it with a thin dense inorganic membrane layer to achieve gas separation [17, 40, 49-51]. However, the main object of this thesis is the development of microporous inorganic membrane material, hybrid silica, to be used as a precursor for thin inorganic membrane layer. Such kind of membranes, with pore sizes smaller than 2 nm, are described as microporous inorganic membranes. Based on synthesis route and material, one can roughly distinguish 5 main types of inorganic microporous membranes that are [52]:

- Sol-gel derived ceramic membranes.
- CVD modified (glass or ceramic) membranes.
- Leached hollow glass fibers.
- Carbon molecular sieve membranes.
- Zeolite membranes.

A microporous ceramic membrane system generally consists of a macroporous ceramic support, some ceramic intermediate layers, and eventually a highly selective

top layer. As this thesis is related to development of hybrid silica as a type of porous inorganic membrane materials, sol-gel derived membrane materials; therefore the membrane preparation will be briefly discussed. In general, silica membranes are prepared on top of a support for mechanical strength to form an asymmetric structure. The support has a principle role in the final morphology of the silica derived films as fine-porous separation layer. The support must have low surface roughness, small pore sizes and low defect or void concentration [53]. Micro-cracks or pin-hole defects may occur if the support has large pores, voids and rough surfaces due to the induced mechanical stress in the films. Hence, the support modification is important issue for membrane preparation.

Indeed, because of the high porosity, relatively low cost and high mechanical stability of α-Al_2O_3 supports, they are widely used for silica membrane preparation. Their modification can be performed by using mesoporous γ-Al_2O_3 as intermediate layers. Such a layer consisting of much smaller pore sizes of ~4 nm and 2 μm thick is able to minimize the defect rate observed [54]. However, γ-Al_2O_3 exhibits low hydrothermal stability, which is of concern if these materials are to be used in applications containing water vapor [55]. Once the coating process completes, the membranes are calcined at high temperatures, which help in silica densification, and hence fix the silica structure resulting in extremely low fluxes. The heating ramp of the calcination process is preferred to be low, at around 1 °C/ min, to minimize the thermal stresses between the substrate and the thin silica film and prevent film cracking and defects. In some cases the coating and calcination processes can be repeated to produce high quality membranes. As environmental dust affects thin film formation, the quality of silica membranes was greatly improved by simply coating in a clean room environment as mentioned earlier. When considering these membranes for gas separation, the most important membrane properties such as permeation and selectivity should be taken into account, as well as, the thermal and mechanical strength.

The permeation and selectivity depend on the microstructures of the membrane/support composites such as pore size and distribution, porosity and the affinity between permeating species and the pore walls. Separation of a gas mixture can take place based on differences in molecular mass, size or shape, or on differences in the affinity of the gas molecules to the membrane material. An increase

in selectivity is generally at the expense of a decrease in membrane permeation, due to decreasing not only the pore size but also the overall porosity of the membrane. The best answer to permeation/selectivity optimization would be to synthesize very thin layers of materials with high porosity and with pore sizes in the range of 0.3–0.8 nm so as to achieve molecular sieving effects [46, 56]. However, this is the challenge in membrane gas separation processes whatever the properties of the membrane material, unsupported one that will be used as a thin separation layer, possess. As the characteristic properties of the unsupported membrane material may differ somehow when it will be supported, therefore, in that sense the understanding of the supported membrane material can be estimated by the mechanisms that control their transport and separation performance, in turn the mechanisms will be mentioned in the next section.

1.3.3. Gas transport and separation mechanisms in porous inorganic membranes

1.3.3.1. An overview

The properties of gas flow in porous media depend on the ratio of the number of molecule-molecule collisions to that of the molecule-wall collisions. The Knudsen number (K_n) is a characteristic parameter defining different regions of this ratio. Its value is defined by $K_n = \lambda/dp$ with λ being the average free path length of the gas molecules and dp the characteristic pore diameter [57].

For evaluating the membrane transport and/or separation performance, following are shown some important parameters commonly used for this purpose [58].

- Membrane flux (J)

$$J = \frac{Q}{At} \qquad 1.1$$

Where Q (mol) is the total amount of gas permeated through the membrane area A (m^2) in a time period of t (s).

- Membrane permeance (F)

$$F = \frac{J}{\Delta P} \qquad 1.2$$

Where ΔP (Pa) is the partial pressure difference between the two sides of the membrane, namely, $\Delta P = P_f - P_p$ and P_p and P_f are partial pressures on the feed side and permeate side, respectively.

Permeability is the rate at which any compound permeates through a membrane; it depends upon a thermodynamic factor (partitioning of species between feed phase and membrane phase) and a kinetic factor (e.g., diffusion in a dense membrane or surface diffusion in a microporous membrane). During the gas transport there are two major processes, sorption and diffusion processes that play important roles in the overall gas transport. Sorption describes the interactions between gas molecules and the membrane surface, and diffusion describes the rate of gas passage through the membrane. Qualitative and quantitative analysis of the involvement of these steps is required to understand the overall gas transport mechanism since each process can contribute to the total permeation rate, and its importance will differ according to such variables as temperature, pressure, and composition [59].

1.3.3.2. Single gas mechanisms

The transport mechanisms of single gases are mainly depending on the pore diameter distribution and/or the temperature-pressure combination. According to these factors, a number of transport mechanisms can be used to describe this phenomenon. In other words, one of these mechanisms might be dominant. In many cases some of them act simultaneously and addition rules must be formulated and each contribution has to be "weighted" according to its own driving force. This is generally not the pressure gradient, but the gradient of the thermodynamic potential. As a consequence a thermodynamic correction factor has to be applied in diffusion or permeation equations expressed in terms of pressure or concentration [57].

In the case of macropores the gas molecule has a higher chance to collide with another gas molecule than with the pore wall. This is because of the mean free path of a molecule is far smaller than the pore diameter. In this regime, which is called viscous flow regime, the dominant mechanism is viscous flow mechanism and can be described by the Poiseuille law [52]:

$$J_{viscous} = \frac{\varepsilon \mu_p \bar{r}^2}{8RT} \frac{P_m}{\eta L} \qquad 1.3$$

Where:

- ε is the porosity.
- μ_p is a shape factor equal to $1/\tau$ and τ is the tortuosity.
- $\bar{r}$ is the modal pore radius (m).
- P_m is the mean pressure (Pa).
- R is the gas constant (J.mol^{-1}.K^{-1}).
- T is the absolute temperature (K).
- η is the gas viscosity (N.s.m^{-2}).
- L is the membrane thickness (m).

On the contrary in the case of mesopores the mean free path of a gas molecule is larger than the size of the pore. The interaction gas molecule-pore wall is therefore more dominant than the interaction molecule-molecule. In this case the transport occurs and described mainly by the Knudsen law [52]:

$$J_{Knudsen,a} = \frac{2}{3} \bar{v}_a \frac{\varepsilon \bar{r}}{\tau RTL} \qquad 1.4$$

Where ν_a is the mean molecular velocity of a species "*a*" in a pore of radius r. According to the kinetic theory of ideal gases this term is given by:

$$\bar{v}_a = \sqrt{\frac{8\,RT}{\pi M_a}} \qquad 1.5$$

The gas flux of species "*a*" in a mesoporous membrane is expressed by (assuming that the pressure gradient is constant across the membrane).

$$J_{Knudsen,a} = K_{Kund} \sqrt{\frac{1}{M_a RT}} \frac{\Delta P_a}{L} \qquad 1.6$$

Form this equation we can observe that the permeation of a single gas in the Knudsen regime is:

- Proportional to the average pore radius.
- Independent of the pressure.

- Inversely proportional to the square root of the molecular mass of the permeating species.

Therefore, molecules with different molecular mass can be separated by Knudsen diffusion which is the dominant mechanism.

Concerning the micropores medium the dominate mechanism is activated transport or diffusion (or called configurational transport or diffusion) which is related mainly to the molecular sieving effect of the pores. Consequently the general Fick law can be applied:

$$J = -D\frac{dC}{dz} \qquad 1.7$$

Where J is the membrane flux, D is the diffusion coefficient (which is in general dependent on the concentration) and dC/dz is the concentration gradient.

If microporous flux is rate determining and the contribution of external surface flux is not significant; the apparent activation energy (E_a) for permeation of gases is determined by:

$$E_a = E_m - Q_{st} \qquad 1.8$$

Where Q_{st} is the isosteric heat of adsorption and E_m is the energy of mobility required for molecules to jump from one site to another inside the micropore. The E_a value is empirically estimated for each species measuring the temperature dependence of permeance and it can be positive or negative.

Q_{st} and E_m can be determined through the van't Hoff relation and the Arrhenius relation, respectively.

$$K = K_0\, exp\left(\frac{Q_{st}}{RT}\right) \qquad 1.9$$

$$D = D_0\, exp\left(\frac{-E_m}{RT}\right) \qquad 1.10$$

K_0 and D_0 are temperature independent proportionality constants and hence the transport through micropores can be written as:

$$J = -J_{0,a}\, exp\left\{\frac{-E_a}{RT}\right\}\frac{\Delta P_a}{L} \qquad 1.11$$

As it can be seen the permeance of microporous membranes is an exponential function of the temperature whereas in mesoporous membranes it decreases with the square root of temperature. Therefore, the study of the permeance of a gas as function of the temperature is an important issue to indicate either the presence or absence of defect-free microporous and mesoporous layers [60] .

1.3.3.3. Gas mixtures mechanisms

In the case of gas mixture, besides the permeation of the gas, there is an important parameter which should be taken into account, the selectivity factor. Separation and permeation are two opposing requirements. As mentioned earlier, an increase in selectivity is generally at the expense of a decrease in membrane permeation. The selectivity is the ability of a membrane to accomplish a given separation (relative permeability of the membrane for the feed species). Selectivity is a key parameter to achieve high product purity at high recoveries. In gas mixtures the permeation of components (and thus the selectivity) is only identical with that of single gases under special conditions such as high temperature and low pressure. This difference is of importance in the transition region between molecular diffusion (Poiseuille flow) and Knudsen diffusion and in that of Knudsen to configurational diffusion [57]. Membrane gas separation has the potential to grow enormously if more selective membranes will become available. Both membrane permeability and selectivity influence the economics of a gas separation membrane process. Therefore, the efficiency of membranes is generally described in terms of permeance and selectivity. In other words it is necessary to have a good separation and at the same time to reduce the size (the cost and the space) of the membrane.

- Membrane selectivity ($S_{i/j}$)

  Membrane selectivity of component *i* over component *j* in a mixture is defined as:

$$S_{i/j} = \frac{\left(y_i/y_j\right)}{\left(x_i/x_j\right)} \qquad 1.12$$

Where *x* and *y* are the molar compositions in the feed side and the permeate side of the membrane, respectively.

The ideal selectivity ($S°_{i/j}$) also called "permselectivity" of gas *i* over gas *j* is defined as the ratio of their pure gas permeance values:

$$S^0_{i/j} = \frac{(P_{m.i})_{pure}}{(P_{m.j})_{pure}} \qquad 1.13$$

Where ($P_{m,i}$) pure is the permeance of pure gas *i*.

The separation factor (α_i) of component *i* from a multicomponent mixture is defined by:

$$\alpha_i = \frac{y_i/(1-y_i)}{x_i/(1-x_i)} \qquad 1.14$$

The gas separation mechanisms in porous membrane are governed by the membrane pores and the permeating gas molecules [58]. In that case there are two possibilities, because in the macropores no gas separation is possible:

- The membrane pores are several times larger than the gas molecules. This case is occurring for mesopores membrane (diameter of pore, 2 nm<dp< 50 nm). Where these large pores do not have a large resistance to gas flow.
- The membrane pores are in the same size or very close to the gas molecules. This case is occurring for micropores membrane (diameter of pore, dp< 2 nm). Where the membrane works as a sort of yes-no filter with a very well defined cut-off. Besides, the interactions between the walls of the pores and gas molecules are dominated and hence the permeance decreases dramatically [60].

Viscous (Poiseuille) flow and molecular diffusion are non-selective. Nevertheless they play an important role in the macroporous substrate(s) supporting the separation layer and can seriously affect the total flow resistance of the membrane system. Mesoporous separation layers or supports are frequently in the transient-regime between Knudsen diffusion (flow) and molecular diffusion, with large effects on the separation factor (selectivity) [57].

There have been many studies in the literature associated with gas transport through membranes. A variety of models have been used to describe the transport through membranes [52, 57, 61-65]. These models have different theoretical bases associated with the details of the gas diffusion mechanism. In membrane applications

for gas separation, adsorption is usually not multilayer, and often well below a monolayer, so is well described by the Langmuir adsorption model [59]. Diffusion of molecules through a membrane can proceed in various ways depending on the nature of the interaction between the diffusing gas molecules and the membrane. Various gas diffusion processes were discussed elsewhere [57, 61]. Gas permeation through mesoporous or macroporous membranes includes viscous flow, molecular diffusion and Knudsen diffusion. The theory governing the transport in these large pore membranes is the Dusty–Gas model [57, 66]. For microporous membranes, the separation of multicomponent gases can be described by the Maxwell–Stefan model [57, 67].

The mechanism of separation is depending on a competitive adsorption-diffusion mechanism which is observed for gas containing adsorbing and non-adsorbing or weakly adsorbing components. During operation, the adsorbing gases are preferentially adsorbed into the internal pore surfaces and permeate through the membrane via surface diffusion. The adsorbed gas molecules drastically reduce the free space of the membrane pores that limits the entry and passage for the non-adsorbing molecules [68-70]. Figure 1.8 shows gas transport mechanisms in porous membranes.

1.4. The need for gas separation

The need for hydrogen will increase dramatically in the coming years due to the increasing demand for it as a raw material for the chemical industry, and for clean fuels in cars and home heating. Today, hydrogen is mostly produced using the steam-reforming process of fossil fuels, especially methane [71]. In this process the reaction is:

$$CH_4 + H_2O \rightleftharpoons CO + 3H_2 \qquad \Delta H = 206\ kJ/mol$$

The problem of hydrogen production in chemical processes and from fossil fuels is that the hydrogen is mixed with large quantities of non-desired components such as light hydrocarbons, CO and CO_2 [72]. In order to maximize H_2 production and reduce concentration of CO_2 the reforming reaction is further processing through shift units. The main reaction in the shift reactors units is water gas shift reaction (WGS) according the following [49]:

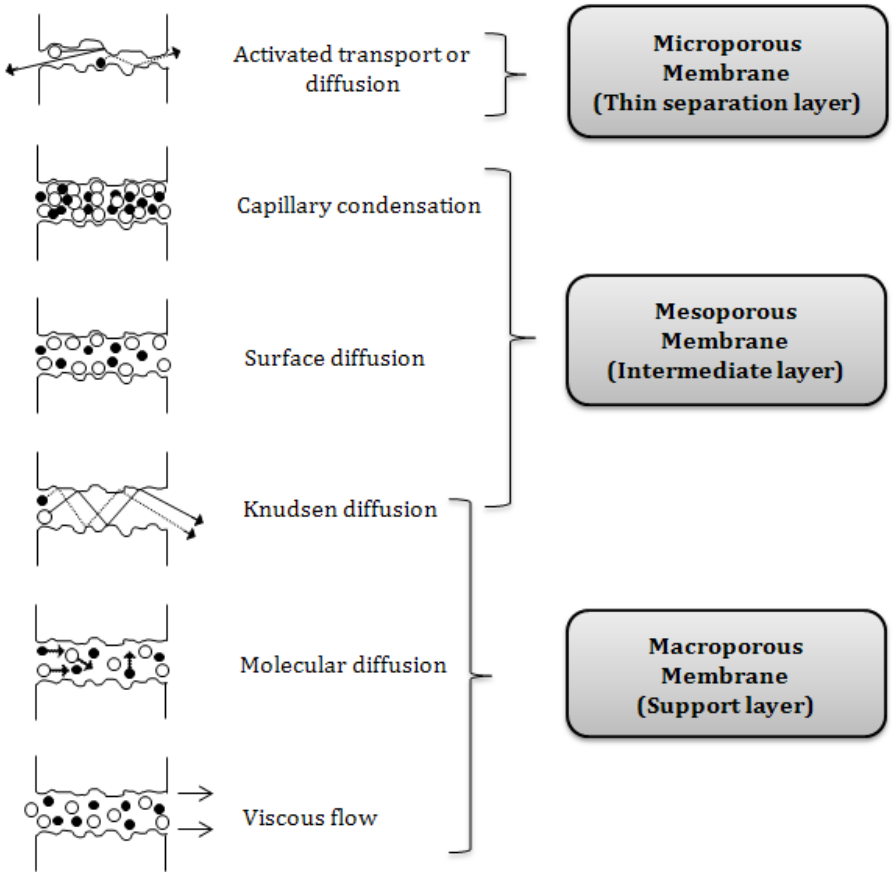

Figure 1.8. Gas transport mechanisms in porous membranes.

$$CO + H_2O \rightleftharpoons CO_2 + H_2 \qquad \Delta H = -41\ kJ/mol$$

Over the last decades, membrane reactor technology has become an important area of increasing research interest in the field of gas separation. Simply a membrane reactor is a chemical equipment that combines a catalyst-filled reaction chamber with a membrane to add reactants or remove products of the reaction. Membrane reactor is a possible way to produce and purify the hydrogen from the steam-reforming process [71]. Figure 1.9 shows schematic representation of a membrane reactor with catalyst for both steam-reforming and WGS reactions. An alternative strategy to optimize the WGS reaction is to employ a membrane reactor unit integrating the reaction with product separation using a selective membrane [49].

In order to obtain high conversion from the reforming unit at a lower temperature, hydrogen must be removed selectively from the reaction zone during the process. This can be performing by using hydrogen selective membrane (also can be called hydrogen purification membrane) with sufficient hydrogen permeability and separation selectivity. Such a membrane reactor, provided with a membrane having a higher affinity toward hydrogen separation compared to the reaction mixture, which are CH_4, H_2O, CO_2 and CO. This would give the same conversion at low temperature as obtained at high temperature in the conventional process. Several types of membranes can be used for that purpose such as dense palladium or palladium composite membranes and its alloys. From the economical points of view, which play an important role for membrane reactor application, in particular, the efforts for fulfilling the continuously increasing hydrogen demand in the refinery industry and for fuel cell technology [73], sol-gel derived microporous silica membranes come into the picture. Thus the development of microporous silica materials, in order to prepare effective silica membranes for molecular sieve separation, is of particular importance in this research field. The modifications of microporous silica materials to work in presence of steam and high pressure and temperature have encouraged an increasing research for that purpose. Thanks to sol-gel technique, the synthesis of molecular sieve silica (MSS) membranes is now simple and effective. Due to the micropores of the silica network, silica membranes allow the permeation of small molecular gases such as H_2. Hence, microporous silica membranes with high flux of H_2 as well as high selectivity of H_2 over others gases such as CO_2 and N_2 have been prepared by sol-gel technique [74, 75]. However, over

the last decades and next decades the development and enhancement of supported/unsupported silica membranes has been and still will be an attractive topic for molecular sieve applications.

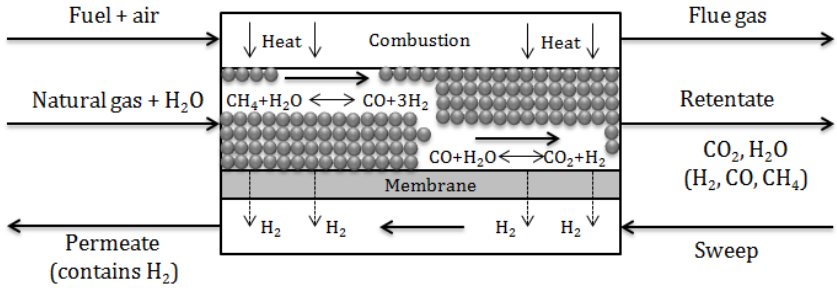

Figure 1.9. Schematic representation of two reactions (steam-reforming + WGS) in a membrane reactor with catalyst.

1.5. References

[1] X. He, M.-B. Hägg, Membranes for environmentally friendly energy processes, Membranes 2 (2012) 706-726.
[2] K.B. Jirage, C.R. Martin, New developments in membrane-based separations, Trends Biotechnol. 17 (1999) 197-200.
[3] W.J. Koros, Evolving beyond the thermal age of separation processes: Membranes can lead the way, AIChE J. 50 (2004) 2326-2334.
[4] P. Bernardo, E. Drioli, G. Golemme, Membrane gas separation: A review/State of the art, Ind. Eng. Chem. Res. 48 (2009) 4638-4663.
[5] US membrane separation technology markets analysed, Membrane Technology 2002 (2002) 10-12.
[6] R.W. Baker, Future directions of membrane gas separation technology, Ind. Eng. Chem. Res. 41 (2002) 1393-1411.
[7] R.W. Baker, K. Lokhandwala, Natural gas processing with membranes: An overview, Ind. Eng. Chem. Res. 47 (2008) 2109-2121.
[8] L. Peters, A. Hussain, M. Follmann, T. Melin, M.B. Hägg, CO_2 removal from natural gas by employing amine absorption and membrane technology–A technical and economical analysis, Chem. Eng. J. 172 (2011) 952-960.
[9] A. Hussain, M.-B. Hägg, A feasibility study of CO_2 capture from flue gas by a facilitated transport membrane, J. Membr. Sci. 359 (2010) 140-148.
[10] R. Beavis, CACHET-II: Carbon capture and hydrogen production with membranes–A new in project in FP7-Energy, Energy Procedia 4 (2011) 745-749.
[11] G. Rebollar-Perez, E. Carretier, N. Lesage, P. Moulin, Volatile organic compound (VOC) removal by vapor permeation at low VOC concentrations: Laboratory scale results and modeling for scale up, Membranes 1 (2011) 80-90.
[12] S. Sá, J.M. Sousa, A. Mendes, Methanol steam reforming in a dual-bed membrane reactor for producing PEMFC grade hydrogen, Catal. Today 156 (2010) 254-260.
[13] E. López, N.J. Divins, J. Llorca, Hydrogen production from ethanol over Pd–Rh/CeO_2 with a metallic membrane reactor, Catal. Today 193 (2012) 145-150.
[14] P. Pandey, R.S. Chauhan, Membranes for gas separation, Prog. Polym. Sci. 26 (2001) 853-893.
[15] W.J. Koros, Y.H. Ma, T. Shimidzu, Terminology for membranes and membrane processes (IUPAC Recommendation 1996), J. Membr. Sci. 120 (1996) 149-159.
[16] M. Elma, C. Yacou, D.K. Wang, S. Smart, J.C. Diniz da Costa, Microporous silica based membranes for desalination, Water 4 (2012) 629-649.
[17] G.Q. Lu, J.C. Diniz da Costa, M. Duke, S. Giessler, R. Socolow, R.H. Williams, T. Kreutz, Inorganic membranes for hydrogen production and purification: A critical review and perspective, J. Colloid Interface Sci. 314 (2007) 589-603.
[18] H.P. Hsieh, Inorganic Membranes for Separation and Reaction; Membrane Science and Technology Series 3, Elsevier, Amsterdam, 1996.

[19] A. Buekenhoudt, A. Kovalevsky, J. Luyten, F. Snijkers, 1.11 - Basic Aspects in Inorganic Membrane Preparation, in: D. Editor-in-Chief: Enrico, G. Lidietta (Eds.), Comprehensive Membrane Science and Engineering, Elsevier, Oxford, 2010, pp. 217-252.

[20] A.F. Ismail, L.I.B. David, A review on the latest development of carbon membranes for gas separation, J. Membr. Sci. 193 (2001) 1-18.

[21] Y. Kase, Gas separation by polyimide membranes, in: N.N. Li, A.G. Fane, W.S.W. Ho,T. Matsuura (Eds.), Advanced Membrane Technology and Applications, John Wiley & Sons, Inc., Hoboken, New Jersey, 2008, pp. 581-598.

[22] K.C.B. Mejías, Carbon Molecular Sieve Membranes for Gas Separation, PhD Thesis, Universitat Rovira i Virgili, 2012.

[23] V. Sebastian, Z. Lin, J. Rocha, C. Tellez, J. Santamaria, J. Coronas, A new titanosilicate umbite membrane for the separation of H_2, Chem. Commun. 0 (2005) 3036-3037.

[24] C.Y. Pan, Gas separation by permeators with high-flux asymmetric membranes, AIChE J. 29 (1983) 545-552.

[25] A. Tabe-Mohammadi, A review of the applications of membrane separation technology in natural gas treatment, Sep. Sci. Technol. 34 (1999) 2095-2111.

[26] S.J. Metz, W.J.C. van de Ven, J. Potreck, M.H.V. Mulder, M. Wessling, Transport of water vapor and inert gas mixtures through highly selective and highly permeable polymer membranes, J. Membr. Sci. 251 (2005) 29-41.

[27] G. Bisio, A. Bosio, G. Rubatto, Thermodynamics applied to oxygen enrichment of combustion air, Energy Convers. Manage. 43 (2002) 2589-2600.

[28] K.S.W. Sing, D.H. Everett, R.A. W. Haul, L. Moscou, R.A. Pierotti, J. Rouquerol, T. Siemieniewska, Reporting physisorption data for gas/solid systems with special reference to the determination of surface area and porosity (Recommendations 1984), Pure Appl. Chem. 57 (1985) 603-619.

[29] T.A. Peters, J. Fontalvo, M.A.G. Vorstman, N.E. Benes, R.A.v. Dam, Z.A.E.P. Vroon, E.L.J.v. Soest-Vercammen, J.T.F. Keurentjes, Hollow fibre microporous silica membranes for gas separation and pervaporation: Synthesis, performance and stability, J. Membr. Sci. 248 (2005) 73-80.

[30] B. Sea, K.H. Lee, Modification of mesoporous γ-alumina with silica and application for hydrogen separation at elevated temperature, J. Ind. Eng. Chem. 7 (2001) 417-423.

[31] Q. Wei, F. Wang, Z.-R. Nie, C.-L. Song, Y.-L. Wang, Q.-Y. Li, Highly hydrothermally stable microporous silica membranes for hydrogen separation, J. Phy. Chem. B 112 (2008) 9354-9359.

[32] Y. Zhang, Q. Li, P. Shen, Y. Liu, Z. Yang, W. Ding, X. Lu, Hydrogen amplification of coke oven gas by reforming of methane in a ceramic membrane reactor, Int. J. Hydrogen Energy 33 (2008) 3311-3319.

[33] D. Casanave, P. Ciavarella, K. Fiaty, J.A. Dalmon, Zeolite membrane reactor for isobutane dehydrogenation: Experimental results and theoretical modelling, Chem. Eng. Sci. 54 (1999) 2807-2815.

[34] J. Yang, J. Čermáková, P. Uchytil, C. Hamel, A. Seidel-Morgenstern, Gas phase transport, adsorption and surface diffusion in a porous glass membrane, Catal. Today 104 (2005) 344-351.

[35] H.B. Park, Y.M. Lee, Pyrolytic carbon–silica membrane: a promising membrane material for improved gas separation, J. Membr. Sci. 213 (2003) 263-272.

[36] D. Uhlmann, S. Liu, B.P. Ladewig, J.C. Diniz da Costa, Cobalt-doped silica membranes for gas separation, J. Membr. Sci. 326 (2009) 316-321.

[37] J.C. Diniz da Costa, G.Q. Lu, V. Rudolph, Y.S. Lin, Novel molecular sieve silica (MSS) membranes: characterisation and permeation of single-step and two-step sol–gel membranes, J. Membr. Sci. 198 (2002) 9-21.

[38] C. Xia, F. Wu, Z. Meng, F. Li, D. Peng, G. Meng, Boehmite sol properties and preparation of two-layer alumina membrane by a sol-gel process, J. Membr. Sci. 116 (1996) 9-16.

[39] D.E. Koutsonikolas, S.P. Kaldis, S.D. Sklari, G. Pantoleontos, V.T. Zaspalis, G.P. Sakellaropoulos, Preparation of highly selective silica membranes on defect-free γ-Al_2O_3 membranes using a low temperature CVI technique, Microporous Mesoporous Mater. 132 (2010) 276-281.

[40] R. Igi, T. Yoshioka, Y.H. Ikuhara, Y. Iwamoto, T. Tsuru, Characterization of Co-doped silica for improved hydrothermal stability and application to hydrogen separation membranes at high temperatures, J. Am. Ceram. Soc. 91 (2008) 2975-2981.

[41] T. Tsuru, R. Igi, M. Kanezashi, T. Yoshioka, S. Fujisaki, Y. iwamoto, Permeation properties of hydrogen and water vapor through porous silica membranes at high temperatures, AIChE J. 57 (2011) 618-629.

[42] H. Qi, J. Han, N. Xu, H.J.M. Bouwmeester, Hybrid organic–inorganic microporous membranes with high hydrothermal stability for the separation of carbon dioxide, ChemSusChem 3 (2010) 1375-1378.

[43] V. Boffa, J.E. ten Elshof, R. Garcia, D.H.A. Blank, Microporous niobia–silica membranes: Influence of sol composition and structure on gas transport properties, Microporous Mesoporous Mater. 118 (2009) 202-209.

[44] K. Brands, D. Uhlmann, S. Smart, M. Bram, J.C.D. da Costa, Long-term flue gas exposure effects of silica membranes on porous steel substrate, J. Membr. Sci. 359 (2010) 110-114.

[45] D.-W. Lee, S.-J. Park, C.-Y. Yu, S.-K. Ihm, K.-H. Lee, Study on methanol reforming–inorganic membrane reactors combined with water–gas shift reaction and relationship between membrane performance and methanol conversion, J. Membr. Sci. 316 (2008) 63-72.

[46] Y.S. Lin, Microporous and dense inorganic membranes: current status and prospective, Sep. Purif. Technol. 25 (2001) 39-55.

[47] K. Li, Ceramic Membranes for Separation and Reaction, John Wiley & Sons, Ltd., West Sussex, England, 2007.

[48] J. Gabitto, C. Tsouris, Hydrogen transport in composite inorganic membranes, J. Membr. Sci. 312 (2008) 132-142.

[49] S. Battersby, M.C. Duke, S. Liu, V. Rudolph, J.C. Diniz da Costa, Metal doped silica membrane reactor: Operational effects of reaction and permeation for the water gas shift reaction, J. Membr. Sci. 316 (2008) 46-52.

[50] V. Boffa, D.H.A. Blank, J.E. ten Elshof, Hydrothermal stability of microporous silica and niobia–silica membranes, J. Membr. Sci. 319 (2008) 256-263.

[51] S. Battersby, S. Smart, B. Ladewig, S. Liu, M.C. Duke, V. Rudolph, J.C. Diniz da Costa, Hydrothermal stability of cobalt silica membranes in a water gas shift membrane reactor, Sep. Purif. Technol. 66 (2009) 299-305.

[52] R.S.A. de Lange, K. Keizer, A.J. Burggraaf, Analysis and theory of gas transport in microporous sol-gel derived ceramic membranes, J. Membr. Sci. 104 (1995) 81-100.

[53] B.C. Bonekamp, Chapter 6 Preparation of Asymmetric Ceramic Membrane Supports by Dip-Coating, in: A.J. Burggraaf, L. Cot (Eds.), Membrane Science and Technology, Elsevier, 1996, pp. 141-225.

[54] B.C. Bonekamp, A. van Horssen, L.A. Correia, J.F. Vente, W.G. Haije, Macroporous support coatings for molecular separation membranes having a minimum defect density, J. Membr. Sci. 278 (2006) 349-356.

[55] A. Nijmeijer, H. Kruidhof, R. Bredesen, H. Verweij, Preparation and properties of hydrothermally stable γ-alumina membranes, J. Am. Ceram. Soc. 84 (2001) 136-140.

[56] Y.S. Lin, I. Kumakiri, B.N. Nair, H. Alsyouri, Microporous inorganic memebranes, Sep. Purif. Rev. 31 (2002) 229-379.

[57] A.J. Burggraaf, Chapter 9 Transport and Separation Properties of Membranes with Gases and Vapours, in: A.J. Burggraaf, L. Cot (Eds.), Membrane Science and Technology, Elsevier, 1996, pp. 331-433.

[58] J. Dong, Y.S. Lin, M. Kanezashi, Z. Tang, Microporous inorganic membranes for high temperature hydrogen purification, J. Appl. Phys. 104 (2008) 121301-121317.

[59] D. Lee, S.T. Oyama, Gas permeation characteristics of a hydrogen selective supported silica membrane, J. Membr. Sci. 210 (2002) 291-306.

[60] V. Boffa, Niobia-Silica and Silica Membranes for Gas Separation, PhD thesis, University of Twente, 2008.

[61] A.J. Burggraaf, Single gas permeation of thin zeolite (MFI) membranes: theory and analysis of experimental observations, J. Membr. Sci. 155 (1999) 45-65.

[62] A.B. Shelekhin, A.G. Dixon, Y.H. Ma, Theory of gas diffusion and permeation in inorganic molecular-sieve membranes, AIChE J. 41 (1995) 58-67.

[63] R.S.A. de Lange, J.H.A. Hekkink, K. Keizer, A.J. Burggraaf, Permeation and separation studies on microporous sol-gel modified ceramic membranes, Microporous Mater. 4 (1995) 169-186.

[64] G.B. van den Berg, C.A. Smolders, Diffusional phenomena in membrane separation processes, J. Membr. Sci. 73 (1992) 103-118.

[65] M. Soltanieh, W.N. Gill, Review of reverse osmosis membranes and transport models, Chem. Eng. Commun. 12 (1981) 279-363.

[66] E.A. Mason, A.P. Malinauskas, Gas Transport in Porous Media : the Dusty-Gas Model, Elsevier, Amsterdam, New York, 1983.

[67] R. Krishna, J.A. Wesselingh, The Maxwell-Stefan approach to mass transfer, Chem. Eng. Sci. 52 (1997) 861-911.

[68] S. Suzuki, H. Takaba, T. Yamaguchi, S.-i. Nakao, Estimation of gas permeability of a zeolite membrane, based on a molecular simulation technique and permeation model, J. Phy. Chem. B 104 (2000) 1971-1976.

[69] A.I. Labropoulos, G.E. Romanos, N. Kakizis, G.I. Pilatos, E.P. Favvas, N.K. Kanellopoulos, Investigating the evolution of N_2 transport mechanism during the cyclic CVD post-treatment of silica membranes, Microporous Mesoporous Mater. 110 (2008) 11-24.

[70] J.-H. Moon, C.-H. Lee, Hydrogen separation of methyltriethoxysilane templating silica membrane, AIChE J. 53 (2007) 3125-3136.

[71] F. Gallucci, E. Fernandez, P. Corengia, M. van Sint Annaland, Recent advances on membranes and membrane reactors for hydrogen production, Chem. Eng. Sci. 92 (2013) 40-66.

[72] A. Brunetti, G. Barbieri, E. Drioli, K.H. Lee, B. Sea, D.W. Lee, WGS reaction in a membrane reactor using a porous stainless steel supported silica membrane, Chem. Eng. Process. Process Intensif. 46 (2007) 119-126.

[73] M. Sjardin, K.J. Damen, A.P.C. Faaij, Techno-economic prospects of small-scale membrane reactors in a future hydrogen-fuelled transportation sector, Energy 31 (2006) 2523-2555.

[74] M.C. Duke, J.C. Diniz da Costa, G.Q. Lu, M. Petch, P. Gray, Carbonised template molecular sieve silica membranes in fuel processing systems: permeation, hydrostability and regeneration, J. Membr. Sci. 241 (2004) 325-333.

[75] R.M. de Vos, H. Verweij, High-selectivity, high-flux silica membranes for gas separation, Science 279 (1998) 1710-1711.

Chapter 2

Sol-Gel Technique

Microporous silica materials have attracted a considerable attention in the last few years because of their properties as molecular sieving materials. Hence, these materials are important categories in gas separation field. Sol-gel technique is a simple, attractive and effective way for facile synthesis of high purity molecular sieve silica materials. Via this technique, the modification to achieve novel materials with enhanced properties could be performed. For instance, tailoring the porosity and surface modification of microporous silica materials. Therefore, Sol-gel technique became the fast growing field in the preparation of precursor membrane materials. This chapter discuses a general description concerning theoretical background of sol-gel technique. Additionally, the use of this technique in microporous silica/modified silica-based membrane materials preparation, (unsupported membranes) and the most characterization techniques that are employed for these materials are also considered.

2.1. Introduction

The sol-gel technique is a wet-chemical technique widely used in the fields of materials science, ceramic engineering and Nanotechnology. Such methods are used primarily for the fabrication of materials (typically metal oxides) starting from a colloidal solution (known as sol which is based on a suspension of particles with diameter of 1 to 100 nm) that acts as the precursor for an integrated network. Generally, the sol particles or clusters may interact or aggregate with each other [1-3]. This process is driven by Van der Waals forces or bond formation between unreacted groups. As a result the particles grow in time, leading eventually to precipitation of larger aggregates, or to the formation of a tri-dimensional network. During the development of this network the viscosity of the sol increases and at a certain point the system behaves like a solid. This point is called the "gel point" and the system after this moment is called a gel. The gels are bi-phasic systems containing both a liquid phase and solid phase whose morphologies range from discrete particles to continuous polymer networks (three dimensional networks) [4, 5] as shown in Figure 2.1.

Removal of the remaining liquid (solvent) phase requires a drying process, which is typically accompanied by a significant amount of shrinkage and densification. The gels can be dried in controlled fashion to produce porous solids with unique thermal, mechanical, optical and chemical properties. The rate at which the solvent can be removed is ultimately determined by the distribution of porosity in the gel. The ultimate microstructure of the final component will clearly be strongly influenced by changes imposed upon the structural template during this phase of processing. If the formed gels are dried by evaporation under normal atmospheric condition, they are called xerogels where the structure of the gel collapses and hence the structure is more or less destroyed. On the other hand, if the formed gels are dried under supercritical conditions, they are called aerogels where the structure of the gel is preserved. However, aerogels are materials with very low densities, high porosities and low refraction indexes [1, 2]. The normal drying of the gel leads to structural collapse, Figure 2.2, due capillary forces drawing the walls of the pores together, and reducing the pore size. In some cases cracking may occur when the tension in the gel is so large that it cannot shrink anymore. Afterwards, a thermal treatment, or firing process, is often necessary in order to favor further

polycondensation and enhance mechanical properties and structural stability via final sintering, densification and grain growth [6].

The precursor sol can be either deposited on a substrate to form a film (e.g., by dip coating or spin coating), cast into a suitable container with the desired shape (e.g., to obtain monolithic ceramics, glasses, fibers, membranes, aerogels), or used to synthesize powders (e.g., microspheres, nanospheres). Even small quantities of dopants can be introduced in the sol and end up uniformly dispersed in the final product. It can be used in ceramics processing and manufacturing as an investment casting material, or as a means of producing very thin films of metal oxides for various purposes. Sol-gel derived materials have diverse applications in optics, electronics, energy, space, (bio)sensors, medicine (e.g., controlled drug release), reactive material and separation technology (e.g., microporous silica membranes) [7-9]. The interest in sol-gel processing can be traced back until the mid-1800s with the observation, by Ebelmanl and Graham, that the hydrolysis of tetraethyl orthosilicate (TEOS), $Si(OC_2H_5)_4$ under acidic conditions yielded SiO_2 in the form of a glass-like material [1, 10]. Hence, the interest in the sol-gel processing of inorganic ceramic and glass materials began. Besides, chemists and engineers have learned how to vary the reactants and processing conditions to tailor material properties for specific applications. Advances in chemistry and the chemical precursors available for sol-gel processing have made it an extremely flexible process for materials synthesis. We are no longer limited to silica gels or even to metals oxides. It is now possible to make sol gels materials from almost any transition metal, as well as make composite materials.

The applications of sol-gel materials have grown as the synthesis and processing methods have opened new vistas of material properties. Figure 2.3 shows some applications for sol-gel technique such as ceramic powders, films and composites. The sol-gel technique is a cheap and low-temperature technique that allows for the fine control of the product's chemical composition. One of the distinct advantages of using this technology as opposed to the more traditional processing techniques is that densification is often achieved at a much lower temperature. Due to the possibility of obtaining high-surface-area solids with homogeneous compositions and controlled porosity, sol–gel methods have been widely employed for the synthesis of micro and mesoporous materials. The sol-gel technology is a typical Nanotechnology because all gel products may contain nanoparticles or are nanocomposites. In this

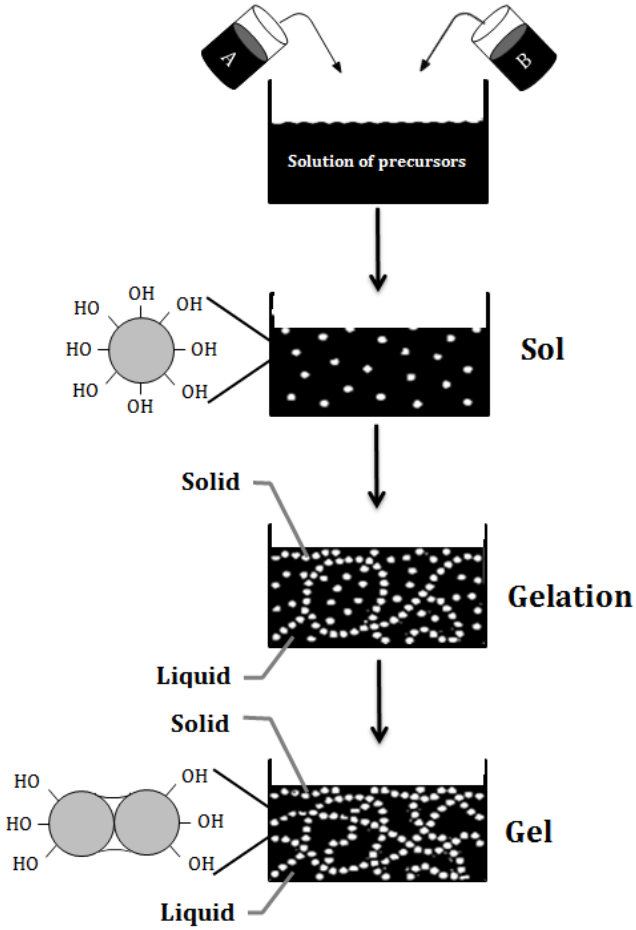

Figure 2.1. Formation of sols and gels.

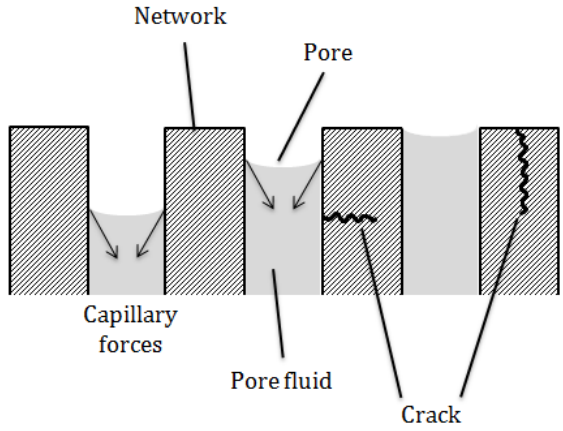

Figure 2.2. Contracting surface forces in pores of different size during drying.[6]

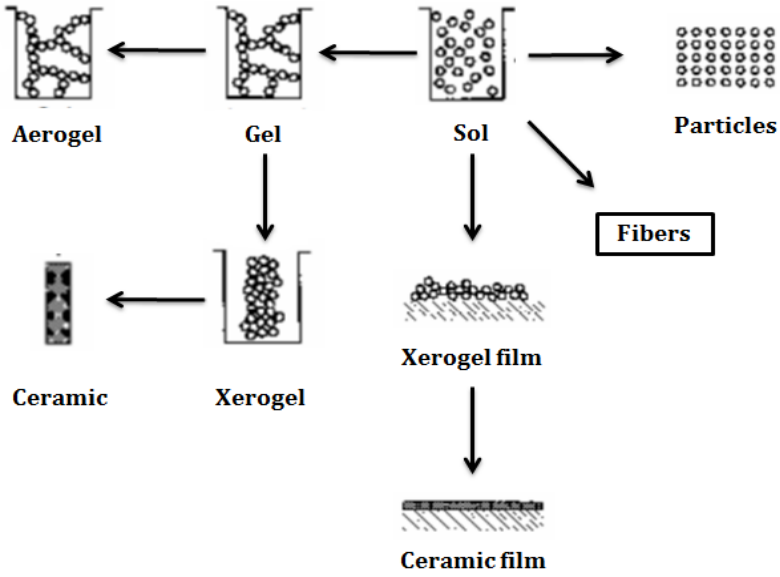

Figure 2.3. Applications of sol-gel technique.[3]

way the sol-gel technique play an important role in the development of modern Nanotechnology for the preparation of new materials [7]. The present thesis studies the development of modified silica-based material, polymeric sols, for molecular sieve applications such as gas separation; therefore, a short description of the chemistry of such systems will be discussed. In particular, a brief description of the chemistry of the silicon alkoxide will be mentioned, because of the fact that microprous silica is the most common material for the preparation of gas selective ceramic membranes.

2.1.1. Chemical reactions during the sol-gel process

The early work with sol-gels focused on those made of silica, derived by condensation of silanols groups (Si-OH), as illustrated by reactions in Figure 2.4. In that reaction the silanols condense by forming water leading to a network of Si-O-Si bonds (the quaternary functionality of the Si results in a three dimensional network) [11]. The most typical precursors for most sol-gel syntheses and applications of silica are based on metal alkoxides such as silicon alkoxide, tetraalkoxysilanes $Si(OR)_4$, which undergo various forms of hydrolysis reactions that leads to produce silanols groups which may be on the surface of nanometer sized silica particles. The silanols subsequently undergo condensation reactions to produce silica gels.. Gelation of silicon alkoxide solutions takes place as a result of the hydrolysis (substitution) of the silicone alkoxides $Si(OR)_4$ and subsequent polycondensation (dehydration) leading to the formation of polymers and particles with siloxane bonds. The reaction can be represented as follows [1, 11]:

$$Si(OR)_4 + 4H_2O \xrightarrow{\text{Catalyst}} Si(OH)_4 + 4ROH \qquad \textit{Hydrolysis}$$

$$Si(OH)_4 + Si(OR)_4 \longrightarrow 2SiO_2 + 4ROH \qquad \textit{Alcohol condensation}$$

$$nSi(OH)_4 \longrightarrow nSiO_2 + 2nH_2O \qquad \textit{Water condensation}$$

Hydrolysis and condensation reactions do not occur independently. Therefore, the mechanisms of these reactions are unknown as result of the complexity of the gelation process. Thus, condensation reactions (2nd reaction) can start already after first hydrolysis reactions (1st reaction) occurred. During this process, intermediate derivatives are generated and subsequently consumed by hydrolysis or condensation reactions as shown in Figure 2.5. Besides, it is also possible the formation of cyclic

structures. The condensation between these kinds of intermediate polyhydroxylated species may be responsible for the gel formation [11]. The catalyst, pH value of the solution, water concentration and silicon alkoxide concentration affect the sol-gel reaction kinetics or rates. Besides, the reaction mechanism of the sol-gel transition, the nature of the polymerized species formed in the sol, the bulk nature of the gel and the gelation time are affected as well. For example depending on the pH value, chain-like or branched networks can be built. Generally the sol-gel reactions are catalyzed by acids or bases and are accompanied by the redistribution reactions [12, 13]:

$$2(RO)_3SiOH \rightleftharpoons (RO)_2Si(OH)_2 + (RO)_4Si$$

$$(RO)_2Si(OH)_2 \rightleftharpoons (RO)_3SiOH + ROSi(OH)_3$$

Therefore, during the process there is a change in the proportion of Si-OH, $Si(OH)_2$ and $Si(OH)_3$ [13]. Acid-catalyzed reactions, represented in Figure 2.6, are performed at pH values below 7. In these processes, first a leaving group is formed by protonation of an alkoxy substituent. Afterwards this is followed by nucleophilic attack of water and the precursor is hydrolyzed. Via a deprotonation step $(RO)_3SiOH$ moieties are obtained which immediately react via condensation to lead siloxanes $(RO)_3Si\text{-}O\text{-}Si(OR)_3$. In acid catalysed hydrolysis the positive transition state is stabilized by the presence of an alkoxy group (electron donor) on the silicon. Therefore the reaction is faster for those species that still have more alkoxy groups on the metallic centre. The breakdown of the Si-O-R bound and the formation of a new Si-O-H bond are synchronized [14]. On the other hand for base-catalyzed reactions, represented in Figure 2.7, the processes occur via an analogous mechanism, but in this case with the formation of a negatively charged transition state. The nucleophilic substitution of alkoxy groups (-OR) by –OH occurs, and the rate of the nucleophilic attack of the hydroxyl anion (electron withdrawing) is dependent on the electron density at reaction site. Hence the opposite behaviour of the acid-catalyzed processes is observed, i.e. the reaction is slower for those species that still have more alkoxy groups on the metallic centre.

One remarkable case to study the reaction rate of organoalkoxysilanes such as $(CH_3)_nSi(OC_2H_5)_{4-n}$, where n= 1, 2 or 3, compared with other silicone alkoxides as $Si(OC_2H_5)_4$ and $Si(OCH_3)_4$ was reported by Schmidt, besides other results were reviewed [15]. The hydrolysis rate increases with “n”, where more positive charge on

the central metal, under acidic conditions. In basic conditions, the reaction speed decreases because the alkyl groups destabilize the intermediate state. The hydrolysis and condensation reactions involve a nucleophilic attack on the electrophilic silicon atom both in acid and basic catalysis. This nucleophilic substitution is known as a bimolecular nucleophilic substitution (SN^2).

In a nucleophilic substitution (SN) both steric and inductive effects play a role in reaction mechanism and should be taken into account [16]. In acid-catalyzed processes after the formation of siloxanes $(RO)_3Si\text{-}O\text{-}Si(OR)_3$ the subsequent hydrolysis reactions is speeded up more efficiently than the condensation reaction. Whereas in base-catalyzed processes the rate of the nucleophilic attack of the hydroxyl anion is dependent on steric effects of the substituents as well as the electron density at reaction site, as mentioned earlier. In general the more the metal centre is accessible to the attack of a nucleophile, the faster is the reaction. Thus the hydrolysis is faster in presence of small and linear alkoxyl chains, as shown in Figure 2.8.

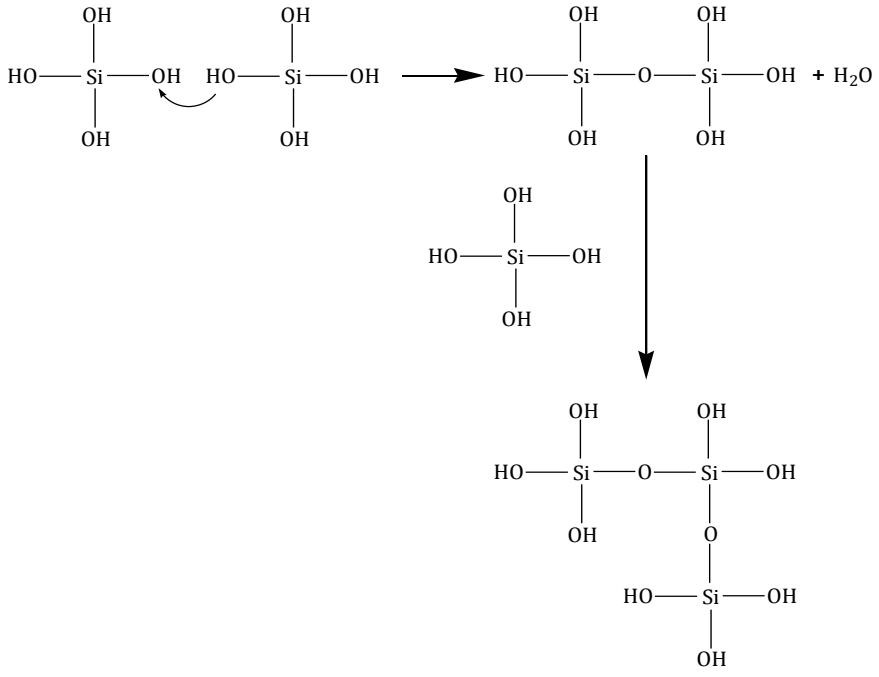

Figure 2.4. Formation of gel via condensation reactions of silanols.

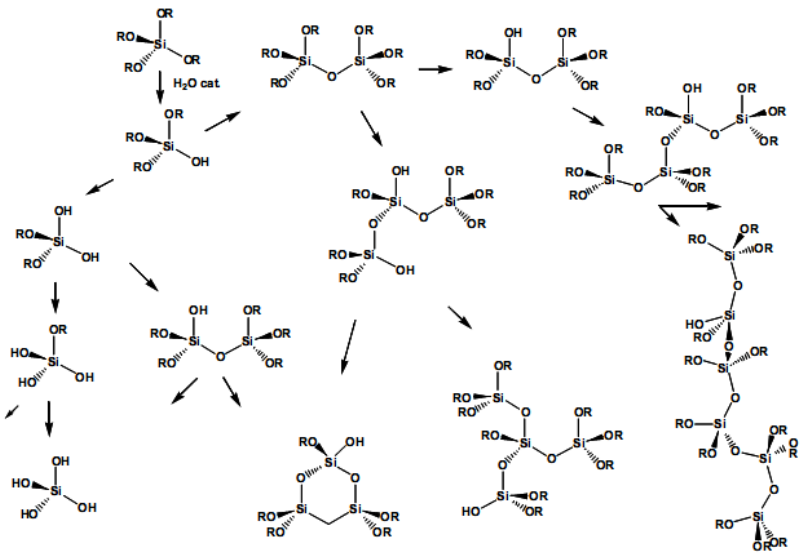

Figure 2.5. Possible intermediates generated during sol-gel process of $Si(OR)_4$ via hydrolysis and condensation reactions. Each intermediate can, in principle, undergo either hydrolysis or condensation reactions.

Hydrolysis

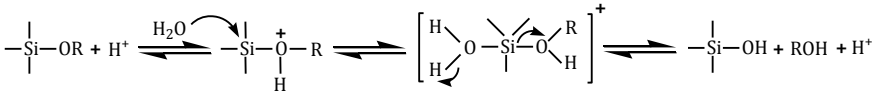

Condensation

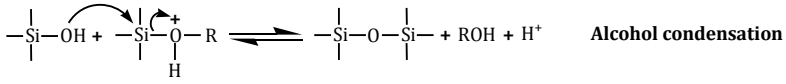

Alcohol condensation

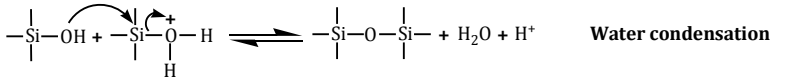

Water condensation

Figure 2.6. Acid-catalyzed reactions where the oxygen atom in Si-OH or Si-OR is protonated and H-OH or H-OR are leaving groups. The electron density are shifted from the Si atom, making it more accessible for reaction with water (hydrolysis) or silanol (condensation).

Hydrolysis

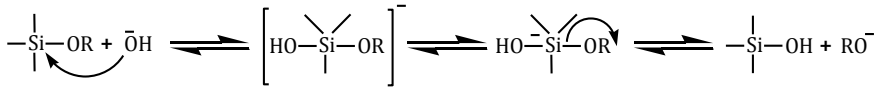

Condensation

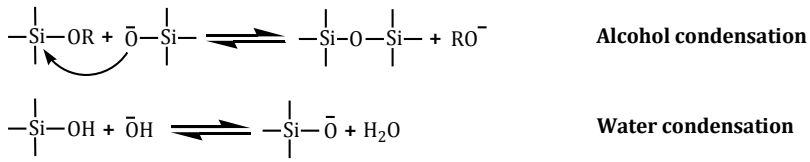

Figure 2.7. Base-catalyzed reactions where nucleophilic attack by OH- or Si-O- on the central Si atom. These species are formed by dissociation of water or Si-OH. The reactions are of SN^2 type where OH- replaces OR- (hydrolysis) or silanolate replaces OH- or OR- (condensation).

2.1.2. Processing

After the sol-gel process is completed, gels have to be dried by thermal treatment or in vacuum conditions. Since the pores of the gels are filled with solvent, capillary forces appear during removal of solvent. These forces induce shrinkage and the formation of cracks in the case of the xerogel. In the next step the obtained xerogels are thermally treated, i.e. calcination and pyrolysis are performed. During calcination step solvent residuals are removed, organic substituents are separated and volatile molecules are released. These processes continue during the pyrolysis step, further thermal treatment thereof at higher temperatures leads to polycrystalline materials.

2.2. Sol-gel derived microporous silica membranes

Porous ceramic, particularly microporous membranes possess high permeability, moderate to high selectivity, and are chemically and thermally stable. Therefore, they are attractive for applications such as hydrogen production reactions. There are various types of porous membranes that have been tested and reported for

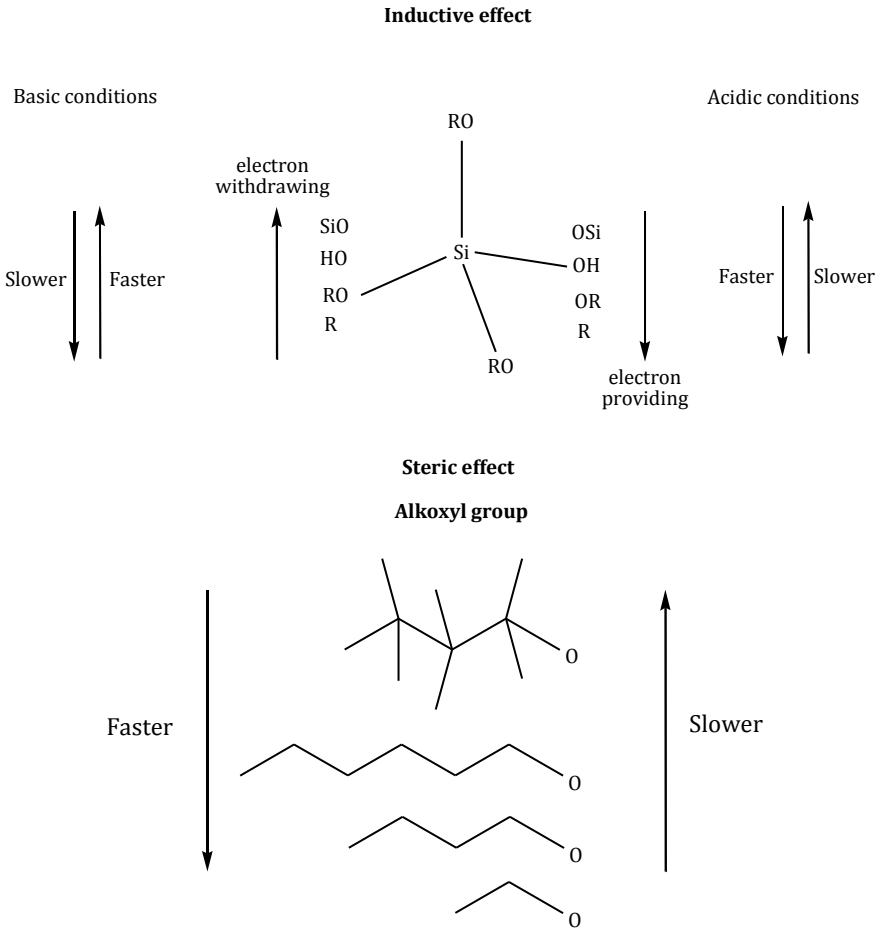

Figure 2.8. Inductive and steric effects on hydrolysis rate.

hydrogen separation or production in the literature. These include carbon molecular sieve membranes [17, 18]. However, another type of porous ceramic membrane reported for use in H_2 production application is based on alumina mesoporous membranes [19]. As mentioned in the previous chapter, the architecture of an inorganic microporous membrane consists of three layers; one of them is the top separation layer. Hence, due to the possibility of obtaining high-surface-area solids with homogeneous compositions and controlled porosity, sol-gel methods have been widely employed for the synthesis of microporous materials that can be used as precursor membrane materials. Due to the micropores of the silica network, silica materials are used to prepare membranes that allow the permeation of small molecular gases such as H_2. Hence, silica membranes with high flux of H_2 as well as high selectivity of H_2 over other gases such as N_2, CO_2 and CH_4 have been prepared by dip or hot coating and sol-gel techniques [19-21].

Silica and silica functionalized ceramic membranes are showing great potential for intended application of molecular sieve application such as gas separation and hydrogen separation and production. Because of the sol-gel technique is a simple and effective way for the synthesis of microporous silica membranes. Therefore, from economical point of view, molecular sieve silica membranes are becoming very competitive against traditional non-hydrostable and expensive metal membranes such as palladium and its alloys [19]. There has been a large development in unsupported and supported silica membranes in the last decade with several groups in the USA, Holland, Germany, Japan and Australia focusing their research efforts in this area.

2.2.1. Preparation of microporous silica membranes

One class of microporous ceramic membranes derived by sol–gel technique is molecular sieve silica (MSS) membranes. The sol-gel technique involves coating of liquid silica precursors on a support and subsequent heat treatment, as shown in Figure 2.9. The most common precursor for the preparation of silica based membranes is usually tetraethylorthosilicate (TEOS) which undergoes hydrolysis followed by further condensation reactions as described earlier. The sol–gel method for preparation of silica membrane materials is divided into two routes, the colloidal suspension route and the polymeric gel route [19].

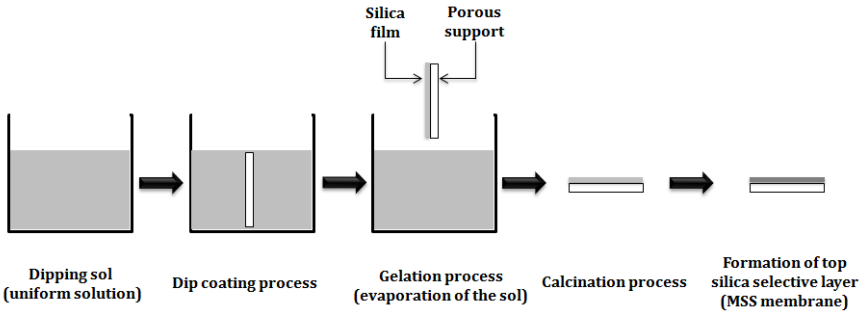

Figure 2.9. Schematic process of sol–gel method for preparing MSS membranes.[19]

2.2.1.1. Colloidal suspension route

In this method the sol consists of a colloidal suspension, containing a particle and agglomerate chain network which is formed by a hydrolysis step using an excess of water. The sols are prepared by the acid catalysed hydrolysis of TEOS precursor, which enables silica particles with different sizes, and then to coat progressively the smaller silica particles onto the support or underlying layers with bigger pore size. By doing so it is possible to modify the α-alumina supports with the colloidal silica sols via the coating process [22, 23]. It is important to take into account the number of layers, and the order in which the various sols are dip coated for the resulting pore size. This is mainly due to the dispersion medium during the dip coating process, which is forced into the pores of the underlying layer by capillary action of the microporous matrices [19]. Colloidal silica sols with small particles can result from fast hydrolysis, slow condensation, and low solubility achieved by acid reaction conditions. All these factors contribute to a high supersaturation level and result in small particles. Particles are much smaller in acidic than in basic reaction conditions due to the slower condensation rate and lower solubility under acidic conditions [24].

2.2.1.2. Polymeric sol-gel route

This is the route that was performed to prepare the unsupported/supported silica-based membranes in the present thesis. The polymeric sol-gel process depends mainly on the control of hydrolysis and condensation reactions. Hence, several studies have been performed to produce high quality silica derived membranes with

very small pore size distribution in the region of ~ 1.0 nm or lower. In this method sols are prepared by the acid-catalyzed hydrolysis of TEOS precursor, which can be a single-step [25, 26] or a two-step catalyzed hydrolysis sol–gel process [27, 28]. Intermediate species are formed through hydrolysis then sol is formed by the condensation of oxygen bridge.

The common recipe of the silica sol preparation, by the acid-catalyzed process, depends on the addition of HNO_3/H_2O mixture to TEOS/ethanol mixture. Premature (partial) hydrolysis can occur during the addition of ethanol to TEOS at room tempreature, therefore, the addition should be done by placing the alkoxide/ethanol mixture in ice bath and afterwards the acid/water mixture is added drop wise with continuous stirring [25, 29]. In some cases the acid-catalyzed hydrolysis of TEOS precursor can be performed by HCl as well [30]. Diniz da Costa *et al.* [27] have reported that sol–gel derived films with a large contribution of silanol groups (SiOH) prepared by the two-step sol gel process have much smaller pore sizes with molecular dimensions in the region of 0.3–0.4 nm than those with a large contribution of siloxane bonds (SiO_4) prepared by the single-step sol–gel process. Water to silica molar ratio is of a particular importance for the microporous structure of the formed gel. A high H_2O/Si molar ratio (>10) provides the sol-gel synthesis with excess water, thus favoring the condensation reaction and the formation of siloxane bridges (Si-O-Si) and larger pore sizes. Contrarily, low H_2O/Si molar ratio (<10) tends to inhibit the condensation reactions, thus favoring the formation of silanol groups (Si-OH) and pore sizes ~ 1 nm or lower. Therefore the gel structure, which contains weakly branched networks, tends to collapse under inhibited condensation reaction conditions. Hence, the formed gel is characterized by exhibiting micropores [3, 27, 31].

Aging, drying, calcination and synthesis procedure affect the micro structure of the layer. Polymeric cross-linking occurs due to heat treatment which further gives strength to the network. As the amount of the alcohol increases, particle size decreases. Structural changes occur from microporous to mesoporous network of the layer due to increasing alkyl chain of solvent. Acid catalysis leads to smaller pore size with weak branched polymer. Generally, membrane produced by base catalysis contains larger pores in colloidal sols. To optimize sol with smaller pores, catalyst concentration and aging time are very important parameters. Catalyst concentration

also affects condensation rate. Low condensation rate is necessary to avoid damage of network during drying stage [32].

2.2.2. Tailoring the porosity of microporous silica materials

As shown above, sol-gel derived microporous silica materials are ideal precursors to prepare membranes with the molecular dimensions required to separate a large gas molecule from a small one. Several works have been performed and intensively cited in the literature in order to prepare unsupported/supported microporous silica/modified silica membranes towards molecular sieve applications with enhanced properties. One of these properties is tailoring the porosity of microporous silica materials to be enhanced as membrane precursor. There are three strategies that enable control of pore size of silica/modified silica materials [6, 33, 34]:

- Solvent-templating of the silica framework (Aerogel, Xerogel).
- Surface derivatization of pre-formed pore networks with well-defined molecular species.
- Template-based approaches (hybrid organic-inorganic materials).

2.2.2.1. Solvent-templating

During drying process the rate at which the solvent can be removed is ultimately determined by the distribution of porosity in the gel. Hence, the formed silica gel is mainly depend on the drying process in order to obtain either aerogel (structure of the gel is preserved) or xerogel (the gel collapses). Besides, during the drying process the development of capillary stress in the pore fluid causes shrinkage of the silica matrix. This shrinkage in turn causes a reduction in pore volume and average pore size. Thus in order to create pores of molecular dimension required for molecular sieving is necessary to promote drying shrinkage. The conventional view of drying shrinkage is that it continues until capillary stress P_C is balanced by the network resistance as expressed in the following equation where the left side represents the capillary stress and the right side, the network modulus [35]:

$$P_c = -\ RT/V_m \ln(P|P_0) = K_0/m\beta C_n\ [(h_0|h)^m - 1] \qquad 2.1$$

Where:

- V_m is the molar volume of the pore liquid.

- K_0 is the initial network bulk modulus at the gel point.
- β and C_n are constants that depend on Poisson's ratio and the ratio of the network and skeletal moduli.
- h_0 is the film thickness at the gel point.
- h is the final film thickness.

However, the balance between the capillary tension and the network resistance (viscosity or modulus) control the final film thickness, pore volume, and pore size which are properties crucial to silica membrane performance. In the case that K_0 is designed to be low, which occurred through catalytic control of the sol-gel reaction, and drying is carried out at low relative pressure (P/P_0). Complete collapse of the developing gel network will occur resulting in small pores within the silica network. This is because the capillary stress, the imposed drying stress, may always exceed the network resistance [36]. Brinker *et al.* demonstrated that by simply changing the solvent composition, it is possible to vary the transport limiting pore size in the approximate range 0.3 to 0.8 ±0.05 nm [37]. The limitation of this approach is that the small pores, which are needed for high selectivity, are obtained at the expense of volume fraction porosity.

2.2.2.2. Surface derivatization

This strategy can be used to modify or "derivatize" the pore surface of the silica matrix. It consists on the fact that certain alkoxides of transition metal, such as Ti and Zr, have more tendencies to interact with water molecules and subsequently undergo hydrolysis reactions. This phenomena can be describe by the following reaction [33]:

$$M\text{-}OH_{surface} + X_X M^* R_{N-X} \longrightarrow M_{surface}\text{-}O\text{-}M^* R_{N-X} X_{X-1} + HX$$

Where M and M* are metals, N represents the coordination number of the transition metal, R is an organic ligand and X is a halide or alkoxide ligand. It could be possible in some cases that the surface chemistry is altered when M ≠ Si. Microporous membranes of titania and zirconia have been prepared. Although the chemical stability of the membrane increases through derivatization process, the preparation of transition metals membrane is a big challenge. Because the tendency to crystallize at relatively low calcination temperatures and the difficulty to synthesize stable polymeric sols in the nanometer region. These kinds of membranes have shown

permeabilities and selectivities for gases that are much lower than those of pure silica membranes [38-40].

2.2.2.3. Template-based approaches

This is the main approach that has been performed in the present thesis to prepare and modify the microporous silica materials to be used as precursor membrane material. Beside, by this approach a novel sol-gel derived microporous silica material was achieved and developed via metal-doping process. This approach depends on preparation of organic-inorganic hybrid materials, which differentiate from traditional polymer composites with respect to the relative sizes of organic and inorganic domains and the level of phase homogeneity. These materials combine the advantages of the inorganic material (e.g., heat resistance, retention of mechanical properties at high temperature, and low thermal expansion) and the organic polymer (e.g., flexibility, low dielectric constant, ductility, and processability of high polymers). Figure 2.10 distinguish between the possible interactions connecting the inorganic and organic species [41]. Class I hybrid materials are those that show weak interactions between the two phases, such as Van der Waals, hydrogen bonding or weak electrostatic interactions. Class II hybrid materials are those that show strong chemical interactions between the components. Because of the gradual change in the strength of chemical interactions it becomes clear that there is a steady transition between weak and strong interactions. For template-based approaches, the organic templates can be classified as covalently or non-covalently organic templates bonded to the siloxane network [30, 34, 42, 43]. The following section will discuss the benefit of template-based approaches for silica-based membrane modification.

2.2.3. Modified microporous silica membranes

Having said and showed that microporous silica materials are considered as promising membrane materials because of the possibility for tailoring their porosity. Other properties can be developed and enhanced such as the silica surface, i.e. surface modification, in order to achieve new materials thanks to the sol gel technique. The surface of the silica sol can be modified by substitution of the silanol groups for different organofunctional groups. This can be achieved by direct substitution of the silanol groups for organic groups, these organic groups are however quickly hydrolyzed in both acidic and alkaline water solutions [44], limiting

their use to completely water free applications. Surface modification can also be achieved via condensation of organofunctional alkoxysilanes to the surface of the silica sol, which is much more stable towards hydrolysis due to the organic group being attached by a carbon-silicon bond and new hybrid material can be achieved (Figure 2.11).

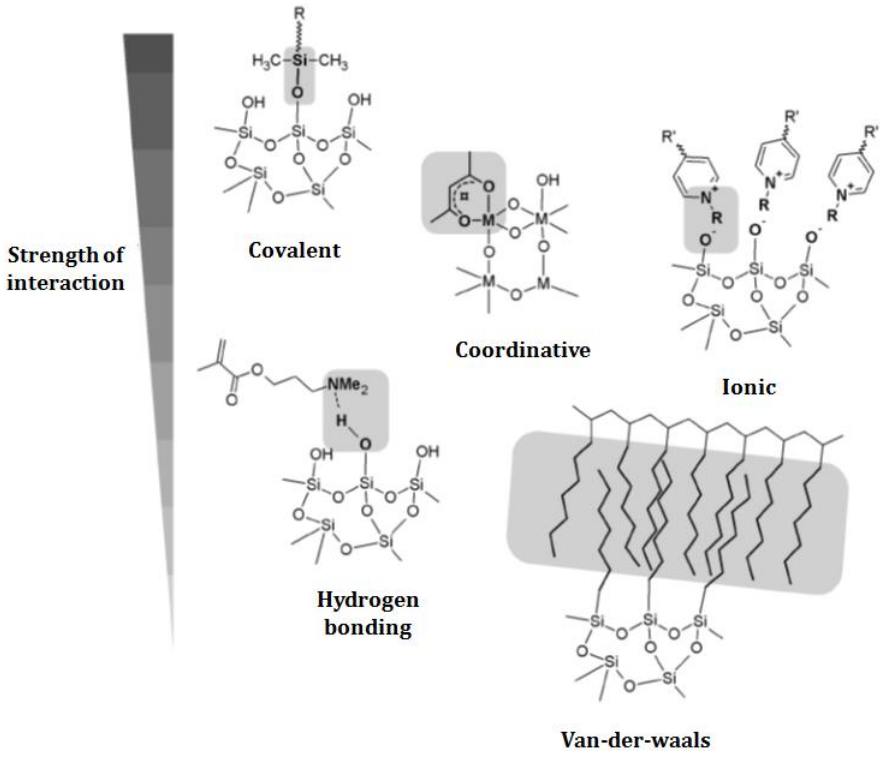

Figure 2.10. Selected interactions typically applied in hybrid materials and their relative strength.[41]

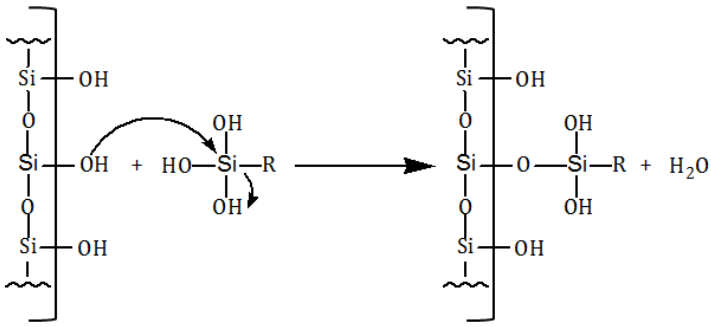

Figure 2.11. Condensation of a hydrolyzed trialkoxysilane to the silica surface.

The present thesis is related to preparation of hybrid materials using covalently organic templates bonded to the siloxane network. The most common precursor that was used to incorporate organic groups within the oxide network is methyltriethoxysilane (MTES) which contains methyl groups as a covalently bonded organic template. The hybrid material can be prepared via co-condensation method between TEOS and MTES, and hence materials with organic residues anchored covalently to the pore walls prepared. The chemical reactivity of the organic template is important to be known, i.e. to investigate their hydrolysis and condensation processes. For MTES, the hydrolysis and condensation rate at room temperature is higher than that of TEOS, the isoelectric point is at a higher pH and MTES has a smaller number of reactive ethoxy groups [45]. Therefore, the formation of xerogels with microporous structure requires controlling the addition time of MTES to the TEOS as well as the whole reaction time [29]. Besides, it is also possible that different type of silica network is formed with MTES than from pure TEOS. This trend has opened new frontiers in the field of microporous silica membrane materials for molecular sieve applications, as new properties can be achieved via this modification. For example, the surface chemistry of these hybrid materials can be altered by the processing gas used for partial sintering, calcination, and pyrolysis of the organic constituents. Therefore, there are two strategies depending on the calcination process of these hybrid materials.

When the organic templates ligands describe above are pyrolyzed under inert atmosphere, such as N_2 or Ar, the membrane is rendered hydrophobic feature. The

idea of doing so is the prevention of the burnt-off the organic template and hence, the membrane water resistance increases [29, 46]. By this strategy, researchers were able to overcome the hydrophilicity problem of the silica membranes. Briefly, silica derived membranes undergo structural degradation when exposed to water, leading to a loss of selectivity [43]. Silica surface materials are prone to rehydration via a mechanism of physisorption of H_2O molecules on silanol groups (Si-OH), via intermolecular hydrogen bonding. As a result, H_2O assists the breakage of Si-O-Si bonds. Therefore, hydrolysed surface siloxanes may become strained, which act as strong acid–base sites, having a rapid uptake of water and becoming mobile [47]. Duke *et al.* [47] proposed that the mobile and strained hydrolysed siloxane groups migrate to smaller pores where they undergo re-condensation to block the pore, whilst the larger pores become even larger. Hydro-stability is therefore a serious problem for the deployment of silica based membranes for molecular sieve applications such as gas separation. Thanks to that strategy by which modification of silica surface can be performed. Hence, the interaction of water molecules with the membrane structure is minimizing.

On the other hand, if the calcination process is performed under oxidizing atmosphere, this leads to create porosity by the removal of the organic constituents. This removal should create pores that mimic the size and shape of the organic constituents [48]. Raman *et al.* [48] have described a strategy for making inorganic membranes using fugitive organic ligands as micropore templates. Organic ligands embedded in a dense inorganic matrix are removed to create a continuous network of micropores. Ideally the organic ligand volume fraction is used to control porosity and hence flux, independently of selectivity, which depends on the ligand size and shape. In order to successfully implement this approach the following criteria must be satisfied:

- The organic ligands must be uniformly incorporated in the inorganic matrix without aggregation or phase separation to avoid creating pores larger than the size of the individual ligands.
- The synthesis and processing conditions should result in a dense embedding matrix so that pores are created only by template removal.
- Template removal should be achieved without collapse of the matrix, so that the pores created preserve the original size and shape of the template.

- After the first three criteria are satisfied, pore connectivity may be achieved by exceeding some percolation threshold of the organic ligands.

Although this strategy has a significant effect on the effect of separation properties of membrane as reported by Raman *et al.* [48], this come at the expense of the membrane hydrophobicity, resulted from the burnt-off the organic templates. These kinds of modified silica membranes have shown a high hydrothermal stability compared with the blank (pure) silica [43, 49]. The thermal stability for MTES as organic template molecule incorporated within the silica matrix was reported to be between 400 and 500 °C either in inert or oxidizing atmosphere [29, 46, 50, 51]. On the other hand, several works have investigated the stability of silica membranes using non-covalently bonded carbon chain surfactants (i.e. as templates) and reported in the literature [30, 42, 43].

The trend to improve the properties of silica membranes towards molecular sieve applications is a topic of growing interest in the research field. Another strategy has attracted the attention of researchers during the last decade to reduce the degradation of hydrophilic silica membranes. This strategy depends on modification of silica structure through the doping of metals or metal oxides within the silica matrix. Very recently, a limited number of research works has been published on high quality metal-doped silica membranes. These metal-based membranes can be prepared via sol–gel or chemical vapour deposition (CVD) methods. For sol-gel method, which was used for unsupported or supported silica membranes preparation, metal oxides or metal-doped silica sols were prepared through the hydrolysis and condensation of TEOS in ethanol and hydrogen peroxide (H_2O_2) or nitric acid with metal salts, such as hydrated cobalt and nickel nitrate salts or niobium alkoxide. Fine control of the silica matrix and pore size tuning was possible using sol-gel processes [52-56].

Fotou *et al.* [57] have reported the doping process through sol-gel method of alumina and magnesia by mixing pure silica sols with ethanol solutions of the metal salts. Alumina doping of 3% and 6% did not change the silica structure and gave enhanced stability against hydrothermal treatment. The magnesia doping of 3% appeared to significantly reduce the silica surface area and not provide enhanced stability. Gu *et al.* [58] have enhanced hydrothermal stability using 3% alumina

doping in CVD membranes and achieved a stable 45% hydrogen permeance reduction after long-term exposure to steam. Igi *et al.* [53] have investigated and characterized the hydrothermal stability of cobalt-doped silica with varying cobalt composition prepared through sol-gel method. The hydrothermal stability of cobalt-doped silica membranes was enhanced at 500 °C under a steam pressure of 300 kPa, where H_2 permeation performance was observed. On the other hand several research works have been performed on nickel doping as well as doping the silica matrix with cobalt to improve hydrothermal stability [52, 55, 59-62]. Darmawan *et al.* [63] reported the effect of iron oxide embedded in silica matrices as a function of Fe/Si molar ratio and sol pH. The effect of sol pH was found to be less significant than the Fe/Si molar ratio in the formation of molecular sieve structures derived from iron oxide silica. Other inorganic oxides such as MgO, TiO_2, ZrO_2 and Al_2O_3 have also been used to improve the performance of membranes in presence of steam [64-67].

The structure of the metal-doped, such as cobalt, in the silica matrices was reported to be in oxide form, which chemically reduced to pure metal by a flow of hydrogen at elevated temperature. These trends, the presence of metal oxide and pure form, were supported by X-ray characterization and Fourier transform infrared characterization (FTIR) [53, 56]. However, the characterization of metal-doped silica membranes and xerogels reported in the literature is also limited regardless the gas permeance for the supported one. In fact the structure of the metal-doped in the silica matrix continues to be controversial. One possible hypothesis for that is the presence of the strong framework by the formation of Si-O-M linkage, for example M= Co [53] or Al [58]. Other possible hypothesizes were intensively reported in the literature [3, 4, 68-70]. In some cases related to the performance of metal-doped silica membranes, the gas flux and selectivity decrease within few hours of testing of the membrane in the presence of steam. Kanezashi *et al.* [52] found that hydrogen and nitrogen permeance decreased by 60% and 93%, respectively up on exposure nickel-doped membrane (33%) to high temperature water vapour, favoring high H_2/N_2 selectivity. Although these metal-doped silica membranes have shown high hydrothermal stability, they are still hydrophilic membranes as they can absorb water as reported by Uhlmann *et al.* [56] concerning the unsupported cobalt-doped silica membranes. However, the cobalt-doped silica xerogel had a lower water adsorption capacity than the pure silica xerogel.

As shown above, the modified silica-based membranes possess new properties compared with the blank silica. Thanks to the facile and effective sol-gel technology which enable the modification process.

Now some questions may be raised:

- What will be achieved if the doping process is performed for organic templated silica matrix (hybrid silica)?
- Are there new properties that can be developed and achieved?
- If so, would it be possible to be used as silica membrane precursor for molecular sieve applications?

These questions will be answered throughout the next chapters.

2.3. Characterization techniques for microporous silica membranes

The characterization techniques that are used for silica or modified silica membranes depend on whether the silica or modified silica membranes are supported or not. Concerning the supported silica or modified silica membranes, as mentioned in chapter 1, the permeance of microporous membranes is an exponential function of the temperature whereas in mesoporous membranes it decreases with the square root of temperature. Therefore, the study of the permeance of a gas as function of the temperature is an interesting tool to indicate either the presence or absence of defect-free microporous and mesoporous layers. On the other hand, for the unsupported one several characterization techniques can be used for that purpose as will be mentioned.

2.3.1. Hydrophobicity of the microporous silica membranes

The hydrophobicity of the silica membrane materials results from the substitution of hydroxyl groups on the surface by organic groups. Possible ways are available for hydrophobicity measurements such as:

2.3.1.1. Contact angle measurements

The contact angle (θ) is the angle, conventionally measured through the liquid, where a liquid interface meets a solid surface. It allows quantifying the wettability of a solid surface by a liquid. It is generally, but rather arbitrarily assumed that $\theta < 90°$ indicates that the solid is partially wetted by a liquid (for example water). Surfaces characterized by a contact angle of water smaller than 90° are usually termed

hydrophilic. Hydrophilic means literally "water preferring", and drops of water placed at such surfaces should spread spontaneously forming a thin water film at the surface when θ ≈ 0° (Figure 2.12). The contact angle θ > 90° indicates non-wetting and hence the surfaces are called hydrophobic. Drops of water tend to form "beads like structure" on hydrophobic (water rejecting) solid surfaces. Surfaces on which the water contact angle is above 140° are termed superhydrophobic and can be obtained from the hydrophobic ones by appropriate modifications [71, 72]. This kind of measurements for the unsupported silica/modified silica membranes give an idea related to the water silica surface interaction. In order to eliminate the capillary effect of the porous supports on the real water contact angle values [73], silica membranes can be coated on a smooth glass substrate for that purpose [50, 74]. This is the technique that was used in the present thesis to investigate the hydrophobicity of the unsupported modified silica membrane; other methods were reported in the literature and briefly mentioned bellow.

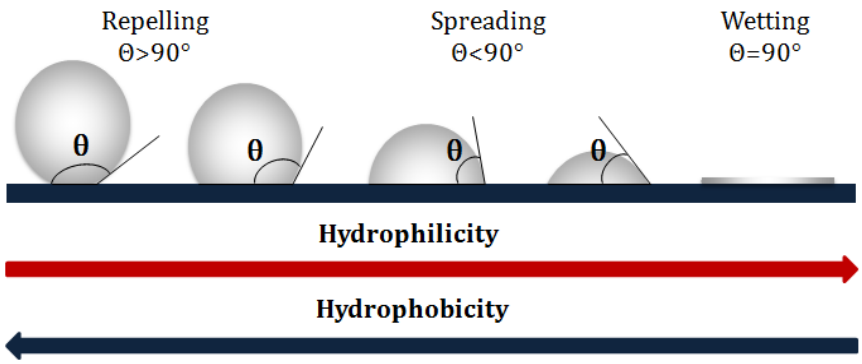

Figure 2.12. Water drop behavior and contact angle values at solid of different hydrophobicity.

2.3.1.2. Hydrophobicity index

The hydrophobic index (HI) represents the hydrophobic effect which lies in the fact that water interacts with itself much more strongly than it does with nonpolar groups. The effect originates from the disruption of highly dynamic hydrogen bonds between molecules of liquid water. For instance, the polar chemical groups, such as OH group in methanol do not cause the hydrophobic effect. However, a pure hydrocarbon molecule, for example octane, cannot accept or donate hydrogen bonds to water. Introduction of octane into water causes disruption of the hydrogen bonding network between water molecules [75, 76]. Therefore, hydrophobic index, which can be represented as HI = x_{octane}/x_{water}, is calculated as a measure of the relative affinity of the sample to these sorbents. As blank silica is hydrophilic so that it has HI value < 1 which indicates it favors water absorption. On the contrary the organic tempalted silica, with CH_3 on the surface, has HI value > 1, which indicates it has high tendency to absorb hydrocarbons [29, 77].

2.3.1.3. Water adsorption isotherms

The water sorption isotherm is the relation between the measured weight adsorbed of water as a function of partial pressure. The sorption isotherm indicates the corresponding water content value at a given, constant temperature. If the composition or quality of the material changes, then its sorption behavior also changes [78]. Hence, the initial shape of the water adsorption isotherm at low partial pressure is determined by the amount of methyl functional groups, for modified silica membrane materials, and the amount of hydroxyl groups, for the blank one. Therefore, hydrophilic silica materials have an initially high water adsorption capacity at very low relative pressures and then show a large increase in adsorption. On the other hand, hydrophobic materials, such as the organic templated silica , have a low water adsorption capacity at very low relative pressures, followed by a small increase in adsorption [42]. This technique is an interesting way for investigation the hydrophobicity of the unsupported organic-templated silica membranes. In some cases after the heat treatment of these materials at elevated temperature, where the pyrolysis of the organic templates occurs, a proportion of the organic templates stay trapped in the silica matrix [51], and hence this assists the ability of the silica material to reduce water adsorption [42].

2.3.2. Thermogravimetric Analysis (TGA)

Thermogravimetric Analysis is a thermal characterization technique in which a sample is subject to heat in a controlled atmosphere, an inert or oxidizing atmosphere, to observe its thermal degradation pattern. The mass of a substance is monitored as a function of increasing temperature with constant heating rate. TGA is commonly used to determine selected characteristics of materials that exhibit either mass loss or gain due to decomposition, oxidation, or loss of volatiles (such as moisture or organic solvents). It can be used for [79]:

- Materials characterization through analysis of characteristic decomposition patterns.
- Studies of degradation mechanisms and reaction kinetics.
- Determination of organic and inorganic content in a sample.

Therefore, in the case of organic template silica materials, this technique offers a possible way by which the stability of organic template in an inert or oxidizing atmosphere can be examined [46, 50, 51, 80].

2.3.3. Fourier Transform Infrared- Attenuated Total Reflectance Spectroscopy (FTIR-ATR)

Fourier transform infrared spectroscopy (FTIR) is a characterization technique in which exposure of a sample to an IR beam yields characteristic peaks of various chemical bonds present in the sample. The attenuated total reflection (ATR) technique operates by measuring the changes in molecular vibration that occur in a totally internally reflected infrared beam when the beam comes into contact with a sample. This internal reflectance creates an evanescent wave that extends beyond the surface of the crystal into the sample held in contact with the crystal [81]. The most characteristic IR bands for silica/modified silica membranes appear in the range from ~ 500 to ~ 1400 cm^{-1} which are shown in Table 2.1.

2.3.4. X-Ray Diffraction (XRD)

X-ray diffraction (XRD) is a versatile, non-destructive technique that offers detailed Information about the chemical composition and crystallographic structure of solid matters which can be described as [82]:

Table 2.1. Characteristic bands (cm^{-1}) in FTIR of spectra silica/modified silica membrane materials.

Bands origin	Silica membrane materials			
	Blank silica	Organic templated silica	Metal-doped silica	Ref.
Si-O-Si*	~1020-1090 and ~770-800			[83, 84]
Si-OH*	~930-950			[80, 84]
CH_3 Vibration	–	~1270	–	[29, 84]
Co(III)-O Vibration	–	–	~570 and ~660	[56, 68]

* These bands are common in silica/modified silica membrane materials. The position of the bands depends on whether the sample is dried or calcined.

- Amorphous: The atoms are arranged in a random way similar to the disorder that could be found in a liquid.
- Crystalline: The atoms are arranged in a regular pattern, and there is a smallest volume element that by repetition in three dimensions describes the crystal. This smallest volume element is called a unit cell which its dimensions can be described by three axes a, b, c and the angles between them alpha, beta and gamma.

This technique is commonly used for metal-doped silica membranes in order to investigate the structure of the metal-doped in the silica matrices. This depends mainly on the calcination process as well as on the metal amounts [50, 53]. For instance, the presence of the strong framework by the formation of Si-O-M linkage is more dominant if the amount of the metal is low. On the other hand, the crystal structure of the metal will be more dominant if the amount of the metal is high [50, 51, 68]. In that latter case, the crystalline size can be determined from the line broadening of the diffraction line at $2\theta = 36.8°$ using the following Scherrer equation (eq. 2.1) [85]:

$$\tau = \frac{K\,\lambda}{\beta \cos\theta} \qquad 2.2$$

Where:

- τ is the crystalline size.
- K is a dimensionless shape factor, with a value close to unity. The shape factor has a typical value of about 0.9, but varies with the actual shape of the crystallite.
- λ is the X-ray wavelength.
- β is the line broadening at half the maximum intensity.
- θ is the Bragg angle.

XRD analysis by Kanezashi *et al.* [60] showed that nickel-doped silica resulted in strong NiO peaks upon calcination at 500 °C. Ikuhara *et al.* [59] further showed that NiO phase changed to pure Ni upon reduction in a H_2 atmosphere. Similarly, cobalt-doped silica resulted in the formation of Co_3O_4 peaks upon calcination at 400–600 °C and the reduction to CoO and Co under calcinations in H_2 atmosphere at 600 °C [53, 56].

2.3.5. Solid-state silicon-29 nuclear magnetic resonance spectroscopy (^{29}Si NMR)

NMR is a research technique that exploits the magnetic properties of certain atomic nuclei, therefore it is the most widely applied magnetic spectroscopy method. It is an important tool for investigating molecular structures and molecular dynamics of both organic and inorganic compounds. The impact of NMR spectroscopy on the research work has been substantial because of the range of information and the diversity of samples, including solutions and solids. When the nuclei of certain atoms are immersed in a static magnetic field and exposed to a second oscillating magnetic field, NMR phenomenon occurs. This phenomenon depends upon whether the nuclei possess a feature called spin, which is a small magnetic field, and will cause the nucleus to produce a NMR signal. Of the naturally occurring isotopes ^{28}Si (92.21%), ^{29}Si (4.70%) and ^{30}Si (3.09%), only ^{29}Si has a spin 1/2 and therefore a magnetic moment [86].

The first major investigation of ^{29}Si NMR of inorganic materials was performed by Lippmaa *et al.* [87, 88], who found a correlation between chemical shift and extent of polymerization in silicate crystals. Since then, ^{29}Si NMR has found significant application in examining the structures of silica-based materials. Besides, it is an

important technique to investigate the hydrolysis and polycondensation processes of the silica network formation. The silicon center in the network can be described by which is called Q^n distribution, where n = 0 to 4. In the case of organic template silica another term is used, referred to as T^n distribution, for differentiation from the silicon nomenclature (Q). This T^n distribution is assigned to the presence of organosiloxane [50, 51, 74, 80].

2.3.6. Gas adsorption/desorption measurements

Gas adsorption is a process that occurs when a gas accumulates on the surface of a solid (adsorbent), forming a molecular or atomic film (the adsorbate). The term sorption encompasses both processes, while desorption is the reverse process. This technique is widely used for characterization of a variety of porous solids, by which the determination of the surface area and pore size distribution of the materials can be concluded. Several procedures have been devised for determining the amount of gas adsorbed. Volumetric methods are generally employed for measuring gas isotherms at specific temperatures. For instance, N_2 isotherms are measuring at temperature of 77 K whereas CO_2 and Ar isotherms are measuring at temperature of 273 K and 87 K, respectively [29, 89]. The isotherm is created point by point by the admission and withdrawal of known amount of gas, with adequate time allowed for equilibration at each point. In fact the shape of the isotherms highly depends on the specific surface interaction and the size of the probe molecule (sorbent gas). Moreover, data that can be determined from the isotherms, such as pore size distribution, depend mainly on the model used for that determination [29, 50, 89, 90]. According to the IUPAC, the adsorption isotherms can be classified as follows (Figure 2.13) [90]:

- Type I isotherm:

It is the most characteristic isotherm for microporous materials which having relatively small external surfaces, such as activated carbons and molecular sieve zeolites. In this case the limiting uptake being governed by the accessible micropore volume rather than by the internal surface area. As it can be observed that this kind of isorthem is concave to the vertical axis (relative pressure), with a knee at low relative pressure.

- Type II isotherm:

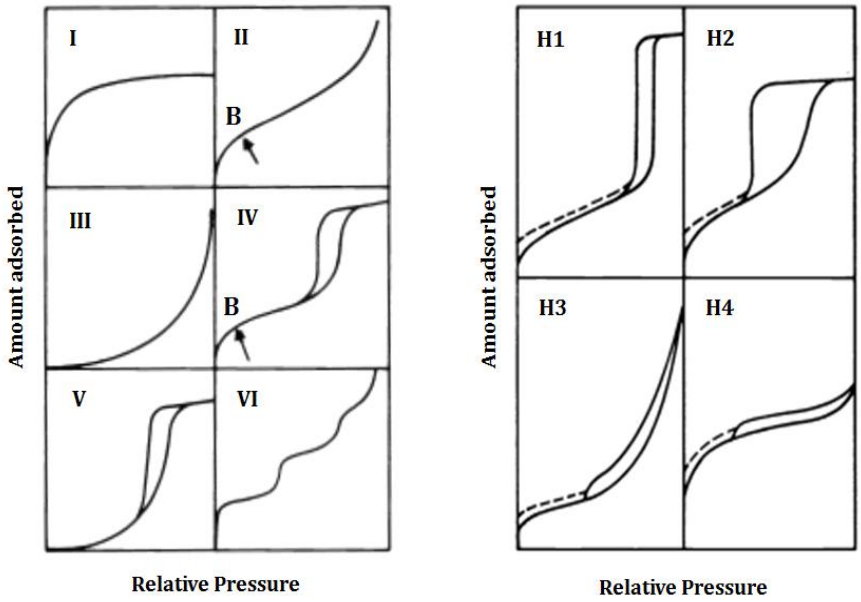

Figure 2.13. Types of physisorption isotherms (left) and types of hysteresis loops (right).[90]

It is the normal form of isotherm obtained with a nonporous or macroporous adsorbent. Besides, this isotherm represents unrestricted monolayer-multilayer adsorption. Point B (Figure 2.13) the beginning of the almost linear middle section of the isotherm, is often taken to indicate the stage at which monolayer coverage is complete and multilayer adsorption is about to begin.

- Type III isotherm:

This kind of isotherms is not common where it is convex to the relative pressure axis over its entire range and therefore does not exhibit point B. There are a number of systems that give isotherms with gradual curvature and indistinct point B. In such cases, the adsorbate-adsorbate interactions play an important role.

- Type IV isotherm:

It is given by many mesoporous industrial adsorbents and present characteristic features called hysteresis loop. It is associated with capillary condensation taking place in mesopores, and the limiting uptake over range of high relative pressure. The initial part of the Type IV isotherm is attributed to monolayer-multilayer adsorption

since it follows the same path as the corresponding part of Type II isotherm obtained with the given adsorptive on the same surface area of the adsorbent in a non-porous form.

- Type V isotherm:

This isotherm is uncommon; it is related to the Type III isotherm in that the adsorbent-adsorbate interaction is weak, but it is obtained with certain porous adsorbents.

- Type VI isotherm:

Consists of several steps in which the sharpness of the steps depends on the system and the temperature, as well as represents stepwise multilayer adsorption on a uniform non-porous surface. The step-height now represents the monolayer capacity for each adsorbed layer and, in the simplest case, remains nearly constant for two or three adsorbed layers.

Hysteresis loops appearing in the multilayer range of physisorption isotherms is usually associated with capillary condensation in mesopores structures. Such hysteresis loops may exhibit a wide variety of shapes. Although the effect of various factors on adsorption hysteresis is not fully understood, the shapes of hysteresis loops have often been identified with specific pore structures. Hence, they can be classified as follows [90]:

- Type H1 loops:

This loop contains two branches that are almost vertical and nearly parallel over an appreciable range of gas uptake. It is often associated with porous materials known, from other evidence, that consist of agglomerates or compacts of approximately uniform spheres in fairly regular array, and hence to have narrow distribution of pore size.

- Type H2 loops:

The H2 loop is especially difficult to interpret: in the past it was attributed to a difference in mechanism between condensation and evaporation processes occurring in pores with narrow necks and wide bodies, but it is now recognized that this provides an over-simplified picture and the role of the network effects must be taken into account. Many porous adsorbents tend to give Type H2 loops, but in such systems the distribution of pore size and shape is not well defined.

- Type H3 loops:

The type H3 loop, which does not exhibit any limiting adsorption at high relative pressure, is observed with aggregates of plate like particles giving rise to slit- shaped pores. These aggregates can be defined as an assemblage of particles that are loosely coherent. In certain respects Type H2 and H3 may be regarded as intermediate between Type H1 and H4 loops.

- Type H4 loops:

This loop contains two branches that remain nearly horizontal and parallel over a wide range of relative pressure. Similarly to the Type H3, Type H4 loop is often associated with narrow slit-like pores, but in this case the Type I isotherm character is indicative of microporosity

A feature common to many hysteresis loops is that the steep region of the desorption branch leading to the lower closure point occurs at a relative pressure which is almost independent of the nature of the porous adsorbent but depends mainly on the nature of the adsorptive. Low hysteresis may be observed extending to the lowest attainable pressures; this could be observed with many systems, especially those containing micropores. Removal of the residual absorbed material is then possible only if the absorbent is out-gassed at higher temperatures. This phenomenon may be associated with the swelling of a non-rigid porous structure or with the irreversible uptake of molecules in pores of about the same width as that of the adsorbate molecule or in some instances with an irreversible chemical interaction of the adsorbate with the adsorbent [90].

2.4. References

[1] L.L. Hench, J.K. West, The sol-gel process, Chem. Rev. 90 (1990) 33-72.
[2] S. Sakka, Handbook of Sol-Gel Science and Technology : Processing, Characterization, and Applications, Kluwer Academic Publishers, Dordrecht, 2005.
[3] C.J. Brinker, G.W. Scherer, SSol-Gel Science : The Physics and Chemistry of Sol-Gel Processing, Academic Press, Boston, 1990.
[4] A.C. Pierre, Introduction to Sol-Gel Processing, Kluwer Academic Publishers, Dordrecht, 1998.
[5] C.J. Brinker, G.W. Scherer, Sol → gel → glass: I. Gelation and gel structure, J. Non-Cryst. Solids 70 (1985) 301-322.
[6] B.J.J. Zelinski, D.R. Uhlmann, Gel technology in ceramics, J. Phys. Chem. Solids 45 (1984) 1069-1090.
[7] Y. Dimitriev, Y. Ivanova, R. Iordanova, History of sol-gel science and technology (review), J. Univ. Chem. Technol. Metallurgy 43, 2, (2008) 181-192.
[8] J.E. Mcgrath, J.P. Pullockaren, J.S. Riffle, S. Kilic, C.S. Elsbernd, Sol-Gel Networks: Fundamental Chemical Studies of Hydrolysis, Condensation and Polysiloxane Toughening of Tetraethylorthosilicate (TEOS) Systems, in: J.D. Mackenzie, D.R. Ulrich (Eds.), Ultrastructure Processing of Advanced Ceramics, Wiley, New York, 1988, pp. 55-75.
[9] C.J. Brinker, G.C. Frye, A.J. Hurd, C.S. Ashley, Fundamentals of sol-gel dip coating, Thin Solid Films 201 (1991) 97-108.
[10] T. Graham, XXXV.-On the properties of silicic acid and other analogous colloidal substances, J. Chem. Soc. 17 (1864) 318-327.
[11] R.K. Iler, The Chemistry of Silica : Solubility, Polymerization, Colloid and Surface Properties, and Biochemistry, John Wiley and Sons, New York, 1979.
[12] W. Stöber, A. Fink, E. Bohn, Controlled growth of monodisperse silica spheres in the micron size range, J. Colloid Interface Sci. 26 (1968) 62-69.
[13] J. Chruściel, L. Ślusarski, Synthesis of nanosilica by the sol-gel method and its activity toward polymers, Mater Sci-Poland 21 (2003) 461-469.
[14] R.J.P. Corriu, M. Henner, The siliconium ion question, J. Organomet. Chem. 74 (1974) 1-28.
[15] H. Schmidt, H. Scholze, A. Kaiser, Principles of hydrolysis and condensation reaction of alkoxysilanes, J. Non-Cryst. Solids 63 (1984) 1-11.
[16] C.J. Brinker, Hydrolysis and condensation of silicates: Effects on structure, J. Non-Cryst. Solids 100 (1988) 31-50.
[17] K.-i. Okamoto, M. Yoshino, K. Noborio, H. Maeda, K. Tanaka, H. Kita, Preparation of Carbon Molecular Sieve Membranes and Their Gas Separation Properties, in: I. Pinnau, B.D. Freeman (Eds.), Membrane Formation and Modification, American Chemical Society, Washington, DC, 2000, pp. 314-329.
[18] C.W. Jones, W.J. Koros, Carbon molecular sieve gas separation membranes-I. Preparation and characterization based on polyimide precursors, Carbon 32 (1994) 1419-1425.

[19] G.Q. Lu, J.C. Diniz da Costa, M. Duke, S. Giessler, R. Socolow, R.H. Williams, T. Kreutz, Inorganic membranes for hydrogen production and purification: A critical review and perspective, J. Colloid Interface Sci. 314 (2007) 589-603.

[20] R.M. de Vos, H. Verweij, High-selectivity, high-flux silica membranes for gas separation, Science 279 (1998) 1710-1711.

[21] A.K. Prabhu, S.T. Oyama, Highly hydrogen selective ceramic membranes: application to the transformation of greenhouse gases, J. Membr. Sci. 176 (2000) 233-248.

[22] M. Naito, K. Nakahira, Y. Fukuda, H. Mori, J. Tsubaki, Process conditions on the preparation of supported microporous SiO_2 membranes by sol-gel modification techniques, J. Membr. Sci. 129 (1997) 263-269.

[23] T. Yoshioka, E. Nakanishi, T. Tsuru, M. Asaeda, Experimental studies of gas permeation through microporous silica membranes, AIChE J. 47 (2001) 2052-2063.

[24] L. Chu, M.I. Tejedor-Tejedor, M.A. Anderson, Particulate sol-gel route for microporous silica gels, Microporous Mater. 8 (1997) 207-213.

[25] R.M. de Vos, H. Verweij, Improved performance of silica membranes for gas separation, J. Membr. Sci. 143 (1998) 37-51.

[26] [26] B.N. Nair, T. Yamaguchi, T. Okubo, H. Suematsu, K. Keizer, S.-I. Nakao, Sol-gel synthesis of molecular sieving silica membranes, J. Membr. Sci. 135 (1997) 237-243.

[27] J.C. Diniz da Costa, G.Q. Lu, V. Rudolph, Y.S. Lin, Novel molecular sieve silica (MSS) membranes: characterisation and permeation of single-step and two-step sol–gel membranes, J. Membr. Sci. 198 (2002) 9-21.

[28] M.C. Duke, J.C. Diniz da Costa, G.Q. Lu, M. Petch, P. Gray, Carbonised template molecular sieve silica membranes in fuel processing systems: permeation, hydrostability and regeneration, J. Membr. Sci. 241 (2004) 325-333.

[29] R.M. de Vos, W.F. Maier, H. Verweij, Hydrophobic silica membranes for gas separation, J. Membr. Sci. 158 (1999) 277-288.

[30] C.-Y. Tsai, S.-Y. Tam, Y. Lu, C.J. Brinker, Dual-layer asymmetric microporous silica membranes, J. Membr. Sci. 169 (2000) 255-268.

[31] C.J. Brinker, K.D. Keefer, D.W. Schaefer, C.S. Ashley, Sol-gel transition in simple silicates, J. Non-Cryst. Solids 48 (1982) 47-64.

[32] H.P. Hsieh, Inorganic Membranes for Separation and Reaction; Membrane Science and Technology Series 3, Elsevier, Amsterdam, 1996.

[33] C.J. Brinker, R. Sehgal, N.K. Raman, S.S. Prakash, L. Delattre, Sol-gel strategies for controlled porosity ceramic materials: Thin film and bulk, Mat. Res. Soc. Symp. Proc. 368 (1994) 329-343.s

[34] N.K. Raman, M.T. Anderson, C.J. Brinker, Template-based approaches to the preparation of amorphous, nanoporous silicas, Chem. Mater. 8 (1996) 1682-1701.

[35] G.W. Scherer, Freezing gels, J. Non-Cryst. Solids 155 (1993) 1-25.

[36] J. Samuel, C.J. Brinker, L.J. Douglas Frink, F. van Swol, Direct measurement of solvation forces in complex microporous media: A new characterization tool, Langmuir 14 (1998) 2602-2605.

[37] C.J. Brinker, S. Wallace, N. Raman, R. Sehgal, J. Samuel, S. Contakes, Sol-Gel Processing of Amorphous Nanoporous Silicas: Thin Films and Bulk, in: T. Pinnavaia, M.F. Thorpe (Eds.), Access in Nanoporous Materials, Springer US, 2002, pp. 123-139.

[38] J. Sekulić, J.E. ten Elshof, D.H. A. Blank, A microporous titania membrane for nanofiltration and pervaporation, Adv. Mater. 16 (2004) 1546-1550.

[39] Y. Hao, J. Li, X. Yang, X. Wang, L. Lu, Preparation of ZrO_2–Al_2O_3 composite membranes by sol–gel process and their characterization, Mater. Sci. Eng., A 367 (2004) 243-247.

[40] J. Etienne, A. Larbot, A. Julbe, C. Guizard, L. Cot, A microporous zirconia membrane prepared by the sol—gel process from zirconyl oxalate, J. Membr. Sci. 86 (1994) 95-102.

[41] G. Kickelbick, Introduction to Hybrid Materials, in: G. Kickelbick (Eds.), Hybrid Materials. Synthesis, Characterization, and Applications, Wiley-VCH Verlag GmbH & Co. KGaA, Weinheim, 2007, pp. 1-48.

[42] S. Giessler, J.C. Diniz da Costa, G.Q. Lu, Hydrophobicity of templated silica xerogels for molecular sieving applications, J. Nanosci. Nanotechnol. 1 (2001) 331-336.

[43] S. Giessler, L. Jordan, J.C. Diniz da Costa, G.Q. Lu, Performance of hydrophobic and hydrophilic silica membrane reactors for the water gas shift reaction, Sep. Purif. Technol. 32 (2003) 255-264.

[44] B. Wind, E. Killmann, Adsorption of polyethylene oxide on surface modified silica – stability of bare and covered particles in suspension, Colloid Polym. Sci. 276 (1998) 903-912.

[45] M.J. van Bommel, T.N.M. Bernards, A.H. Boonstra, The influence of the addition of alkyl-substituted ethoxysilane on the hydrolysis—condensation process of TEOS, J. Non-Cryst. Solids 128 (1991) 231-242.

[46] H.L. Castricum, A. Sah, M.C. Mittelmeijer-Hazeleger, C. Huiskes, J.E.t. Elshof, Microporous structure and enhanced hydrophobicity in methylated SiO_2 for molecular separation, J. Mater. Chem. 17 (2007) 1509-1517.

[47] M.C. Duke, J.C.D. da Costa, D.D. Do, P.G. Gray, G.Q. Lu, Hydrothermally robust molecular sieve silica for wet gas separation, Adv. Funct. Mater. 16 (2006) 1215-1220.

[48] N.K. Raman, C.J. Brinker, Organic "template" approach to molecular sieving silica membranes, J. Membr. Sci. 105 (1995) 273-279.

[49] J. Campaniello, C.W.R. Engelen, W.G. Haije, P.P.A.C. Pex, J.F. Vente, Long-term pervaporation performance of microporous methylated silica membranes, Chem. Commun. 0 (2004) 834-835.

[50] H.H. El-Feky, K. Briceño, E.d.O. Jardim, J. Silvestre-Albero, T. Gumí, Novel silica membrane material for molecular sieve applications, Microporous Mesoporous Mater. 179 (2013) 22-29.

[51] H.H. El-Feky, K. Briceño, M. A. G. Hevia, T. Gumí, Characterization of metal-doped methylated microporous silica for molecular separations, submitted to Microporous Mesoporous Materials.

[52] M. Kanezashi, M. Asaeda, Hydrogen permeation characteristics and stability of Ni-doped silica membranes in steam at high temperature, J. Membr. Sci. 271 (2006) 86-93.

[53] R. Igi, T. Yoshioka, Y.H. Ikuhara, Y. Iwamoto, T. Tsuru, Characterization of Co-doped silica for improved hydrothermal stability and application to hydrogen separation membranes at high temperatures, J. Am. Ceram. Soc. 91 (2008) 2975-2981.

[54] V. Boffa, D.H.A. Blank, J.E. ten Elshof, Hydrothermal stability of microporous silica and niobia–silica membranes, J. Membr. Sci. 319 (2008) 256-263.

[55] S. Battersby, S. Smart, B. Ladewig, S. Liu, M.C. Duke, V. Rudolph, J.C. Diniz da Costa, Hydrothermal stability of cobalt silica membranes in a water gas shift membrane reactor, Sep. Purif. Technol. 66 (2009) 299-305.

[56] D. Uhlmann, S. Liu, B.P. Ladewig, J.C. Diniz da Costa, Cobalt-doped silica membranes for gas separation, J. Membr. Sci. 326 (2009) 316-321.

[57] G.P. Fotou, Y.S. Lin, S.E. Pratsinis, Hydrothermal stability of pure and modified microporous silica membranes, J. Mater. Sci. 30 (1995) 2803-2808.

[58] Y. Gu, P. Hacarlioglu, S.T. Oyama, Hydrothermally stable silica–alumina composite membranes for hydrogen separation, J. Membr. Sci. 310 (2008) 28-37.

[59] Y.H. Ikuhara, H. Mori, T. Saito, Y. Iwamoto, High-temperature hydrogen adsorption properties of precursor-derived nickel nanoparticle-dispersed amorphous silica, J. Am. Ceram. Soc. 90 (2007) 546-552.

[60] M. Kanezashi, T. Fujita, M. Asaeda, Nickel-doped silica membranes for separation of helium from organic gas mixtures, Sep. Sci. Technol. 40 (2005) 225-238.

[61] S. Battersby, M.C. Duke, S. Liu, V. Rudolph, J.C. Diniz da Costa, Metal doped silica membrane reactor: Operational effects of reaction and permeation for the water gas shift reaction, J. Membr. Sci. 316 (2008) 46-52.

[62] D. Uhlmann, S. Smart, J.C. Diniz da Costa, High temperature steam investigation of cobalt oxide silica membranes for gas separation, Sep. Purif. Technol. 76 (2010) 171-178.

[63] A. Darmawan, S. Smart, A. Julbe, J.C. Diniz da Costa, Iron oxide silica derived from sol-gel synthesis, Materials 4 (2011) 448-456.

[64] J.-H. Lee, S.-C. Choi, D.-S. Bae, K.-S. Han, Synthesis and microstructure of silica-doped alumina composite membrane by sol-gel process, J. Mater. Sci. Lett. 18 (1999) 1367-1369.

[65] K. Yoshida, Y. Hirano, H. Fujii, T. Tsuru, M. Asaeda, Hydrothermal stability and performance of silica-zirconia membranes for hydrogen separation in hydrothermal conditions, J. Chem. Eng. Jpn. 34 (2001) 523-530.

[66] M. Asaeda, M. Kanezashi, T. Yoshioka, T. Tsuru, Gas permeation characteristics and stability of composite silica-metal oxide membranes, Mater. Res. Soc. Symp. Proc. 752 (2002) 213-218.

[67] J. Sekulić, M.W.J. Luiten, J.E. ten Elshof, N.E. Benes, K. Keizer, Microporous silica and doped silica membrane for alcohol dehydration by pervaporation, Desalination 148 (2002) 19-23.

[68] S. Esposito, M. Turco, G. Ramis, G. Bagnasco, P. Pernice, C. Pagliuca, M. Bevilacqua, A. Aronne, Cobalt–silicon mixed oxide nanocomposites by modified sol–gel method, J. Solid State Chem. 180 (2007) 3341-3350.

[69] G. Ortega-Zarzosa, C. Araujo-Andrade, M.E. Compeán-Jasso, J.R. Martínez, F. Ruiz, Cobalt oxide/silica xerogels powders: X-ray diffraction, infrared and visible absorption studies, J. Sol-Gel Sci. Technol. 24 (2002) 23-29.

[70] K. Kojima, H. Taguchi, J. Matsuda, Optical and magnetic properties of Co^{2+} ions in dried and heated silica gels prepared by the sol-gel process, J. Phys. Chem. 95 (1991) 7595-7598.

[71] Y. Yuan, T.R. Lee, Contact Angle and Wetting Properties, in: G. Bracco, B. Holst (Eds.), Surface Science Techniques, Springer Berlin Heidelberg, 2013, pp. 3-34.

[72] C.R. Crick, I.P. Parkin, Preparation and characterisation of super-hydrophobic surfaces, Chem. Eur. J. 16 (2010) 3568-3588.

[73] J. Bico, U. Thiele, D. Quéré, Wetting of textured surfaces, Colloids Surf., A 206 (2002) 41-46.

[74] Q. Wei, Y.-L. Wang, Z.-R. Nie, C.-X. Yu, Q.-Y. Li, J.-X. Zou, C.-J. Li, Facile synthesis of hydrophobic microporous silica membranes and their resistance to humid atmosphere, Microporous Mesoporous Mater. 111 (2008) 97-103.

[75] T. Lazaridis, Hydrophobic Effect, John Wiley & Sons, Ltd, Chichester, 2013.

[76] K.M. Biswas, D.R. DeVido, J.G. Dorsey, Evaluation of methods for measuring amino acid hydrophobicities and interactions, J. Chromatogr. A 1000 (2003) 637-655.

[77] S. Klein, W.F. Maier, Microporous mixed oxides—catalysts with tunable surface polarity, Angew. Chem. Int. Ed. 35 (1996) 2230-2233.

[78] S. Inagaki, Y. Fukushima, K. Kuroda, K. Kuroda, Adsorption isotherm of water vapor and its large hysteresis on highly ordered mesoporous silica, J. Colloid Interface Sci. 180 (1996) 623-624.

[79] A.W. Coats, J.P. Redfern, Thermogravimetric analysis. A review, Analyst 88 (1963) 906-924.

[80] J.C. Diniz da Costa, G.Q. Lu, V. Rudolph, Characterisation of templated xerogels for molecular sieve application, Colloids Surf., A 179 (2001) 243-251.

[81] F.M. Mirabella, Internal Reflection Spectroscopy : Theory and Applications, Marcel Dekker, New York, 1993.

[82] A. Guinier, X-Ray Diffraction in Crystals, Imperfect Crystals, and Amorphous Bodies, Dover, New York, 1994.

[83] H. Qi, J. Han, N. Xu, Effect of calcination temperature on carbon dioxide separation properties of a novel microporous hybrid silica membrane, J. Membr. Sci. 382 (2011) 231-237.

[84] Z. Olejniczak, M. Łęczka, K. Cholewa-Kowalska, K. Wojtach, M. Rokita, W. Mozgawa, ^{29}Si MAS NMR and FTIR study of inorganic–organic hybrid gels, J. Mol. Struct. 744–747 (2005) 465-471.

[85] A.L. Patterson, The Scherrer formula for X-ray particle size determination, Physical Review 56 (1939) 978-982.

[86] C. Brevard, P. Granger, Handbook of High Resolution Multinuclear NMR, Wiley, New York, 1981.

[87] E. Lippmaa, M. Maegi, A. Samoson, G. Engelhardt, A.R. Grimmer, Structural studies of silicates by solid-state high-resolution silicon-29 NMR, J. Am. Chem. Soc. 102 (1980) 4889-4893.

[88] E. Lippmaa, M. Maegi, A. Samoson, M. Tarmak, G. Engelhardt, Investigation of the structure of zeolites by solid-state high-resolution silicon-29 NMR spectroscopy, J. Am. Chem. Soc. 103 (1981) 4992-4996.

[89] R.V.R.A. Rios, J. Silvestre-Albero, A. Sepulveda-Escribano, M. Molina-Sabio, F. Rodriguez-Reinoso, Kinetic restrictions in the characterization of narrow microporosity in carbon materials, J. Phys. Chem. C 111 (2007) 3803-3805.

[90] K.S.W. Sing, D.H. Everett, R.A. W. Haul, L. Moscou, R.A. Pierotti, J. Rouquerol, T. Siemieniewska, Reporting physisorption data for gas/solid systems with special reference to the determination of surface area and porosity (Recommendations 1984), Pure Appl. Chem. 57 (1985) 603-619.

Chapter 3

General Objectives of the Thesis

General objectives of the thesis

The main objective of the present thesis is combining both template-based approach and metal-doped approach to develop and achieve novel silica material with well enhanced surface and microstructural properties and subsequently, the use of the novel material as silica membrane precursor to prepare the proper membrane for molecular sieve silica applications such as gas separation. The detailed objectives of the present thesis are the following:

1- The synthesis and development of novel unsupported silica membrane by sol-gel technique.

It implies the first synthesis of the novel hybrid silica material. Preparation by acid-catalyzed hydrolysis and condensation of TEOS and MTES (co-precursor method) with 50:50% TEOS:MTES molar ratio is involved. Afterwards, Cobalt-doping within the hybrid silica matrix is considered. The characteristic features of the four different silica membrane materials, which are:

- Blank silica membrane material.
- Hydrophobic silica membrane material (hybrid silica material).
- Metal-doped silica membrane material.
- Hydrophobic metal-doped silica membrane material (metal-hybrid silica material).

are compared by means of contact angle measurements, FTIR, X-ray, solid-state ^{29}Si MAS NMR, TGA and N_2 adsorption measurements.

2- The characterization of the novel silica membrane material and the study of the effect of different MTES and cobalt-doped contents.

Investigation of the influence of the content of both MTES and cobalt-doped needs to be carried out by means of FTIR, X-ray, solid-state ^{29}Si MAS NMR, TGA and N_2 adsorption measurements.

3- The preparation and characterization of the novel microporous silica membrane (supported material).

Two different methodologies are considered; preparation under normal conditions and preparation under clean room conditions. In both methodologies the performance of the novel membrane (cobalt-doped hybrid silica membrane) is compared with the non-doped one. Investigation of the membrane performance

towards gas transport, as well as the governing mechanisms is studied. Gas transport is the proper way for membrane performance characterization and this is by means of study the variation of membrane pressure and temperature. Top silica selective layers are prepared in both methodologies by diluted sols; therefore, the characterization of the diluted unsupported silica membranes (cobalt-doped and non-doped silica membranes) is also performed by means of TGA and microporosity measurements.

Chapter 4

Novel Silica Membrane Material for Molecular Sieve Applications

Development of new silica membranes properties, e.g, molecular sieving properties, has been increasingly gaining importance in the last few years. A novel unsupported silica membrane, referred to as hydrophobic metal-doped silica, was developed by cobalt-doping within the organic templated silica matrix. The novel material was prepared by the acid-catalyzed hydrolysis and condensation process of tetraethylorthosilicate (TEOS) and methyltriethoxysilane (MTES), which is the precursor for methyl ligand covalently bounded to the silica matrix. The synthesis and surface properties of the novel unsupported silica membrane as well as the unsupported blank silica and modified silica membranes were revealed by surface and microstructural techniques, such as water contact angle measurement, FTIR, X-ray, solid-state ^{29}Si MAS NMR, TGA and N_2 and CO_2 adsorption measurements. The results showed that the thermal stability of the organic templated silica matrix was enhanced by cobalt-doping process. A hydrophobic microporous silica membrane material with high thermal stability up to ~ 560 °C in oxidizing atmosphere and a narrow pore size distribution centered at 1.1 nm was obtained. Therefore, a novel precursor material for molecular sieve silica membranes applications has been achieved and developed.

Novel silica membrane materials for molecular sieve applications

4.1. Introduction

In recent years microporous materials have attracted considerable attention because of their characteristics features as molecular sieving materials. The use of microporous materials to make membranes for molecular sieve applications such as gas separation is an ever-growing area of research [1]. Over the last decade, microporous silica membranes have been considered to be promising materials for clean-energy systems since they can separate small molecules from gas mixtures based on their different kinetic diameter [2]. Due to the microporous nature of the silica network, silica membranes allow the permeation of small gas molecules such as H_2. Hence, silica membranes with high flux of H_2 as well as high selectivity of H_2 over others gases such as CO_2, N_2 and CH_4 have been prepared by sol-gel method and dip-coating [3, 4]. Sol-gel technique is a simple and effective way for the synthesis of microporous silica membranes. Therefore, from economical point of view, molecular sieve silica membranes are becoming very competitive against traditional non-hydrostable and expensive metal membranes such as palladium and its alloys.

Several studies have been performed to produce high quality silica derived membranes with very small pore size distribution in the region of ~ 1.0 nm or lower [5-9]. These silica membranes are ideal for molecular sieve applications but they suffer from extensive water adsorption if exposed to moisture. This is due to the high affinity between water molecules and hydroxyl surface groups of the silica matrix [10]. In wet atmosphere, such as water gas shift reaction environments where steam together with carbon monoxide are converted to CO_2 and H_2 [11], interaction of the silica membrane with water from process streams leads to degradation phenomena due to dissociation of Si–O–Si bonds. Because of the hydrothermally instability, the hydrogen flux and selectivity decrease within few hours of testing of the membrane in the presence of steam [12, 13]. This trend can be mainly attributed to the hydrophilic nature of silica membranes. It is well documented in the literature that water can be adsorbed on silica materials via the intermolecular hydrogen bonding between water molecules and silanol (hydroxyl) surface groups of silica membranes, thus resulting in further changes in the matrix of silica-derived materials [10, 14, 15]. For that reason, the use of molecular sieve silica membranes requires modifications of these membranes to stand for temperature, pressure and work in presence of

water vapor. These drawbacks have encouraged an increasing research to overcome these limitations and to enable these materials to be used in large-scale industrial applications.

Several novel strategies of synthesis were designed to prepare modified silica membrane materials in order to improve the surface properties of the silica matrix towards molecular sieve applications in moisture environments. Over the last decades, the sol-gel technique was postulated as an interesting strategy to prepare new hybrid organic-inorganic silica-based microporous materials with enhanced properties. For example, surface modification using different organic template agents increase the hydrophobicity of the silica membranes. Using this technique, researchers have prepared molecular sieving architectures by calcining templated sol-gels in inert atmospheres [14-16]. However, such methods may alter the micropore structure of the materials and hinder their molecular separation properties [16, 17]. Templates can be classified as organic covalent ligands, such as methyl groups, or non-covalently bonded, such as surfactants. One remarking case to introduce hydrophobic moieties in the silica membrane material was reported by De Vos *et al.* [16]. Methyltriethoxysilane (MTES) was embedded into a sol-gel process prepared with tetraethylorthosilicate (TEOS), water, ethanol and nitric acid. This process introduces methyl groups to the silica matrix as template agents to enhance hydrophobicity. These silica membrane materials showed high hydrophobicity compared with silica membrane material prepared without MTES. On the other hand, various research groups have used non-covalently bonded organic templates, such as C6 and C16 surfactants [5, 17] and alkyltriethoxysilanes [18], to tailor the pore size of intermediate or top layers of membranes. At high temperature under oxidizing conditions these organic templates trapped in the gel structure are burnt off, thus producing a cavity with similar dimensions to that of the template molecule [19, 20].

Another strategy investigated to modify the silica membrane materials consists in incorporating a metal and/or metal oxide in the sol-gel process to produce metal-doped molecular sieve silica membrane materials. For that purpose metal oxides or metal doped silica sols were prepared through the hydrolysis and condensation of TEOS in ethanol and hydrogen peroxide (H_2O_2) or nitric acid with metal salts, such as hydrated cobalt and nickel nitrate salts or niobium alkoxide. Fine control of the silica

matrix and pore size tuning was possible using sol-gel processes [12, 21-24]. However, metal-doped silica membrane material as cobalt-doped one showed hydrophilic behavior as it can adsorb water, with a lower water adsorption capacity compared with the blank (non-doped) silica membrane material, as reported by Uhlmann *et al.* [25].

For the unsupported silica or modified silica membrane, the microporous structure can be estimated by means of gas sorption as well as the pore size distribution (PSD). PSD is an interesting tool to estimate the pore width of these materials from the adsorption data. However, the microporosity results reported in the literature highly depends on the probe molecules used for the sorption analysis, either N_2, CO_2 and/or Ar. In addition to that, the PSD results could differ somehow depending mainly on the model used for the PSD determination [14-16, 20, 26, 27]. The earlier mentioned strategies (preparation of hybrid silica and metal-doped silica) enabled researchers to produce sol-gel derived microporous silica or modified silica materials. However, the actual values of the pores width for the supported silica or modified silica materials may differ somehow compared with the PSD results for the unsupported one. This is because there are several factors should be considered such as the support resistance and membrane thickness.

The aim of this work is the preparation of novel unsupported modified silica membrane for molecular sieve applications. The preparation involves cobalt- doping within the matrix of organic templated silica material (hybrid silica). In the present study a novel modified molecular sieve silica membrane material derived from a standard TEOS sol plus MTES and cobalt nitrate salt is prepared and labeled as hydrophobic metal-doped silica membrane material. The present study provides initial results on the synthesis and surface properties of the novel unsupported silica membrane together with a comparison of these aspects with the unsupported blank, hydrophobic and metal-doped silica membrane.

4.2. Experimental part

4.2.1. Materials and methods

Tetraethylorthosilicate (TEOS, 98%, Acros Organics), methyltriethoxysilane (MTES, 98%, Acros Organics), ethanol (EtOH, 96% V/V extra pure, Acros Organics),

nitric acid (HNO_3, Acros Organics) and cobalt nitrate (99% pure, Acros Organics) were purchased from Scharlab. Distilled water was used for the sols preparation.

4.2.2. Preparation of silica membrane materials

The silica sols were prepared by the acid-catalyzed hydrolysis and condensation process. TEOS and MTES were used as the silica precursors mixed with ethanol (EtOH), nitric acid (HNO_3), cobalt nitrate, as metal salt, and distilled water. To avoid the partial hydrolysis while mixing H_2O/HNO_3 mixture with TEOS/EtOH mixture, the latter was placed in an ice bath and then H_2O/HNO_3 mixture was added drop wise under continuous stirring [16]. The different molar compositions investigated in this work as well as the sample notations are listed in Table 4.1. For the cobalt-doping within the hybrid silica matrix, a solution of cobalt nitrate in ethanol was prepared. Ethanol was chosen as the solvent for the salt solution because it was the same solvent used in the sols preparation. Moreover, the nitrate salt was used because it is compatible with the silica sol which was catalyzed by nitric acid [28].

For the blank silica, indicated as B-Si, a mixture of HNO_3/H_2O was added under vigorous stirring to TEOS/EtOH and then the sol was refluxed in water bath at 60 °C for 180 minutes [16].

For the Co-doped silica (Co-Si) the doping was performed by mixing the sol, with the same composition as the blank silica sol, with the ethanol solution of the metal salt. The metal salt to the metal alkoxide (Co:Si) weight ratio used was 3% [28].

For the hydrophobic silica (Hyd-Si) the initial sol, with the same composition as the blank silica sol, was stirred for 165 minutes (1st step). Afterwards, a mixture of MTES/EtOH solution with 1 : 3.8 molar ratio, which had been cooled for 5-10 minutes in ice, was added to the reaction mixture (2nd step) and the final sol was refluxed for an additional 15 minutes [16].

The novel silica sol (Hyd-Co-Si) was prepared as the hydrophobic one but in the second step the sol was mixed with a MTES/EtOH solution plus the ethanol solution of the cobalt salt. The metal salt to the metal alkoxide (Co:Si) weight ratio used was 3%.

All silica sols were allowed to evaporate in a Petri-dish at room temperature so that silica flakes, xerogels, were obtained overnight. Xerogels were crushed finely to obtain powders, which were used for characterization, and calcined in air at a heating and cooling rate of 1 °C/min, and held for 3 hours at 400 °C.

For water contact angle measurements, silica membrane materials were coated on a glass substrate. The coated film of the novel silica material was calcined in air with the same conditions as mentioned earlier. The hydrophobic silica, powder and coated film, were calcined under nitrogen atmosphere, in order to prevent the burn-off of the methyl groups, at a heating and cooling rate of 1 °C/min and held for 3 hours at 400 °C.

In order to compare X-ray of Hyd-Co-Si, two additional samples were prepared. Silica powders were mixed with Co_3O_4 with weight ratio 3%. Cobalt oxide was prepared by calcination cobalt nitrate in air as xerogels. The other one was prepared as the novel sol but with higher weight ratio, 10%, and calcined in air at a heating and cooling rate of 1 °C/min, and held for 3 hours at 400 and 500 °C.

Table 4.1. Molar compositions of the used sols.

Sample	Step	TEOS	MTES	EtOH	HNO_3	H_2O	$Co(NO_3)_2.6H_2O$*
B-Si	1st step	1	0	3.8	0.085	6.4	
Co-Si	1st step	1	0	3.8	0.085	6.4	3 wt%
Hyd-Si	1st step	1	0	3.8	0.085	6.4	
	2nd step	1	1	7.6	0.085	6.4	
Hyd-Co-Si	1st step	1	0	3.8	0.085	6.4	
	2nd step	1	1	7.6	0.085	6.4	3 wt%

* Amounts were calculated in order to prepare solution of 10% wt/vol of cobalt nitrate in ethanol.

4.2.3. Characterization of the silica membrane materials

Water contact angles were measured on a Dataphysics OCA 15EC video-based contact angle system at ambient temperature. Water droplets (3 µl) were dropped onto the coating silica membranes.

Fourier transform infrared characterization was carried out to determine functional groups within the bulk silica matrix using ATR cell (FTIR 680 Plus JASCO). The absorption spectra were recorded in the 500-1500 cm^{-1} range. The spectrum of each sample represents an average of 32 scans. With the aim of comparison, all FTIR spectra were normalized with respect to the maximum absorbance value for each sample.

XRD for phase detection was conducted using a Siemens D500 diffractometer (Bragg-Brentano parafocusing geometry and vertical θ-θ goniometer). The angular 2θ diffraction range was 5° to 70°. The crystalline size was determined from the line broadening of the diffraction line at $2\theta = 36.8°$ using the Scherrer equation (eq. 2.2).

Solid-state ^{29}Si MAS NMR spectra were recorded on a Varian Mercury_Vx 400MHz spectrometer according to the following measurement conditions: 7mm CPMAS probe, 79.577 MHz resonance frequency, 5 µs pulse width, 3 kHz rotation speed, 20 s delay time, and 30 scans. The spectra were fitted using MestReNova fitting software.

Thermogravimetric analysis was used to investigate the processes taking place during the heat treatment. This analysis was carried out for the calcined samples, in a Perkin Elmer model Thermobalance TGA7 device, in synthetic air and in nitrogen with constant flow rate of 290 cm^3 min^{-1} and heating rate of 10 °C min^{-1} from room temperature to 900 °C.

Textural characterization of the synthesized samples was determined by N_2 and CO_2 adsorption/desorption measurements at -196 °C and 0 °C, respectively. Gas adsorption measurements were performed in a homemade fully automated manometric equipment. Before any adsorption experiment, samples were degassed at 250 °C for 4h. The pore size distribution was calculated from the nitrogen adsorption data using the NLDFT model (Non Localized Density Functional Theory) based on a cylindrical pore-equilibrium model.

4.3. Results and discussion

4.3.1. Hydrophobicity of the modified silica membrane materials

The unsupported hydrophobic silica membranes were generally produced by using co-precursor method. In the present work, the hydrophobic properties of TEOS based silica membrane materials were obtained by using MTES as the hydrophobic additive. In the sol-gel process, initially TEOS was acid-hydrolyzed and condensed as described by the following reactions:

Hydrolysis:

$$Si(OC_2H_5)_4 + 4H_2O \longrightarrow Si(OH)_4 + 4C_2H_5OH$$

Condensation:

Water condensation:

$$nSi(OH)_4 \longrightarrow nSiO_2 + 2n\,H_2O$$

Alcohol condensation:

$$Si(OH)_4 + Si(OC_2H_5)_4 \longrightarrow 2SiO_2 + 4C_2H_5OH$$

However, using MTES as a co-precursor in the sol-gel process, the hydrogen from –OH groups on the silica surface are replaced by $\equiv Si-CH_3$ through –O–$SiCH_3$ bonds as shown in the following reaction:

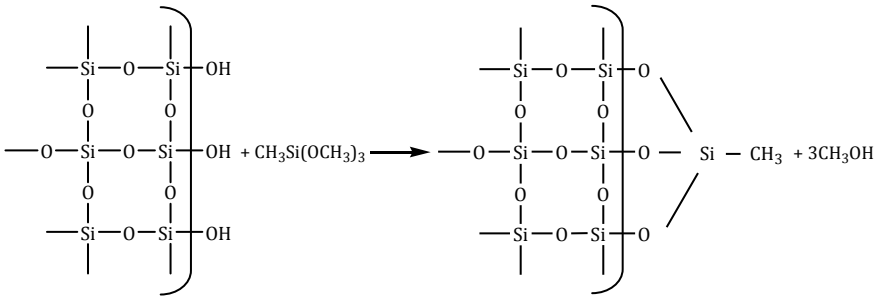

Several methods have been reported in the literature concerning the cobalt-silicon mixed oxide [29-31] among them the sol-gel technique. It is a better way for control the textural properties of the silica matrix as well as an effective way for

cobalt-doping within the matrix on a nanometric scale [32, 33]. Possible hypothesis for the interaction between cobalt species and silica matrix, prepared via sol-gel way, is the formation of Si-O-Co bridges. These bridges were suggested to be formed through the condensation reaction between the silicone complexes $[Si(OC_2H_5)_{4-n}(OH)_n]$ and oxo-hydroxy complexes $[Co(H_2O)_{6-x-y}(HO)_xO_y]$. Oxo-hydroxy complexes can be formed through the acid-base equilibria of the $[Co(H_2O)_6]^{2+}$ aquo-ion, which resulted from the addition of $Co(NO_3)_2.6H_2O$ to the TEOS sol (a pinkish colored solution) [34-36].

Figure 4.1 shows the wettability for silica materials. The water contact angle for the B-Si is smaller than 5° indicating the hydrophilic behavior of this material. Whereas for Hyd-Si is 108.1±3.3° and for the Hyd-Co-Si is 110.9±3.1° indicating in both cases that a hydrophobic surface was obtained. Contact angle measurements correspond to the mean value of the measurements, after 5 analyses, which were performed at different parts of the material surface. It has been reported in the literature that the blank silica showed the superhydrophilicity behavior because of the presence of silanol (hydroxyl) groups on the surface [10, 14-16]. Therefore, they can physically adsorb water via intermolecular hydrogen bonding. When silica materials are modified by organic templates, most of silanol groups are replaced by the hydrophobic group of the organic templates [14]. Uhlmanna *et al.* reported that the cobalt-doped silica and the blank silica membrane materials were hydrophilic as both samples adsorbed water. However, the cobalt-doped silica xerogel had a lower water adsorption capacity than the blank silica xerogel [25]. Superhydrophobic silica film material, i.e. water contact angle higher than 150°, was prepared via sol-gel method using MTES as hydrophobic reagent. Interestingly, the film became superhydrophilic when the material was heated in air at temperature higher than 290 °C [37]. Therefore, the organic templated silica xerogels (hybrid silica) should be calcined in inner atmosphere to prevent the burn-off of the hydrophobic group of the organic templates. Concerning the novel silica membrane material, the cobalt impregnated in the silica matrix may exist as covalently bound cobalt, forming Si-O-Co. This perhaps facilitates the surface to substitute the –OH groups, along with the hydrophobic $-CH_3$ groups, on the surface making the silica surface hydrophobic and decreasing the possibilities for the burn-off of the methyl groups upon heat treatment at 400 °C in air.

4.3.2. Infrared spectroscopy

Figure 4.2 compares the FTIR spectra of the dried, 2a, and calcined, 2b, samples of B-Si, Hyd-Si, Co-Si and Hyd-Co-Si. The IR bands corresponding to silanol and siloxane bonds appear in the range from ~ 600 to ~ 1400 cm^{-1}. For the dried samples, bands at ~ 770 - 800 cm^{-1} and at ~ 1045 cm^{-1} were assigned to siloxane bonds (Si-O-Si). Band at ~ 940 cm^{-1} was assigned to silanol bonds (Si-O-H) [27, 38]. For the calcined samples, the silanol bonds decrease in intensity after the calcination process for B-Si and Co-Si whereas for Hyd-Si and Hyd-Co-Si that band was almost unobservable. This indicates that the calcination process significantly improves the condensation process by enhancing the formation of siloxane bonds [9, 27, 39, 40]. The siloxane bonds at ~ 770 - 800 cm^{-1} are also appearing whereas the band at ~ 1045 cm^{-1} shifted to ~ 1055 cm^{-1}. This shift is due to the shrinkage produced by polymeric bonding, this shift was also obtained for silica and modified silica materials, organic templated silica and metal-doped one [9, 26, 27, 40]. The band at ~ 1270 cm^{-1} for dried and calcined Hyd-Si and Hyd-Co-Si was assigned to asymmetric vibration of the CH_3 group [16, 38]. Tiny small bands at ~ 570 and 660 cm^{-1} for Co-Si and Hyd-Co-Si were assigned to the vibration of Co(III)-O bonds for cobalt, in oxide form Co_3O_4, these 2 bands appeared after the calcination process whereas these bands were no present before the calcination process [25, 34, 41]. This result suggests that the Co-doped in the silica matrix exists not only as covalently bound cobalt, forming Si-O-Co, but also as extremely tiny crystals as will be mentioned in the X-ray section. Moreover, these results strongly prove that the novel silica membrane material possess the characteristic FTIR features of B-Si, Co-Si and Hyd-Si as reported in the literature.

4.3.3. X-ray analysis for the metal-doped membrane materials

The calcined samples of Co-Si and Hyd-Co-Si were X-ray amorphous (as shown in Figure 4.3) indicating that the nature of the cobalt species and their interactions with the silica matrix were strongly depending on both, the cobalt content and the heat treatment. Igi *et al.* [21] reported that as the cobalt content increased from 0-30 mol %, the peak intensity of (100) for Co_3O_4 (2θ = 36.8°) increased. At cobalt compositions > 30 mol %, the peak intensity remained relatively constant. In that later case, certain amount of cobalt form crystalline Co_3O_4 with a size of about 20 nm

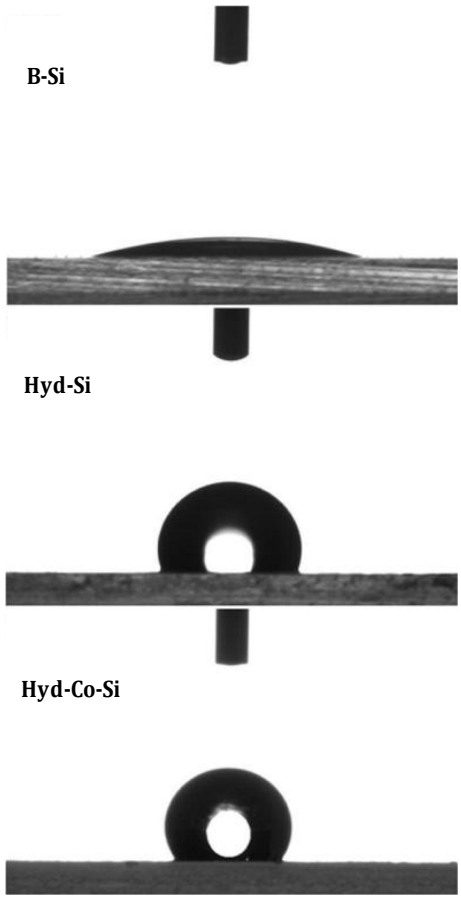

Figure 4.1. Contact angles of silica membrane materials surface.

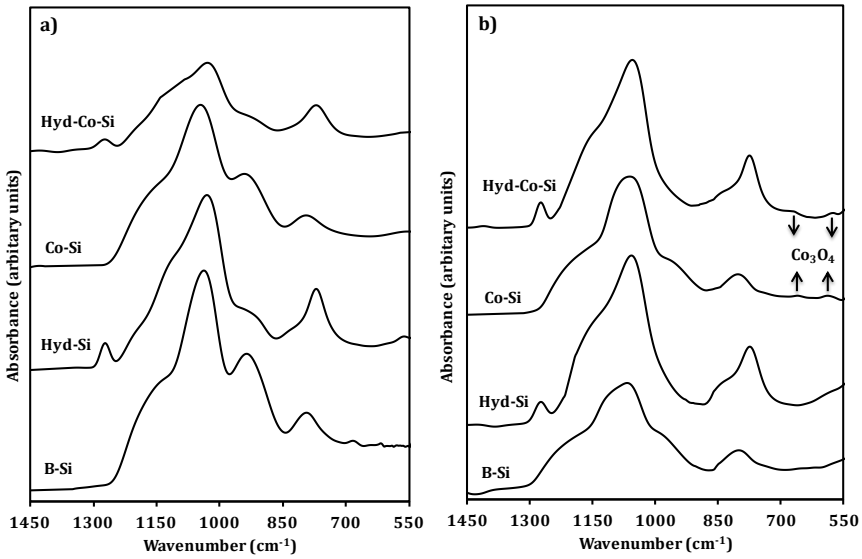

Figure 4.2. FTIR spectra of a) dried and b) calcined silica membrane materials.

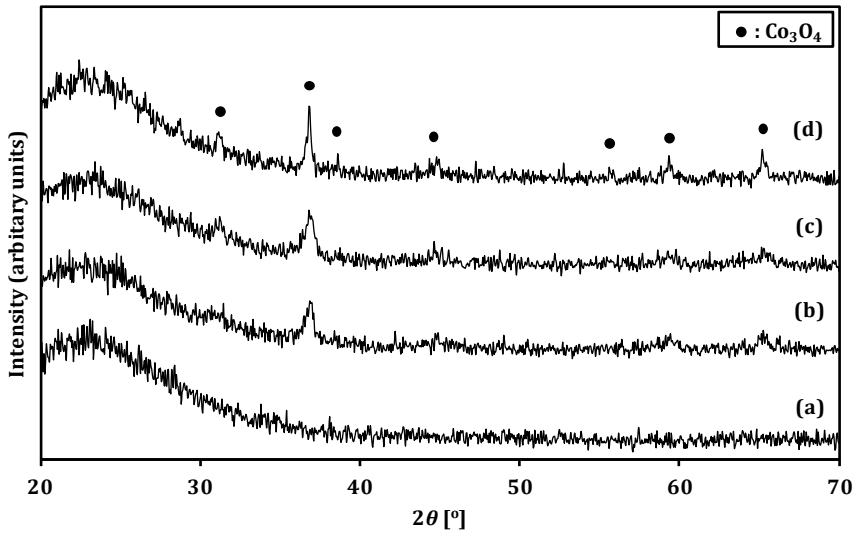

Figure 4.3. XRD diffractogramms of Hyd-Co-Si, (a) 3 wt% Co, (b) 10 wt% Co calcined at 400 °C, (c) 10 wt% Co calcined at 500 °C and (d) mixture of SiO_2 and Co_3O_4. Solid circles represent Co_3O_4 reference pattern.

which exists outside the silica matrix and hence can be detected by XRD. Esposito *et al.* [34] reported the same case and the size of crystalline Co_3O_4 was about 13 nm. Moreover, the sample with lowest cobalt content appeared amorphous after heat treatment at 400 °C and contained Co^{2+} ions which strongly bonded to the silica matrix. However, at high cobalt content the extent of the interaction between Co^{2+} ions and the silica matrix appeared to be low and the formation of crystalline Co_3O_4 was obtained. In the present study, it is also the same case so that as the amount of doped cobalt was increased from 3 wt% to 10 wt%, and silica membrane materials were calcined at 400 and 500 °C, certain amounts of the cobalt impregnated in the silica matrix form crystalline Co_3O_4 with a size of about 6 nm, as determined using the Scherrer equation (eq. 2.2), and hence can be detected by XRD. Moreover, the peak intensity of the mixture of silica powder, SiO_2, and Co_3O_4 (3%) was higher than that of the peak intensity of cobalt-doped in the silica matrix (10%). These results strongly indicate that the cobalt-doped in silica matrix existed not only as crystalline Co_3O_4 powder, but also as noncrystalline compounds, such as extremely tiny or fine particles that could not be detected by XRD. In fact, the structure of cobalt impregnated in the silica matrix is controversial so that the possible hypothesizes for the existence of the cobalt is the following: ionic metal as Co^{2+}; covalently bound cobalt strongly interacting with the silica matrix forming Si-O-Co; or tiny crystal that could not be detected by XRD.

4.3.4. Solid-state ^{29}Si NMR spectroscopy

The surface chemical properties of silica membrane materials can be revealed by the Solid-state ^{29}Si MAS NMR, as shown in Figure 4.4, where the Q^n distribution (describe silicon center in the silica matrix, n= 0 to 4) can be observed. For all silica membrane materials, the resonances at a chemical shift from -90 to -120 ppm were assigned to the structure unit Q^4 [$Si(OSi)_4$], Q^3 [$Si(OSi)_3(OH)$] and Q^2 [$Si(OSi)_2(OH)_2$] silicon atoms, respectively. By Solid-state ^{29}Si MAS NMR investigation the hydrolysis and condensation processes can be monitored. Therefore, the presence of Q^3 and/or Q^2 species provides evidence of incomplete polymerization of the gel structure, which indicates weakly branched networks. These weakly branched networks tend to collapse under inhibited condensation reaction conditions, which is caused by the low H_2O/Si ratio, so that the xerogel is characterized by exhibiting micropores [42,

43]. For Hyd-Si and Hyd-Co-Si, two additional resonances can be observed at chemical shift from -50 to -70 ppm. These two resonances were indicating the presence of organosiloxane which is referred to as Tn, for differentiation form the silicon nomenclature (Q) where [$T^n = RSi(OSi)_n(OH)_{3-n}$, n=1-3, and R=$CH_3$]. The ability of hydrophobic silica membrane materials to repel water molecules is attributed to the presence of condensed species Q^4 and organosiloxane species T^3 and T^2. Hence, the novel silica membrane material possesses these species. The chemical shifts of the species Q^n and T^n are shown in Table 4.2. These resonances at different chemical shifts concerning the novel silica membrane material are in a good agreement with the literature concerning organic templated silica materials [27, 38, 44-48].

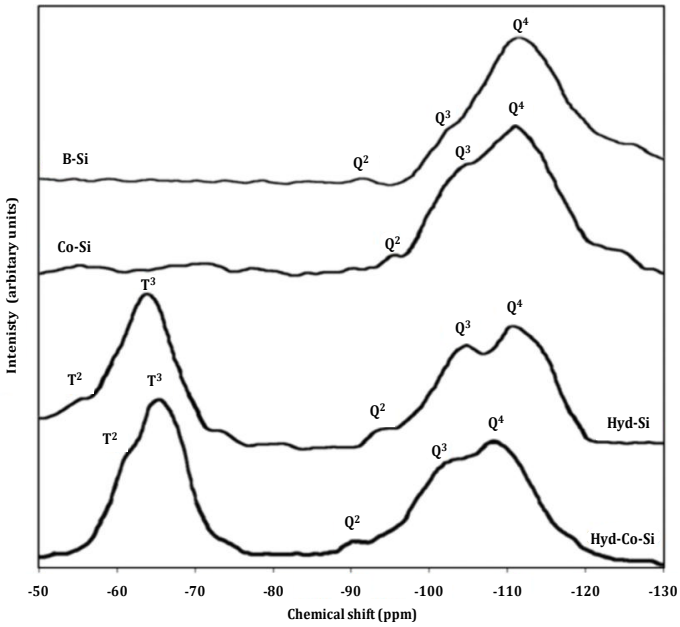

Figure 4.4. Solid-state ^{29}Si MAS NMR spectra of the silica membrane materials.

Table 4.2. Solid-state ^{29}Si MAS NMR of silica membrane materials.

Sample	Chemical shifts (ppm)				
	Q^4	Q^3	Q^2	T^3	T^2
B-Si	-112.69	-102.49	-92.68	-	-
Co-Si	-111.95	-104.75	-95.15	-	-
Hyd-Si	-111.15	-104.63	-93.98	-64.95	-55.92
Hyd-Co-Si	-108.68	-101.93	-90.53	-66.28	-61.48

4.3.5. Thermal stability of the membrane materials

Thermogravimetric results for the calcined samples are shown in Figure 4.5. The analyses were performed under synthetic air flow as well as under nitrogen flow for Hyd-Si and Hyd-Co-Si [16]. The initial weight losses from room temperature to ~ 150 °C are mainly attributed to physisorbed water molecules trapped in the silica matrix [20, 27]. Although the Hyd-Si and Hyd-Co-Si membrane materials are hydrophobic (contact angle > 90°, see Figure 4.1) these water molecules trapped in the silica matrix could be attributed to the presence of some silanol bonds (Si-O-H) on the surface. This is in agreement with solid-state ^{29}Si MAS NMR results where the resonances, Q^3 and Q^2, corresponding to that bond were observed. In some cases the absence of Q^2 indicates that there are only few –OH groups remaining after hydrolysis and condensation processes, and hence a high condensation degree between TEOS and the organic template [14, 44]. Sharp weight losses are observed for the B-Si and Co-Si, as they show the hydrophilic behavior, however the Co-Si is less hydrophilic than B-Si [25]. Hyd-Si was stable up to ~ 450 °C in both atmospheres whereas it can be observed that Hyd-Co-Si exhibited high thermal stability up to ~ 560 °C in oxidative atmosphere. Besides, Hyd-Co-Si was more thermally stable under inert atmosphere compared with the non-doped one (Hyd-Si). This higher thermal stability for the Hyd-Co-Si could be attributed to the cobalt composites with silica matrix, e.g., formation of Si-O-Co species. The weight loss after that temperature might be due to

the loss of incorporated CH_3 group [15, 16, 27]. On the other hand, the other hydrophilic materials, B-Si and Co-Si, exhibited high thermal stability as well.

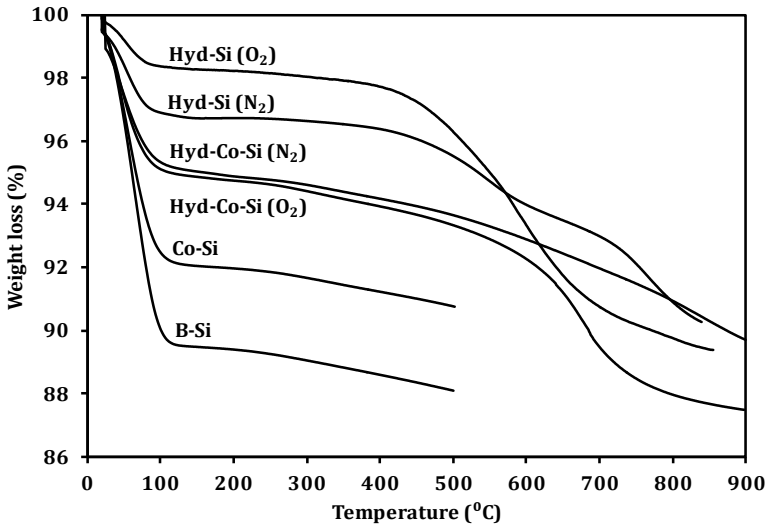

Figure 4.5. TGA curve, relative weight loss vs. temperature for silica/modified silica membrane materials.

4.3.6. Micropore structure

Textural properties were determined using N_2 adsorption/desorption isotherms at -196 °C, Figure 4.6a, and CO_2 adsorption/desorption isotherms at 0 °C, Figure 4.6b, for the silica membrane materials. Taking into account that N_2 adsorption isotherms at -196 °C and atmospheric pressure achieves a relative pressure of 1 whereas CO_2 adsorption isotherms at 0 °C and atmospheric pressure achieves only a final relative pressure of 0.03, the porosity analyzed using these two probe molecules is different [49]. CO_2 adsorption measures preferentially narrow micropores, pores < 0.7 nm, which sometimes are inaccessible to nitrogen at -196 °C, due to its slightly larger kinetic diameter (0.36 nm for N_2 vs. 0.33 nm for CO_2) and the lower adsorption temperature compared to CO_2 (-196 °C vs. 0 °C) [50]. On the contrary, N_2 adsorption at -196 °C measures the whole microporosity, pores < 2 nm, plus the presence of

larger pores (meso/macropores). Table 4.3 reports the parameters obtained from the N_2 and CO_2 adsorption data after application of different mathematical equations. Micropore volume (V_0) was calculated by applying the Dubinin-Radushkevich equation to the nitrogen adsorption data (eq. 4.1) [51].

$$V = V_0 \, exp\left[-\left(\frac{RT}{\beta E} ln \frac{P_0}{P}\right)^2\right] \qquad 4.1$$

Where V is the volume adsorbed at a given relative pressure (P/P_0) and temperature (T), V_0 is the micropore volume, E is the energy of adsorption, β is the affinity coefficient of the adsorbate, and R is the universal gas constant. The total pore volume, V_T, was obtained from the amount adsorbed at a relative pressure (P/P_0) of 0.95 while the mesopore volume, V_{meso}, was obtained from the difference between the total pore volume and the micropore volume. The surface area was obtained by application of the BET (Brunauer, Emmett and Teller) equation to the nitrogen adsorption data [52]. Finally, narrow micropore volume, V_n, was calculated from the CO_2 adsorption data by applying the Dubinin-Radushkevich equation. As it can be observed in Table 4.3, samples B-Si and Co-Si exhibit a larger total micropore and narrow micropore volume compared to samples Hyd-Si and Hyd-Co-Si, which is accompanied also by a larger BET surface area. Apparently, the incorporation of $-CH_3$ groups on the surface of the silica materials gives rise to a partial blocking/narrowing of the microporous structure. Similar results were reported elsewhere [14, 15] where the B-Si was accompanied also by a larger BET surface area than Hyd-Si.

Figure 4.6a shows the N_2 adsorption/desorption isotherms for all silica membrane materials. All isotherms exhibit the characteristic Type I with a knee at low relative pressures ($P/P0 < 0.1$) characteristic of microporous materials. The variation in the amount of nitrogen adsorbed is attributed to the limiting capacity for each sample, which is dependent on the available micropore volume where the adsorbent-adsorbate interaction occurs. Furthermore, a decrease in the micropore width results in both an increase in the adsorption potential and a decrease in the relative pressure at which the micropore filling occurs (narrow knee in the isotherm). Besides, the appearance of a nearly horizontal plateau indicates the absence of larger pores (meso-/macropores) [53]. As it can be observed in Figure 4.6a, samples B-Si

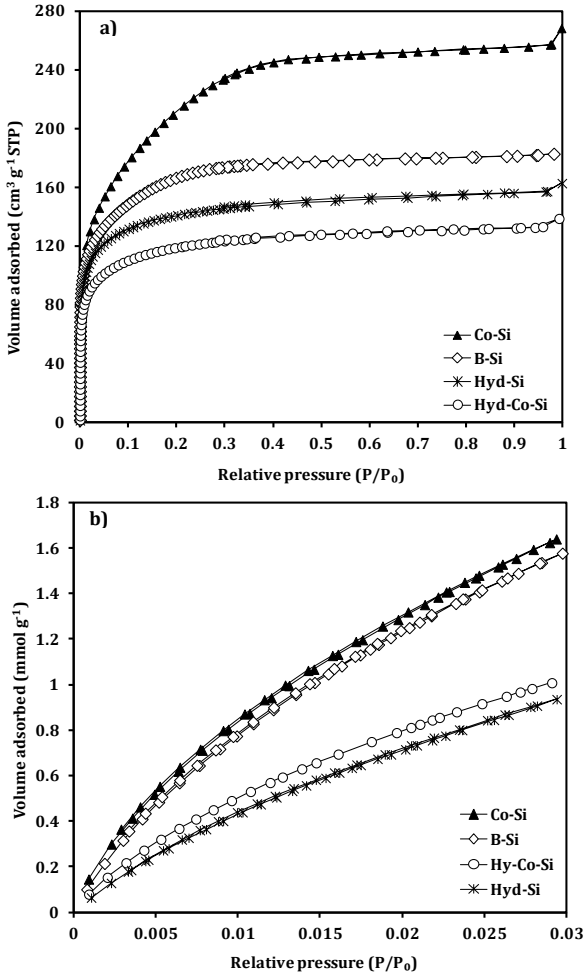

Figure 4.6. a) N_2 at -196 °C and b) CO_2 at 0 °C adsorption isotherms for the silica/modified membrane materials.

Table 4.3. Compilation of structural parameters deduced from N_2 adsorption data at -196 °C and CO_2 adsorption data at 0 °C.

Sample	S_{BET} ($m^2\ g^{-1}$)	$V_{T0.95}$ ($cm^3\ g^{-1}$)	V_{micro} ($cm^3\ g^{-1}$)	V_{meso} ($cm^3\ g^{-1}$)	V_n ($cm^3\ g^{-1}$)
B-Si	590	0.28	0.22	0.06	0.16
Co-Si	780	0.40	0.26	0.14	0.16
Hyd-Si	520	0.24	0.21	0.03	0.10
Hyd-Co-Si	435	0.21	0.17	0.04	0.11

S_{BET}: Surface area (after application of the Brunauer, Emmett and Teller equation to the nitrogen adsorption data).
$V_{T0.95}$: Total pore volume (from the amount adsorbed at $P/P_0 = 0.95$).
V_{micro}: Micropore volume (after applying the Dubinin-Radushkevich equation to the nitrogen adsorption data).
V_{meso}: Mesopore volume ($V_{meso} = V_{T0.95} - V_{micro}$).
V_n: Narrow micropore volume (from the CO_2 adsorption data by applying the Dubinin-Radushkevich equation).

and Co-Si exhibit a broad knee in the nitrogen isotherm at low relative pressures (P/P0 < 0.1) , thus suggesting a wider micropore size distribution (PSD) compared to samples Hyd-Si and Hyd-Co-Si were the incorporation of –CH3 groups on the silica surface gives rise to a narrower PSD. In general, the presence of larger pores (mesopores) is negligible for all samples (except for sample Co-Si).

Figure 4.6b shows the CO_2 adsorption isotherms for all silica membrane materials. As it can observed, all isotherms exhibit Langmuir-type with approximately linear region [54]. The adsorbate-adsorbent interactions are dependent on the polarity of the interacting functional groups, the adsorption temperature and the particular surface composition and/or the pore structure [53]. As it can be observed in Figure 6b, samples B-Si and Co-Si exhibit a higher adsorption capacity and a higher adsorption potential for CO_2 compared to samples Hyd-Si and Hyd-Co-Si. This observation must be related to the presence of a highly developed narrow microporous structure (larger values of V_n) together with the presence of a larger proportion of hydroxyl groups on the surface of hydrophilic samples. Hence

the adsorption occurs with these active sites at the surface at the range of very low relative pressure resulting enhanced micropore filling. On the contrary, for samples Hyd-Si and Hyd-Co-Si, due to the presence of CH_3 groups on the surface, the interaction of the CO_2 molecule with the surface is weaker and occurs at the range of higher relative pressure. A similar effect of the probe molecule has been reported in the literature for N_2 and Ar (kinetic diameter is 0.34 nm) adsorption on samples B-Si and Hyd-Si, where the shape of the isotherms highly depended on the specific surface interaction and the size of the sorbent gas [16].

Figure 4.7 shows the pore size distributions (PSD) for the silica membrane materials; they were calculated by applying the NLDFT model to the nitrogen adsorption data at -196 ºC based on a cylindrical pore model. Although the PSD determined by BJH (Barrett, Joyner and Halenda) method is more accurate than other method such as HK (Horváth-Kawazoe) method [14], the NLDFT adsorption kernels recently developed by Neimark *et al.* [55] describe the position of the pore condensation (i.e. adsorption branch) by taking into account the pressure range of metastable pore fluid prior to condensation. Hence, the application of this NLDFT adsorption branch kernel allows obtaining a correct pore size distribution curve also from the adsorption branch. As it can be seen, the novel silica membrane material, Hyd-Co-Si, exhibit a narrow pore size distribution centered at 1.1 nm suggesting that the novel material can be used for molecular sieving applications. Similar results were reported for Hyd-Si with the same pore size distribution [15]. The PDS for Co-Si is centered at 1.4 nm; Darmawan *et al.* [26] have obtained a metal oxide silica derived from sol-gel method with an average pore radius of 1nm and 1.2 nm. There are distinctive peaks over 2 nm, this could be attributed to the fact that silica materials possess wider micropores and mesopores (see Table 4.3). In fact the actual values of the pore widths for the unsupported silica or modified silica membrane may differ somehow in the supported membrane one. Therefore, this could explain why Hyd-Si showed lower selectivity and the contrary for Co-Si [16, 17, 25].

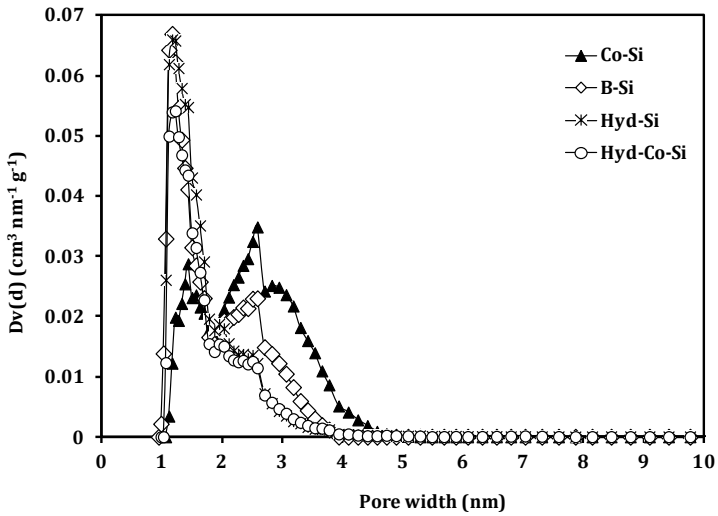

Figure 4.7. Pore size distributions of the silica membrane materials, calculated according to NLDFT model (cylindrical pore-equilibrium model), from N_2 adsorption data at -196 °C.

4.4. Conclusions

A novel unsupported hydrophobic cobalt-doped silica membrane was derived from the sol-gel process by the acid-catalyzed hydrolysis and condensation of TEOS with MTES and cobalt nitrate salt. The surface properties as well as thermal stability of the novel unsupported silica membrane were enhanced by cobalt-doping within the organic templated silica material (hybrid silica). The novel material showed a hydrophobic behavior after heat treatment in air at 400 °C. Moreover, the novel silica material is thermally stable up to ~ 560 °C in oxidizing atmosphere and inert atmosphere as well. This enhancement could be attributed to the presence cobalt as covalently bound cobalt strongly interacting with the silica matrix forming Si-O-Co as well as tiny crystal of Co_3O_4 as confirmed by FTIR where tiny small bands at ~ 570 and 660 cm^{-1} were assigned to Co_3O_4. These two bands appeared after the calcination process whereas they were no present before calcination process. In addition to these results, the N_2 and CO_2 isotherms confirmed the formation of microporous material with a narrow pore size distribution centered at 1.1 nm, i.e. the novel silica membrane material exhibited trend toward micropores formation. This is in a good agreement with solid-state ^{29}Si MAS NMR results where the resonances, Q^3 and Q^2, were observed. These two resonances results in silica matrix with smaller pore sizes. The objective of the present study was to demonstrate the development of a novel unsupported organic templated silica membrane. The results obtained concerning the Hyd-Co-Si membrane material are in a good agreement with what have been reported in the literature concerning the B-Si, Co-Si and Hyd-Si. Therefore, a novel hydrophobic microporous silica membrane material, with high thermal stability, have been achieved which can be a precursor material for molecular sieve silica membranes applications.

4.5. References

[1] G.Q. Lu, X.S. Zhao, Nanoporous Materials : Science and Engineering, Imperial College Press, London, 2004.

[2] G.Q. Lu, J.C. Diniz da Costa, M. Duke, S. Giessler, R. Socolow, R.H. Williams, T. Kreutz, Inorganic membranes for hydrogen production and purification: A critical review and perspective, J. Colloid Interface Sci. 314 (2007) 589-603.

[3] R.M. de Vos, H. Verweij, High-selectivity, high-flux silica membranes for gas separation, Science 279 (1998) 1710-1711.

[4] A.K. Prabhu, S.T. Oyama, Highly hydrogen selective ceramic membranes: application to the transformation of greenhouse gases, J. Membr. Sci. 176 (2000) 233-248.

[5] C.-Y. Tsai, S.-Y. Tam, Y. Lu, C.J. Brinker, Dual-layer asymmetric microporous silica membranes, J. Membr. Sci. 169 (2000) 255-268.

[6] B.N. Nair, T. Yamaguchi, T. Okubo, H. Suematsu, K. Keizer, S.-I. Nakao, Sol-gel synthesis of molecular sieving silica membranes, J. Membr. Sci. 135 (1997) 237-243.

[7] M.C. Duke, J.C. Diniz da Costa, G.Q. Lu, M. Petch, P. Gray, Carbonised template molecular sieve silica membranes in fuel processing systems: permeation, hydrostability and regeneration, J. Membr. Sci. 241 (2004) 325-333.

[8] R.M. de Vos, H. Verweij, Improved performance of silica membranes for gas separation, J. Membr. Sci. 143 (1998) 37-51.

[9] J.C. Diniz da Costa, G.Q. Lu, V. Rudolph, Y.S. Lin, Novel molecular sieve silica (MSS) membranes: characterisation and permeation of single-step and two-step sol–gel membranes, J. Membr. Sci. 198 (2002) 9-21.

[10] L.T. Zhuravlev, The surface chemistry of amorphous silica. Zhuravlev model, Colloids Surf., A 173 (2000) 1-38.

[11] S. Battersby, M.C. Duke, S. Liu, V. Rudolph, J.C. Diniz da Costa, Metal doped silica membrane reactor: Operational effects of reaction and permeation for the water gas shift reaction, J. Membr. Sci. 316 (2008) 46-52.

[12] M. Kanezashi, M. Asaeda, Hydrogen permeation characteristics and stability of Ni-doped silica membranes in steam at high temperature, J. Membr. Sci. 271 (2006) 86-93.

[13] G.R. Gallaher, P.K.T. Liu, Characterization of ceramic membranes I. Thermal and hydrothermal stabilities of commercial 40 Å membranes, J. Membr. Sci. 92 (1994) 29-44.

[14] Q. Wei, Y.-L. Wang, Z.-R. Nie, C.-X. Yu, Q.-Y. Li, J.-X. Zou, C.-J. Li, Facile synthesis of hydrophobic microporous silica membranes and their resistance to humid atmosphere, Microporous Mesoporous Mater. 111 (2008) 97-103.

[15] H.L. Castricum, A. Sah, M.C. Mittelmeijer-Hazeleger, C. Huiskes, J.E.t. Elshof, Microporous structure and enhanced hydrophobicity in methylated SiO_2 for molecular separation, J. Mater. Chem. 17 (2007) 1509-1517.

[16] R.M. de Vos, W.F. Maier, H. Verweij, Hydrophobic silica membranes for gas separation, J. Membr. Sci. 158 (1999) 277-288.

[17] S. Giessler, L. Jordan, J.C. Diniz da Costa, G.Q. Lu, Performance of hydrophobic and hydrophilic silica membrane reactors for the water gas shift reaction, Sep. Purif. Technol. 32 (2003) 255-264.

[18] K. Kusakabe, S. Sakamoto, T. Saie, S. Morooka, Pore structure of silica membranes formed by a sol–gel technique using tetraethoxysilane and alkyltriethoxysilanes, Sep. Purif. Technol. 16 (1999) 139-146.

[19] J.S. Beck, J.C. Vartuli, G.J. Kennedy, C.T. Kresge, W.J. Roth, S.E. Schramm, Molecular or supramolecular templating: Defining the role of surfactant chemistry in the formation of microporous and mesoporous molecular sieves, Chem. Mater. 6 (1994) 1816-1821.

[20] S. Giessler, J.C. Diniz da Costa, G.Q. Lu, Hydrophobicity of templated silica xerogels for molecular sieving applications, J. Nanosci. Nanotechnol. 1 (2001) 331-336.

[21] R. Igi, T. Yoshioka, Y.H. Ikuhara, Y. Iwamoto, T. Tsuru, Characterization of Co-doped silica for improved hydrothermal stability and application to hydrogen separation membranes at high temperatures, J. Am. Ceram. Soc. 91 (2008) 2975-2981.

[22] V. Boffa, D.H.A. Blank, J.E. ten Elshof, Hydrothermal stability of microporous silica and niobia–silica membranes, J. Membr. Sci. 319 (2008) 256-263.

[23] S. Battersby, S. Smart, B. Ladewig, S. Liu, M.C. Duke, V. Rudolph, J.C. Diniz da Costa, Hydrothermal stability of cobalt silica membranes in a water gas shift membrane reactor, Sep. Purif. Technol. 66 (2009) 299-305.

[24] V. Boffa, J.E. ten Elshof, R. Garcia, D.H.A. Blank, Microporous niobia–silica membranes: Influence of sol composition and structure on gas transport properties, Microporous Mesoporous Mater. 118 (2009) 202-209.

[25] D. Uhlmann, S. Liu, B.P. Ladewig, J.C. Diniz da Costa, Cobalt-doped silica membranes for gas separation, J. Membr. Sci. 326 (2009) 316-321.

[26] A. Darmawan, S. Smart, A. Julbe, J.C. Diniz da Costa, Iron oxide silica derived from sol-gel synthesis, Materials 4 (2011) 448-456.

[27] J.C. Diniz da Costa, G.Q. Lu, V. Rudolph, Characterisation of templated xerogels for molecular sieve application, Colloids Surf., A 179 (2001) 243-251.

[28] G.P. Fotou, Y.S. Lin, S.E. Pratsinis, Hydrothermal stability of pure and modified microporous silica membranes, J. Mater. Sci. 30 (1995) 2803-2808.

[29] T.r. Vrålstad, G. Øye, J. Sjöblom, M. Stöcker, Cobalt functionalization of mesoporous silica by organosilane grafting, J. Dispersion Sci. Technol. 27 (2006) 489-496.

[30] Q. Tang, Q. Zhang, P. Wang, Y. Wang, H. Wan, Characterizations of cobalt oxide nanoparticles within faujasite zeolites and the formation of metallic cobalt, Chem. Mater. 16 (2004) 1967-1976.

[31] C.L. Bianchi, V. Ragaini, Co/SiO_2 for Fischer–Tropsch synthesis: comparison among different preparation methods, Catal. Lett. 95 (2004) 61-65.

[32] K. Okabe, X. Li, M. Wei, H. Arakawa, Fischer–Tropsch synthesis over Co–SiO_2 catalysts prepared by the sol–gel method, Catal. Today 89 (2004) 431-438.

[33] K. Okabe, X. Li, T. Matsuzaki, H. Arakawa, K. Fujimoto, Application of sol-gel method to preparation of ultra-uniform Co-based catalysts for Fischer-Tropsch reaction, J. Sol-Gel Sci. Technol. 19 (2000) 519-523.

[34] S. Esposito, M. Turco, G. Ramis, G. Bagnasco, P. Pernice, C. Pagliuca, M. Bevilacqua, A. Aronne, Cobalt–silicon mixed oxide nanocomposites by modified sol–gel method, J. Solid State Chem. 180 (2007) 3341-3350.

[35] K. Kojima, H. Taguchi, J. Matsuda, Optical and magnetic properties of Co^{2+} ions in dried and heated silica gels prepared by the sol-gel process, J. Phys. Chem. 95 (1991) 7595-7598.

[36] G. Ortega-Zarzosa, C. Araujo-Andrade, M.E. Compeán-Jasso, J.R. Martínez, F. Ruiz, Cobalt oxide/silica xerogels powders: X-ray diffraction, infrared and visible absorption studies, J. Sol-Gel Sci. Technol. 24 (2002) 23-29.

[37] S.S. Latthe, H. Imai, V. Ganesan, A. Venkateswara Rao, Porous superhydrophobic silica films by sol–gel process, Microporous Mesoporous Mater. 130 (2010) 115-121.

[38] Z. Olejniczak, M. Łęczka, K. Cholewa-Kowalska, K. Wojtach, M. Rokita, W. Mozgawa, ^{29}Si MAS NMR and FTIR study of inorganic–organic hybrid gels, J. Mol. Struct. 744–747 (2005) 465-471.

[39] A. Bertoluzza, C. Fagnano, M. Antonietta Morelli, V. Gottardi, M. Guglielmi, Raman and infrared spectra on silica gel evolving toward glass, J. Non-Cryst. Solids 48 (1982) 117-128.

[40] Duran, C. Serna, V. Fornes, J.M. Fernandez Navarro, Structural considerations about SiO_2 glasses prepared by sol-gel, J. Non-Cryst. Solids 82 (1986) 69-77.

[41] Pejova, A. Isahi, M. Najdoski, I. Grozdanov, Fabrication and characterization of nanocrystalline cobalt oxide thin films, Mater. Res. Bull. 36 (2001) 161-170.

[42] C.J. Brinker, K.D. Keefer, D.W. Schaefer, C.S. Ashley, Sol-gel transition in simple silicates, J. Non-Cryst. Solids 48 (1982) 47-64.

[43] C.J. Brinker, G.W. Scherer, Sol–Gel Science: The Physics and Chemistry of Sol–Gel Processing, Academic Press, Boston, 1990.

[44] Yang, J. Li, Y. Xu, D. Wu, Y. Sun, H. Zhu, F. Deng, Direct formation of hydrophobic silica-based micro/mesoporous hybrids from polymethylhydrosiloxane and tetraethoxysilane, Microporous Mesoporous Mater. 95 (2006) 180-186.

[45] A.S. Maria Chong, X.S. Zhao, A.T. Kustedjo, S.Z. Qiao, Functionalization of large-pore mesoporous silicas with organosilanes by direct synthesis, Microporous Mesoporous Mater. 72 (2004) 33-42.

[46] T. Förster, S. Scholz, Y. Zhu, J.A. Lercher, One step synthesis of organofunctionalized transition metal containing meso- and macroporous silica spheres, Microporous Mesoporous Mater. 142 (2011) 464-472.

[47] N. Baccile, F. Babonneau, Organo-modified mesoporous silicas for organic pollutant removal in water: Solid-state NMR study of the organic/silica interactions, Microporous Mesoporous Mater. 110 (2008) 534-542.

[48] C.D. Nunes, J. Pires, A.P. Carvalho, M.J. Calhorda, P. Ferreira, Synthesis and characterisation of organo-silica hydrophobic clay heterostructures for volatile organic compounds removal, Microporous Mesoporous Mater. 111 (2008) 612-619.

[49] J. Garrido, A. Linares-Solano, J.M. Martin-Martinez, M. Molina-Sabio, F. Rodriguez-Reinoso, R. Torregrosa, Use of nitrogen vs. carbon dioxide in the characterization of activated carbons, Langmuir 3 (1987) 76-81.

[50] R.V.R.A. Rios, J. Silvestre-Albero, A. Sepulveda-Escribano, M. Molina-Sabio, F. Rodriguez-Reinoso, Kinetic restrictions in the characterization of narrow microporosity in carbon materials, J. Phys. Chem. C 111 (2007) 3803-3805.

[51] M.M. Dubinin, Physical Adsorption of Gases and Vapors in Micropores, in: D. A. Cadenhead, J. F. Danielli, M. D. Rosenberg (Eds), Progress in Surface and Membrane Science, Academic Press, New York, 1975, pp. 1-70.

[52] S. Brunauer, P.H. Emmett, E. Teller, Adsorption of gases in multimolecular layers, J. Am. Chem. Soc. 60 (1938) 309-319.

[53] F. Rouquerol, J. Rouquerol, K. Sing, Adsorption by Powders and Porous Solids, Principles, Methodology and Applications, Academic Press, London, 1999.

[54] R.S.A. de Lange, K. Keizer, A.J. Burggraaf, Analysis and theory of gas transport in microporous sol-gel derived ceramic membranes, J. Membr. Sci. 104 (1995) 81-100.

[55] A.V. Neimark, P.I. Ravikovitch, Capillary condensation in MMS and pore structure characterization, Microporous Mesoporous Mater. 44–45 (2001) 697-707.

Chapter 5

Characterization of Metal-Doped Methylated Microporous Silica for Molecular Separations

The trend to improve the properties of silica membrane materials towards molecular sieve applications is a topic of growing interest. In the present chapter novel organic templated silica xerogels are prepared by sol-gel method. The preparation involves cobalt-doping within the organic templated silica matrices, where methyltriethoxysilane (MTES) which contains methyl groups as a covalently bonded organic template was used. The synthesis and surface properties of cobalt-doped methylated microporous silica xerogels with different MTES content are revealed by surface and microstructural techniques, such as TGA, FTIR, X-ray, solid-state ^{29}Si MAS NMR and N_2 adsorption measurements. The doping process enhances the thermal stability of the silica xerogels up to ~ 560 °C in oxidizing atmosphere. Besides, this process has no significant effect on the incorporation of the organic template within the silica matrix. As result of the promoted densification of the xerogels either by increasing MTES content and heat treatment, there is structural change of the silica xerogels such as decreasing the micropore volume and broadening of the pore size distribution. Despite of these changes, the cobalt-doped methylated microporous silica xerogels exhibit trend toward micropores formation suggesting that these cobalt-doped silica xerogels can be precursor materials for molecular sieve silica membranes applications.

Characterization of metal-doped methylated microporous silica for molecular sepatations

5.1. Introduction

Microporous silica materials have been attracted a considerable attention in the last few years in the research field such as gas separation, pervaporation, catalytic reactors and molecular sieving [1-4]. This is due to the microporosity of the silica network which can be tailored to achieve novel materials with enhanced properties [5-9]. Sol-gel technique is a simple, attractive and effective way for facile synthesis of high purity microporous silica membrane materials with well-controlled physical and chemical properties [2, 10, 11]. This process consists on the formation of a macromolecular oxide network by the polymerization reaction of metal alkoxide in organic or aqueous solvents. The precursor for the preparation of silica based materials is usually tetraethylorthosilicate (TEOS). Two main steps are involved in the sol-gel way, hydrolysis, either acid or base catalyzed, and condensation reactions of the metal alkoxide as described by equations 1-3.

$$Si(OC_2H_5)_4 + 4H_2O \longrightarrow Si(OH)_4 + 4C_2H_5OH \qquad \text{Eq. (1) } \textit{Hydrolysis}$$

$$Si(OH)_4 + Si(OC_2H_5)_4 \longrightarrow 2SiO_2 + 4C_2H_5OH \qquad \text{Eq. (2) } \textit{Alcohol condensation}$$

$$nSi(OH)_4 \longrightarrow nSiO_2 + 2n\,H_2O \qquad \text{Eq. (3) } \textit{Water condensation}$$

The alkoxide groups are replaced by hydroxyl groups during the hydrolysis reaction, equation 1. In the condensation reaction, the siloxane bonds (Si-O-Si) are formed with by-products as alcohol (equation 2) or water (equation 3). The formed gels are called xerogels, if they are dried by evaporation under normal atmospheric conditions, or aerogels, if they are dried under supercritical conditions [12].

The heat treatment of silica materials, especially at high temperature, leads to removal of nearly all silanol (hydroxyl) surface groups, resulting in an almost complete loss of porosity of silica materials which is needed for the molecular sieve applications [13]. Over the last decade, tailoring the porosity of these materials has been increasingly gaining importance. One strategy for doing that is template-based approach which depends on the preparation of new hybrid organic-inorganic silica-based microporous materials [14]. In turn, hybrid silica materials have been prepared by the sol-gel technique and they offer a versatile range of applications. Therefore, they are considered as promising molecular sieve membrane materials [5-

7, 15-17]. The incorporation of organic groups in the oxide network leads to reduction of the degree of cross-linking which helps in structural flexibility. Hence, the silica material will have new functional properties such as improvement in thermal stability, hydrophobicity and tunable pore size of the xerogel [5-7]. The most common precursor that was used to incorporate organic groups within the oxide network is methyltriethoxysilane (MTES) which contains methyl groups as a covalently bonded organic template.

By incorporation of organic groups of MTES template it is possible that different type of silica network is formed with MTES than pure TEOS. For instance, the surface chemistry of these hybrid materials can be altered by the processing gas used for partial sintering, calcination, and pyrolysis of the organic constituents. Therefore, there are two strategies depending on the calcination process of these hybrid materials. When the calcination is performed under inert atmosphere, below 450 °C, the membrane is rendered hydrophobic feature. By that way, high quality hydrophobic molecular sieve membranes have been derived from the methyl ligand templated xerogel [5, 6, 16]. On the other hand, if the calcination process is performed under oxidizing atmosphere, this leads to create porosity by the removal of the organic constituents. This removal, that depends on the temperature at which it occurs, should create pores that mimic the size and shape of the organic constituents, resulting in the formation of a microporous network [17]. However, the common trend for the calcination of these materials is performed under inert atmosphere to prevent pyrolyzes of the methyl ligands and hence maintains the hydrophobicity of the membrane [5-7, 16]. This will limit the applications of the hydrophobic microporous silica membranes to the non-oxidative environments.

The chemical reactivity of the organic template is important to be known, i.e. to investigate their hydrolysis and condensation processes. For MTES, the hydrolysis and condensation rate at room temperature is higher than that of TEOS [18]. Therefore, the formation of xerogels with microporous structure requires controlling the addition time of MTES to the TEOS as well as the whole reaction time [16]. Moreover, of particular importance for the microporous structure of the xerogel is the water to silica molar ratio. A high H_2O/Si molar ratio (>10) provides the sol-gel synthesis with excess water, thus favoring the condensation reaction and the

formation of siloxane bridges (Si-O-Si) and larger pore sizes. Contrarily, low H_2O/Si molar ratio (<10) tends to inhibit the condensation reactions, thus favoring the formation of silanol groups (Si-OH) and pore sizes ~ 1 nm or lower [19-21]. Solid-state ^{29}Si NMR was used to investigate the hydrolysis and polycondensation processes of the xerogel formation. In that technique the Q^n distribution factor is used to describe silicon center in the network, where n = 0 to 4 [5-7, 22-25]. Therefore, for the xerogels that were prepared and reported in the literature with low H_2O/Si molar ratio (<10), the presence of Q^3 and/or Q^2 peaks, which indicate weakly branched networks, is an evidence of incomplete polymerization of the gel structure. These weakly branched networks tend to collapse under inhibited condensation reaction conditions so the xerogel is characterized with micropores formation [5, 9, 15, 26].

In the previous chapter, a novel unsupported silica membrane was reported and the preparation involved cobalt-doping within the matrix of organic templated silica material (hybrid silica). By doing so, a hydrophobic material with a high thermal stability, up to ~ 560 °C, was achieved [5]. Therefore, the aim of this work is to study the characteristics of cobalt-doped organic templated xerogels containing different contents of covalently bonded methyl ligands. Investigation of the heat treatment, especially in oxidizing atmosphere, on the silica matrices was studied as well. For comparison, the temperatures selected in this work are below and above the temperature at which the removal of the organic constituents occur for cobalt-doped hybrid silica (around 560 °C) [5]. The organic templated xerogel was prepared by acid catalyzed and condensation reaction of different molar ratio of TEOS : MTES with constant amount of cobalt to be doped. The fundamental aspects of xerogel characterization such as Fourier transform infrared (FTIR), solid-state ^{29}Si nuclear magnetic resonance (NMR), Thermogravimetric analysis (TGA) and the micropore structure are reported in this study.

5.2. Experimental part

5.2.1. Materials and methods

Tetraethylorthosilicate (TEOS, 98%, Acros Organics), methyltriethoxysilane (MTES, 98%, Acros Organics), ethanol (EtOH, 96% V/V extra pure, Acros Organics),

nitric acid (HNO_3, Acros Organics) and cobalt nitrate (99% pure, Acros Organics) were purchased from Scharlab. Distilled water was used for the sols preparation.

5.2.2. Xerogels preparation

The silica sols were prepared by the acid-catalyzed hydrolysis and condensation process. Tetraethylorthosilicate (TEOS) and Methyltriethoxysilane (MTES) were used as the silica precursors mixed with ethanol (EtOH), nitric acid (HNO_3), cobalt nitrate (as metal salt) and distilled water as described previously [5]. Partial hydrolysis can occur during the addition of EtOH to TEOS at room temperature. Therefore, alkoxide/ethanol mixture was placed in ice bath and then acid/water mixture was added drop wise with continuous stirring [16]. For metal doping, a solution of cobalt nitrate in ethanol was used as described previously [5, 27].

Cobalt-doped methyl ligand templated silica xerogels were prepared as follow: after addition of HNO_3/H_2O mixture to TEOS/EtOH mixture. The sol was refluxed under stirring in water bath at 60 °C for 165 minutes. The reaction mixtures had a (based on starting materials) TEOS : EtOH : H_2O : HNO_3 molar ratio of 1 : 3.8 : 6.4 : 0.085 according to the recipe of the silica sol preparation [28]. Afterwards, mixture of MTES/EtOH solution, which has been placed for 5-10 minutes in ice, and the ethanol solution of the metal salt were added to the reaction mixture and the final sol was refluxed for an additional 15 minutes [5]. The molar ratio of MTES/EtOH solution was X : 3.8, where X = 0.25 - 4, in order to have different mol % of MTES such as 20, 40, 50, 60 and 80 mol %. For instance, for 50% MTES, the mixture had a (based on starting materials) TEOS : MTES : EtOH : H_2O : HNO_3 molar ratio of 1 : 1 : 7.6 : 6.4 : 0.085. The metal salt to metal alkoxide (Co:Si) weight ratio used was 3% for all modified materials. The amounts of metal salt were calculated in order to prepare solution of 10% wt/vol of cobalt nitrate in ethanol [5, 27]. For thermal stability comparison, a methyl ligand templated silica xerogel was prepared with 50% MTES (non-doped sample). Throughout this study the cobalt-doped methyl ligand template silica xerogels are referred to as Co-X% MTES, where X=20, 40, 50, 60 and 80, to differentiate from the methyl ligand templated silica xerogel, which is referred to as 50% MTES.

All silica sols were allowed to evaporate in Petri-dish at room temperature so that silica flakes, xerogels, were obtained overnight. Xerogels samples were crushed finely to obtain powders, which were used for characterization, and calcined in air at a heating and cooling rate of 1 °C/min, and held for 3 hours at 400 °C and 2 hour at 600 °C.

5.2.3. Characterization of the xerogels

Thermogravimetric analysis (thermogravimetry, TGA and differential thermal analysis, DTA) was used to investigate the processes taking place during the heat treatment. This analysis was carried out for dried xerogels, in a Perkin Elmer model Thermobalance TGA7 device, in synthetic air with constant flow rate of 290 cm^3 min^{-1} and heating rate of 10 °C min^{-1} from room temperature to 900 °C.

Fourier transform infrared characterization was carried out to determine functional groups within the bulk silica matrix using ATR cell (FTIR 680 Plus JASCO). The absorption spectra were recorded in the 500-1500 cm^{-1} range. The spectrum of each sample represents an average of 32 scans. With the aim of comparison, all FTIR spectra were normalized with respect to the maximum absorbance value for each sample.

XRD for phase detection was conducted using a Siemens D500 diffractometer (Bragg-Brentano parafocusing geometry and vertical θ-θ goniometer). The angular 2θ diffraction range was 5° to 70°.

Solid-state ^{29}Si MAS NMR spectra were recorded on a Varian Mercury_Vx 400MHz spectrometer according to the following measurement conditions: 7mm CPMAS probe, 79.577 MHz resonance frequency, 5 μs pulse width, 3 kHz rotation speed, 20 s delay time, and 30 scans. The spectra were deconvoluted using MestReNova fitting software (© 2009, Mestrelab Research S.L).

Textural characterization of the synthesized samples was determined by nitrogen isotherms measurements at -196 °C. Gas adsorption measurements were performed in the range of $3\times10^{-7} < P/P_0 < 0.995$. The measurements were performed in a Quantachrome Autosorb-iQ adsorption analyzer. Before analysis, the samples were degassed at 250 °C under vacuum for 12 h. The pore size distribution was

calculated from the nitrogen adsorption data using the NLDFT model (Non Localized Density Functional Theory) based on a cylindrical pore-equilibrium model.

5.3. Results and discussion

5.3.1. Thermogravimetric analysis

Thermogravimetric analysis was used to investigate the processes occurred during the heat treatment as well as the stability of the organic template (methyl ligands) in oxidizing atmosphere. The weight loss curves of 50% MTES and Co-X% MTES as function of temperature (TGA curves) and the differential weight loss (DTA curves) are shown in Figure 5.1. For all samples, the initial weight losses from room temperature to ~ 150 °C are mainly attributed to physisorbed water molecules trapped in the silica matrix in addition to the loss of free solvent molecules [9, 15]. For Co-X% MTES, from ~ 150 to ~ 240 °C, the weight loss is due to the dehydration of cobalt nitrate and the removal of the nitrous gases [29, 30]. The weight losses from ~ 150 °C to ~ 460 °C, for 50% MTES, and from ~ 240 °C to ~ 560 °C, for Co-X% MTES, are attributed to the condensation reaction which leads to continuously removal of the water and alcohol from the silica matrix due to heat treatment [15]. For 50% MTES, the weight losses after ~ 460 °C are due to the oxidative pyrolysis of the methyl ligands. The weight loss between 400-500 °C is 5.94 % and this is in good agreement as reported by Diniz da Costa *et al.* [15] concerning organic template xerogel with 50% MTES (non-doped xerogel).

Castricum *et al.* [6] have studied the thermal stability of the methyl ligand templated silica xerogels. It was found that the decomposition or pyrolysis processes did not occur for these materials, regardless the MTES content, at temperatures below 312 °C and the samples were stable up to at least 400 °C in N_2. The effect of cobalt-doping within the matrix of the methyl ligand templated silica xerogel (hybrid silica) was studied (chapter 4) [5]. Doping process led to more thermal stability compared with the non-doped one in both inert and oxidizing atmospheres. As shown in Figure 5.1 the Co-X% MTES samples, regardless the MTES content, are stable up to ~ 560 °C in oxidizing atmosphere. This high thermal stability could be attributed to cobalt composites with silica matrix results in formation of Si-O-Co [5, 31-33]. It has been reported that the weight losses of the organic templated increased with

increasing the molar ratio of MTES in the silica matrix and it is also the same case in the present study [15]. Table 5.1 shows the weight losses of the organic template between 500-800 °C.

Table 5.1. Weight losses between 500-800 °C of different Co-X% MTES.

% MTES	20	40	50	60	80
Wt loss (%)	2.40	2.56	5.28	5.85	8.12

5.3.2. Infrared spectroscopy

Figure 5.2 shows the FTIR spectra of dried and calcined Co-X% MTES. The IR bands corresponding to silanol and siloxane bonds appear in the range from ~ 600 to ~ 1400 cm^{-1}, for all Co-X% MTES that were treated at various temperatures.

Bands at ~ 770 - 810 cm^{-1} and at ~ 1035 cm^{-1} were assigned to siloxane bonds (Si-O-Si) [5, 22, 34, 35]. Bands at ~ 930 cm^{-1} was assigned to silanol bonds (Si-O-H). This band appears strongly for the dried silica and decrease in intensity after calcination process at 400 and 600 °C. This is in good agreement with what have been reported in the literatures [5, 15, 26, 36]. This decrease in intensity is attributed to the polycondensation process which is responsible for the transformation of silanol to siloxane bonds. The band at ~1273 cm^{-1} was assigned to asymmetric vibration of the CH_3 group [5, 16, 22, 34]. This band appears strongly for the dried and the calcined sample at 400 °C whereas it is unobservable for Co-X% MTES samples, where X = 20, 40 and 50, calcined at 600 °C. Inset graph in Figure 5.2 shows the FTIR spectra of Co-60% and Co-80% MTES samples calcined at 600 °C where the band of the CH_3 group is still observable. These results clearly indicate that for Co-X% MTES samples with low MTES content (when X = 20, 40 and 50) most of the organic template (methyl ligands) decomposed or pyrolyzed due to heat treatment in oxidizing atmosphere. According to TGA results around that temperature the decomposition process occurred for all Co-X% MTES samples. Although a high decomposition or pyrolysis processes (high weight losses) occurred as the MTES content increased, when X > 50 mol % a proportion of the methyl ligands still trapped in the silica matrix. Therefore, the band that was assigned to asymmetric vibration of

the CH_3 group was observed (see inset graph in Figure 5.2). The solid-state ^{29}Si MAS NMR results, as will be mentioned later, prove these results.

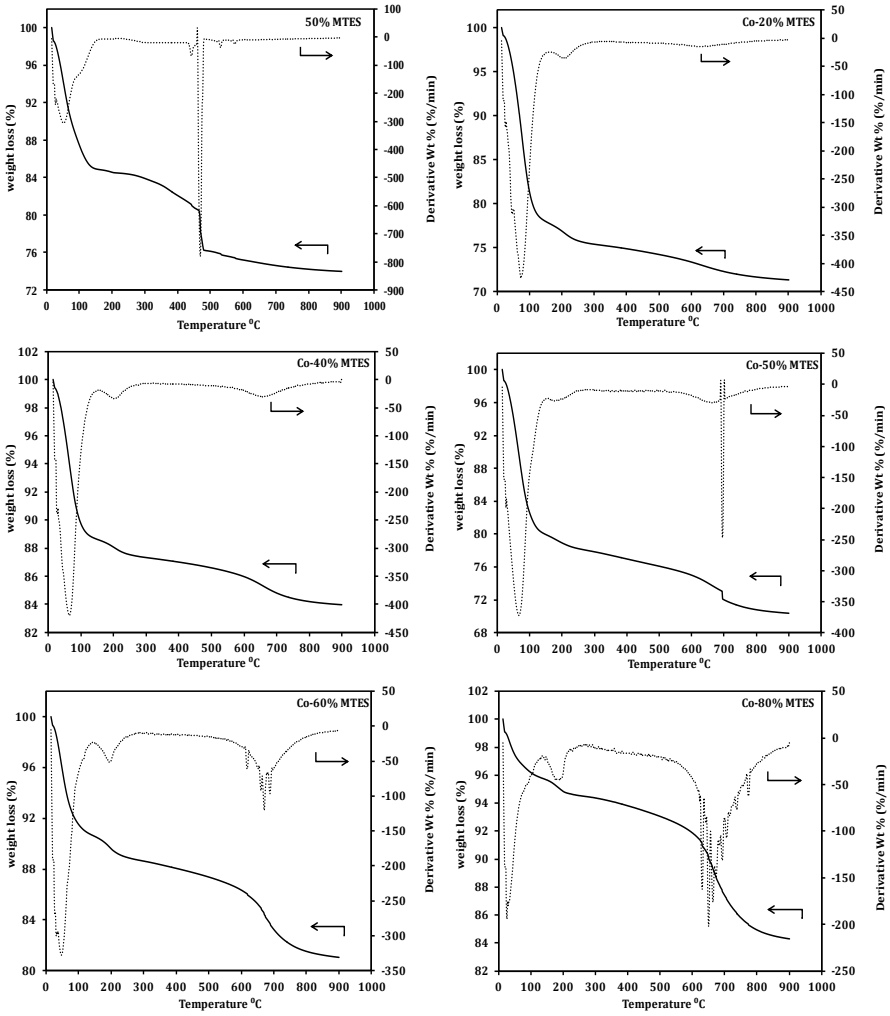

Figure 5.1. TGA (solid lines) and DTA (dashed lines) of 50% MTES (top left) and Co-X% MTES.

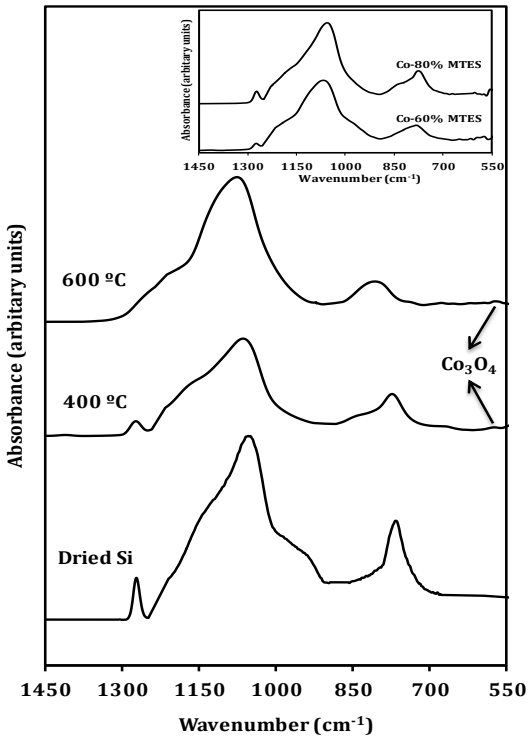

Figure 5.2. FTIR spectrum of sample Co-50% MTES. Inset shows the FTIR spectra of samples Co-60% and Co-80% MTES calcined at 600 °C.

As the calcination temperature increased, the band at ~ 1035 cm^{-1}, which was assigned to siloxane bonds (Si-O-Si) for the dried samples, shifted with a broad shoulder towards ~ 1040 and 1050 cm^{-1} at 400 and 600 °C, respectively. This shift is attributed to the change in the xerogel network resulted by the shrinkage in the silica polymeric bonding [5, 34, 36]. Tiny small band at ~ 570 cm^{-1} was assigned to cobalt, in oxide form Co_3O_4, this band appeared after the calcination process whereas this band was no present before the calcination process [5, 32, 37]. As there is no distinguishable peak at ~ 670 cm^{-1} that assigned to cobalt in oxide form, these results suggest that the interaction between the methyl ligand templated xerogel matrix and cobalt species depend on the cobalt content as will be mentioned in X-ray section.

5.3.3. X-ray analysis

The calcined samples of Co-X% MTES are X-ray amorphous. This indicates that the nature of the cobalt species and their interaction with the silica matrix was strongly depending on the cobalt content. In our previous study, we have reported that as the amount of cobalt content increase the formation of crystalline Co_3O_4 was obtained [5]. The same case was reported by Esposito *et al.* [32] and Igi *et al.* [38] where they have studied the interaction between different cobalt content and silica matrix. According to the study of Esposito *et al.* [32] the sample with lowest cobalt content appeared amorphous after heat treatment at 400 °C and contained Co^{2+} ions which strongly bonded to the silica matrix. Whereas, at high cobalt content the extent of the interaction between Co^{2+} ions and the silica matrix appeared to be low and the formation of crystalline Co_3O_4 was obtained. he same case was reported where sample with low cobalt content (3 wt%) was amorphous. However, as the amount increased from 3 to 10 wt% the crystalline structure was obtained [5]. As the cobalt content, in the present study, for all cobalt-doped methyl ligand templated silica xerogels was constant amount (3 wt%) that being low, hence the X-ray results are amorphous.

In general the structure of cobalt impregnated in the silica matrix continues to be controversial. Therefore, at low cobalt content and by heat treatment, these may result in the formation of a mixed matrix due to cobalt composites with silica matrix. In that later case, it is supposed that the cobalt-doped may exist as covalently bound cobalt strongly interacting with the siloxane matrix forming Si-O-Co bridges. The formation of Si-O-Co bridges was postulated through the condensation reaction between cobalt oxo-hydroxy complexes $[Co(H_2O)_{6-x-y}(HO)_xO_y]$ with silicone complexes $[Si(OC_2H_5)_{4-n}(OH)_n]$ [32, 33]. As result of these, it is supposed that the cobalt-doped may exist as the following: ionic metals, such as Co^{2+}; covalently bound cobalt strongly interacting with the siloxane matrix forming Si–O–Co; as well as extremely tiny crystals that could not be detected by XRD.

5.3.4. Solid-state ^{29}Si NMR spectroscopy

Figure 5.3 shows the solid-state ^{29}Si MAS NMR spectrum of Co-X% MTES which was deconvoluted using MestReNova fitting software. The resonances at a chemical

shift from -120 to -90 ppm are associated with Q^4 [$Si(OSi)_4$], Q^3 [$Si(OSi)_3(OH)$] and Q^2 [$Si(OSi)_2(OH)_2$] silicon atoms, respectively. The resonances at a chemical shift from -50 to -70 ppm, donating the presence of organosiloxane which is referred to as T^n, for differentiation from the silicon nomenclature (Q) where [$T^n = RSi(OSi)_n(OH)_{3-n}$, n=1-3, and R=$CH_3$]. For Co-X% MTES, they are characterized by the presence of T^3 and T^2. These resonances at different chemical shifts are in good agreement with the findings of several other works in the literature [5, 6, 15, 24, 25, 39-41]. Table 5.2 shows the peak areas and chemical shifts of the species Q^n and T^n at 400 °C, i.e. before the high decomposition of the organic template, and at 600 °C where high ratio of the decomposition process occurred (see TGA and FTIR results).

As it can be seen at 400 °C the peaks associated with T^n species, especially T^3, are very strong and their contribution increase as the molar ratio of MTES increase. For example 20% contains 11.0% of T^3 while 80% contains 57.9% of T^3. Moreover, the contribution of uncondensed species (i.e. Q^3, Q^2 , T^3 and T^2) at that temperature is higher than fully condensed species (Q^4). On the other hand, as the samples were calcined at 600 °C, this significantly improves the condensation process by enhancing the formation of siloxane bonds and hence more contribution of Q^4 occurred. This is also in agreement with FTIR results where at higher temperature there is much decrease in the intensity of the band assigned to silanol bonds (Si-O-H). Besides, the uncondensed species ($Q^{2,3}$) increased at the expenses of the T^n species. This resulted from the burnt off the methyl ligands and hence a continuous condensation reactions replace the lost of carbon with hydroxyl and/or siloxane bonds [15]. Moreover, in some cases the less contribution of uncondensed species, especially Q^2, indicates that there are only few –OH groups remaining after hydrolysis and condensation processes, and hence a high condensation degree between TEOS and the organic template [7, 41]. However, as it can be observed in Table 5.2 the samples show that a proportion of the methyl ligands still trapped in the silica matrix at high temperature indicated by T^n species. This proportion of the methyl ligands is higher for samples with X > 50 mol %. This is consistent with the FTIR results for the samples with X > 50 mol % where the band at ~ 1273 cm^{-1} that was assigned to asymmetric vibration of the CH_3 group was observed (see inset graph of Figure 5.2). Giessler *et al.* [9] have reported the presence of a proportion of the methyl ligands still trapped in the silica matrix with 50% MTES, but the sample was calcined at 500 °C in N_2. The same case

was also reported where a proportion of the methyl ligands still trapped in the silica matrix with different MTES contents after calcination at 550 °C [15]. The results presented above showed that the novel cobalt-doped organic templated silica xerogels possess the characteristic FTIR and NMR features of the non-doped silica xerogels, besides the high thermal stability.

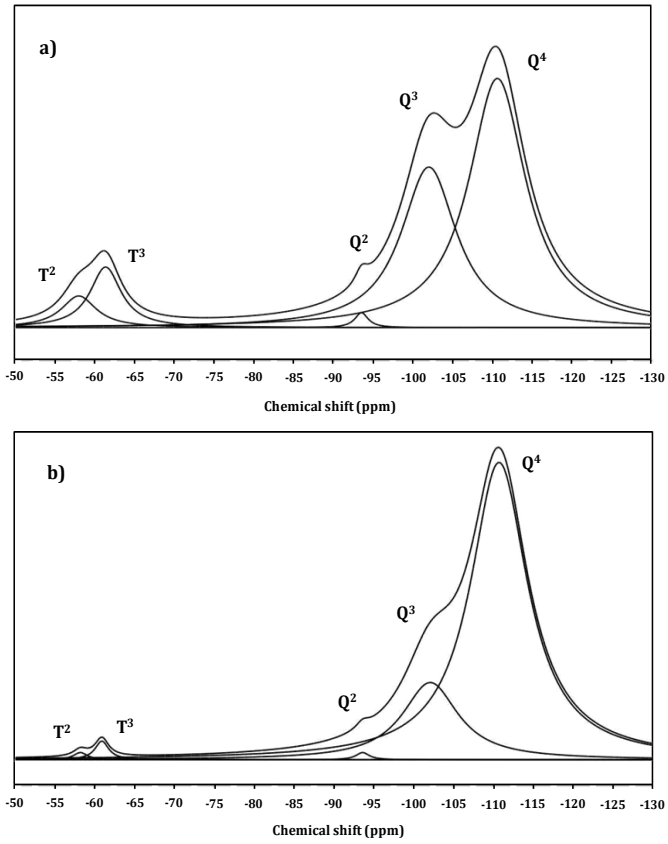

Figure 5.3. Deconvoluted solid-state ^{29}Si NMR spectrum of sample Co-20% MTES at a) 400 °C and b) 600 °C.

Table 5.2. Solid-state ^{29}Si MAS NMR of Co-X% MTES.

% MTES	Q^4		Q^3		Q^2		T^3		T^2	
	chemical shifts	% Area	chemical shifts	% Area	chemical shifts	% Area	chemical shifts	% Area	chemical shifts	% Area
20, 400 °C	-110.9	51.8	-102.4	32.4	-93.8	0.8	-61.8	11.0	-58.4	4.0
20, 600 °C	-110.4	82.8	-102.3	15.6	-93.5	0.3	-61.6	1.1	-58.1	0.2
40, 400 °C	-109.0	33.6	-101.5	27.7	-91.1	1.5	-63.5	34.7	-55.8	2.5
40, 600 °C	-109.3	69.9	-101.1	25.4	-91.3	3.1	-63.8	1.0	-55.5	0.6
50, 400 °C	-108.9	29.2	-103.3	30.5	-90.6	1.6	-65.8	35.3	-54.1	3.4
50, 600 °C	-108.4	64.5	-103.6	33.2	-90.2	1.1	-65.0	0.9	-54.3	0.3
60, 400 °C	-111.0	41.8	-103.1	14.5	-92.0	0.4	-64.9	38.6	-54.5	4.7
60, 600 °C	-111.0	69.2	-103.4	20.4	-92.3	0.7	-64.7	5.8	-54.7	3.9
80, 400 °C	-112.7	18.0	-105.4	11.8	-90.5	0.4	-65.7	57.9	-55.6	11.9
80, 600 °C	-112.5	43.1	-105.3	10.8	-90.8	0.5	-65.3	34.7	-55.9	10.9

5.3.5. Micropore structure

Textural properties were determined using N_2 adsorption isotherms at -196 °C. Table 5.3 and 5.4 represent the parameters obtained from the N_2 adsorption data for the samples calcined at 400 °C and 600 °C, respectively. The total pore volume, V_T, was obtained from the amount adsorbed at a relative pressure (P/P_0) of 0.99 while the surface area was obtained by application of the BET (Brunauer, Emmett and Teller) method to the nitrogen adsorption data [42]. Micro- and mesoporosity were discriminated using the *t*-plot method [43]. The pore size distributions (PSD) were calculated by applying the NLDFT model to the nitrogen adsorption data at -196 °C based on a cylindrical pore model [44].

Figure 5.4a and 5.4b show the N_2 adsorption isotherms for the Co-X% MTES calcined at 400 °C and 600 °C, respectively. In Figure 5.4a, all isotherms exhibit the characteristic Type I isotherm with a knee at low relative pressures ($P/P_0 < 0.1$) where the majority of pores filling occur and this is a characteristic of microporous materials [45]. At higher relative pressures ($P/P_0 > 0.4$) the isotherms of samples Co-60% and Co-80% MTES present a positive slope which will most probably correspond to the adsorption in the external area of the samples [40]. The trend is quite clear in the variation in the amount of nitrogen adsorbed which is related to the limiting capacity for each sample. This is mainly dependent on the available micropore volume (rather than the internal surface area) where the adsorbent-adsorbate interaction occurs. Furthermore, a decrease in the micropore width results in both an increase in the adsorption energy and a decrease in the relative pressure at which the micropore filling occurs (narrow knee in the isotherm) [46]. Apparently, Co-20% and Co-40% MTES samples exhibit a broader knee in the nitrogen isotherm at low relative pressure whereas the incorporation of $-CH_3$ groups on the surface of the silica materials, i.e. as the amount of MTES increases, gives rise to a partial blocking/narrowing of the micropores, accompanied by smaller surface area. This trend was observed by Castricum *et al.* [6] for methyl ligand templated xerogel with different MTES amount. In fact it is a general trend for organic templated xerogel, that the incorporation of organic template results in decreasing the surface area [5, 7].

On the other hand, Figure 5.4b shows the N_2 adsorption isotherms Co-X% MTES calcined at 600 °C. At this temperature a high ratio of the decomposition process

occurred (see TGA and NMR results). No difference in the isotherm type is observed with regard to the samples calcined at 400 °C. Raman *et al.* [17] have reported criteria that must be satisfied in order to achieve molecular sieve silica membranes by organic template approach. One of them is that the organic ligands must be uniformly incorporated in the inorganic matrix without aggregation or phase separation to avoid creating pores larger than the size of the individual ligands. It seems that a non-uniform incorporation of the organic template in the silica matrix occurs in excess of 50:50% MTES:TEOS molar ratio. This could be a possible hypothesis for the behavior of the isotherms of samples Co-60% and Co-80% MTES calcined at both temperatures.

Figure 5.5a and 5.5b show the PSD for the Co-X% MTES calcined at 400 °C and 600 °C, respectively. It can be observed that samples calcined at 400 °C are microporous or bordering the mesoporous region, exhibiting an average pore width between ~ 0.7 and 1.7 nm for Co-20 and Co-40% MTES, between ~ 0.7 and 1.3 nm for Co-50 and Co-60% MTES, and a peak at ~ 1.3 nm for Co-80% MTES. Samples calcined at 600 °C are exhibiting an average pore width between ~ 0.7 and 1.1 nm. This corresponds to the pores filling at low relative pressure leading to a narrow PSD. This is also proven by the solid-state ^{29}Si MAS NMR results where the resonances Q^3 and Q^2 were observed (besides the other uncondensed species, T^n). These resonances result in silica matrix with smaller pore sizes because of the low H_2O/Si ratio, therefore the gel structure contains weakly branched networks tending to collapse under inhibited condensation reaction conditions. Hence the xerogel is characterized by exhibiting micropores [19-21]. For Co-X% MTES calcined at 400 °C where X > 50 mol %, peaks over 1 nm broaden, more apparently for Co-80% MTES, which is attributed to the increasing of the organic template content. This is in good agreement with the PSD results reported in the literature where the PSD broadens as the MTES content increases [6, 15]. There is a distinctive peak over 2 nm that could be attributed to the fact that silica materials possess wider micropores and mesopores as well. However, a higher template concentration induces the collapse of the xerogel matrix due to capillary stress promoting dense xerogels as well as a broader PSD. This trend was reported by Castricum *et al.* [6] where pore sizes around 1-1.5 nm were obtained, becoming 2 nm pores more apparent as the MTES content increased. Further, such xerogels showed smaller ultramicropores, down to 0.2 nm

diameter, as determined from adsorption of various probe molecules with different critical diameters.

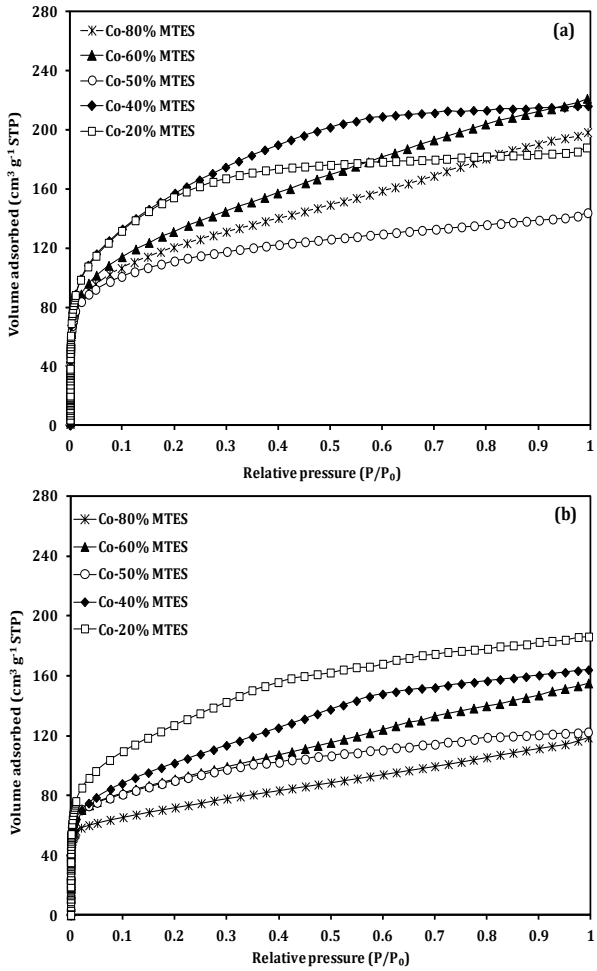

Figure 5.4. N_2 adsorption isotherms of Co-X% MTES calcined at a) 400 °C and b) 600 °C.

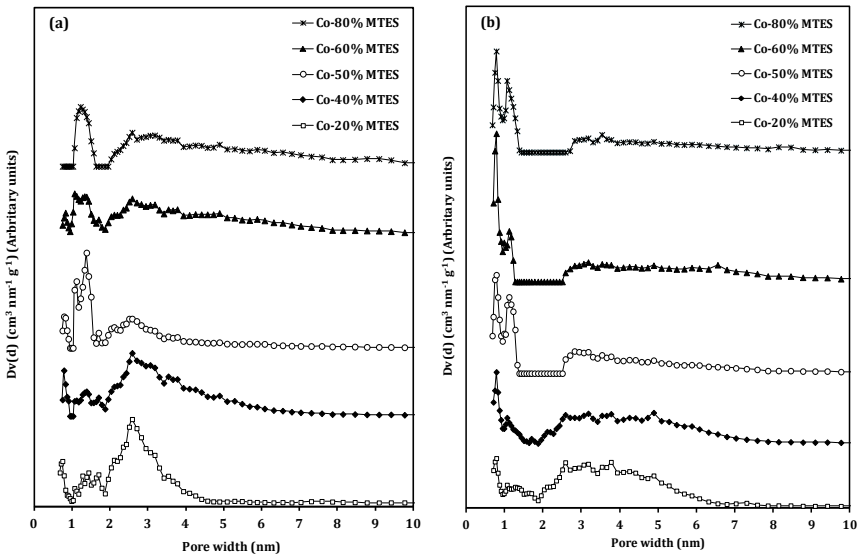

Figure 5.5. PSD of Co-X% MTES calcined at a) 400 °C and b) 600 °C.

The effect of the calcination process on the inorganic matrix lead to structural changes, in particular densification of the matrix, due to the reduction in silanol groups. Moreover, a reduction in the micropore volume, the micropore area, and the surface area is obtained. The calcination process leads to the burnt off the methyl ligands and, as a consequence, continuous condensation reactions replace the lost of carbon with hydroxyl and/or siloxane bonds. This leads to the creation of a continuous microporous network which depends on the uniform incorporation of the organic templates. Raman *et al.* [17] encountered some structural changes derived from adsorption isotherms. Thus, for the 10 mol% MTES/TEOS xerogels, as function of the calcination temperature, the N_2 sorption isotherms changed from Type I at 150 °C and 400 °C to Type II at 550 °C which is characteristic to non-porous or macroporous materials. However, the CO_2 isotherm showed that the 550 °C sample was microporous. This indicates that the densification of the inorganic matrix was virtually complete.

In the present study, these structural changes are also observed (see Table 5.3 and 5.4), however N_2 adsorption isotherms show a knee at low relative pressures ($P/P_0 < 0.1$) which is a characteristic of microporous materials. This indicates that further densification can occur for Co-X% MTES, and hence a continuous network of micropores can be formed even at temperature higher than 550 °C. These changes are observable when comparing the samples calcined at 400 °C and 600 °C. This is quite clear in the PSD curves; Figure 5.5, where the peaks over 1.1 nm are not observable for samples calcined at 600 °C as a result of the heat treatment which reduced the micropore volume. Sample Co-20% MTES calcined at 600 °C still showed some peaks over 1.1 nm but with very small height. Thus, it is supported the hypothesis of silica densification because of the heat treatment that leads to a reduction of the pore volume. These structural changes due to heat treatment are in conjugation with the solid-state ^{29}Si MAS NMR results where more contribution of the fully condensed species Q^4 is observed and other Q species ($Q^{2,3}$) as well. These changes are associated with lower pore volume as observed from N_2 adsorption data (see Table 5.4).

In fact, the PSD for Co-80% MTES calcined at 600 °C changed and the heat treatment could be a possible reason of that change. These results indicate that microporous network formation as well as further densification can occur at higher temperature compared with non-doped materials. Such difference is the consequence of the high thermal stability and the organic templates removal at high temperature shown by the material essayed in this work. In general, as can be seen in Table 5.3 and 5.4, the micropore area and micropore volume decrease as the MTES content increases. Accordingly, Diniz da Costa *et al.* [15] and Fahrenholtz *et al.* [47] reported that the micropore area for 50% MTES concentration was almost halved with regard to lower MTES content. In spite of having obtained the same trend in this work, such a big decrease is obtained only for Co-80% MTES compared to Co-20% calcined at 600 °C. The increase in the MTES content leads to the collapse of the xerogel matrix and promotes denser xerogel formation and lower pore volume [15], which has been attributed to the lower reaction kinetics during gelatin and ageing, and the longer duration of these steps [6].

Table 5.3. Compilation of structural parameters deduced from N_2 adsorption data at -196 °C for Co-X% MTES calcined at 400 °C.

Sample (% MTES)	S_{BET} (m^2g^{-1})	Micropore surface (m^2g^{-1})	$V_{T0.99}$ ($cm^3\ g^{-1}$)	V_{micro} ($cm^3\ g^{-1}$)
20	563	528	0.29	0.25
40	568	526	0.36	0.30
50	406	393	0.22	0.20
60	471	451	0.34	0.30
80	462	432	0.37	0.32

Table 5.4. Compilation of structural parameters deduced from N_2 adsorption data at -196 °C for Co-X% MTES calcined at 600 °C.

Sample (% MTES)	S_{BET} (m^2g^{-1})	Micropore surface (m^2g^{-1})	$V_{T0.99}$ ($cm^3\ g^{-1}$)	V_{micro} ($cm^3\ g^{-1}$)
20	457	418	0.30	0.26
40	364	343	0.27	0.23
50	320	299	0.22	0.18
60	325	303	0.25	0.21
80	253	243	0.18	0.16

S_{BET}: Surface area (after application of the Brunauer, Emmett and Teller equation to the nitrogen adsorption data).
$V_{T0.99}$: Total pore volume (from the amount adsorbed at $P/P_0 = 0.95$).
V_{micro}: Micropore volume.

It seems that the constant content (3 wt%) cobalt doping process studied in this work has no effect on the uniform incorporation of organic template. On the other hand, this process improved the thermal stability for the whole xerogel network comparing with the non-doped xerogel. These micropore results strongly suggest that a cobalt-doped methylated microporous silica xerogels were successfully achieved in the present study by sol-gel method, although some supermicroporosity was observed. In addition to that, the narrow PSD suggests that these xerogels can be used as precursor materials for molecular sieve silica applications. In a field such as gas separation involving large molecules and small diffusing molecules; these materials with supermicropores may facilitate the transport of gas molecules towards narrower pores of the silica membranes. In fact the actual values of the pore width interval of the unsupported cobalt-doped methylated microporous silica may differ somehow from the supported one as well as the actual separation behavior. Moreover, the sintering of the supported material might be enhanced due to the lower connectivity of the siloxane network imposed by the inclusion of the non-hydrolyzable methyl ligands as well as the cobalt-doping [17]. Hence, the novel organic templated silica membrane materials with high thermal stability will open new frontiers in the field of microporous materials for molecular sieve applications. Besides, these materials can be considered as promising membrane materials for particular applications such as gas separation and pervaporation.

5.4. Conclusions

The sol-gel technique used in this study makes possible a fine control of the silica matrix and a satisfactory pore size tuning. Novel organic templated silica xerogels, with different contents of the template molecule, were developed by cobalt-doping within the silica matrix, where the organic template molecule incorporated into silica matrix is a methyl ligand covalently bonded to the silica matrix in the form of MTES. The results showed that the thermal stability of the cobalt-doped organic templated silica xerogels was enhanced up to a range of ~ 500-600 °C in oxidizing atmosphere, regardless the MTES content, compared with the non-doped organic templated silica xerogel. Such enhancement in the silica properties could be attributed to the presence of cobalt as covalently bound cobalt strongly interacting with the siloxane matrix forming Si–O–Co. The covalent methyl ligands are burnt off at that temperature range according to TGA analysis. These results are also confirmed by the solid-state ^{29}Si MAS NMR spectroscopy which showed a reduction in the contribution of the T^3 and T^2 species as a function of calcination temperature. The losses of methyl templates are proportional to each sample MTES concentration as revealed by TGA and NMR.

The doping process had no significant effect on the incorporation of the organic template within the silica matrix. Moreover, a non-uniform incorporation of the template in the silica matrix occurs in excess of 50:50% MTES:TEOS molar ratio due to phase separation causing poor pore size control. Hence, molar ratios of sols prepared with MTES:TEOS are generally preferred to be limited to 50:50% or lower. A structural change of the silica xerogels such as a decreased micropore volume and broadened pore size distribution occurred as a result of increasing MTES content and the heat treatment. However, complete densification tending to smaller pores can be achieved at high temperature compared with the non-doped hybrid materials. Despite of these changes, the cobalt-doped methylated microporous silica xerogels exhibited trend toward micropores formation along with some supermicroporosity was observed. This resulted from the high thermal stability and hence removal of the organic templates at high temperature. The results obtained demonstrate the potential of high thermally stable materials that can be precursor materials for molecular sieve silica membranes applications.

5.5. References

[1] B.N. Lukyanov, D.V. Andreev, V.N. Parmon, Catalytic reactors with hydrogen membrane separation, Chem. Eng. J. (Lausanne) 154 (2009) 258-266.

[2] S. Smart, J.F. Vente, J.C. Diniz da Costa, High temperature H_2/CO_2 separation using cobalt oxide silica membranes, Int. J. Hydrogen Energy 37 (2012) 12700-12707.

[3] L. Wang, X. Han, J. Li, X. Zhan, J. Chen, Hydrophobic nano-silica/polydimethylsiloxane membrane for dimethylcarbonate–methanol separation via pervaporation, Chem. Eng. J. (Lausanne) 171 (2011) 1035-1044.

[4] A. Javaid, Membranes for solubility-based gas separation applications, Chem. Eng. J. (Lausanne) 112 (2005) 219-226.

[5] H.H. El-Feky, K. Briceño, E.d.O. Jardim, J. Silvestre-Albero, T. Gumí, Novel silica membrane material for molecular sieve applications, Microporous Mesoporous Mater. 179 (2013) 22-29.

[6] H.L. Castricum, A. Sah, M.C. Mittelmeijer-Hazeleger, C. Huiskes, J.E.t. Elshof, Microporous structure and enhanced hydrophobicity in methylated SiO_2 for molecular separation, J. Mater. Chem. 17 (2007) 1509-1517.

[7] Q. Wei, Y.-L. Wang, Z.-R. Nie, C.-X. Yu, Q.-Y. Li, J.-X. Zou, C.-J. Li, Facile synthesis of hydrophobic microporous silica membranes and their resistance to humid atmosphere, Microporous Mesoporous Mater. 111 (2008) 97-103.

[8] A. Darmawan, S. Smart, A. Julbe, J.C. Diniz da Costa, Iron oxide silica derived from sol-gel synthesis, Materials 4 (2011) 448-456.

[9] S. Giessler, J.C. Diniz da Costa, G.Q. Lu, Hydrophobicity of templated silica xerogels for molecular sieving applications, J. Nanosci. Nanotechnol. 1 (2001) 331-336.

[10] C.-Y. Tsai, S.-Y. Tam, Y. Lu, C.J. Brinker, Dual-layer asymmetric microporous silica membranes, J. Membr. Sci. 169 (2000) 255-268.

[11] B.N. Nair, T. Yamaguchi, T. Okubo, H. Suematsu, K. Keizer, S.-I. Nakao, Sol-gel synthesis of molecular sieving silica membranes, J. Membr. Sci. 135 (1997) 237-243.

[12] L.L. Hench, J.K. West, The sol-gel process, Chem. Rev. (Washington, DC, U. S.) 90 (1990) 33-72.

[13] R.K. Iler, The chemistry of Silica : Solubility, Polymerization, Colloid and Surface Properties, and Biochemistry, John Wiley and Sons, New York, 1979.

[14] N.K. Raman, M.T. Anderson, C.J. Brinker, Template-based approaches to the preparation of amorphous, nanoporous silicas, Chem. Mater. 8 (1996) 1682-1701.

[15] J.C. Diniz da Costa, G.Q. Lu, V. Rudolph, Characterisation of templated xerogels for molecular sieve application, Colloids Surf., A 179 (2001) 243-251.

[16] R.M. de Vos, W.F. Maier, H. Verweij, Hydrophobic silica membranes for gas separation, J. Membr. Sci. 158 (1999) 277-288.

[17] N.K. Raman, C.J. Brinker, Organic "template" approach to molecular sieving silica membranes, J. Membr. Sci. 105 (1995) 273-279.

[18] M.J. van Bommel, T.N.M. Bernards, A.H. Boonstra, The influence of the addition of alkyl-substituted ethoxysilane on the hydrolysis—condensation process of TEOS, J. Non-Cryst. Solids 128 (1991) 231-242.

[19] C.J. Brinker, G.W. Scherer, Sol-Gel Science: The Physics and Chemistry of Sol-Gel Processing, Academic Press, Boston, 1990.

[20] C.J. Brinker, Hydrolysis and condensation of silicates: Effects on structure, J. Non-Cryst. Solids 100 (1988) 31-50.

[21] C.J. Brinker, K.D. Keefer, D.W. Schaefer, C.S. Ashley, Sol-gel transition in simple silicates, J. Non-Cryst. Solids 48 (1982) 47-64.

[22] Z. Olejniczak, M. Łęczka, K. Cholewa-Kowalska, K. Wojtach, M. Rokita, W. Mozgawa, ^{29}Si MAS NMR and FTIR study of inorganic–organic hybrid gels, J. Mol. Struct. 744–747 (2005) 465-471.

[23] G. Morales, R. van Grieken, A. Martín, F. Martínez, Sulfonated polystyrene-modified mesoporous organosilicas for acid-catalyzed processes, Chem. Eng. J. (Lausanne) 161 (2010) 388-396.

[24] T. Förster, S. Scholz, Y. Zhu, J.A. Lercher, One step synthesis of organofunctionalized transition metal containing meso- and macroporous silica spheres, Microporous Mesoporous Mater. 142 (2011) 464-472.

[25] N. Baccile, F. Babonneau, Organo-modified mesoporous silicas for organic pollutant removal in water: Solid-state NMR study of the organic/silica interactions, Microporous Mesoporous Mater. 110 (2008) 534-542.

[26] J.C. Diniz da Costa, G.Q. Lu, V. Rudolph, Y.S. Lin, Novel molecular sieve silica (MSS) membranes: characterisation and permeation of single-step and two-step sol–gel membranes, J. Membr. Sci. 198 (2002) 9-21.

[27] G.P. Fotou, Y.S. Lin, S.E. Pratsinis, Hydrothermal stability of pure and modified microporous silica membranes, J. Mater. Sci. 30 (1995) 2803-2808.

[28] R.M. de Vos, H. Verweij, Improved performance of silica membranes for gas separation, J. Membr. Sci. 143 (1998) 37-51.

[29] K. Sinkó, G. Szabó, M. Zrínyi, Liquid-phase synthesis of cobalt cxide nanoparticles, J. Nanosci. Nanotechnol. 11 (2011) 4127-4135.

[30] S.A.A. Mansour, Spectrothermal studies on the decomposition course of cobalt oxysalts Part II. Cobalt nitrate hexahydrate, Mater. Chem. Phys. 36 (1994) 317-323.

[31] K. Kojima, H. Taguchi, J. Matsuda, Optical and magnetic properties of Co^{2+} ions in dried and heated silica gels prepared by the sol-gel process, J. Phys. Chem. 95 (1991) 7595-7598.

[32] S. Esposito, M. Turco, G. Ramis, G. Bagnasco, P. Pernice, C. Pagliuca, M. Bevilacqua, A. Aronne, Cobalt–silicon mixed oxide nanocomposites by modified sol–gel method, J. Solid State Chem. 180 (2007) 3341-3350.

[33] G. Ortega-Zarzosa, C. Araujo-Andrade, M.E. Compeán-Jasso, J.R. Martínez, F. Ruiz, Cobalt oxide/silica xerogels powders: X-ray diffraction, infrared and visible absorption studies, J. Sol-Gel Sci. Technol. 24 (2002) 23-29.

[34] H. Qi, J. Han, N. Xu, Effect of calcination temperature on carbon dioxide separation properties of a novel microporous hybrid silica membrane, J. Membr. Sci. 382 (2011) 231-237.

[35] J. Ma, M. Zhang, L. Lu, X. Yin, J. Chen, Z. Jiang, Intensifying esterification reaction between lactic acid and ethanol by pervaporation dehydration using chitosan–TEOS hybrid membranes, Chem. Eng. J. (Lausanne) 155 (2009) 800-809.

[36] A. Duran, C. Serna, V. Fornes, J.M. Fernandez Navarro, Structural considerations about SiO_2 glasses prepared by sol-gel, J. Non-Cryst. Solids 82 (1986) 69-77.

[37] D. Uhlmann, S. Liu, B.P. Ladewig, J.C. Diniz da Costa, Cobalt-doped silica membranes for gas separation, J. Membr. Sci. 326 (2009) 316-321.

[38] R. Igi, T. Yoshioka, Y.H. Ikuhara, Y. Iwamoto, T. Tsuru, Characterization of Co-doped silica for improved hydrothermal stability and application to hydrogen separation membranes at high temperatures, J. Am. Ceram. Soc. 91 (2008) 2975-2981.

[39] N. Abidi, B. Deroide, J.V. Zanchetta, L.C. de Menorval, J.B. d'Espinose, ^{29}Si and ^{129}Xe NMR of Mn^{2+} doped silica xerogels, J. Non-Cryst. Solids 231 (1998) 49-57.

[40] C.D. Nunes, J. Pires, A.P. Carvalho, M.J. Calhorda, P. Ferreira, Synthesis and characterisation of organo-silica hydrophobic clay heterostructures for volatile organic compounds removal, Microporous Mesoporous Mater. 111 (2008) 612-619.

[41] D. Yang, J. Li, Y. Xu, D. Wu, Y. Sun, H. Zhu, F. Deng, Direct formation of hydrophobic silica-based micro/mesoporous hybrids from polymethylhydrosiloxane and tetraethoxysilane, Microporous Mesoporous Mater. 95 (2006) 180-186.

[42] S. Brunauer, P.H. Emmett, E. Teller, Adsorption of gases in multimolecular layers, J. Am. Chem. Soc. 60 (1938) 309-319.

[43] J.H. de Boer, B.C. Lippens, B.G. Linsen, J.C.P. Broekhoff, A. van den Heuvel, T.J. Osinga, The t-curve of multimolecular N_2-adsorption, J. Colloid Interface Sci. 21 (1966) 405-414.

[44] A.V. Neimark, P.I. Ravikovitch, Capillary condensation in MMS and pore structure characterization, Microporous Mesoporous Mater. 44–45 (2001) 697-707.

[45] K.S.W. Sing, D.H. Everett, R.A.W. Haul, L. Moscou, R.A. Pierotti, J. Rouquerol, T. Siemieniewska, Reporting physisorption data for gas/solid systems with special reference to the determination of surface-area and porosity (Recommendation 1984), Pure Appl. Chem. 57 (1985) 603-619.

[46] F. Rouquerol, J. Rouquerol, K. Sing, Adsorption by Powders and Porous Solids, Principles, Methodology and Applications, Academic Press, London, 1999.

[47] W.G. Fahrenholtz, D.M. Smith, D.-W. Hua, Formation of microporous silica gels from a modified silicon alkoxide. I. Base-catalyzed gels, J. Non-Cryst. Solids 144 (1992) 45-52.

Chapter 6

Thermally Enhanced Methylated Microporous Silica for Molecular Sieve Applications

Enhancement in molecular sieving properties of silica materials has attracted considerable attention. In this chapter we investigate the effect of cobalt-doping within organic templated silica xerogel. Thermally stable methylated microporous silica, up to ~ 560 °C, is prepared via sol-gel technique. The preparation involves different cobalt amount to be doped within the matrix of 50:50 % molar ratio of tetraethylorthosilicate (TEOS) to methyltriethoxysilane (MTES). MTES is the precursor for methyl ligand covalently bonded to the silica matrix. Structural changes such as decrease in the surface area and in the micropore volume and area are obtained as result of heat treatment, which promotes the silica matrix densification. However, calcination at 600 °C resulted in samples with approximately the same structural parameters as the cobalt oxide content increased from 5 to 10% weight ratio. This suggests that the cobalt particles were homogeneously dispersed in the silica matrix and opposed the silica structure collapse. The densification of silica matrices with trend to small pores and narrow pore size distribution is achieved. The results suggest that the cobalt-doping within the MTES templated silica xerogel further provides beneficial structural stability and thermal stability as well. Hence, novel cobalt-doped methylated microporous silica with high thermal stability for molecular sieve silica membranes applications is achieved and developed.

Thermally enhanced methylated microporous silica for molecular sieve applications

6.1. Introduction

The development of microporous silica membranes have attracted great interest since they can be used as inorganic membranes for water-gas shift reaction, coal gasification, steam methane reforming and fuel cell systems . These industries may require a high temperature, between 100 and 500 °C, and the modification of the silica membranes to achieve high performance [1-8]. Over the last decade, thermal stability as well as the hydrothermal stability of microporous silica materials is an area of increasing research interest [9-14]. Microporous silica materials with well-controlled physical and chemical properties can be easily synthesized by sol-gel method. The most common precursor for the preparation of silica based materials is usually tetraethylorthosilicate (TEOS). Two main steps are involved in the sol-gel way, hydrolysis, either acid or base catalyzed, and condensation reactions of the metal alkoxide as described previously [15-17]. The polymeric sol-gel process depends mainly on the control of hydrolysis and condensation reactions. In turn, several research works have been performed to produce molecular sieving structures with very small pore size distribution in the region of ~ 1 nm or lower [5, 18-23]. The acid catalyzed hydrolysis of TEOS can be a single-step or a two-step process [18-21, 24-27]. During the sol-gel process the silanol bonds (SiOH) as well as the siloxane bonds are formed. The advantage of silanol bonds is that they form weakly branched silica networks, causing the collapse of the silica structure and, therefore, resulting in low pore volume with molecular dimensions. Hence, the sol–gel process is a promising way for producing microporous silica materials for molecular sieve silica membranes applications such as gas separation [17, 28, 29].

Several novel strategies of synthesis were designed to prepare unsupported/supported silica/modified silica membranes in order to improve the surface properties of the silica matrix towards molecular sieve applications. For instance, one strategy consists on template-based approach [30]. This approach depends on preparation of organic-inorganic hybrid materials, which differentiate from traditional polymer composites with respect to the relative sizes of organic and inorganic domains and the level of phase homogeneity. These materials combine the advantages of the inorganic material (e.g., heat resistance, retention of mechanical properties at high temperature, and low thermal expansion) and the organic polymer

(e.g., flexibility, low dielectric constant, ductility, and processability of high polymers). For template-based approaches, the organic templates can be classified as covalently or non-covalently organic templates bonded to the siloxane network. By doing so, surface modification using different organic template agents have been reported intensively in the literature [9, 12, 19, 26, 30-35].

Methyltriethoxysilane (MTES), which contains methyl groups as a covalently bonded organic template, is the most common precursor that was used to incorporate organic groups within the oxide network. For that purpose, the investigation of the hydrolysis and condensation processes of MTES is of particular importance to be known. Van Bommel *et al.* [36] have reported that the hydrolysis and condensation rate for MTES, at room temperature is higher than that of TEOS. Therefore, De Vos *et al.* [35] when reported on the addition of MTES to the standard TEOS sol, the hydrolysis and condensation reaction time were taken into account. By doing so, the formation of polymer particles with dimension > 10 nm, which would hamper the formation of a microporous membrane structure in the later stages of the process, was prevented. The same procedures have been followed for producing molecular sieving silica architectures. Tailoring the silica architectures was achieved via sols that were prepared using TEOS, MTES, in absolute ethanol, water and nitric acid. By that way, the organic templates were trapped in the silica matrix [9-12, 31, 37]. At high temperature these templates are burnt off under oxidizing atmosphere [9, 10, 32]. Whatever the kind of the organic templates that are using to be incorporated within the silica matrix, they are showing the same behavior at high temperature. The thermal stability of the organic templated silica xerogels, containing MTES, has been studied in both inert and oxidizing atmosphere. They are stable up to temperature range of 400-500 °C in both atmospheres [9]. However, this burnt off can be exploited to produce more micropores silica network and hence this has a significant effect on the separation properties of silica membrane as reported by Raman *et al.* [38].

Most of silanol bonds (surface hydroxyls) of the silica material can be removed by thermal treatment, especially at high temperature (800 °C), and upon exposure to water very slow subsequent rehydroxylation can occurs. Moreover, this thermal treatment leads to sintering of silica materials with complete loss of their porosity

[39]. Due to the removal of the organic template of the hybrid silica that depends mainly on the temperature at which it occurs, therefore continuous condensation reactions talk place to replace the lost of carbon with hydroxyl and/or siloxane bonds. This leads to continuous microporous network formation as well as silica densification results from the reduction in the number of silanol groups [32, 38]. Giessler *et al.* [12] have prepared two different templated silica xerogels using MTES as organic covalent ligand template and C6 surfactant as non-covalent ligand template. It was found that surfactant templated silica xerogel was stable up to temperature range of 250-320 °C, and MTES templated silica xerogel was stable up to temperature range of 400-500 °C. Raman *et al.* [38] have reported that at high temperature, 550 °C, the scale of the porosity of the MTES templated silica xerogel was apparently quite small and the densification of the silica matrix was virtually complete. This resulted in membranes exhibited increasing CO_2/ CH_4 selectivity, as small pores allow permeance of smaller molecular diameter gas (0.33 nm for CO_2 vs 0.38 nm for CH_4).

As mentioned in chapters 4 and 5, a novel unsupported silica membrane was reported and the preparation involved cobalt-doping within the matrix of organic templated silica material (hybrid silica) [9, 10]. Hydrophobic material with high thermal stability up to temperature range of 500-600 °C in oxidizing atmosphere was achieved. Besides, the novel material showed high thermal stability in inert atmosphere as well compared with the non-doped material. In chapter 5 concerning the effect of cobalt-doping on hybrid silica with different content of organic templates, and at high temperature, 600 °C, the metal-doped methylated microporous silica showed uptake of N_2 as indicated by the adsorption isotherm. This indicated that microporous network formation and further densification can occur at high temperature. This is a consequence of the high thermal stability and the organic templates removal at high temperature as non-uniform incorporation of the organic template in the silica matrix occurs in excess of 50:50% molar ratio of TEOS : MTES [10, 32]. Therefore, the aim of the present work is to investigate the effect of different cobalt amounts to be doped within the organic templated xerogel matrix, which contains constant content of covalently bonded methyl ligands (50% TEOS : 50% MTES). The fundamental aspects of xerogel characterization such as Fourier transform infrared (FTIR), X-ray diffraction, Thermogravimetric analysis (TGA) as

well as the micropore, and molecular sieve characterization aspects are reported in this chapter.

6.2. Experimental part

6.2.1. Materials and methods

Tetraethylorthosilicate (TEOS, 98%, Acros Organics), methyltriethoxysilane (MTES, 98%, Acros Organics), ethanol (EtOH, 96% V/V extra pure, Acros Organics), nitric acid (HNO_3, Acros Organics) and cobalt nitrate (99% pure, Acros Organics) were purchased from Scharlab. Distilled water was used for the sols preparation.

6.2.2. Xerogels preparation

The silica sols were prepared by the acid-catalyzed hydrolysis and condensation process. Tetraethylorthosilicate (TEOS) and Methyltriethoxysilane (MTES) were used as the silica precursors mixed with ethanol (EtOH), nitric acid (HNO_3), cobalt nitrate (as metal salt) and distilled water as described previously [9]. To prevent the partial (premature) hydrolysis during the addition of EtOH to TEOS at room temperature, the alkoxide/ethanol mixture was placed in ice bath and then acid/water mixture was added drop wise with continuous stirring [35]. For metal doping, a solution of cobalt nitrate in ethanol was used as described previously [9, 14].

Different cobalt- doped methyl ligand templated silica xerogels were prepared as follow: after addition of HNO_3/H_2O mixture to TEOS/EtOH mixture, the sol was refluxed under stirring in water bath at 60 °C for 165 minutes. The reaction mixtures had a (based on starting materials) TEOS : EtOH : H_2O : HNO_3 molar ratio of 1 : 3.8 : 6.4 : 0.085 according to the recipe of the silica sol preparation [24].

Afterwards, mixture of MTES/EtOH solution, which has been placed for 5-10 minutes in ice, and the ethanol solution of the metal salt were added to the reaction mixture and the final sol was refluxed for an additional 15 minutes. The molar ratio of MTES/EtOH solution was 1 : 3.8 and hence the mixture had a (based on starting materials) TEOS : MTES : EtOH : H_2O : HNO_3 molar ratio of 1 : 1 : 7.6 : 6.4 : 0.085. The metal salt to metal alkoxide (Co:Si) weight ratio used was varied from 3% to 10% for all modified silica materials. In the present study different cobalt- doped methyl ligand templated silica xerogels are referred as X%-Co, where X=3, 5, 8 and 10. The

first work on this novel silica membrane material was performed by cobalt-doping (3wt%) [9], therefore, the amounts from 5 to 10 wt% are chosen for studying the gradual increase of cobalt content.

All silica sols were allowed to evaporate in Petri-dish at room temperature so that silica flakes, xerogels, were obtained overnight. Xerogels samples were crushed finely to obtain powders, which were used for characterization, and were calcined in air at a heating and cooling rate of 1 °C/min, and held for 3 hours at 400 °C and 2 hour at 600 °C. For X-ray comparison of the different xerogels, silica powders were mixed with Co_3O_4 with weight ratio 3%. Cobalt oxide was prepared by calcination cobalt nitrate in air at 400 °C as the silica xerogels.

6.2.3. Characterization of the xerogels

Thermogravimetric analysis (thermogravimetry, TGA and differential thermal analysis, DTA) was used to investigate the processes taking place during the heat treatment. This analysis was carried out for dried xerogels, in a Perkin Elmer model Thermobalance TGA7 device, in synthetic air with constant flow rate of 290 $cm^3\ min^{-1}$ and heating rate of 10 °C min^{-1} from room temperature to 900 °C.

Fourier transform infrared characterization was carried out to determine functional groups within the bulk silica matrix using ATR cell (FTIR 680 Plus JASCO). The absorption spectra were recorded in the 500-1500 cm^{-1} range. The spectrum of each sample represents an average of 32 scans. With the aim of comparison, all FTIR spectra were normalized with respect to the maximum absorbance value for each sample.

XRD for phase detection was conducted using a Siemens D500 diffractometer (Bragg-Brentano parafocusing geometry and vertical θ-θ goniometer). The angular 2θ diffraction range was 5° to 70°. The crystalline size was determined from the line broadening of the diffraction line at 2θ = 36.8° using the Scherrer equation (eq. 2.2).

Textural characterization of the synthesized samples was determined by nitrogen isotherms measurements at -196 °C. Gas adsorption measurements were performed in the range of $3\times10^{-7} < P/P_0 < 0.995$. The measurements were performed in a Quantachrome Autosorb-iQ adsorption analyzer. Before analysis, the samples were degassed at 250 °C under vacuum for 12 h. The pore size distribution was

calculated from the nitrogen adsorption data using the NLDFT model (Non Localized Density Functional Theory) based on a cylindrical pore-equilibrium model.

6.3. Results and discussion

6.3.1. Thermogravimetric analysis

The stability of the organic templates as well as the condensation occurred during the heat treatment in an oxidizing atmosphere was assessed by thermogravimetric analysis. The weight loss curves of the X%-Co as function of temperature (TGA curve) and the differential weight loss (DTA curve) are shown in Figure 6.1. For all samples, the initial weight losses from room temperature to ~ 150 °C are mainly attributed to physisorbed water molecules trapped in the matrix of the xerogels, and to the loss of free solvent molecules [9, 10, 12, 32, 37]. From ~ 150 to ~ 240 °C, the weight loss is due to the dehydration of cobalt nitrate and to the removal of the nitrous gases [10, 40]. That weight loss increased as the cobalt-doped content increased in the xerogels. The heat treatment from ~ 240 to ~ 500 °C, leads to further condensation reaction, i.e. removal of the water and alcohol from the silica matrix [10, 32, 38]. In the first study on metal-doped organic templated silica xerogel, chapter 4, it was reported that this material is thermally stable in oxidizing atmosphere up to ~ 560 °C, and more thermally stable than the non-doped one in inert atmosphere [9]. Later, we have studied the effect of constant amount of cobalt to be doped within the matrix of the methyl ligand templated silica xerogel, chapter 5. It was found that this doping led to more thermal stability in oxidizing atmosphere, regardless the MTES content [10]. This is also the same case in the present study where the methyl ligand templated silica xerogels, with 50% MTES, show high thermal stability in oxidizing atmosphere regardless the cobalt amount.

For 50% MTES templated silica xerogel (non-doped one) the oxidative pyrolysis of the methyl ligands was found to be around ~ 450 °C in oxidizing atmosphere [10, 12, 32]. Castricum *et al.* [41] have reported that the decomposition or pyrolysis processes did not occur for the methyl ligand templated silica xerogels, regardless the MTES content, at temperatures below ~ 312 °C and the samples were stable up to at least 400 °C in N_2. In a comparison with other organic templated silica xerogels (non-doped xerogels), the novel one is more thermally stable. For instance, surfactant

templated silica xerogel was stable up to temperature range of 250-320 °C, whereas MTES templated silica xerogel was stable up to temperature range of 400-500 °C [12]. On the other hand, organic templated silica xerogels using TEOS, 3-(Trimethoxysilyl)propyl methacrylate (MPTMA) and the urethane acrylate organic resin showed thermal stability up to temperature range of 400-500 °C [42]. As it can be seen from TGA and DTA curves, the decomposition or pyrolysis processes for the methyl ligands occurred at high temperature range of 500-600 °C, regardless the cobalt content, as they are stable up to ~ 560 °C in oxidizing atmosphere. The high thermal stability of the X%-Co could be attributed to the presence of the strong framework by the formation of Si-O-Co linkage [9, 10, 43-45].

6.3.2. Infrared spectroscopy

Figure 6.2 shows the FTIR spectra of dried and calcined 10%-Co at 400 and 600 °C (other xerogels show the same spectra as well). From ~ 600 to ~ 1400 cm^{-1}, this is the range of IR bands corresponding to silanol and siloxane bonds for all cobalt-doped methyl ligand templated silica xerogels.

Bands assigned to siloxane bonds (Si-O-Si) appears at ~ 760 - 807 cm^{-1} and bands at ~ 935 cm^{-1} were assigned to silanol bonds (Si-O-H) [46, 47]. This latest band appears strongly for the dried silica and its intensity decrease after calcination process at 400 °C and 600 °C. This change intensity is attributed to the condensation process, and also support the hypothesis that polycondesation allows for the transformation of silanols to silicons as reported elsewhere [48, 49]. The band at ~ 1278 cm^{-1} was assigned to asymmetric vibration of the CH_3 group [9, 35, 47]. This band is unobservable for the calcined sample at 600 °C whereas it appears strongly for the dried and the calcined sample at 400 °C. This result is in agreement with TGA results, where around that temperature a high ratio of the decomposition or pyrolysis processes occurred for the organic templates (methyl ligands) in oxidizing atmosphere [10]. Stretching vibrations at around 1000–1100 cm^{-1} [17, 47] were assigned to Si–O–Si, and shifting with a broad shoulder can be found from 1022 cm^{-1} (for dried samples), 1035 cm^{-1} (for samples calcined at 400 °C) to 1040 cm^{-1} (for samples calcined at 600 °C). This shift is interpreted as changes in the xerogel matrix as result of the shrinkage in the silica polymeric bonding derived from heat treatment [9, 18, 48, 50]. Tiny small bands at ~ 570 and ~ 670 cm^{-1} were assigned to cobalt, in

oxide form Co_3O_4. These two bands appeared after the calcination process whereas these bands were no present before the calcinations process [9, 44, 51, 52].

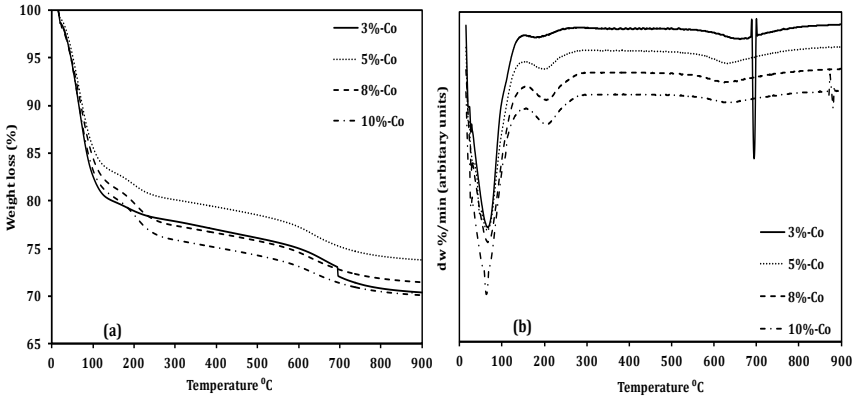

Figure 6.1. TGA (a) and DTA (b) of different cobalt content organic templated xerogels.

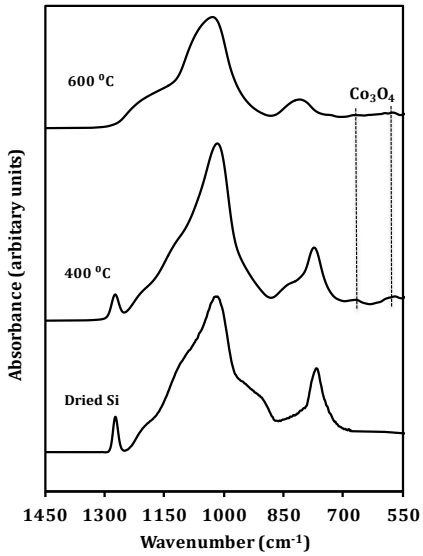

Figure 6.2. FTIR spectrum of 10%-Co.

6.3.3. X-ray analysis

The X-ray results of the calcined samples of the X%-Co are shown in Figure 6.3. As it can be seen, the difference in their XRD diffractogramms, which is an indication that the nature of the cobalt species and their interaction with the silica matrix were strongly depending on both, the cobalt content and heat treatment. The X-ray result of the 3%-Co appear amorphous [9, 10]. Whereas as the cobalt content increase from 5 to 10%, the peak intensity of (100) for Co_3O_4 (2θ = 36.8°) increase as well. Moreover, the crystalline size of Co_3O_4 species, as determined using the Scherrer equation (eq. 2.2), increase to be about 5 nm for 5%-Co, 7 nm for 8%-Co and 8 nm for 10%-Co. Besides, as it can be seen the peak intensity of the mixture of silica powder, SiO_2, and Co_3O_4 (3 wt%) was higher than that of the peak intensity of the all different cobalt-doped in the silica matrix.

These results strongly support the following interpretation: at low cobalt content the formation of a mixed matrix of polymeric silica and cobalt oxide particles will be more dominant than the formation of crystalline Co_3O_4. Contrarily, at high cobalt content certain amounts of the cobalt-impregnated in the silica matrix will form crystalline Co_3O_4 along with the interaction between the ionic metal as Co^{2+} and the siloxane matrix will take place as reported elsewhere [44]. The formation of Si-O-Co linkage was postulated through condensation of cobalt oxo-hydroxy complexes $[Co(H_2O)_{6-x-y}(HO)_xO_y]$ with silicone complexes $[Si(OC_2H_5)_{4-n}(OH)_n]$ [44, 45]. As result of these, the possible hypotheses for the existences of the cobalt within the silica matrix are the following: ionic metal as Co^{2+}; covalently bound cobalt strongly interacting with the siloxane matrix forming Si-O-Co; or tiny crystal that could not be detected by XRD for the low cobalt content sample, 3%-Co, and detectable crystals for the high cobalt content samples, 5-10%-Co [8, 9, 44, 45].

6.3.4. Micropore structure

Textural properties were determined using N_2 adsorption isotherms at -196 °C. The surface area was obtained by application of the BET (Brunauer, Emmett and Teller) equation to the nitrogen adsorption data [53]. The total pore volume, V_T, was obtained from the amount of N_2 adsorbed at a relative pressure (P/P_0) of 0.99. The pore size distributions (PSD) were calculated by applying the NLDFT model to the

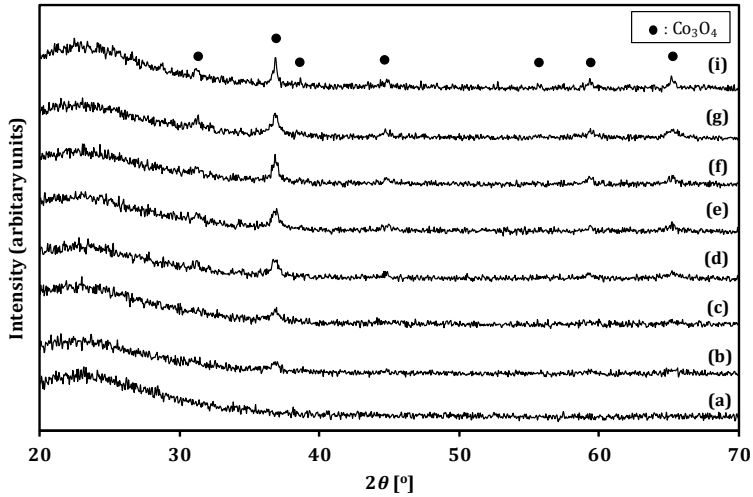

Figure 6.3. XRD diffractogramms of X%-Co calcined at 400 °C (a) 3%-Co, (b) 5%-Co, (d) 8%-Co and (f) 10%-Co. Samples calcined at 600 °C (c) 5%-Co, (e) 8%-Co and (g) 10%-Co. (i) SiO_2+Co_3O_4 mixture and solid circles represent Co_3O_4 reference pattern.

nitrogen adsorption data at -196 °C based on a cylindrical pore model [54]. Micro-and mesoporosity were determined using the *t*-plot method [55]. Table 6.1 and 6.2 represent the compilation of structural parameters deduced from the N_2 adsorption data at -196 °C for the samples calcined at 400 °C and 600 °C, respectively.

Figure 6.4a and 6.4b represent the N_2 adsorption isotherms for the calcined X%-Co samples at 400 °C and 600 °C, respectively. At 400 °C the isotherms represent high amount of N_2 adsorbed at low relative pressure, a knee at low relative $P/P_0 < 0.1$ where the majority of the pores filling, which is a characteristic of microporous materials [56]. As the amount of the cobalt increase the isotherms show a slight increase at relative pressure of 0.4 and this could be attributed to the presence and the formation of crystalline Co_3O_4. Esposito *et al.* [44] confronted change in the adsorption isotherm of cobalt-doped silica, of Type IV isotherm with large adsorption volumes at relative pressure > 0.4, as the cobalt content increased to 30 mol%. However, the samples in the present study still show the characteristic isotherm of microporous materials. At 600 °C, no difference in the isotherms type is observed

with regard to the samples calcined at 400 °C, except that the amount of N_2 uptake is less due to the heat treatment which leads to densification of the silica matrix.

Figure 6.5a and 6.5b show the PSD of the calcined X%-Co samples at 400 °C and 600 °C, respectively. As it can be noticed, all samples are micropores or border the mesoporous region by exhibiting an average pore widths at ~ 0.8, ~ 1.1 nm (more apparently for 3%-Co) and ~ 1.4 nm at 400 °C and at ~ 0.8 and ~ 1.1 nm at 600 °C. This corresponding to the pores fill at low relative pressure and thus a narrow PSD produced. Some supermicropores are obtained and this could be attributed to the presence of cobalt in the oxide form as reported elsewhere [44]. However, the PSD results could differ somehow depending mainly on the model used for the PSD determination [9].

From the data in Table 6.1 and 6.2 it seems that at each specific temperature, either at 400 °C or 600 °C, the variation in the obtained results is not dramatically, as the PSD remained similar and the variations in the pore volumes and specific areas are not so large. In fact the only noticeable change is that the 3%-Co at both temperatures differs from the other samples that have approximately the same structural parameters at each temperature separately, only 5%-Co shows high micropore surface area at 400 °C. This could be attributed to the fact that the dominant case for 3%-Co is the formation of the strong framework by the formation of Si-O-Co linkage at low cobalt content, whereas the dominant case for the other samples is the crystalline structure. In general, due to the metal-doping process, the surface area and the micropore volume should be reduced as the amount of the metal increases. Esposito *et al.* [44] encountered a decrease in the micropore volume as the cobalt content increased, and also a decrease in the surface area for 20 mol% cobalt. Generally the metal content, especially in the oxide form, has low surface area as compared to polymeric silica. The obtained results show no significant effect of the cobalt-doping at each temperature, despite that of the 3%-Co sample which deviates from the other samples, i.e. its structural parameters lower than the other samples, this strongly suggests that over 3%-Co the cobalt particles, in oxide form, were homogeneously dispersed in the hybrid silica matrix. Similar case have been reported concerning investigation the effect of iron oxide embedded in conventional silica

matrices [57]. In addition, this supports that cobalt composite with the silica matrix results in the formation of Si-O-Co linkage for the 3%-Co sample.

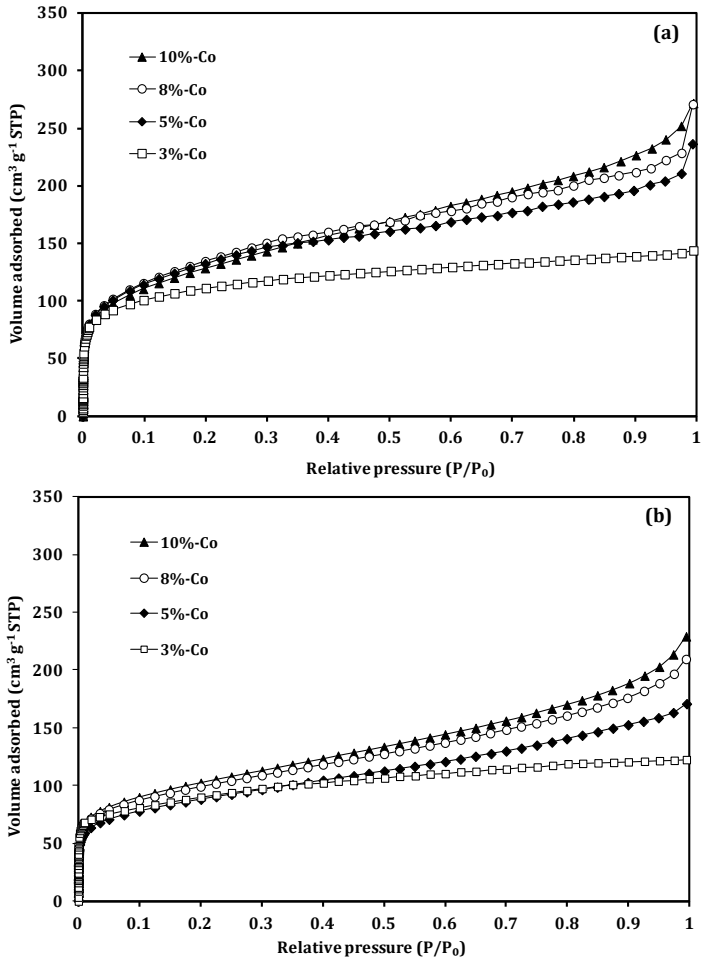

Figure 6.4. N_2 adsorption isotherms of X%-Co calcined at a) 400 °C and b) 600 °C.

Thermally enhanced methylated microporous silica for molecular sieve applications

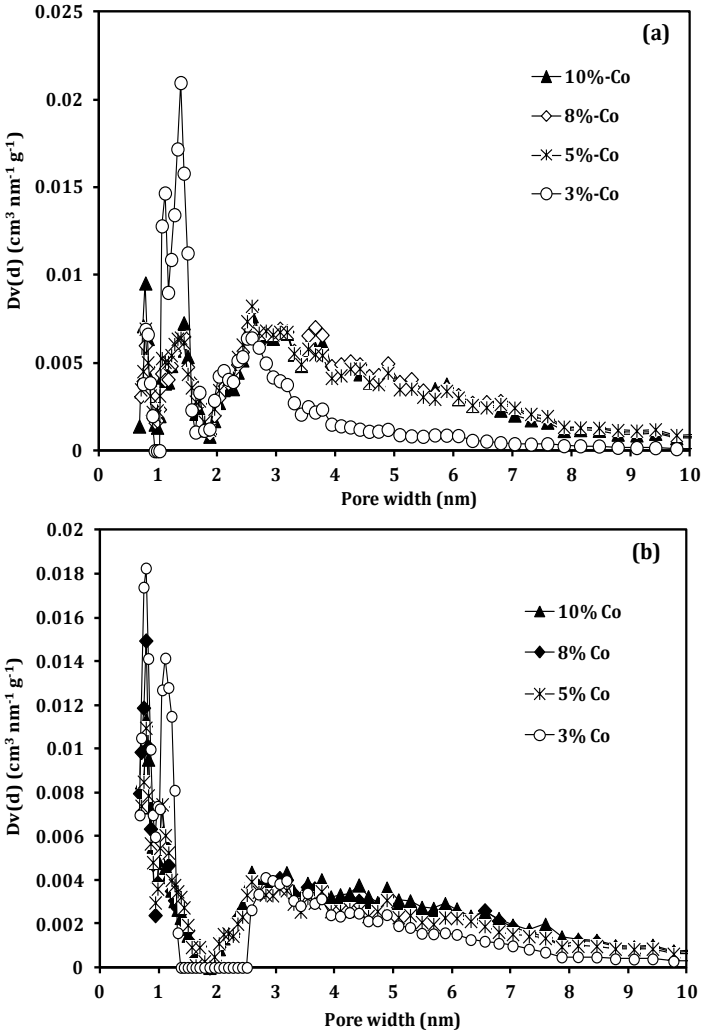

Figure 6.5. PSD of X%-Co calcined at a) 400 °C and b) 600 °C.

Table 6.1. Compilation of structural parameters deduced from N_2 adsorption data at -196 °C for X%-Co calcined samples at 400 °C.

Sample (% Co)	S_{BET} (m^2g^{-1})	Micropore surface (m^2g^{-1})	$V_{T0.99}$ ($cm^3\ g^{-1}$)	V_{micro} ($cm^3\ g^{-1}$)
3	406	393	0.22	0.20
5	476	422	0.40	0.29
8	484	375	0.45	0.23
10	462	372	0.42	0.23

Table 6.2. Compilation of structural parameters deduced from N_2 adsorption data at -196 °C for X%-Co calcined at 600 °C.

Sample (% Co)	S_{BET} (m^2g^{-1})	Micropore surface (m^2g^{-1})	$V_{T0.99}$ ($cm^3\ g^{-1}$)	V_{micro} ($cm^3\ g^{-1}$)
3	320	299	0.21	0.18
5	351	277	0.40	0.19
8	353	275	0.45	0.17
10	365	273	0.42	0.17

S_{BET}: Surface area (after application of the Brunauer, Emmett and Teller equation to the nitrogen adsorption data).
$V_{T0.99}$: Total pore volume (from the amount adsorbed at $P/P_0 = 0.95$).
V_{micro}: Micropore volume.

The only difference between the samples can be observed due to the calcination process. It is well known that the heat treatment has a significant effect on the silica structures. In particular leads to structural changes as the densification of the silica matrix occur, due to the reduction of silanol (hydroxyl) surface groups, especially at high temperatures. For MTES templated silica xerogel, as result of the organic templates burnt off, replacement of the lost carbon with hydroxyl and/or siloxane bonds occur. Subsequently, continuous microporous networks are formed that depend on the temperature at which burnt off occurs (between 400-500 °C). At 550 °C , i.e. after the temperature rang at which removal of the organic templates take place, complete densification of the hybrid silica matrix was observed [38]. However, the formation of more microporous networks had a significant effect on the hybrid silica material towards gas separation. This was observed for the unsupported silica that exhibited uptake of CO_2 rather than N_2 that were used as molecular probes to check the efficacy of templated molecular sieving films. Whereas for the supported one exhibited very high permeability combined with high selectivity towards CO_2 over CH_4 [38]. In some cases at 550 °C the MTES templated silica xerogels showed N_2 uptake but not such as at 400 °C as reported by Diniz da Costa *et al.* [32].

Alongside the matrix densification due to heat treatment, changes in the micropore volume and area as well as surface area occurred [10, 32]. In the present study, due to the calcination process, these structural changes are also observed when comparing the samples calcined at 400 °C and 600 °C. Moreover, for the samples calcined at 600 °C the peak at ~ 1.4 nm is not observable as result of reduction of the micropore volume and area by heat treatment. This supports the view of the formation of continuous microporous network at high temperature. In general, the average of the narrow PSD is still quite constant for all samples at each temperature separately. For samples 5 to 10%-Co, calcination at 600 °C results in densification of the silica matrix that is accompanied with approximately similar structural parameters. Therefore, this indicates that cobalt-doping process apposed greater collapse of the silica structure and this could be attributed to the homogeneity dispersion of the cobalt oxide within the silica matrix. Figure 6.6 represents the percent of structural changes in surface area and micropore surface area because of the heat treatment from 400 °C to 600 °C. As it can be observed that sample 5%-Co exhibit major structural change in the micropore surface area

comparing with the other samples. However, the samples show large structural changes in micropore surface area (~ 24% to ~ 35%) compared with surface area (~ 21% to ~ 27%). This could be attributed to the presence of cobalt that has a significant effect on modifying the PSD by reducing the micropore volume, and hence the micropore surface area compared with the surface area [44].

Due to the heat treatment the non-doped MTES templated silica xerogels showed large percent of structural change in micropore surface area. For instance, 30 and 40 mol % MTES/TEOS xerogels showed reduction in micropore surface areas of ~ 57% and ~ 51% by heat treatment from 400 °C to 550 °C and 450 °C to 500 °C, respectively [32]. The samples in the present study have a high MTES content, which should lead to collapse of the silica structure, than other materials [32]. However, they show a smaller reduction in the micropore surface area, although the temperature range is higher (from 400 °C to 600 °C). Obviously, the cobalt-doping within the MTES templated silica xerogel further provides beneficial structural stability.

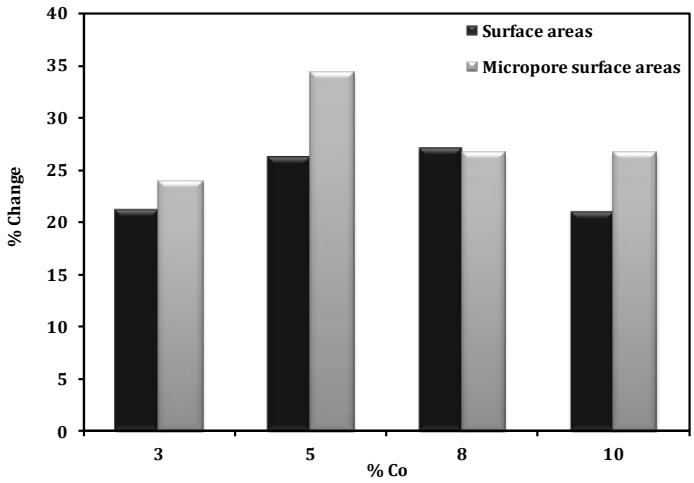

Figure 6.6. Structural changes in surface and micropore surface area.

As reported on MTES templated silica xerogels, with different MTES content and 3 wt% cobalt (chapter 5), the structural changes were observed as the MTES content increased along with heat treatment [10]. Besides, by varying the organic template content, pore control could be achieved, and hence 3wt% cobalt content had no effect except the thermal stability enhancement. Therefore, this interprets the obtained results in the present work where cobalt-doping, more than 3 wt%, has a significant role in opposing the hybrid silica structure collapse. As the cobalt-doping process leads to more thermal stability of the hybrid silica materials, and hence the burnt off for the organic templates occur at higher temperature range compared with the non-doped materials. Continuous microporous formation, i.e. the tendency for more small pores formation, as well as further densification can occur at higher temperature and not complete as reported at temperature of 550 °C [38]. Therefore, fine control of the silica matrix and pore size tuning is possible in the present study by metal-doping within the organic templated silica matrix.

In any case the modification of the silica materials to achieve new materials with enhanced thermal properties in the present study has been proved. Besides, the micropores results (with narrow PSD) suggest that these novel unsupported hybrid materials can be used as precursor materials for molecular sieve silica applications. However, for the supported materials the actual values of the pores width may differ somehow regardless the obtained results for the unsupported materials. As these materials possess micropores as well as supermicropores, therefore, for gas separation, as a type of the molecular sieve silica applications, these supermicropores can be exploited to facilitate the transport of small diffusing molecules towards narrow pores of the silica membranes on the expenses of larger molecules. Hence, these materials can be considered as promising membrane materials for the particular applications of pervaporation and gas separation.

6.4. Conclusions

A novel highly thermally stable organic templated silica xerogels were prepared by the sol-gel technique. The sol-gel method allowed a better control of the textural properties of the silica matrix and a more effective dispersion of cobalt oxide in the matrix on a nanometric scale. Enhancement in the thermal properties of the silica matrix was achieved via cobalt-doping process. The cobalt-doped methylated microporous silica xerogels with different cobalt content were prepared via the acid-catalyzed and condensation of TEOS and MTES with 50:50% molar ratio. This molar ratio was chosen because non-uniform incorporation of the organic templates in the silica matrix occurs in excess of that molar ratio. MTES was used as precursor for the methyl ligand covalently bounded to the silica matrix. The high thermal stability of the novel silica material could be attributed to the presence and the strong framework by the formation of Si-O-Co linkages. The X-ray results showed that these linkages were the dominant case at low cobalt content, and hence amorphous structure was obtained. Whereas as the cobalt content increased the formation of crystalline Co_3O_4 species were the dominant case. As result of the promoted densification of the xerogels by heat treatment, there were structural changes such as decrease in the surface areas and the micropore volumes and areas. However, calcination at 600 °C resulted in samples with approximately the same structural parameters though the cobalt oxide content increased from 5 to 10% weight ratio. This suggested that the cobalt particles were homogeneously dispersed in the silica matrix and opposed the silica structure collapse.

The burnt off process of the organic templates occurred at high temperature range for the novel material compared with the non-doped material. Therefore, microporous network formation and further densification can be occurred even at high temperature and not complete as the non-doped materials showed at 550 °C. The cobalt-doped methylated microporous silica exhibited trend towards micropores formation, although some supermicropores were observed. In any case, the high thermal stability can be achieved by cobalt-doping regardless its amount, while cobalt content over 3 wt% resulted in silica matrix with approximately the same structural parameters even at high temperature. However, the obtained results

demonstrate the potential of these highly thermally stable silica materials to be used as membrane precursor materials for molecular sieve silica membranes applications.

6.5. References

[1] G.Q. Lu, J.C. Diniz da Costa, M. Duke, S. Giessler, R. Socolow, R.H. Williams, T. Kreutz, Inorganic membranes for hydrogen production and purification: A critical review and perspective, J. Colloid Interface Sci. 314 (2007) 589-603.

[2] G. Barbieri, A. Brunetti, T. Granato, P. Bernardo, E. Drioli, Engineering evaluations of a catalytic membrane reactor for the water gas shift reaction, Ind. Eng. Chem. Res. 44 (2005) 7676-7683.

[3] M.D. Dolan, N.C. Dave, A.Y. Ilyushechkin, L.D. Morpeth, K.G. McLennan, Composition and operation of hydrogen-selective amorphous alloy membranes, J. Membr. Sci. 285 (2006) 30-55.

[4] L. Barelli, G. Bidini, F. Gallorini, S. Servili, Hydrogen production through sorption-enhanced steam methane reforming and membrane technology: A review, Energy 33 (2008) 554-570.

[5] M.C. Duke, J.C. Diniz da Costa, G.Q. Lu, M. Petch, P. Gray, Carbonised template molecular sieve silica membranes in fuel processing systems: permeation, hydrostability and regeneration, J. Membr. Sci. 241 (2004) 325-333.

[6] K. Damen, M.v. Troost, A. Faaij, W. Turkenburg, A comparison of electricity and hydrogen production systems with CO_2 capture and storage. Part A: Review and selection of promising conversion and capture technologies, Progr. Energy Combust. Sci. 32 (2006) 215-246.

[7] S. Battersby, M.C. Duke, S. Liu, V. Rudolph, J.C. Diniz da Costa, Metal doped silica membrane reactor: Operational effects of reaction and permeation for the water gas shift reaction, J. Membr. Sci. 316 (2008) 46-52.

[8] R. Igi, T. Yoshioka, Y.H. Ikuhara, Y. Iwamoto, T. Tsuru, Characterization of Co-doped silica for improved hydrothermal stability and application to hydrogen separation membranes at high temperatures, J. Am. Ceram. Soc. 91 (2008) 2975-2981.

[9] H.H. El-Feky, K. Briceño, E.d.O. Jardim, J. Silvestre-Albero, T. Gumí, Novel silica membrane material for molecular sieve applications, Microporous Mesoporous Mater. 179 (2013) 22-29.

[10] H.H. El-Feky, K. Briceño, M. A. G. Hevia, T. Gumí, Characterization of metal-doped methylated microporous silica for molecular separations, submitted to Microporous Mesoporous Materials.

[11] H.L. Castricum, A. Sah, R. Kreiter, D.H.A. Blank, J.F. Vente, J.E. ten Elshof, Hydrothermally stable molecular separation membranes from organically linked silica, J. Mater. Chem. 18 (2008) 2150-2158.

[12] S. Giessler, J.C. Diniz da Costa, G.Q. Lu, Hydrophobicity of templated silica xerogels for molecular sieving applications, J. Nanosci. Nanotechnol. 1 (2001) 331-336.

[13] D.-H. Park, N. Nishiyama, Y. Egashira, K. Ueyama, Enhancement of hydrothermal stability and hydrophobicity of a silica MCM-48 membrane by silylation, Ind. Eng. Chem. Res. 40 (2001) 6105-6110.

[14] G.P. Fotou, Y.S. Lin, S.E. Pratsinis, Hydrothermal stability of pure and modified microporous silica membranes, J. Mater. Sci. 30 (1995) 2803-2808.
[15] L.L. Hench, J.K. West, The sol-gel process, Chem. Rev. (Washington, DC, U. S.) 90 (1990) 33-72.
[16] S. Sakka, Handbook of Sol-Gel Science and Technology: Processing, Characterization, and Applications, Kluwer Academic Publishers, Dordrecht, 2005.
[17] C.J. Brinker, G.W. Scherer, Sol-Gel Science: The Physics and Chemistry of Sol-Gel Processing, Academic Press, Boston, 1990.
[18] J.C. Diniz da Costa, G.Q. Lu, V. Rudolph, Y.S. Lin, Novel molecular sieve silica (MSS) membranes: characterisation and permeation of single-step and two-step sol–gel membranes, J. Membr. Sci. 198 (2002) 9-21.
[19] C.-Y. Tsai, S.-Y. Tam, Y. Lu, C.J. Brinker, Dual-layer asymmetric microporous silica membranes, J. Membr. Sci. 169 (2000) 255-268.
[20] W.J. Elferink, B.N. Nair, R.M. de Vos, K. Keizer, H. Verweij, Sol–gel synthesis and characterization of microporous silica membranes: II. Tailor-making porosity, J. Colloid Interface Sci. 180 (1996) 127-134.
[21] B.N. Nair, W.J. Elferink, K. Keizer, H. Verweij, Sol–gel synthesis and characterization of microporous silica membranes I: SAXS study on the growth of polymeric structures, J. Colloid Interface Sci. 178 (1996) 565-570.
[22] M.-J. Muñoz-Aguado, M. Gregorkiewitz, Sol–gel synthesis of microporous amorphous silica from purely inorganic precursors, J. Colloid Interface Sci. 185 (1997) 459-465.
[23] S. Smart, J.F. Vente, J.C. Diniz da Costa, High temperature H_2/CO_2 separation using cobalt oxide silica membranes, Int. J. Hydrogen Energy 37 (2012) 12700-12707.
[24] R.M. de Vos, H. Verweij, Improved performance of silica membranes for gas separation, J. Membr. Sci. 143 (1998) 37-51.
[25] B.N. Nair, T. Yamaguchi, T. Okubo, H. Suematsu, K. Keizer, S.-I. Nakao, Sol-gel synthesis of molecular sieving silica membranes, J. Membr. Sci. 135 (1997) 237-243.
[26] S. Giessler, L. Jordan, J.C. Diniz da Costa, G.Q. Lu, Performance of hydrophobic and hydrophilic silica membrane reactors for the water gas shift reaction, Sep. Purif. Technol. 32 (2003) 255-264.
[27] J.C.D. Da Costa, G.Q. Lu, H.Y. Zhu, V. Rudolph, Novel composite membranes for gas separation: Preparation and performance, J. Porous Mater. 6 (1999) 143-151.
[28] C.J. Brinker, Hydrolysis and condensation of silicates: Effects on structure, J. Non-Cryst. Solids 100 (1988) 31-50.
[29] C.J. Brinker, K.D. Keefer, D.W. Schaefer, C.S. Ashley, Sol-gel transition in simple silicates, J. Non-Cryst. Solids 48 (1982) 47-64.

[30] N.K. Raman, M.T. Anderson, C.J. Brinker, Template-based approaches to the preparation of amorphous, nanoporous silicas, Chem. Mater. 8 (1996) 1682-1701.

[31] Q. Wei, Y.-L. Wang, Z.-R. Nie, C.-X. Yu, Q.-Y. Li, J.-X. Zou, C.-J. Li, Facile synthesis of hydrophobic microporous silica membranes and their resistance to humid atmosphere, Microporous Mesoporous Mater. 111 (2008) 97-103.

[32] J.C. Diniz da Costa, G.Q. Lu, V. Rudolph, Characterisation of templated xerogels for molecular sieve application, Colloids Surf., A 179 (2001) 243-251.

[33] K. Kusakabe, S. Sakamoto, T. Saie, S. Morooka, Pore structure of silica membranes formed by a sol–gel technique using tetraethoxysilane and alkyltriethoxysilanes, Sep. Purif. Technol. 16 (1999) 139-146.

[34] Y. Lu, G.Z. Cao, R.P. Kale, L. Delattre, C.J. Brinker, G.P. Lopezl, Controlling the porosity of microporous silica by sol-gel processing using an organic template approach, Mat. Res. Soc. Symp. Proc. 435 (1996) 271-275.

[35] R.M. de Vos, W.F. Maier, H. Verweij, Hydrophobic silica membranes for gas separation, J. Membr. Sci. 158 (1999) 277-288.

[36] M.J. van Bommel, T.N.M. Bernards, A.H. Boonstra, The influence of the addition of alkyl-substituted ethoxysilane on the hydrolysis—condensation process of TEOS, J. Non-Cryst. Solids 128 (1991) 231-242.

[37] S. Giessler, M.C. Duke, J.C. Diniz da Costa, G.Q. Lu, Hydrothermal stability of modified silica membranes for gas separation, D. G. Wood 6th World Congress of Chemical Engineering (2001) 1-10.

[38] N.K. Raman, C.J. Brinker, Organic "template" approach to molecular sieving silica membranes, J. Membr. Sci. 105 (1995) 273-279.

[39] R.K. Iler, The Chemistry of Silica: Solubility, Polymerization, Colloid and Surface Properties, and Biochemistry, John Wiley and Sons, New York, 1979.

[40] K. Sinkó, G. Szabó, M. Zrínyi, Liquid-phase synthesis of cobalt oxide nanoparticles, J. Nanosci. Nanotechnol. 11 (2011) 4127-4135.

[41] H.L. Castricum, A. Sah, M.C. Mittelmeijer-Hazeleger, C. Huiskes, J.E.t. Elshof, Microporous structure and enhanced hydrophobicity in methylated SiO_2 for molecular separation, J. Mater. Chem. 17 (2007) 1509-1517.

[42] Y.-H. Han, A. Taylor, M.D. Mantle, K.M. Knowles, Sol–gel-derived organic–inorganic hybrid materials, J. Non-Cryst. Solids 353 (2007) 313-320.

[43] K. Kojima, H. Taguchi, J. Matsuda, Optical and magnetic properties of Co^{2+} ions in dried and heated silica gels prepared by the sol-gel process, J. Phys. Chem. 95 (1991) 7595-7598.

[44] S. Esposito, M. Turco, G. Ramis, G. Bagnasco, P. Pernice, C. Pagliuca, M. Bevilacqua, A. Aronne, Cobalt–silicon mixed oxide nanocomposites by modified sol–gel method, J. Solid State Chem. 180 (2007) 3341-3350.

[45] G. Ortega-Zarzosa, C. Araujo-Andrade, M.E. Compeán-Jasso, J.R. Martínez, F. Ruiz, Cobalt oxide/silica xerogels powders: X-ray diffraction, infrared and visible absorption studies, J. Sol-Gel Sci. Technol. 24 (2002) 23-29.

[46] Z. Olejniczak, M. Łęczka, K. Cholewa-Kowalska, K. Wojtach, M. Rokita, W. Mozgawa, ^{29}Si MAS NMR and FTIR study of inorganic–organic hybrid gels, J. Mol. Struct. 744–747 (2005) 465-471.

[47] H. Günzler, H.M. Heise, IR Spectroscopy: An Introduction, Wiley-VCH, Weinheim, 2002.

[48] A. Duran, C. Serna, V. Fornes, J.M. Fernandez Navarro, Structural considerations about SiO_2 glasses prepared by sol-gel, J. Non-Cryst. Solids 82 (1986) 69-77.

[49] A. Bertoluzza, C. Fagnano, M. Antonietta Morelli, V. Gottardi, M. Guglielmi, Raman and infrared spectra on silica gel evolving toward glass, J. Non-Cryst. Solids 48 (1982) 117-128.

[50] H. Qi, J. Han, N. Xu, Effect of calcination temperature on carbon dioxide separation properties of a novel microporous hybrid silica membrane, J. Membr. Sci. 382 (2011) 231-237.

[51] A.Y. Khodakov, J. Lynch, D. Bazin, B. Rebours, N. Zanier, B. Moisson, P. Chaumette, Reducibility of cobalt species in silica-supported Fischer–Tropsch catalysts, J. Catal. 168 (1997) 16-25.

[52] D. Uhlmann, S. Liu, B.P. Ladewig, J.C. Diniz da Costa, Cobalt-doped silica membranes for gas separation, J. Membr. Sci. 326 (2009) 316-321.

[53] S. Brunauer, P.H. Emmett, E. Teller, Adsorption of gases in multimolecular layers, J. Am. Chem. Soc. 60 (1938) 309-319.

[54] A.V. Neimark, P.I. Ravikovitch, Capillary condensation in MMS and pore structure characterization, Microporous Mesoporous Mater. 44–45 (2001) 697-707.

[55] J.H. de Boer, B.C. Lippens, B.G. Linsen, J.C.P. Broekhoff, A. van den Heuvel, T.J. Osinga, The t-curve of multimolecular N_2-adsorption, J. Colloid Interface Sci. 21 (1966) 405-414.

[56] K.S.W. Sing, D.H. Everett, R.A.W. Haul, L. Moscou, R.A. Pierotti, J. Rouquerol, T. Siemieniewska, Reporting physisorption data for gas/solid systems with special reference to the determination of surface-area and porosity (Recommendation 1984), Pure Appl. Chem. 57 (1985) 603-619.

[57] A. Darmawan, S. Smart, A. Julbe, J.C. Diniz da Costa, Iron oxide silica derived from sol-gel synthesis, Materials 4 (2011) 448-456.

Chapter 7

Novel Hydrophobic Silica Membrane for Gas Separation

A new class of hybrid molecular sieve silica membrane is developed and reported in this chapter. The novel hydrophobic cobalt-doped silica membrane is prepared by the standard sol-gel process, integrating an organic template (methyltriethoxysilane, MTES) into the silica film matrix that provides the membrane hydrophobicity. Cobalt-doping process results in a membrane retaining the hydrophobic feature after calcinations in air and high thermal stability as well. Two different methodologies are reported for membrane preparation, one under normal conditions and the other one under clean room conditions. Top silica selective layers are prepared by different dilution process, 20-fold dilution (20x) for membrane preparation in both methodologies and 6-fold dilution (6x) for clean room case. The transport of diffusing gases is governed by specific mechanisms depending mainly on the way of preparation. Molecular sieve silica membrane is achieved under clean room conditions, especially with 20x top silica selective layers. Tuning pore control in the region of < 0.3 nm is achieved indicated by the high flux of He compared with other gases. This is accompanied with high activation energy and permselectivity for some gases such as H_2/CH_4 and CO_2/CH_4, varying with temperature as result of the activated transport. Generally, novel hybrid silica membrane is developed and achieved for the particular applications of gas separation.

Novel hydrophobic silica membrane for gas separation

7.1. Introduction

Gas separation using inorganic membranes has emerged into a commercial technology for several industrially important gas separations such as O_2/N_2, CO_2/CH_4, dehydrogenation and hydrogen separation and purification [1]. Defect–free inorganic micropouros membranes can work under conditions where polymeric membranes cannot be used. This is due to the characteristic feature that inorganic membranes posses such as: relatively high thermal stability, compatibility with high-temperature operations, and suitability for real reaction–filtration integration, allowing therefore; for example, a shift of the reaction equilibrium as in membrane reactors. Also they possess high mechanical strength and surface modification to improve hydrothermal stability. Therefore, these kinds of membranes have attracted great interest in research and industrial fields [2-4]. Microporous inorganic membranes generally consist of a macroporous ceramic support, ceramic intermediate layers and eventually a highly top selective layer [5]. This selective layer is playing an important role in separation capability and permeation of the membrane. Molecular sieving materials offer potential advantages for the separation of gases either at elevated temperatures or in the presence of vapors. Microporous silica materials can be easily synthesized by sol-gel technique which is an effective and cheap method [6-9]. Over the last decades, these materials have been increasingly gaining importance in the research field, especially for molecular sieve applications such as gas separation. Hence, they were used as top selective layer for inorganic membranes, and there are intensive research works on silica membranes in the literature [10-17].

It is well known that the micropores of silica network allow for the permeation of small kinetic diameter gases such as helium and hydrogen. In turn, several research works have been performed to produce high molecular sieving silica membranes with very small pore size distribution in the region of ~ 1 nm or lower [14, 16, 18-20]. Furthermore, silica membranes were reported to be very effective in separation and purification of hydrogen as they have large permeation and selectivity for that gas [3, 21]. Besides, silica membranes were considered as efficient separation technique for CO_2/CH_4 and other hydrocarbon mixtures [22]. Separation processes of CO_2 from CH_4 have potential applications in several fields such as enhanced oil

recovery, flue gas recovery, CO_2 recovery from landfills and natural gas purification [23].

Nowadays, hydrogen is considered as a clean energy source for different fields such as electricity sector and transportation. In the next decades, the demand for clean energy, as well as energy generation with zero carbon emissions and the growth of the so-called hydrogen economy, will increase. Modern technology is exploited for production and purification of hydrogen. For instance, membrane reactors, where reaction and separation occur in one unit, have attracted considerable attention for hydrogen production via steam reforming of methane. In order to maximize hydrogen production through steam reforming, further processing such as water gas shift reaction is needed, but gas streams contain water vapor [24, 25].

It was reported in the literature that microporous silica membranes allowed for the permeation of small kinetic diameter gases, but this is only for dry gases. Microporous silica membranes suffer from water sorption at relatively low temperature [26, 27]. Therefore, upon exposure to steam, the morphology of silica membranes is altered and leads to loss of selectivity [28]. Water can be adsorbed on silica materials via the intermolecular hydrogen bonding between water molecules and silanol (hydroxyl) surface groups of silica membranes, thus resulting in further changes in the matrix of silica-derived membranes. This is mainly attributed to the collapse of small pores and expansion of larger pores [29]. To address this problem, modification of the silica surface is required. Several works have been performed and intensively reported in the literature concerning that problem. Template-based approach is one strategy for modification of silica membrane materials [30]. Incorporation of organic templates into the silica film whereby the silica membrane (top selective layer) showed decrease in water interaction, increasing hydrophobicity of silica surface was achieved by calcination in inert atmospheres [6, 31-34]. These organic templates can be classified as organic covalent ligands, such as methyl groups, or non-covalently bonded, such as surfactants (C6 and C16 surfactants) [17, 35]. Gas selectivity was lowered as covalent ligand methyl template in methyltriethoxysilane (MTES) was incorporated in the silica film. This is due to the

formation of slightly broader pore sizes [32]. On the other hand, the selectivity was improved by incorporation of C6 surfactant triethylhexylammonium bromide [19].

Metal-doped approach is an alternative strategy to reduce the degradation of a hydrophilic silica membrane. Various metal and metal oxide doped silica membranes have been prepared. For instance, metal oxide such as Co_3O_4, NiO, TiO_2, ZrO_2 and Fe_2O_3 have been trialed and, in most cases, provide membranes with higher flux, lower cost and improved durability [28, 36-39]. The structure of the metal-doped in the silica matrices was reported to be in oxide form, which chemically reduced to pure metal by a flow of hydrogen at elevated temperature [40]. However, the structure of the metal-doped in the silica matrix continues to be controversial. One possible hypothesis for that is the presence of the strong framework is due to the formation of Si-O-M linkage [6, 41]. For example, Gu *et al.* [39] have reported that the addition of titania and alumina to the silica matrix resulted in membranes of good permeability and stability. The essential reason for the improvement is likely the enhanced resistance of Ti–O–Si and Al–O–Si bonds to hydrolytic bond cleavage.

As shown in chapter 4, the possibility of combing template-based approach and metal-doped approach was reported. A novel unsupported silica membrane, referred to as hydrophobic metal-doped silica, was achieved. The preparation involved cobalt-doping within the matrix of organic templated silica material (hybrid silica). By doing so, the novel silica membrane material retained the hydrophobic behavior after calcinations in oxidizing atmosphere. Besides, the material showed a high thermal stability, up to ~ 560 °C. The aims of the present work are the preparation of the supported material, cobalt-doped hybrid silica, and comparison of its gas separation behavior with the non-doped hybrid silica. Moreover, in the present work the possibility of membrane preparation under normal conditions as well as the clean room conditions is report.

7.2. Experimental part

7.2.1. Materials and methods

Tetraethylorthosilicate (TEOS, for synthesis) and ethanol (ethanol dried, max. 0.01 % H_2O, SeccoSolv®) were purchased Merck, Polyvinylalcohol (PVA, Mowiol 8-88) and nitric acid (HNO_3, 69%) were purchased from Sigma-Aldrich,

methyltriethoxysilane (MTES, 98%, Acros Organics) and cobalt nitrate (99% pure, Acros Organics) were purchased from Scharlab. Distilled water was used for the sols preparation.

7.2.2. Unsupported hydrophobic silica membranes preparation

All sols prepared in this work are based on the acid-catalyzed hydrolysis and condensation process. TEOS and MTES were used as the silica precursors mixed with ethanol (EtOH), nitric acid (HNO_3), and distilled water. To prevent partial hydrolysis while mixing EtOH and TEOS, the mixture was placed in an ice bath then acid/water mixture was added drop wise with continuous stirring [32]. The different molar compositions investigated in this work as well as the sample notations are listed in Table 7.1. For the cobalt-doping within the hybrid silica matrix, a solution of cobalt nitrate in ethanol was prepared. Ethanol was chosen as the solvent for the salt solution because it was the same solvent used in the sols preparation. Moreover, the nitrate salt was used because it is compatible with the silica sol which was catalyzed by nitric acid [6, 36].

Unsupported hydrophobic silica membrane (Hyd-Si) was prepared as follows: a mixture of HNO_3/H_2O was added under vigorous stirring to TEOS/EtOH, which was placed in ice bath, and then the sol was refluxed in water bath at 60 °C for 165 minutes (1st step). Afterwards, a mixture of MTES/EtOH solution with 1 : 3.8 molar ratio, which had been cooled for 5-10 minutes in ice, was added to the reaction mixture (2nd step) and the final sol was refluxed for an additional 15 minutes [32].

Unsupported hydrophobic cobalt-doped silica membrane (Hyd-Co-Si) was prepared as the hydrophobic one but in the second step the sol was mixed with a MTES/EtOH solution plus the ethanol solution of the cobalt salt. The metal salt to the metal alkoxide (Co:Si) weight ratio used was 3%.

All silica sols were allowed to evaporate in a Petri-dish at room temperature so that silica flakes, xerogels, were obtained overnight. Xerogels were crushed finely to obtain powders, which were used for characterization, and calcination of Hyd-Co-Si was done in air and for Hyd-Si in nitrogen atmosphere, in order to prevent the burn-off of the methyl groups, at a heating and cooling rate of 0.5 °C/min, and held for 3 hours at 400 °C.

7.2.3. Supported hydrophobic silica membranes preparation

In the present work, two different methodologies for membrane preparation are report, one under normal conditions, where tubular supports were used, and the other under clean room conditions, where disk-shaped supports were used. Concerning the preparation under normal conditions, the membranes were coated on inside monochannel γ-Al_2O_3 substrates supported by α-Al_2O_3 (inopor, Germany) with porosity of 3 μm and 5 nm, respectively. The outer and inner diameters of the support are 10 and 7 mm, respectively. The supports were modified and coated several times with the prepared, fresh, sol and diluted one, 1:2 EtOH (3-fold dilution, 3x). The coating processes were performed by using vacuum pump (THOMAS Picolino VTE 3) in order to withdraw the sols inside the support channel. After the sol had been withdrawn, it was kept for an appropriate time inside the support channel; the idea of doing so is to give more time for the sol to penetrate in the pores of the support, and therefore a kind of modification of the intermediate layers of the hydrophobic membranes. These coating processes of the support were repeated four times for each membrane. Finally, the separation layer consisted of the 1:19 EtOH diluted sol (20x dilution) and this layer was coated six times. After each coating, either for the intermediate or separation layers, the membranes were calcined in air, for Hyd-Co-Si, or in N_2, for Hyd-Si, at a heating and cooling rate of 1 °C/min, and held for 3 hours at 400 °C. The trend of several coating for intermediate layers preparation and top separation layers was reported by Diniz da Costa *et al.* [14].

On the other hand, concerning the preparation under clean room conditions the membranes were coated on top of γ-Al_2O_3 membranes carried by porous α- Al_2O_3 discs that had a Ø of 39 and 2 mm thickness. The porous α-alumina discs were purchased from Pervatech BV (The Netherlands) whereas the γ-Al_2O_3 membranes were prepared by dip coating the α-Al_2O_3 supports in a boehmite colloidal suspension (γ-AlOOH) sol followed by drying and calcining. Polyvinylalcohol (PVA) was added to the boehmite precursor to improve the dip coating of the α-Al_2O_3 supports. This addition resulted in a less critical and better controllable drying and calcining procedure. The addition of PVA has no significant effect on the resultant microstructure of the γ-alumina film, provided all PVA is removed by appropriate thermal treatment. The dip coating was performed in a class 1000 clean room, in

order to minimize particle contamination of the membrane layer, using an automatic dip-coating device (Velterop DA 3960/02). After dipping, the membranes were dried in a climate chamber at 40 °C and 60% relative humidity (VTRK300, Heraeus, Vötsch, Balingen, Germany). Subsequently, the γ-Al_2O_3 membranes were formed by calcination process at 650 °C for 3 h in air with a heating and cooling rate of 1°C/min.

The whole process of dipping, drying and calcination was repeated once again, to avoid any defects in the first γ-Al_2O_3 layer. This process leads to γ-Al_2O_3 layer thickness in the order of 3-5 μm, with an average pore diameter of about 5 nm as reported by Uhlhon *et al.* [42]. Hyd-Si and Hyd-Co-Si top selective layers were prepared by diluting the fresh sol 1:5 EtOH (6-fold dilution, 6x) and 1:19 EtOH (20-fold dilution, 20x). These diluting sols were coated, one time for 6x sols and two times for 20x sols, on the γ-Al_2O_3 membranes by dip coating with speed of 1.4 cm s^{-1}. The membranes were calcined in air, for Hyd-Co-Si, and in N_2, for Hyd-Si, at a heating and cooling rate of 0.5 °C/min, and held for 3 hours at 400 °C. The membrane notations throughout the present work are listed in Table 7.2.

Table 7.1. Molar compositions of the used sols for hydrophobic silica membranes preparation.

Sample	Step	TEOS	MTES	EtOH	HNO_3	H_2O	$Co(NO_3)_2.6H_2O$*
Hyd-Si	1st step	1	0	3.8	0.085	6.4	
	2nd step	1	1	7.6	0.085	6.4	
Hyd-Co-Si	1st step	1	0	3.8	0.085	6.4	
	2nd step	1	1	7.6	0.085	6.4	3 wt%

* Amounts were calculated in order to prepare solution of 10% wt/vol of cobalt nitrate in ethanol.

Table 7.2. Membranes notations in the present study.

Membrane code	Membrane type	Support	Number of coating	
			Intermediate layer	Top layer
M1	Hyd-Si	Tubular	4 (N) + 4 (3x)	6 (20x)
M2	Hyd-Co-Si	Tubular	4 (N) + 4 (3x)	6 (20x)
M3	Hyd-Si	Disk-shaped	2 γ-Al_2O_3	1 (6x)
M4	Hyd-Co-Si	Disk-shaped	2 γ-Al_2O_3	1 (6x)
M5	Hyd-Si	Disk-shaped	2 γ-Al_2O_3	2 (20x)
M6	Hyd-Co-Si	Disk-shaped	2 γ-Al_2O_3	2 (20x)

N: refers to coating with non-diluted sol (fresh prepared sol).
For disk-shaped support, the intermediate layers were prepared as mentioned in experimental section.

7.2.4. Membranes characterization

Water contact angles were measured on a Dataphysics OCA 15EC video-based contact angle system at ambient temperature. Water droplets (3 μl) were dropped directly onto the surfaces of the silica membranes.

Dynamic Light Scattering (DLS) measurements were carried out in order to determine the hydrodynamic radius of the sols in the freshly prepared sols and diluted one. The measurements were performed on a Malvern Zetasizer Nano ZS.

Thermogravimetric analysis (thermogravimetry, TGA and differential thermal analysis, DTA) was used to investigate the processes taking place during the heat treatment. This analysis was carried out for dried xerogels, in a Perkin Elmer model Thermobalance TGA7 device, in synthetic air and nitrogen with constant flow rate of 290 cm^3 min^{-1} and heating rate of 10 °C min^{-1} from room temperature to 900 °C.

Textural characterization of the synthesized samples was determined by N_2 adsorption/desorption measurements at -196 °C. Gas adsorption measurements were performed with the Quantachrome Autosorb 1 MP. Before any adsorption experiment, samples were degassed overnight at 300 °C. The pore size distribution

was calculated from the nitrogen adsorption data using the NLDFT model (Non Localized Density Functional Theory) based on a cylindrical pore-equilibrium model.

Morphological characterization of the hydrophobic silica membranes were determined by high resolution scanning electron microscopy (LEO Gemini 1550 FEG-SEM).

7.2.5. Gas permeance measurements

Membranes performance was characterized by means of single gas permeation. Both tubular and disk-shaped membranes were measured in a dead-end mode as depicted in Figure 7.1 and 7.2, respectively. The set-up for tubular membranes consists of a tubular membrane module and the temperature was controlled with a PID controller. Concerning the tubular membranes, single gas component permeance measurements were carried out for He, H_2 and N_2 at temperatures ranging from ambient to 150 °C and pressure differences ranging from 0.5 bar to 3 bar. Ambient moisture can easily condense inside silica micropores, therefore the membranes were dried overnight at 150 °C.

On the other hand, concerning the disk-shaped membranes a feed pressure of 3 bar was applied to the membranes, while the permeate pressure is the atmospheric pressure, i.e. the pressure difference for measurement was 2 bar. The flow through the membranes was determined by a mass flow meter. The permeances of gases He, N_2, CH_4, H_2, CO_2, and SF_6 were measured in that sequence. The membranes were pretreated by heating up to 200 °C under He flow to ensure a complete removal of water that can be condensed inside silica micropores. The measurements were preformed with temperatures ranging from 50 °C to 200 °C. All gases, either in testing tubular or disk-shaped membranes, were equilibrated for at least half an hour to ensure a constant flow.

7.3. Results and discussion

7.3.1. Membranes hydrophobicity

Figure 7.3 shows the water contact angles for the disk-shaped membranes and the support as well. The support γ-Al_2O_3/α-Al_2O_3 shows hydrophilicity behavior, as the contact angle is 25°. The support plus the silica layer, membranes M3 to M6, show

Novel hydrophobic silica membrane for gas separation

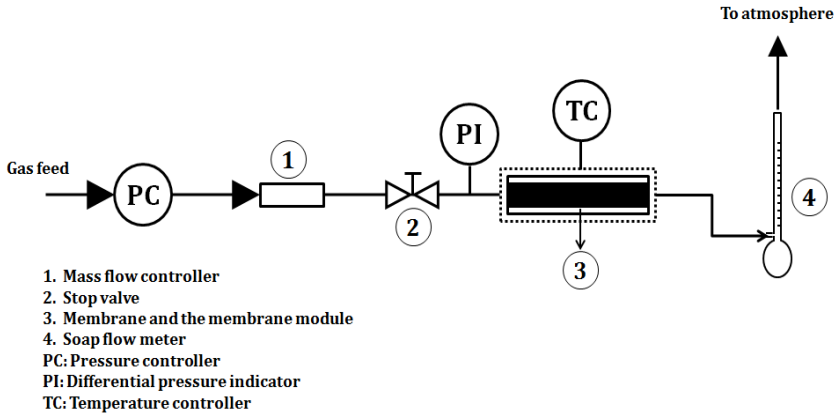

Figure 7.1. Experimental set-up for tubular hydrophobic membranes.

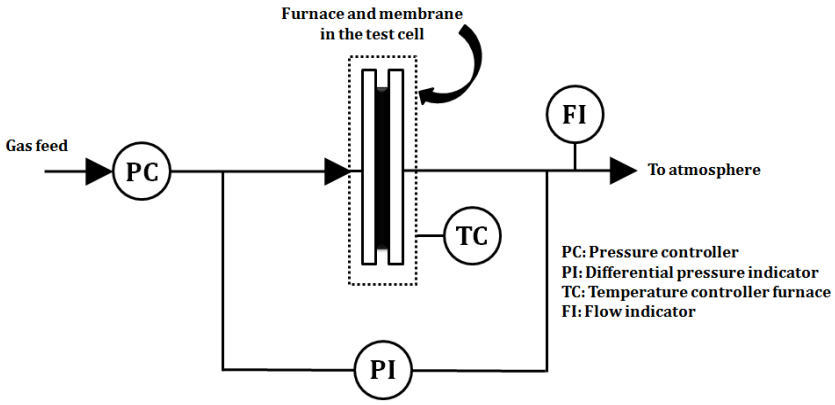

Figure 7.2. Experimental set-up for disk-shaped hydrophobic membranes.

contact angles ranging between 80° and 90°. Although the hydrophobic materials are characterized with contact angle larger than 90° [43], the membranes show very less hydrophilic behavior than the support. In fact the reason for the obtained contact angles is mainly attributed to the capillary effect of the porous γ-Al_2O_3/α-Al_2O_3 supports on the real water contact angles values. Therefore, in our first study on the novel unsupported silica membrane materials, chapter 4, they were coated on a glass substrate for the contact angle measurements [6]. In any case, this gives an indication to the less wettability of the prepared membranes. As it can be seen in Figure 7.4, water drop upon the membranes surfaces still has curvature and not spread out as the hydrophilic silica materials showed [32]. This indicates that the novel material has low water affinity after calcination in air. It is well known in the literature that the hybrid silica membranes are rendered hydrophobic feature by calcination under inert atmosphere. However, the novel membrane still posses the hydrophobic behavior after the heat treatment in air. This may be attributed to that cobalt composite with silica matrix results in a strong framework by the formation of Si-O-Co linkage [41, 44]. This perhaps facilitates the surface to substitute the –OH groups, along with the hydrophobic -CH_3 groups, on the surface, making the silica surface hydrophobic and decreasing the possibilities for the burn-off of the methyl groups upon heat treatment at 400 °C in air.

7.3.2. Characterization of the sols

Figure 7.5 shows the particles size distributions by DLS of the fresh (non-diluted) and diluted sols (6x and 20x). Intensity distribution, particle volume and particle number distributions are given for each fresh and diluted sols. The graph of each distribution is represented as function of the hydrodynamic radius (R_H), which is defined as the effective size of the molecules as detected by its diffusion, or the radius of a hard sphere having the same diffusion coefficient as the sol particles [45]. In Table 7.3, $(R_H)_I$, $(R_H)_V$ and $(R_H)_N$ refer to the average of (R_H) that are calculated from the intensity, volume and number distributions, respectively.

The polydispersity index of polymer is defined as M_W/M_N and M_Z/M_N, where M_W, M_N and M_Z represent the weight, number and z average (which can be determined by certain method such as DLS and sedimentation equilibrium) of molecular mass of a polymer, respectively [46]. Subsequently, for the polymer-colloidal silica the ratio

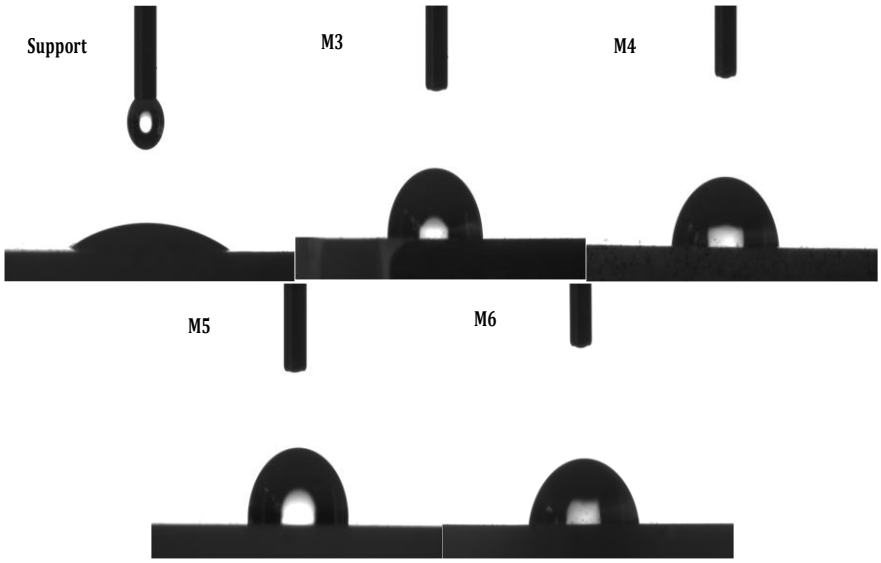

Figure 7.3. Contact angles of the support and hydrophobic silica membranes.

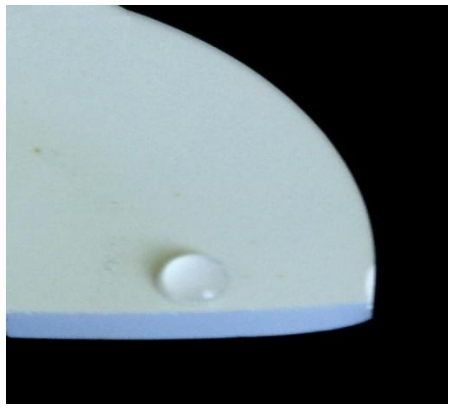

Figure 7.4. Drop of water on Hyd-Co-Si membrane (M6).

$(R_H)_V/(R_H)_N$ and $(R_H)_I/(R_H)_N$ are qualitatively similar to M_W/M_N and M_Z/M_N. Therefore, they can reflect the polydispersity index of the polymer-colloidal silica. However, for monodisperse sample the values of $(R_H)_I$, $(R_H)_V$ and $(R_H)_N$ should match, whereas in polydisperse sample their values are different [45]. As it can be noticed from Table 7.3 the average values of (R_H) increase in the order $(R_H)_I > (R_H)_V > (R_H)_N$. This is because the intensity of scattering of particles is proportional to the sixth power of its diameter $I \, \alpha \, R_H^6$ (from Rayleigh's approximation). Besides, the volume distribution was calculated by assuming volume of sphere that equals to $\left({}^{4}/_{3\pi(r)^3}\right)$ [47]. The values of the polydispersity index that are obtained from the ratio $(R_H)_V/(R_H)_N$ are approximately similar for all samples regardless the doping and dilution process.

On the other hand, the values from the ration $(R_H)_I/(R_H)_N$ show different values between fresh and diluted sols and this is quite clear in the intensity distribution. The doping process leads to the peak shift, and hence this interprets the large $(R_H)_I$ for Hyd-Co-Si compared with Hyd-Si. However, the narrow peak particle size distribution indicates low polydispersity. This may reflect the homogeneity of particle size of the sol, i.e., the dilution process may give better homogeneity of the sol due to the low polydispersity. Hence, this may give better homogeneity of the membrane porosity during the coating process of the silica membranes. In any case, the obtained results show the same trend of modified-silica membranes, niobia-silica one [45]. In the present study the DLS data reveal that none of the sols contained particles with a (R_H) larger than 60 nm. The modified–silica sols presented are therefore potentially suitable precursors for making microporous thin layers.

7.3.3. Thermogravimetric analysis

Thermogravimetric analyses for the uncalcined unsupported membranes were performed under synthetic air flow as well as under nitrogen flow. The aim of these analyses is to investigate the processes occurred during the heat treatment, beside the stability of the organic template (methyl ligands) in both inert and oxidizing atmospheres. The weight loss curves, as function of temperature (TGA curves) and the differential weight loss (DTA curves) in inert and oxidizing atmospheres are depicted in Figure 7.6 and 7.7, respectively. For all samples and under both

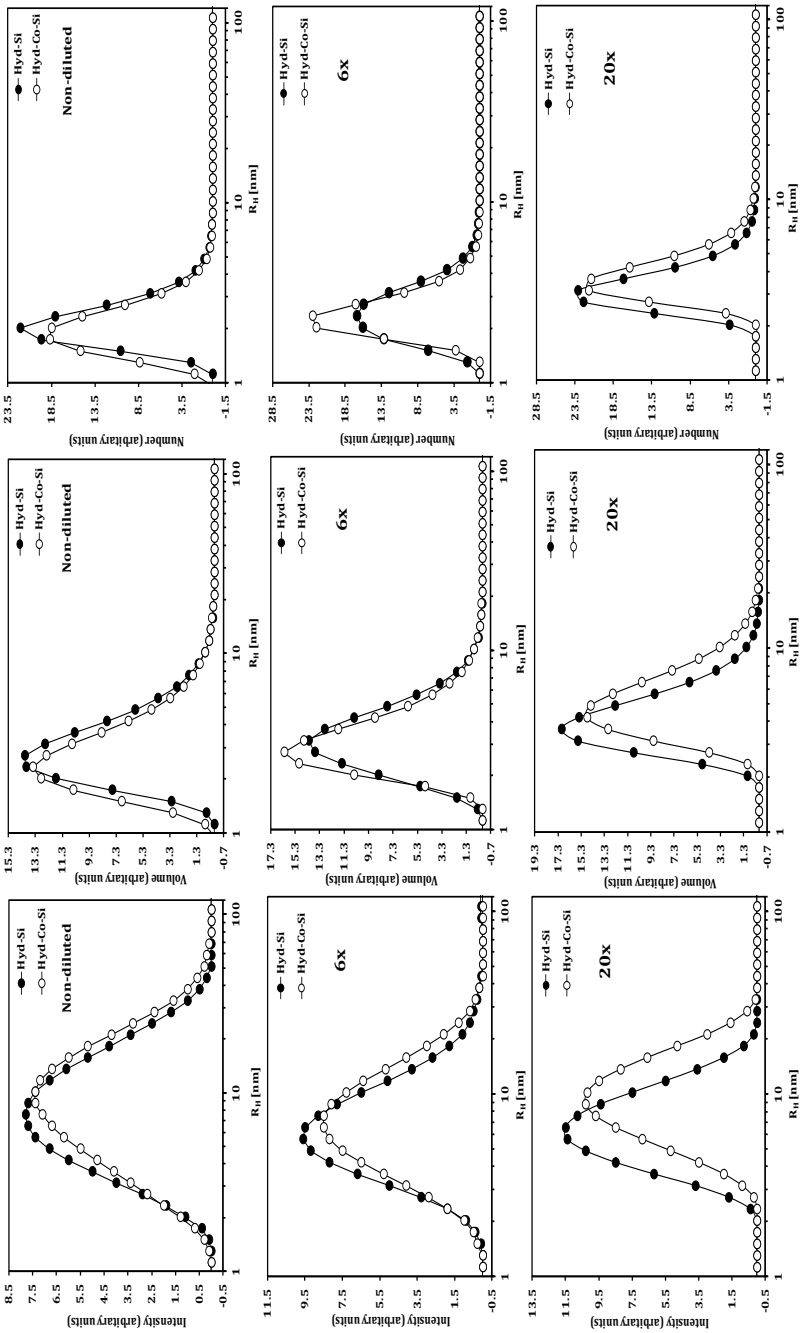

Figure 7.5. Particle size distribution of the non-diluted and diluted sols. Intensity (left), volume (middle) and number (right) distribution curves.

Table 7.3. Characteristics of the sols used for the preparation of hydrophobic membranes.

Sol	Dilution factor	R_H (nm)*			Polydispersity	
		$(R_H)_I$	$(R_H)_V$	$(R_H)_N$	$(R_H)_I/(R_H)_N$	$(R_H)_V/(R_H)_N$
Hyd-Si	Non-diluted	5.0	1.7	1.1	4.5	1.5
	6x	3.8	1.8	1.3	2.9	1.4
	20x	3.5	2.2	1.7	2.1	1.3
Hyd-Co-Si	Non-diluted	5.6	1.6	1.1	5.1	1.4
	6x	4.2	1.7	1.2	3.5	1.4
	20x	5.1	2.8	1.9	2.7	1.5

* Hydrodynamic radius as obtained from DLS (average in number). $(R_H)_I$ = average on scattered intensity, $(R_H)_V$ = average on particle volume, $(R_H)_N$ = average on particle number.

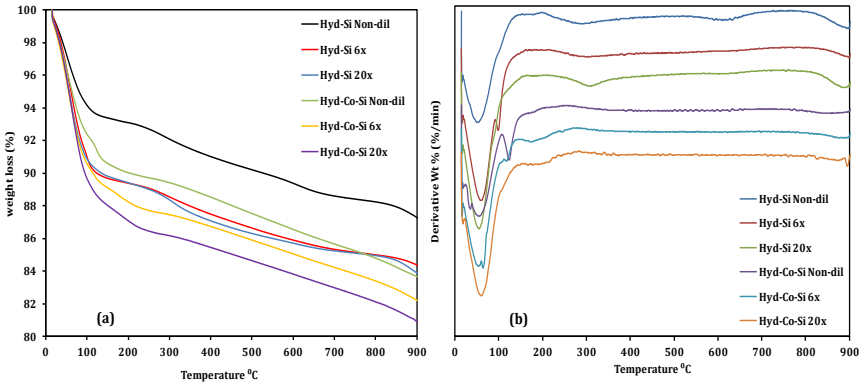

Figure 7.6. Weight losses vs. temperature (a) and differential weight loss curves (b) in inert atmosphere.

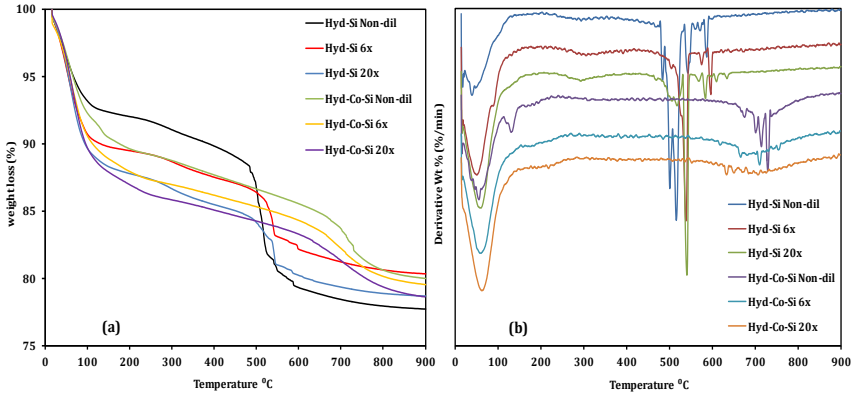

Figure 7.7. Weight losses vs. temperature (a) and differential weight loss curves (b) in oxidizing atmosphere.

atmospheres, the initial weight losses from room temperature to ~ 150 °C are mainly attributed to physisorbed water molecules trapped in the silica matrix, and to the loss of free solvent molecules [7, 35, 48]. For the Hyd-Co-Si, the weight-loss processes in the temperature ranges from ~ 150 °C t ~ 240 °C is due to the dehydration process of cobalt nitrate and the removal of the nitrous gases [49, 50]. The weight-loss processes for Hyd-Si after ~ 150 °C and for Hyd-Co-Si after ~ 240 °C are generally associated with the condensation reactions due to heat treatment, resulting in the production of water and ethanol, which evaporate from the silica matrix [7, 48, 51].

As it can be noticed from the TGA and DTA curves, the cobalt-doping process enhances the thermal stability of the hybrid silica materials in both atmospheres. Besides, the dilution process enhances the thermal stability of the Hyd-Si in both atmospheres compared with the non-diluted sample. The enhancement in thermal stability of the non-doped hybrid silica by dilution process was reported by Castricum *et al.* [33]. In comparison of the thermal stability of the Hyd-Si and Hyd-Co-Si, it is clear that they are more stable in inert atmosphere compared with oxidizing atmosphere. However, the Hyd-Co-Si exhibit high thermal stability compared with the Hyd-Si (non-doped). The non-diluted Hyd-Si is thermally stable up to ~ 450 °C in oxidizing atmosphere, while the diluted samples are thermally stable up to ~ 500 °C. The weight-loss processes after that temperature are due to the oxidative pyrolysis,

decomposition, of the methyl ligands [7, 48]. On the other hand the Hyd-Co-Si, regardless the dilution process, are thermally stable up to ~ 560 °C. This high thermal stability could be attributed to cobalt composites with silica matrix which results in formation of Si-O-Co. This is in good agreement with our first study on the Hyd-Co-Si and the other investigation works on that material (chapters 4 and 5) [6, 7].

7.3.4. Micropore structure

Textural properties of the unsupported membranes were determined using N_2 adsorption isotherms at -196 °C. Top selective layers with 20x dilution were used for membrane preparation under normal conditions (M1 and M2) and clean room conditions (M5 and M6), while top selective layers with 6x dilution were used for M3 and M4. Table 7.4 reports the parameters obtained from the N_2 adsorption data after application of different mathematical equations. Micropore volume (V_0) was calculated by applying the Dubinin Radushkevich equation to the N_2 adsorption data (eq. 4.1) [52]. The total pore volume, V_T, was obtained from the amount adsorbed at a relative pressure (P/P_0) of 0.99 while the surface area was obtained by application of the BET (Brunauer, Emmett and Teller) method to the nitrogen adsorption data [53]. The pore size distributions (PSD) were calculated by applying the NLDFT model to the nitrogen adsorption data at -196 °C based on a cylindrical pore model [54].

As it can be noticed from Figure 7.8, the N_2 adsorption isotherms, for the samples, exhibit the characteristic Type I isotherm with a knee at low relative pressures ($P/P_0 < 0.1$) where the majority of pores filling occur and this is a characteristic of microporous materials. At high relative pressure ($P/P_0 > 0.4$), the isotherm of Hyd-Si 6x shows an increase of the adsorbed amount. This is probably corresponding to the adsorption in the external area of the sample. Figure 7.9 shows the PSD of the unsupported membranes. It can be observed that samples are microporous or bordering the mesoporous region. The samples exhibit an average pore radius of 0.6 nm for both Hyd-Si 6x and Hyd-Co-Si 6x, 0.5 and 0.6 nm for Hyd-Si 20x and 0.5 to 0.8 nm for Hyd-Co-Si 20x. This corresponds to the pores filling at low relative pressure leading to a narrow PSD. However, it is clear in PSD curves that the Hyd-Si samples have broader peaks than the Hyd-Co-Si samples which have very narrow peaks. This trend was observed and reported by De Vos *et al.* [32] concerning

the Hyd-Si and this had a significant effect on the membrane selectivity and permenace.

The samples have one peak over 1 nm (at 1.2 nm) and no distinguished peaks over 2 nm. This indicates that no presence of wider micropores and mesopores as well. Besides, the appearance of a nearly horizontal plateau indicates the absence of larger pores (meso-/macropores). Only sample Hyd-Si 6x has a broad peak over 1.2 nm and this is attributed to the fact that this sample has wider micropores compared with the other ones (see Table 7.4) and also mesopores. However, the PSD results may differ somehow depending mainly on the model used for the PSD determination.

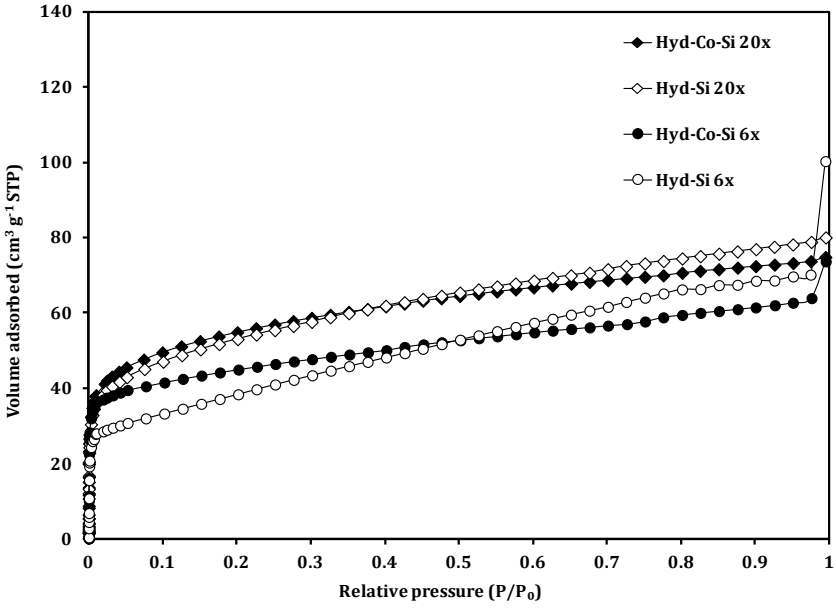

Figure 7.8. N_2 adsorption isotherms of the unsupported hydrophobic membranes.

Table 7.4. Compilation of structural parameters deduced from N_2 adsorption data at -196 °C for the unsupported hydrophobic membranes.

Sample	S_{BET} (m^2g^{-1})	Micropore surface (m^2g^{-1})	$V_{T0.99}$ ($cm^3\ g^{-1}$)	V_{micro} ($cm^3\ g^{-1}$)
Hyd-Si (6x)	130	534	0.115	0.190
Hyd-Co-Si (6x)	163	190	0.114	0.068
Hyd-Si (20x)	189	246	0.124	0.088
Hyd-Co-Si (20x)	198	226	0.116	0.081

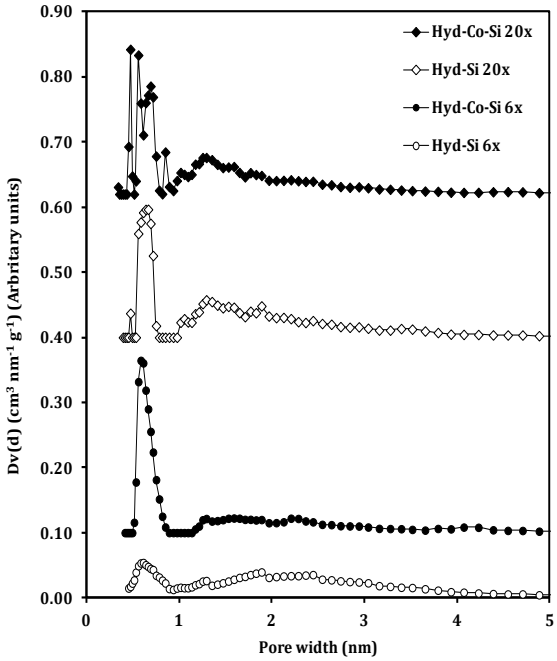

Figure 7.9. PSD of the unsupported hydrophobic membranes.

7.3.5. Permenace of the hydrophobic membranes

7.3.5.1. Tubular hydrophobic silica membranes

M1 and M2 were prepared under normal conditions in the laboratory of METEOR research group, URV, Spain. A relevant example of the permeance of He, H_2 and N_2 gases, at different temperatures and pressures, for M1 and M2 are shown in Figure 7.10 and 7.11, respectively. Apparently, M1 shows an increase in the gas permeance with the average pressure difference at all temperatures. Whereas, M2 at low temperature shows the same trend while temperature increases, the gas permeance shows a slight increase, through the permeance may be slightly higher at low pressures. It is known that the independece of gas permeance with pressure is a trend of molecular sieving silica membranes [14, 18]. However, the permeance increases with pressure difference is a consequence of defects or pinholes that exist in the final membrane. Hence, the membrane performance can be controlled by other mechanisms, such as viscous flow or Knudsen diffusion, rather than activation mechanism which is a characteristic behavior for molecular sieve membranes [55]. Accordingly, this could indicate that M2 has fewer defects than M1.

Figure 7.12 shows the single gas permeance as function of the kinetic diameter (d_k) of the permeating molecules measured at (Δ P = 2 bar) and 150 °C. The M1 and M2 show approximately the same permeance behavior, i.e. discriminate He and H_2 against large diffusing molecule N_2, with the same order of magnitude. The permeance data for M1 and M2 are reported in Table 7.5. For better understanding the performance of the membranes prepared by that simple way, a further investigation was done in order to discriminate the mechanism that control the membrane permeance. Figure 7.13 displays the membrane permeance for He, H_2 and N_2 at (Δ P = 2 bar) and different temperature for M1 and M2. As it can be observed, the permeance of all gases is temperature dependence, i.e. decreases as temperature increases. On the other hand, Figure 7.14 displays the permselectivity for the probing molecules. The trend is clear in the permselectivity difference between the both membranes. This could be attributed to the lower number of defects or pinholes of M2 compared with M1.

M2 shows higher selectivity compared with M1, and this is due to the fact that its permselectivity exceed the Knudsen values as well as the lower number of defects in the separation layer. The only exception is that M2 shows lower selectivity or exactly Knudsen selectivity for H_2/He. This selectivity is approximately constant with increasing temperature. Both membranes show high selectivity with increasing temperature, however, M1 selectivity is approximately on the boundary of Knudsen values. At low temperature, M1 selectivity is lower than the Knudsen values and this could be attributed to the influence of viscous flow. Although the obtained results indicate that these membranes are non defect-free membranes, as first sight this suggests that the way that was used in the present study is an appropriate way for support modification, especially with the cobalt-doped sol. This could be attributed to the possibility that cobalt has an affinity to alumina, thus forming $CoOAl_2O_3$ [40].

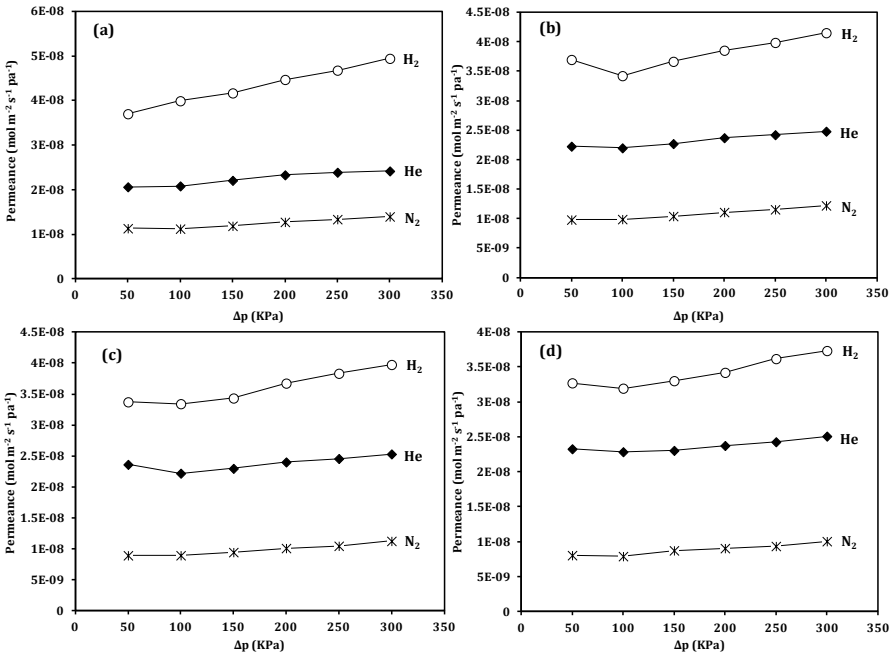

Figure 7.10. Gas permeance vs. pressure difference for M1 where a) at 25 °C, b) at 50 °C, c) at 100 °C and d) at 150 °C.

Table 7.5. M1 and M2 permeance depending on the d_k of the probe molecule at (Δ P = 2 bar) and 150 °C.

Probe molecule	Permeance (mol. m^{-2}. s^{-1}. Pa^{-1})	
	M1	M2
He	2.37×10^{-8}	4.65×10^{-8}
H_2	3.42×10^{-8}	6.6×10^{-8}
N_2	9.06×10^{-9}	1.38×10^{-8}

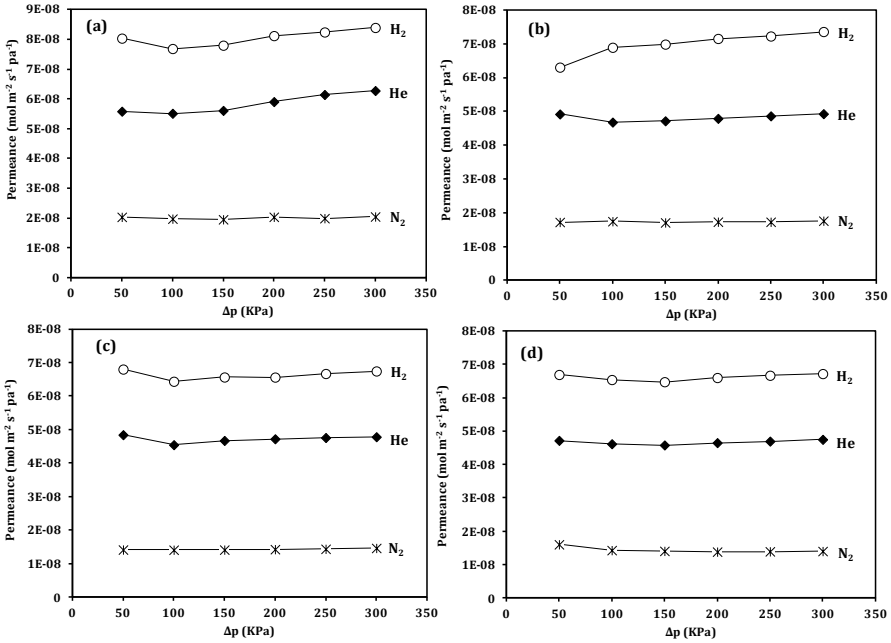

Figure 7.11. Gas permeance vs. pressure difference for M2 where a) at 25 °C, b) at 50 °C, c) at 100 °C and d) at 150 °C.

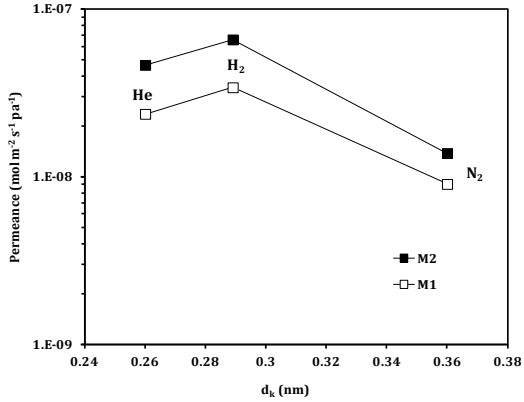

Figure 7.12. Gas permence vs. kinetic diameter for M1 and M2 at (Δ P = 2 bar) and 150 °C.

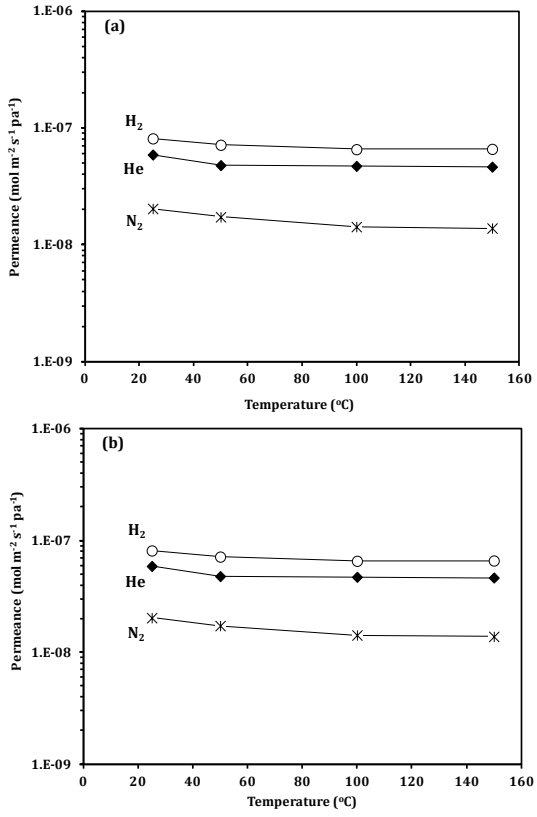

Figure 7.13. Gas permence vs. temperature for a) M1 and b) M2.

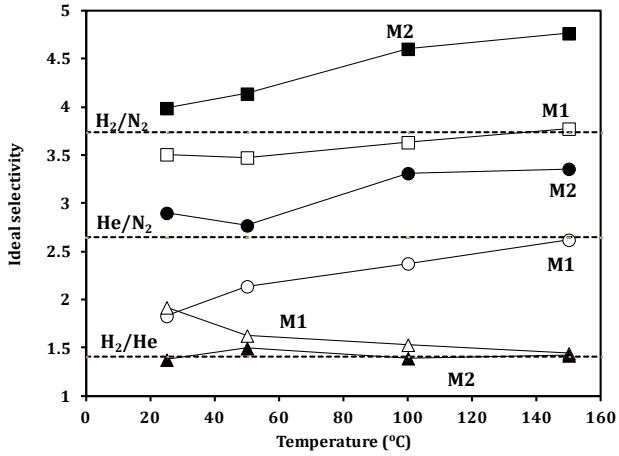

Figure 7.14. Selectivity of M1 (hollow symbols) and M2 (solid symbols). Dashed lines represent Knudsen selectivity (Δ P = 2 bar).

In any case, the study of the permeance of a gas as function of the inverse square root of the temperature (Arrhenius plot) is an interesting tool for determining if a microporous membrane has been obtained or not. Besides, calculation of the apparent activation energy gives an indication for that also. In some cases, Knudsen diffusion is affecting the membrane performance and therefore, cannot be neglected. This is mainly attributed to the effect of membrane support. As mentioned in chapter 1, in gas transport section, Knudsen diffusion is a well-known transport mechanism which occurs when the mean free path of gas molecules is much larger than the size of the pores. In this regime, gas molecules diffuse through the pores by colliding with the pore walls under the driving force of a concentration gradient. The Knudsen permeance is given by

$$Q = \frac{\varepsilon d_p}{\tau L}\left(\frac{8}{9\pi MRT}\right)^{1/2} \qquad 7.1$$

where Q is the permeance (mol m^{-2} s^{-1} Pa^{-1}), ε the porosity, dp the pore diameter (m), τ the tortuosity, L the membrane thickness (m), R the gas constant (8.314 J mol^{-1} K^{-1}), T the temperature (K), and M the molecular weight (kg mol^{-1}). The Knudsen

diffusion equation predicts that gas permeance will have an inverse square root dependency on both the molecular weight and temperature.

In Figure 7.15, the permeance data are plotted vs. the inverse square root of the molecular weight at different temperatures for M1 and M2. A good fit to linear regression is obtained (r^2 = 0.917 to 0.993) for M1 and (r^2 = 0.997 to 0.999) for M2. This indicates that the main transport is Knudsen mechanism and this is what was expected [56]. On the other hand, the permeance data are plotted vs. the inverse square root of the temperature, Figure 7.16. In that later case, the linear regression fits are lower than the previous ones (r^2 = 0.639 to 0.932) for both M1 and M2. Hence, the temperature influence on the whole transport mechanism of the membrane is still evident [55]. On addition to that, the apparent activation energy can be calculated from fitting those experimental data to an Arrhenius equation.

$$Q = Q_0 \, exp\left(\frac{-E_a}{RT}\right) \qquad 7.2$$

Where Q is the gas permeance, Q_0 the pre-exponential factor (mol.m^{-2}.s^{-1}.Pa^{-1}), E_a the apparent activation energy (KJ mol^{-1}), R the gas constant and T the absolute temperature (K). The fitting results and associated Ea are listed in Table 7.6. The E_a for both membranes are negative values, therefore, the gas transport is not controlled by activation mechanism. These negative values of E_a can be obtained if the gas molecules and pore wall interaction are varied by changes in surface polarity and pore size diameter. The same trend was reported for microporous silica membrane and carbon membranes [12, 55]. Subsequently, the possible hypotheses for the obtained results concerning the permeation of M1 and M2 are:

- The membrane support has a significant effect on the whole transport mechanism due to the way of support modification and membrane preparation that do not lead to highly microporous silica membranes.
- Not only one mechanism is dominant and governs the gas transport, but it seems a combination of various mechanisms that controls the whole gas transport through the membranes.
- The possible mechanisms are viscous flow, Knudsen diffusion and surface diffusion and/or adsorption.

The support performance can be governed by Knudsen and viscous flow, while the surface diffusion is almost associated to the temperature effect on the microporous domain. The cohabitation of more than one mechanism to govern gas transport was reported elsewhere [55, 57]. In some cases, especially at low temperature, the gas adsorption and diffusion can exist with the predominance for adsorption as reported for nanoporous carbon membranes [58].

However, as first approach, for the novel supported silica membrane presented in this study, we can conclude that the cobalt-doping within the hybrid silica material leads to better membrane performance compared with the non-doped silica membrane, regardless the selectivity and the permeation data that were obtained, in the case of preparation under normal conditions. Moreover, it is considered as simple and cheap way for support modification as well.

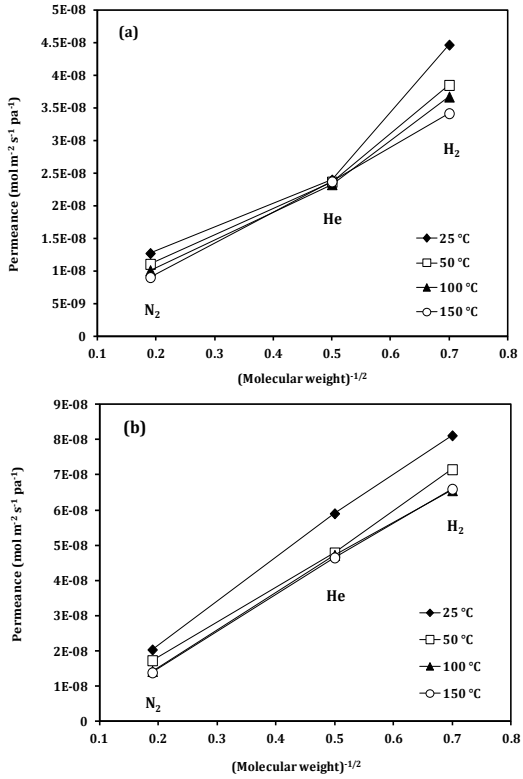

Figure 7.15. Gas permeance vs. molecular weight $^{-1/2}$ for different gases a) M1 and b) M2 (Δ P = 2 bar).

Table 7.6. Apparent activation energies for M1 and M2 at (ΔP= 2 bar).

Probe molecule	Activation energy (E_a) KJ/mol	
	M1	M2
He	-0.13	-1.70
H_2	-2.03	-1.71
N_2	-2.69	-3.29

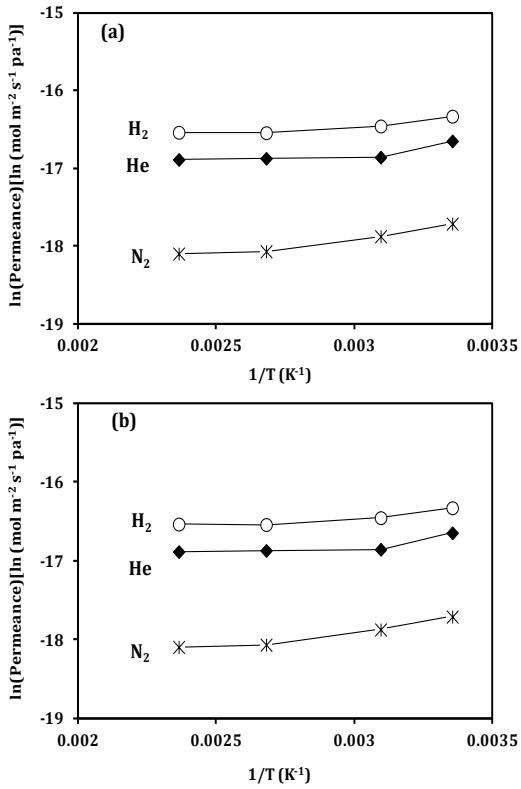

Figure 7.16. Temperature dependency for several gases a) M1 and b) M2 (Δ P = 2 bar).

7.3.5.2. Disk-shaped hydrophobic silica membranes

The preparation under clean room conditions, in the laboratory of IM group, University of Twente, Holland, was investigated in the present study as well. The disk-shaped membranes were tested for various probe molecules at (Δ P = 2 bar) and different temperatures. Figure 7.17 shows the morphological characterization of the hydrophobic silica membranes. As mentioned in experimental section, these membranes were prepared using diluted sols as a top selective layer and the presented cross section SEM images were obtained from the middle of the membranes. As can be noticed, looking at the membrane architecture, the support, intermediate and the top selective layer are present. The thickness of the top selective layers are; 120 nm and 150 nm for M3 and M4, respectively, and 50 nm and 70 nm for M5 and M6, respectively. These differences in membrane thickness are mainly attributed to the dilution process. As it was expected, the less diluted sol leads to thicker top separation layer.

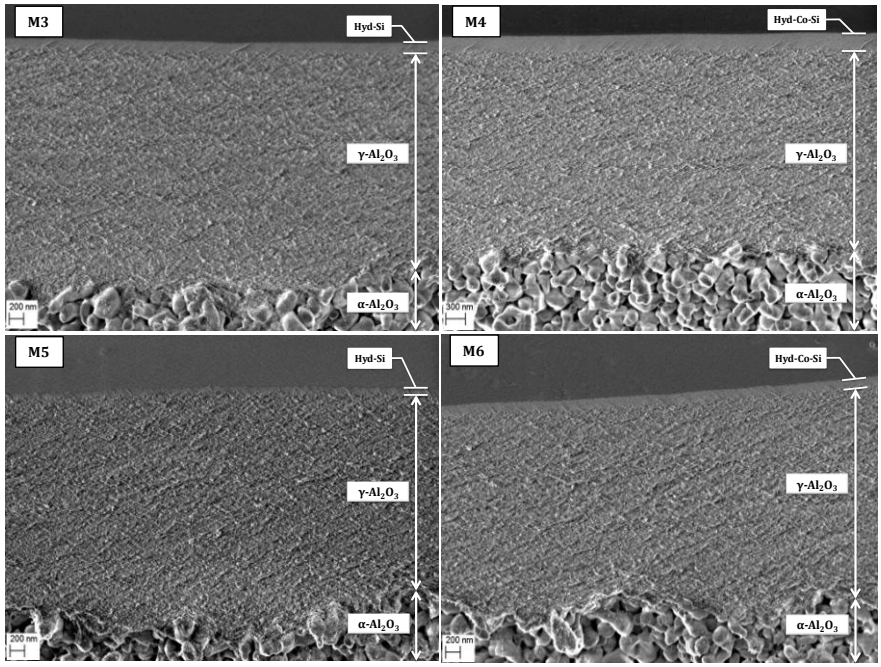

Figure 7.17. SEM images of cross-sections of the membranes prepared in clean room.

Table 7.7 listed the single gas permeance of the probe molecules at 200 °C, and Figure 7.18 shows the single gas permeance as function of the kinetic diameter of the probe molecules at the same temperature. It is clear that the four membranes (M3 to M6) have very small permeance for large gas such as SF_6, and hence a microporous membranes with a pore size smaller that 0.55 nm are achieved. In addition to that, all membranes have permeance with the same order of magnitude, except M6 that shows different behavior. The permeance of M6 is one order of magnitude lower than the other membranes with respect to large gases (> He and H_2). The temperature dependency of the permeance of various gases was studied to determine the transport mechanism that governs the permeance in M3 to M6, and the results are plotted in Figure 7.19.

As can be seen, the flux of most gases across the membranes increases exponentially with increasing temperature, and the reverse trend is observed for CO_2. This trend is characteristic for microporous silica membranes with activated transport or diffusion which is related mainly to the molecular sieving effect of the pores. M6 shows the opposite trend only for CO_2, slight increase in the flux of CO_2 gas with respect to the other membranes. This behavior could be attributed to the interaction between CO_2 molecules and the pore wall of the membrane, which is lower, compared with the other gases; i.e. CO_2 is less adsorbed or CO_2 capillary condensation is less significant; therefore, a gradual increase in CO_2 permeance with temperature (activated transport) is observed for M6. However, this behavior does not exclude the main mechanism of transport, activated one, of this membrane (M6). As it can be seen in Figure 7.19, M6 possesses approximately a high flux for He compared with other gases with increasing temperature (see Table 7.7). Moreover, other membranes show the opposite behavior, i.e. their high flux is for H_2. Therefore, it may be interpreted that the pore tuning control in the region of pore size of < 0.3 nm is taking place for M6. The obtained results concerning the permeance of H_2 or He are in good agreement with the finding in the literature where the permeance of these gases in the silica/modified silica membranes were normally in the range of ~ 10^{-8} to 10^{-7} mol. m^{-2}. s^{-1}. Pa^{-1} [14, 32, 40, 45, 59].

The activation energies of permeation were obtained by fitting the experimental gas permeance data to an Arrhenius expression (eq. 7.2). The permeance data are

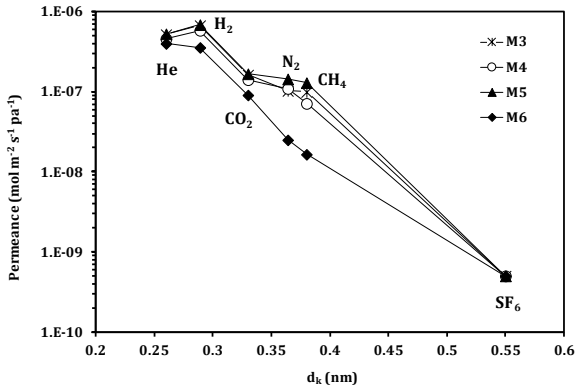

Figure 7.18. Gas permence vs. kinetic diameter for M3 to M6.

Table 7.7. M3 to M6 permeance depending on the d_k of the probe molecule at (Δ P = 2 bar) and 200 °C.

Probe molecule	Permeance (mol. m^{-2}. s^{-1}. Pa^{-1})			
	M3	M4	M5	M6
He	5.18×10^{-7}	4.58×10^{-7}	5.26×10^{-7}	3.98×10^{-7}
H_2	6.71×10^{-7}	5.83×10^{-7}	6.85×10^{-7}	3.55×10^{-7}
N_2	1.03×10^{-7}	1.09×10^{-7}	1.44×10^{-7}	2.49×10^{-8}
CH_4	9.93×10^{-8}	7.12×10^{-8}	1.29×10^{-7}	1.64×10^{-8}

plotted vs. the inverse square root of the temperature, Figure 7.20, and the values of E_a are listed in Table 7.8 together with some data on silica/modified silica membranes that have been prepared by sol-gel and reported elsewhere [5, 18, 37, 40, 60-63]. It is clear that the obtained values in the present study are close to the reported data. The E_a for all gases show positive value, while the negative value is observed for CO_2 which is generally interpreted as being caused by strong adsorption of the molecule on the pore surface. M3 shows higher E_a compared with M4 although they were prepared with the same procedure of dilutions. On the other hand, M6 shows higher E_a compared with all membranes in the present study, except for CO_2. However, this high E_a can be explained as reported by Hacarlioglu *et al.* [64], where they calculated the activation energies of H_2 permeance through $H_{2n}Si_nO_n$ (n = 4-8) cyclosilixane n-membered rings, which corresponds to the pore sizes of silica networks. They have showed that activation energy increased with a decrease in silica members rings. Besides, as repelling force increased as pore size decreased, the activation energy of H_2 permeance indicated the pore size that is effective for H_2 permeation. Hence, the activation energy can be interpreted as a measure of pore sizes of silica networks; the smaller the pore size, the larger the activation energy. This coincides with the obtained result concerning the high flux of small kinetic diameter gas such as He for M6 compared with the other gases (see Figure 7.19 and Table 7.7).

The permselectivity of each membrane are listed in Table 7.9. The larger variations in the selectivity are observed as a function of temperature, as the activated transport occurs during the permeation, and therefore it is expected that permselectivity results will vary with temperature. It seems that the cobalt-doping as well as dilution process lead to a better control of the pore size of the top selective layer. As a consequence, this has a significant effect on the membrane permeance and selectivity compared with the other membranes. Especially, the higher dilution process (20x) by which the top selective layer of M6 was prepared, where this membrane shows higher *Ea* and permselectivity as well. The behavior of M6 compared with the other cobalt-doped membrane (M4) is quite clear; M6 has a better performance compared with the corresponding non-doped membrane (M5), while M4 do showed. This could be attributed to the fact that the polydispersity of M4 is higher than M6, and hence the homogeneity of particle size of the sol may have a

significant effect in the membrane preparation and performance as well (see section 7.3.2).

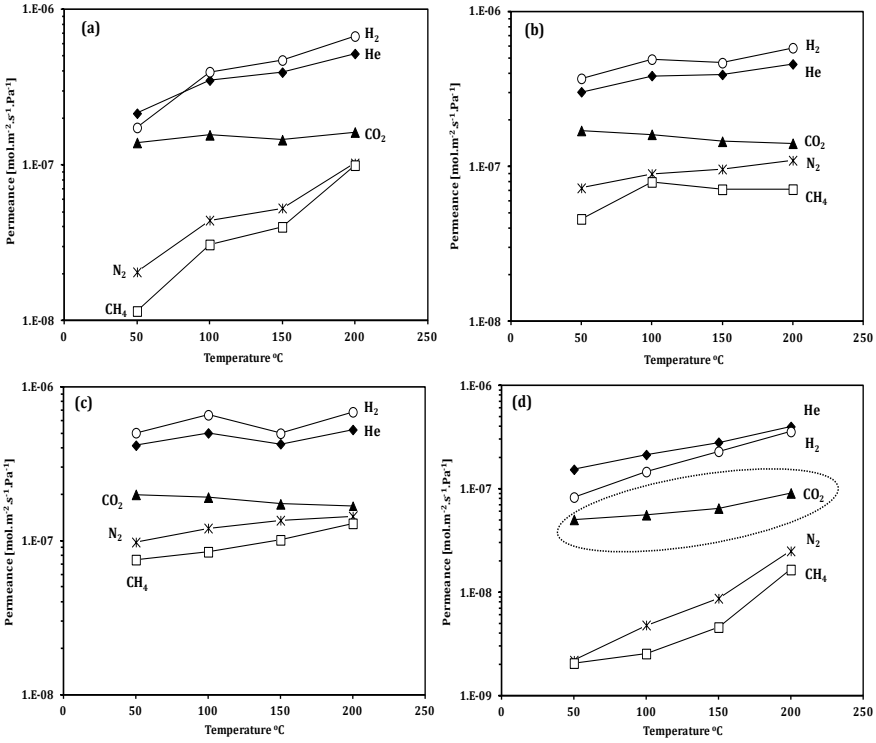

Figure 7.19. Gas permence vs. temperature for a) M3, b) M4, c) M5 and d) M6 (Δ P = 2 bar).

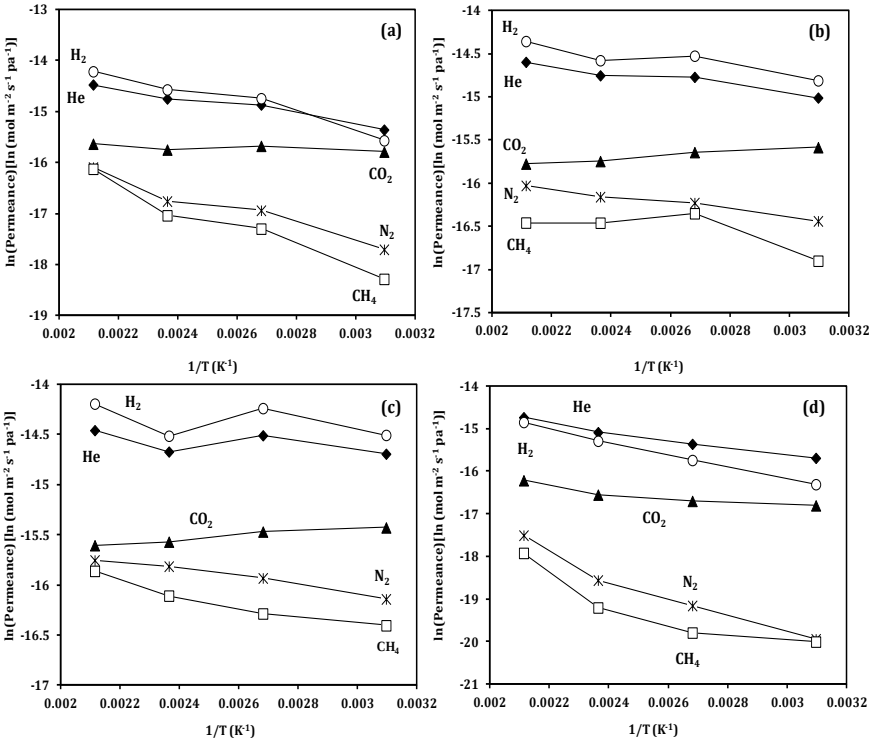

Figure 7.20. Temperature dependency for several gases for a) M3, b) M4, c) M5 and d) M6 (Δ P = 2 bar).

Table 7.8. Apparent activation energies for M3 to M6 at (ΔP= 2 bar) together with reported data in the literature.

Membranes	Activation energy (E_a) KJ/mol					
	He	H_2	CO_2	N_2	CH_4	Ref.
M3	7.1	10.9	-0.16	12.6	17.0	
M4	3.2	3.3	-1.7	3.3	3.4	
M5	1.3	1.6	-1.5	3.3	4.4	
M6	7.8	12.2	4.6	19.7	16.5	
SiO_2	–	8	-2	6	10	[18]
SiO_2	1.7:4.0*	-1.3:2.9*	-9.2:-11.2*	–	–	[60]
Hyd-Si(1)	–	5	-1	–	–	[61]
Hyd-Si(2)	–	6	3.3	–	–	[62]
Surfactant templated silica	–	4	-4	–	–	[61]
Co-SiO_2 (dry conditions)	9.5	–	–	-5	–	[40]
Co-SiO_2	–	21.3	–	–	–	[5]
33% Ni/SiO_2	7.1	–	–	–	–	[63]
10% ZrO_2/SiO_2	4.7	3.4	–	–	–	[37]

* When more values were presented in a single study, the lowest and the highest one are reported in Table 7.8.

(1) Hyd-Si refers to silica membrane prepared with 50% MTES : 50% TEOS.

(2) Hyd-Si refers to silica membrane prepared with molar ratio 0.2-0.6 TFPTES : 1 TEOS, where TFPTES is (trifluoropropyl)triethoxysilane.

Table 7.9. Permselectivity of M3 to M6 membrane at (ΔP= 2 bar).

	H_2/N_2	He/N_2	H_2/CH_4	He/CH_4	CO_2/CH_4
Knudsen value	**3.73**	**2.65**	**2.83**	**2.0**	**1.66**
M3	6-9	5-11	6-15	5-19	1.5-14
M4	5-6	4-7	6-8.5	4-6.5	2-4
M5	3.5-5	3-4.5	5-8	4-6.5	1.5-2.7
M6	**14-40**	**16-70**	**20-60**	**21-74**	**5-24**

From Figures 7.12 and 7.18, M1 to M5 have the same trend to He, H_2 and N_2, i.e. high permeability to H_2 with respect to He. The permeance of M1 and M2 are one order of magnitude lower compared with M3 to M5. This could be attributed to the increase the number of solubility sites for H_2 of the amorphous silica materials with respect to He, which is essentially non-adsorbing gas as reported by Bakker *et al.* [65]. Generally, the overall behavior of the hydrophobic membranes can be explained as reported by Kanezashi *et al.* [66]. The formation of interparticle and intraparticle pores can occur during the preparation of sol-gel derived microporous silica membranes. The interparticle pores are formed by voids between gel particles, while intraparticle pores result from the silica network structure. This silica structures facilitates the transport of small kinetic diameter gases via interparticle pores, whereas the intraparticle pores facilitates the other large gases. Moreover, concerning hybrid silica with MTES we have to take into account that their selectivity was reported to be low resulted from the broader PSD. In the present study, the PSD of unsupported (silica layer) M3 and M5 is a bit broader than M4 and M6 (see Figure 7.9). This means that the doping process has a significant effect on pore size control, however it is worth to say that the selectivity and permeation of M3 (non-doped membrane) is higher than M4 (doped one). This strongly supports the hypothesis that the behavior of supported material may differ somehow from the unsupported one.

7.4. Conclusions

Novel hydrophobic silica membranes were prepared by acid-catalyzed and condensation of TEOS and MTES. The hydrophobic properties of the silica membranes were obtained by using MTES as the hydrophobic additive. The preparation involved cobalt-doping within the hybrid silica matrix. The novel hydrophobic cobalt-doped silica membranes were prepared by two different methodologies. The clean room conditions resulted in membranes with better performance than those membranes prepared under normal conditions. However, in both methodologies even with different kind of support, the novel hydrophobic cobalt-doped silica membrane showed better results than the conventional hydrophobic silica membranes (non-doped membrane). Doping process and dilution process resulted in coating sols with less polydispersity. Hence, this led to membrane with better level of pore tuning control indicated by He permeance (d_k = 0.3 nm).

According to the preparation methodology, the transport of diffusing gases is governed by different mechanisms. The preparation under normal conditions led to non defect-free membranes; therefore, the support has a significance effect on the gas transport. In that later case, the gas transport in the membranes is governed by the coexistence of more than one transport mechanism, such as Knudsen and viscous flows, which are related to the mesoporous part of the structure, while surface diffusion is closely related to the effect of temperature on the microporous domain. Such kind of reported tubular silica membrane (novel hydrophobic cobalt-doped silica membrane) in the present study, with selectivity that exceed Knudsen or even on the boundary of Knudsen values, could be a good candidate among existing membrane materials for separation process. To that respect, the separation of hydrogen from larger molecules such as hydrocarbons could be more favorable with the membrane investigated in this work.

On the other hand, membrane preparation under clean room conditions led to molecular sieve disk-shaped silica membranes. This is indicated by the very low permeance of lager gases, such as SF_6 in the novel membranes. Moreover, the transport of gases through the novel cobalt-doped silica membrane was activated as the flux increased with temperature for membranes M3 to M5. M6 deviated from the other membranes, especially for CO_2 transport, and this may be due to the fact that

CO_2 is less adsorbed or CO_2 capillary condensation is less significant; therefore, a gradual increase in CO_2 permeance with temperature is observed for M6. However, this membrane showed high flux of He compared with the other gases. Besides, the highest activation energy and ideal selectivity was achieved by M6.

Generally, both methodologies in the present work introduced novel hydrophobic cobalt-doped silica membranes. Separation processes of some gases, such as CO_2 from CH_4, have potential applications in several fields such as enhanced oil recovery. In addition to that, the need for H_2 is increasing in the coming decades. The presented work shows promising membrane materials for membranes to be used for H_2 separation and purification, CO_2 separation as indicated, for instance, by the high CO_2/CH_4 and H_2/CH_4 permselectivity. From the economical point of view the membrane preparation presented in the present thesis, especially the preparation under normal conditions is simple and at least an appropriate and effective way for support modification to achieve separation that exceeds Knudsen separation values. Accordingly, this procedure significantly reduced the cost of the membrane production and support modification as well.

7.5. References

[1] H.P. Hsieh, Inorganic Membranes for Separation and Reaction; Membrane Science and Technology Series 3, Elsevier, Amsterdam, 1996.

[2] A. Buekenhoudt, A. Kovalevsky, J. Luyten, F. Snijkers, 1.11 - Basic Aspects in Inorganic Membrane Preparation, in: D. Editor-in-Chief: Enrico, G. Lidietta (Eds.), Comprehensive Membrane Science and Engineering, Elsevier, Oxford, 2010, pp. 217-252.

[3] G.Q. Lu, J.C. Diniz da Costa, M. Duke, S. Giessler, R. Socolow, R.H. Williams, T. Kreutz, Inorganic membranes for hydrogen production and purification: A critical review and perspective, J. Colloid Interface Sci. 314 (2007) 589-603.

[4] Y.S. Lin, Microporous and dense inorganic membranes: current status and prospective, Sep. Purif. Technol. 25 (2001) 39-55.

[5] R. Igi, T. Yoshioka, Y.H. Ikuhara, Y. Iwamoto, T. Tsuru, Characterization of Co-doped silica for improved hydrothermal stability and application to hydrogen separation membranes at high temperatures, J. Am. Ceram. Soc. 91 (2008) 2975-2981.

[6] H.H. El-Feky, K. Briceño, E.d.O. Jardim, J. Silvestre-Albero, T. Gumí, Novel silica membrane material for molecular sieve applications, Microporous Mesoporous Mater. 179 (2013) 22-29.

[7] H.H. El-Feky, K. Briceño, M. A. G. Hevia, T. Gumí, Characterization of metal-doped methylated microporous silica for molecular separations, submitted to Microporous Mesoporous Materials.

[8] G. Xomeritakis, S. Naik, C.M. Braunbarth, C.J. Cornelius, R. Pardey, C.J. Brinker, Organic-templated silica membranes: I. Gas and vapor transport properties, J. Membr. Sci. 215 (2003) 225-233.

[9] B.N. Nair, T. Yamaguchi, T. Okubo, H. Suematsu, K. Keizer, S.-I. Nakao, Sol-gel synthesis of molecular sieving silica membranes, J. Membr. Sci. 135 (1997) 237-243.

[10] R.M. de Vos, H. Verweij, High-selectivity, high-flux silica membranes for gas separation, Science 279 (1998) 1710-1711.

[11] T.A. Peters, J. Fontalvo, M.A.G. Vorstman, N.E. Benes, R.A.v. Dam, Z.A.E.P. Vroon, E.L.J.v. Soest-Vercammen, J.T.F. Keurentjes, Hollow fibre microporous silica membranes for gas separation and pervaporation: Synthesis, performance and stability, J. Membr. Sci. 248 (2005) 73-80.

[12] V. Richard, E. Favre, D. Tondeur, A. Nijmeijer, Experimental study of hydrogen, carbon dioxide and nitrogen permeation through a microporous silica membrane, Chem. Eng. J. 84 (2001) 593-598.

[13] C. Barboiu, B. Sala, S. Bec, S. Pavan, E. Petit, P. Colomban, J. Sanchez, S. de Perthuis, D. Hittner, Structural and mechanical characterizations of microporous silica–boron membranes for gas separation, J. Membr. Sci. 326 (2009) 514-525.

[14] J.C. Diniz da Costa, G.Q. Lu, V. Rudolph, Y.S. Lin, Novel molecular sieve silica (MSS) membranes: characterisation and permeation of single-step and two-step sol–gel membranes, J. Membr. Sci. 198 (2002) 9-21.

[15] J. Dong, Y.S. Lin, M. Kanezashi, Z. Tang, Microporous inorganic membranes for high temperature hydrogen purification, J. Appl. Phys. 104 (2008) 121301-121317.

[16] [16] S. Smart, J.F. Vente, J.C. Diniz da Costa, High temperature H_2/CO_2 separation using cobalt oxide silica membranes, Int. J. Hydrogen Energy 37 (2012) 12700-12707.

[17] C.-Y. Tsai, S.-Y. Tam, Y. Lu, C.J. Brinker, Dual-layer asymmetric microporous silica membranes, J. Membr. Sci. 169 (2000) 255-268.

[18] R.M. de Vos, H. Verweij, Improved performance of silica membranes for gas separation, J. Membr. Sci. 143 (1998) 37-51.

[19] M.C. Duke, J.C. Diniz da Costa, G.Q. Lu, M. Petch, P. Gray, Carbonised template molecular sieve silica membranes in fuel processing systems: permeation, hydrostability and regeneration, J. Membr. Sci. 241 (2004) 325-333.

[20] D. Lee, S.T. Oyama, Gas permeation characteristics of a hydrogen selective supported silica membrane, J. Membr. Sci. 210 (2002) 291-306.

[21] S.J. Khatib, S.T. Oyama, Silica membranes for hydrogen separation prepared by chemical vapor deposition (CVD), Sep. Purif. Technol. 111 (2013) 20-42.

[22] N.K. Raman, C.J. Brinker, Organic "template" approach to molecular sieving silica membranes, J. Membr. Sci. 105 (1995) 273-279.

[23] J. M. S. Henis, Commercial and Practical Aspects of Gas Separation, In : D. R. Paul, Y. P. Yampol'skii (Eds.), Polymeric Gas Separation Membranes, CRC Press, Boca Raton, 1994, pp. 441- 512.

[24] F. Gallucci, E. Fernandez, P. Corengia, M. van Sint Annaland, Recent advances on membranes and membrane reactors for hydrogen production, Chem. Eng. Sci. 92 (2013) 40-66.

[25] S. Battersby, M.C. Duke, S. Liu, V. Rudolph, J.C. Diniz da Costa, Metal doped silica membrane reactor: Operational effects of reaction and permeation for the water gas shift reaction, J. Membr. Sci. 316 (2008) 46-52.

[26] L.T. Zhuravlev, The surface chemistry of amorphous silica. Zhuravlev model, Colloids Surf., A 173 (2000) 1-38.

[27] R.K. Iler, The Chemistry of Silica: Solubility, Polymerization, Colloid and Surface Properties, and Biochemistry, John Wiley and Sons, New York, 1979.

[28] M. Kanezashi, M. Asaeda, Hydrogen permeation characteristics and stability of Ni-doped silica membranes in steam at high temperature, J. Membr. Sci. 271 (2006) 86-93.

[29] M.C. Duke, J.C.D. da Costa, D.D. Do, P.G. Gray, G.Q. Lu, Hydrothermally robust molecular sieve silica for wet gas separation, Adv. Funct. Mater. 16 (2006) 1215-1220.

[30] N.K. Raman, M.T. Anderson, C.J. Brinker, Template-based approaches to the preparation of amorphous, nanoporous silicas, Chem. Mater. 8 (1996) 1682-1701.

[31] Q. Wei, Y.-L. Wang, Z.-R. Nie, C.-X. Yu, Q.-Y. Li, J.-X. Zou, C.-J. Li, Facile synthesis of hydrophobic microporous silica membranes and their resistance to humid atmosphere, Microporous Mesoporous Mater. 111 (2008) 97-103.

[32] R.M. de Vos, W.F. Maier, H. Verweij, Hydrophobic silica membranes for gas separation, J. Membr. Sci. 158 (1999) 277-288.

[33] H.L. Castricum, A. Sah, M.C. Mittelmeijer-Hazeleger, C. Huiskes, J.E.t. Elshof, Microporous structure and enhanced hydrophobicity in methylated SiO_2 for molecular separation, J. Mater. Chem. 17 (2007) 1509-1517.

[34] J.C.D. da Costa, S. Coombs, J. Lim, G.Q. Lu, Characterisation of xerogels derived from sucrose templated sol-gel synthesis, J. Sol-Gel Sci. Technol. 31 (2004) 215-218.

[35] S. Giessler, J.C. Diniz da Costa, G.Q. Lu, Hydrophobicity of Templated Silica Xerogels for Molecular Sieving Applications, J. Nanosci. Nanotechnol. 1 (2001) 331-336.

[36] G.P. Fotou, Y.S. Lin, S.E. Pratsinis, Hydrothermal stability of pure and modified microporous silica membranes, J. Mater. Sci. 30 (1995) 2803-2808.

[37] K. Yoshida, Y. Hirano, H. Fujii, T. Tsuru, M. Asaeda, Hydrothermal stability and performance of silica-zirconia membranes for hydrogen separation in hydrothermal conditions, J. Chem. Eng. Jpn. 34 (2001) 523-530.

[38] Y. Gu, P. Hacarlioglu, S.T. Oyama, Hydrothermally stable silica–alumina composite membranes for hydrogen separation, J. Membr. Sci. 310 (2008) 28-37.

[39] Y. Gu, S.T. Oyama, Permeation properties and hydrothermal stability of silica–titania membranes supported on porous alumina substrates, J. Membr. Sci. 345 (2009) 267-275.

[40] D. Uhlmann, S. Liu, B.P. Ladewig, J.C. Diniz da Costa, Cobalt-doped silica membranes for gas separation, J. Membr. Sci. 326 (2009) 316-321.

[41] S. Esposito, M. Turco, G. Ramis, G. Bagnasco, P. Pernice, C. Pagliuca, M. Bevilacqua, A. Aronne, Cobalt–silicon mixed oxide nanocomposites by modified sol–gel method, J. Solid State Chem. 180 (2007) 3341-3350.

[42] R.J.R. Uhlhorn, M.H.B.J.H.t. Veld, K. Keizer, A.J. Burggraaf, Synthesis of ceramic membranes, J. Mater. Sci. 27 (1992) 527-537.

[43] Y. Yuan, T.R. Lee, Contact Angle and Wetting Properties, in: G. Bracco, B. Holst (Eds.), Surface Science Techniques, Springer Berlin Heidelberg, 2013, pp. 3-34.

[44] G. Ortega-Zarzosa, C. Araujo-Andrade, M.E. Compeán-Jasso, J.R. Martínez, F. Ruiz, Cobalt oxide/silica xerogels powders: X-ray diffraction, infrared and visible absorption studies, J. Sol-Gel Sci. Technol. 24 (2002) 23-29.

[45] V. Boffa, J.E. ten Elshof, R. Garcia, D.H.A. Blank, Microporous niobia–silica membranes: Influence of sol composition and structure on gas transport properties, Microporous Mesoporous Mater. 118 (2009) 202-209.

[46] R.J.L.P.A. Young, Introduction to polymers, Chapman & Hall, London; New York, 1991.

[47] M.S. Dyuzheva, O.V. Kargu, V.V. Klyubin, The effect of polydispersity on the size of colloidal particles determined by the dynamic light scattering, Colloid J. 64 (2002) 33-38.

[48] J.C. Diniz da Costa, G.Q. Lu, V. Rudolph, Characterisation of templated xerogels for molecular sieve application, Colloids Surf., A 179 (2001) 243-251.

[49] K. Sinkó, G. Szabó, M. Zrínyi, Liquid-phase synthesis of cobalt oxide nanoparticles, J. Nanosci. Nanotechnol. 11 (2011) 4127-4135.

[50] S.A.A. Mansour, Spectrothermal studies on the decomposition course of cobalt oxysalts Part II. Cobalt nitrate hexahydrate, Mater. Chem. Phys. 36 (1994) 317-323.

[51] A. Darmawan, S. Smart, A. Julbe, J.C. Diniz da Costa, Iron oxide silica derived from sol-gel synthesis, Materials 4 (2011) 448-456.

[52] M.M. Dubinin, Physical Adsorption of Gases and Vapors in Micropores, in: D. A. Cadenhead, J. F. Danielli, M. D. Rosenberg (Eds), Progress in Surface and Membrane Science, Academic Press, New York, 1975, pp. 1-70.

[53] S. Brunauer, P.H. Emmett, E. Teller, Adsorption of gases in multimolecular layers, J. Am. Chem. Soc. 60 (1938) 309-319.

[54] A.V. Neimark, P.I. Ravikovitch, Capillary condensation in MMS and pore structure characterization, Microporous Mesoporous Mater. 44–45 (2001) 697-707.

[55] K. Briceño, A. Iulianelli, D. Montané, R. Garcia-Valls, A. Basile, Carbon molecular sieve membranes supported on non-modified ceramic tubes for hydrogen separation in membrane reactors, Int. J. Hydrogen Energy 37 (2012) 13536-13544.

[56] D. Lee, L. Zhang, S.T. Oyama, S. Niu, R.F. Saraf, Synthesis, characterization, and gas permeation properties of a hydrogen permeable silica membrane supported on porous alumina, J. Membr. Sci. 231 (2004) 117-126.

[57] D. Wang, W.K. Teo, K. Li, Permeation of H_2, N_2, CH_4, C_2H_6, and C_3H_8 through asymmetric polyetherimide hollow-fiber membranes, J. Appl. Polym. Sci. 86 (2002) 698-702.

[58] B.S. Liu, N. Wang, F. He, J.X. Chu, Separation performance of nanoporous carbon membranes fabricated by catalytic decomposition of CH_4 Using Ni/Polyamideimide templates, Ind. Eng. Chem. Res. 47 (2008) 1896-1902.

[59] H. Qi, J. Han, N. Xu, Effect of calcination temperature on carbon dioxide separation properties of a novel microporous hybrid silica membrane, J. Membr. Sci. 382 (2011) 231-237.

[60] T. Yoshioka, E. Nakanishi, T. Tsuru, M. Asaeda, Experimental studies of gas permeation through microporous silica membranes, AIChE J. 47 (2001) 2052-2063.

[61] S. Giessler, M.C. Duke, J.C. Diniz da Costa, G.Q. Lu, Hydrothermal stability of modified silica membranes for gas separation, in: 6th World Congress of Chemical Engineering, Melbourne, Australia, 2001, pp. 1-10.

[62] Q. Wei, F. Wang, Z.-R. Nie, C.-L. Song, Y.-L. Wang, Q.-Y. Li, Highly hydrothermally stable microporous silica membranes for hydrogen separation, J. Phys. Chem. B 112 (2008) 9354-9359.

[63] M. Kanezashi, T. Fujita, M. Asaeda, Nickel-doped silica membranes for separation of helium from organic gas mixtures, Sep. Sci. Technol. 40 (2005) 225-238.

[64] P. Hacarlioglu, D. Lee, G.V. Gibbs, S.T. Oyama, Activation energies for permeation of He and H2 through silica membranes: An ab initio calculation study, J. Membr. Sci. 313 (2008) 277-283.

[65] W.J.W. Bakker, L.J.P. Van Den Broeke, F. Kapteijn, J.A. Moulijn, Temperature dependence of one-component permeation through a silicalite-1 membrane, AIChE J. 43 (1997) 2203-2214.

[66] M. Kanezashi, A. Yamamoto, T. Yoshioka, T. Tsuru, Characteristics of ammonia permeation through porous silica membranes, AIChE J. 56 (2010) 1204-1212.

Chapter 8

General Conclusions and Future Work

General conclusions and future work

The present thesis presented an alternative and novel methodology to develop and modify microporous silica membrane material. The aim of doing so is to obtain novel material with well enhanced surface and microstructural properties for molecular sieve applications, such as gas separations. In the present thesis the novel material, cobalt-doped hybrid silica, was prepared by the acid-catalyzed hydrolysis and condensation process of tetraethylorthosilicate (TEOS) and methyltriethoxysilane (MTES). The preparation involved cobalt-doping within the matrix of organic templated silica material (hybrid silica). The fine control of the silica matrix and the satisfactory pore size tuning presented in this thesis was possible thanks to sol-gel technique. Moreover, by that technique a better control of the textural properties of the silica matrix and a more homogeneity dispersion of cobalt oxide in the silica matrix on a nanometric scale was achieved as well.

The main conclusions of this research work can be summarized as follow:

- Novel molecular sieve silica membrane material with high thermal stability was achieved.
- The novel silica membrane material possesses all the characteristic feature of silica and modified silica membrane materials together (hybrid and metal-doped silica).
- The novel silica membrane material was rendered the hydrophobic feature after heat treatment,i.e. calcination process, in air (oxidizing atmosphere).
- This novel material exhibited a trend towards micropore formation.
- The PSD of silica matrices was only affected by MTES content, and hence the cobalt content (3 wt%) had no influence on both PSD and the uniformly incorporation of different MTES content.
- At 400 °C, i.e. before the temperature where the pyrolysis or decomposition of the organic template occurs, the contribution of the organic templates were very strong, indicated by the resonances T^2 and T^3. These resonances increased as the MTES content increased.
- Reduction in the contribution of T^2 and T^3 occurred at 600 °C, moreover the losses of organic templates are proportional to the sample MTES concentration as indicated by TGA analysis.
- Broader pore size distribution was obtained by increasing MTES content.

- The molar ratio of the hybrid silica sols prepared by MTES:TEOS are generally preferred to be limited to 50:50% or lower. This is due to the non-uniform incorporation of the organic template over that ratio due to phase separation causing poor pore size control.
- Interaction between the cobalt species and silica matrix depend mainly on the cobalt content. At low cobalt content (3 wt%) the dominate case was amorphous structure, and hence the formation of the strong framework of Si-O-Co linkages was achieved. As the cobalt content increased the formation of the crystalline Co_3O_4 species was the dominant case.
- The enhanced properties of the novel silica membrane material were achieved thanks to the doping process and the presence of the Si-O-Co linkages as well as the tiny crystal of Co_3O_4 species that could be detected by FTIR. Tiny small bands observed were assigned to Co_3O_4 were observed.
- As result of the promoted densification of the novel silica matrix by heat treatment, there were structural changes such as decrease in the surface area and micropore volume and area. However, these structural changes occurred at higher temperature compared with the hybrid silica materials (non-doped) that reported in the literature. Therefore, complete densification tending to smaller pores can be achieved at high temperature compared with the non-doped materials. Such difference is the consequence of the high thermal stability and the organic templates removal at high temperature shown by the novel silica membrane material reported in the present thesis.
- Increasing the organic template concentration with constant cobalt content induced the collapse of the silica matrix. While with constant template concentration and increasing the cobalt content, the homogeneity dispersion of the cobalt oxide opposed the silica structure collapse.
- Despite of these structural changes, the novel material exhibited a trend towards micropores formation. Hence, this novel material can be considered as promising membrane precursor for silica membranes preparation, and therefore for particular molecular sieve applications such as gas separation.

- Both doping and dilution processes led to coating sols with low polydispersity.
- The supported novel material showed a better result compared with the non-doped one regardless the way of membrane preparation. The novel supported room temperature tubular membrane showed an ideal selectivity over Knudsen values, although the gases transport mechanism was governed by the coexistence of more than one mechanism. This indicated that the support had a significant participation on the membrane separation performance. However, in the present thesis we demonstrated a simple way for support modification and hence such kind of membrane could be good candidate among existing reported membranes for gas separation. Especially for the separation of hydrogen from larger molecules such as hydrocarbons.
- Membranes prepared under clean room conditions resulted in membranes with defect-free thin top selective layer, and hence the gases transport was governed by activated transport mechanism. In addition, the membrane prepared with 20x coating sol showed higher selectivity compared with the other membranes.

As the novel silica membrane material presented in this thesis can be considered as promising membrane precursor for silica membrane preparation. Therefore, this novel silica membrane material will open new research lines in the field of microporous silica materials for molecular sieve applications. The following points are interesting research lines that could be covered in the future work:

- The study of the hydrothermal stability of the unsupported and supported material.
- Investigation of the surface and microstructural properties of the novel silica membrane material after heat treatment in inert atmosphere and comparison between this aspect and the heat treatment in oxidizing atmosphere.
- Testing the novel silica membrane in a membrane reactor for investigation the membrane performance in presence of steam.

List of Publications and Congresses

Contributions

List of publications

Directly related with the thesis:

I- Novel silica membrane material for molecular sieve applications
Hany Hassan El-Feky, Kelly Briceño, Erika de Oliveira Jardim, Joaquín Silvestre-Albero, Tània Gumí
Microporous and Mesoporous Materials 179 (2013) 22-29

II- Characterization of metal-doped methylated microporous silica for molecular separations
Hany Hassan El-Feky, Kelly Briceño, Miguel A. G. Hevia, Tània Gumí
Submitted for publication

III- Thermally enhanced methylated microporous silica for molecular sieve applications
Hany Hassan El-Feky, Kelly Briceño, Miguel A. G. Hevia, Tània Gumí
Prepared for submission

IV- Novel hydrophobic silica membrane for gas separation
Hany Hassan El-Feky, Marcel ten Hove, Kelly Briceño, Louis Winnubst, Tània Gumí
Prepared for submission

V- Facile preparation of supported hydrophobic silica membrane for gas separation
Hany Hassan El-Feky, Kamila Szałata, Kelly Briceño, Tània Gumí
Prepared for submission

Derived from other research lines (Master work):

I- Facile synthesis of porous monolithic membrane microdevice
Hany Hassan El-Feky, Àngels Cano-Òdena, Tània Gumí
Journal of Membrane Science 439 (2013) 96-102

Congresses contributions

I- Preparation of novel silica membrane material for gas separation (poster)

Hany Hassan, Kelly Briceño, Tània Gumí

EUROMAT 2011, Montpellier, France, September 12-15, 2011

II- Preparation, characterization and application of a membrane microdevice (master work, poster)

Hany Hassan, Àngels Cano-Òdena, Tània Gumí

Euromembrane 2009, Montpellier, France, September 6-10, 2009

III- Preparation, characterization and application of a membrane microdevice (master work, presentation)

Hany Hassan

11th Network Young Membrains (NYM) 2009, Mèze, France, September 3-4, 2009.

Curriculum Vitae

Hany Hassan El-Feky has got his Bachelor of Science with honor grade, Chemistry major, in May 2002 from Alexandria University, Egypt. From October 2004 to November 2005, he joined Advanced Technology and New Materials Research Institute (ATNMRI) at the City of Scientific Research and Technological Applications (SRTA-City), New Borg El-Arab city, Alexandria, Egypt.

He was with the chemical sector, operational quality control labs sector, Abu Qir Fertilizers and Chemicals Industries Company (AFC), Alexandria, Egypt, as a shift manager, from November 2005 till now. In 2008, he was awarded a master grant from Universitat Rovira i Virgili (URV), Tarragona, Spain. In October 2008, he had started his master work at the Department of Chemical Engineering at URV, and in September 2009, he got the master degree in Nanoscience and Nanotechnology. His research work was focused on preparation, characterization and application of a membrane microdevice.

In 2010, he was awarded a doctoral grant from ''Departament d' Economia i Coneixement'' de la ''Generalitat de Catalunya'' and its department of Support to Universities and Research (SUR del DEC), together with Fons Social Europeu (FSE) for the period 2010-2013. He started his PhD within the doctorate program of Nanoscience and Nanotechnology in METEOR research group at the Department of Chemical Engineering at URV. His current research interests include preparation and characterization of sol-gel derived silica membrane materials by sol-gel technique, and preparation of microporous ceramic membranes for gas separation, of which the results are described in this thesis.